Univerza v Ljubljani
Fakulteta za elektrotehniko

mag. Peter Kramar

ELEKTRIČNA PORUŠITEV RAVNINSKEGA LIPIDNEGA DVOSLOJA

DOKTORSKA DISERTACIJA

MENTORICA

doc. dr. Alenka Maček Lebar

Ljubljana, 2010

Zahvala

Za strokovno vodstvo in pomoč pri nastajanju disertacije se iskreno zahvaljujem mentorici docentki dr. Alenki Maček Lebar, ki je z nasveti in potrpežljivostjo spremljala in usmerjala moje delo.

Še med dodiplomskim študijem me je v področje biomedicinske tehnike in v resnično prijetno okolje Laboratorija za biokibernetiko pritegnil moj prvi mentor in predstojnik Laboratorija, profesor dr. Damijan Miklavčič. Za vse najlepša hvala!

Večina eksperimentalnega dela s tokovnim vzbujanjem je bila opravljena na Politehnični Univerzi v Wroclavu, Poljska, v okviru Poljsko-Slovenskega bilateralnega projekta. Zahvaljujem se profesorici dr. Malgorzati Kotulski za gostoljubje, izkazano strokovno pomoč in nasvete ter da je omogočila izvedbo poizkusov v laboratorijih svoje skupine.

Simulacije molekularne dinamike so bile opravljene na Univerzi Henri Ponicare, Nancy, Francija, v okviru Francosko-Slovenskega bilateralnega projekta PROTEUS. Zahvaljujem se profesorju dr. Mounirju Tareku za gostoljubje, izkazano strokovno pomoč in nasvete. Zahvaljujem tudi raziskovalki Lucie Delemotte za pomoč pri učenju modeliranja z molekularno dinamiko.

Zahvaljujem se diplomantu Izidorju Sabotinu za izkazano pomoč pri eksperimentalnem delu, pogovoru ter reševanju prenekaterih praktičnih vprašanj.

Hvala vsem sodelavcem Laboratorija za biokibernetiko, ki so vsak na svoj način pripomogli s svojim vzdušjem in posledično k nastajanju te disertacije.

Zahvala gre tudi mami.

Največja zahvala gre ženi Andrejki in hčerki Katji, za izredno potrpežljivost pri nastajanju tega dela.

Kazalo

Povzetek IX

Abstract XI

1 Uvod 1

2 Materiali in metode 11

2.1 Priprava ravninskega lipidnega dvosloja 11

2.2 Napetostno vzbujanje ravninskega lipidnega dvosloja 12

2.2.1 Sistem za elektroporacijo ravninskih lipidnih dvoslojev 12

2.2.2 Merilni protokol 13

2.2.3 Porušitvena napetost in življenjska doba ravninskega lipidnega dvosloja ob napetostnem vzbujanju 14

2.3 Tokovno vzbujanje ravninskega lipidnega dvosloja 15

2.3.1 Sistem za opazovanje ravninskih lipidnih dvoslojev s tokovnim vzbujanjem 15

2.3.2 Merilni protokol 16

2.3.3 Porušitvena napetost in porušitveni tok ravninskega lipidnega dvosloja ob tokovnem vzbujanju 16

2.3.4 Opazovanje por v ravninskem lipidnem dvosloju 17

2.4 Merjenje kapacitivnosti ravninskega lipidnega dvosloja 20

2.4.1 Merjenje kapacitivnosti s časovno konstanto razelektritve 20

2.4.2 Merjenje kapacitivnosti s pretvorbo kapacitivnosti v periodo 22

2.5 Statistika 24

2.5.1 Določitev porušitvene napetosti ravninskega lipidnega dvosloja 25

2.6 Simulacije molekularne dinamike 25

2.6.1 Gradnja modela ravninskega lipidnega dvosloja 34

2.6.2 Ravninski lipidni dvosloj v električnem polju 36

2.6.3 Model ravninskega lipidnega dvosloja zgrajen iz lipidnih molekul POPC 37

3 Merjenje kapacitivnosti ravninskega lipidnega dvosloja 39

3.1 Merjenje kapacitivnosti s časovno konstanto razelektritve 39
3.2 Merjenje kapacitivnosti s pretvorbo kapacitivnosti v periodo 40
3.3 Zaključek 40
4 Merjenje porušitvene napetosti ravninskega lipidnega dvosloja z linearno naraščajočim signalom 41
4.1 POPC:POPS (1:0) 41
4.2 POPC:POPS (3:1) 43
4.3 POPC:POPS (1:1) 45
4.4 POPC:POPS (1:3) 47
4.5 POPC:POPS (0:1) 49
4.6 Primerjava porušitvenih napetosti različnih mešanic ravninskega lipidnega dvosloja. 51
4.7 Zaključki 52
5 Določitev viskoelastičnih lastnosti ravninskega lipidnega dvosloja na podlagi porušitvene napetosti izmerjene z linearno naraščajočim signalom 55
5.1 Viskoelastični model ravninskega lipidnega dvosloja 56
5.1.1 Predstavitev modela 56
5.1.2 Uporaba modela 62
5.1.3 POPC:POPS (1:0) 63
5.1.4 POPC:POPS (3:1) 64
5.1.5 POPC:POPS (1:1) 65
5.1.6 POPC:POPS (1:3) 66
5.1.7 POPC:POPS (0:1) 67
5.1.8 Primerjava mešanic 68
5.2 Zaključki 69
6 Dinamični model ravninskega lipidnega dvosloja 73
6.1 Molekularna dinamika 73
6.2 Tokovno vzbujanje ravninskega lipidnega dvosloja 74
6.3 Opazovanje por v ravninskem lipidnem dvosloju 76

6.4 Zaključki ... 79

7 Razprava ... 81

8 Izvirni prispevki k znanosti ... 89

Merjenje porušitvene napetosti ravninskega lipidnega dvosloja z linearno naraščajočim signalom 89

Določitev viskoelastičnih lastnosti ravninskega lipidnega dvosloja na podlagi porušitvene napetosti izmerjene z linearno naraščajočim signalom ... 89

Ocena prevodnosti in gostote por v ravninskem lipidnem dvosloju ... 89

9 Literatura ... 91

Spletni viri ... 101

Izjava ... 103

Dodatek ... 105

Članek 1 ... 107

Članek 2 ... 115

Članek 3 ... 125

Članek 4 ... 135

Poglavje v knjigi ... 143

Povzetek

V živih organizmih imajo membrane celic in celičnih organelov ključno vlogo. Sestavljene so iz različnih lipidnih in beljakovinskih molekul. Naloga celične membrane je vzdrževati kemijsko ravnovesje v celici, ter selektivno prepuščati molekule in ione, ki lahko vstopijo v celico. Lipidne molekule so sestavljene iz polarne hidrofilne glave ter nepolarnega hidrofobnega repa. Skupek molekul v vodi tvori energijsko ugodno strukturo tako, da hidrofobni repi nikoli niso izpostavljeni vodnim molekulam. Ravno zaradi teh lastnosti obstaja široka paleta umetnih lipidnih struktur: enoslojev, dvoslojev, večslojev, zaprtih dvoslojev oziroma veziklov in zaprtih enoslojev oziroma micel. Lastnosti celične membrane lahko preučujemo tudi na omenjenih strukturah; vezikel, na primer, ohranja geometrijo celice, ravninski lipidni dvosloj, pa lahko ponazarja majhen košček celične membrane. Umetne lipidne strukture so seveda mnogo bolj preproste kot celice zaradi geometrije, sestave in odsotnosti aktivnih procesov.

Elektroporacijo raziskujemo na različnih področjih biološke kompleksnosti: ravninskem lipidnem dvosloju, lipidnih veziklih ter celicah v *in vitro* in *in vivo* pogojih. Raziskave na ravninskih lipidnih dvoslojih so postavile temelje teorije vodnih por, katerih pa kasnejši eksperimenti niso neposredno potrdili niti na lipidnih dvoslojih niti na kompleksnejših modelih.

Lastnosti, ki jih opazujemo na ravninskem lipidnem dvosloju, so: kapacitivnost, debelina, upornost oziroma prevodnost, pretok snovi in porušitvena napetost. Vsaka lastnost zahteva svoj način merjenja. Signale, s katerimi ravninski lipidni dvosloj vzbujamo, delimo na napetostne in tokovne. Ena najpomembnejših in najdlje opazovanih lastnosti ravninskih lipidnih dvoslojev je kapacitivnost. Z merjenjem kapacitivnosti ravninskega lipidnega dvosloja ugotavljamo njegovo kvaliteto.

Kadar raziskujemo pojav elektroporacije v biomedicini in biotehnologiji, je porušitvena napetost ena izmed pomembnejših lastnosti ravninskega lipidnega dvosloja. Znano je, da je porušitvena napetost odvisna od sestave ravninskega lipidnega dvosloja, okoliškega elektrolita in trajanja izpostavitve električnemu polju.

V doktorski disertaciji smo predlagali metodo, s katero bi omejili vlogo pred-izpostavitve ter naključnosti življenjskega časa ravninskega lipidnega dvosloja in mu določiti najmanjšo porušitveno napetost. Predlagali smo merilni protokol, ki je sestavljen iz dveh korakov. V prvem koraku izmerimo kapacitivnost ravninskega lipidnega dvosloja s pravokotnim pulzom nizke napetosti. Le-ta mora biti dovolj nizka, da ravninskega lipidnega dvosloja ne poruši. V drugem koraku izmerimo porušitveno napetost ravninskega lipidnega dvosloja z linearno naraščajočim signalom.

Za določitev viskoelastičnih lastnosti ravninskega lipidnega dvosloja smo uporabili model, ki ga je postavil Dimitrov s sodelavci. Model povezuje kapacitivnost, elastični modul, viskoznost, površinsko napetost, življenjski dobo in porušitveno napetost ravninskega lipidnega dvosloja. Modelu so bile očitane pomanjkljivosti, ker ne upošteva stohastične narave procesa porušitve ob izpostavitvi konstantni napetosti. Ker z merjenjem porušitvene napetosti ravninskega dvosloja z uporabo linearno naraščajočega signala naključnost pojava močno zmanjšamo, se model bolje prilega eksperimentalnim rezultatom. Ujemanje izračunanih vrednosti Youngovega modula elastičnosti in površinske napetosti z vrednostmi iz literature je potrdilo pravilno izbiro linearno naraščajočega signala kot metodo za določanje porušitvene napetosti ravninskega lipidnega dvosloja.

Do sedaj rezultati med molekularno dinamiko in poizkusi na ravninskih lipidnih dvoslojih še niso bili primerjani in ovrednoteni. V naših poizkusih smo uporabili linearno naraščajoče tokovne signale različnih naklonov, s katerimi smo se želeli izogniti dlje trajajočemu odpiranju in zapiranju por v ravninskem lipidnem dvosloju ter doseči čimprejšnje porušenje ravninskega lipidnega dvosloja. Iz primerjave simulacij molekularne dinamike ter poizkusov smo ocenili prevodnost, število in gostoto por v ravninskem lipidnem dvosloju.

Abstract

Biological membranes play a crucial role in living organisms. They are soft condensed matter structures that envelope the cells and their inner organelles. Biological membranes maintain relevant concentration gradients by acting as selective filters for ions and molecules. Besides their passive role, they also host a number of metabolic and biosynthetic activities. Artificially built planar lipid bilayer can be considered as a small fraction of total cell membrane. It represents the simplest model for experimental studies of membrane properties; especially because it is accessible from both sides.

An exposure of a cell to an electric field of an adequate strength and duration leads to a transient increase of cell membrane permeability. This phenomenon, termed electroporation allows various otherwise nonpermeant molecules to cross the membrane and enter the cell. It is believed that structural changes, which are the reason for increased permeability, are formed in lipid part of biological membranes. Therefore electroporation is studied on all levels of biological complexity: form planar lipid bilayers and vesicles to cells in vitro, in vivo, and tissues. Experimental and theoretical studies performed on planar lipid bilayers gave an idea of water pores formation due to external electric field. Although water pores were later confirmed by molecular dynamic simulations, there is still gap between model parameters and experimental results.

Breakdown voltage is one of the most important properties of a planar lipid bilayer when biomedical and biotechnological applications of electroporation are under consideration. It has been known that the breakdown voltage depends on the lipid membrane composition, ionic bath solution, amplitude and electric field exposure duration. The breakdown voltage of the lipid bilayer is usually determined by repeatedly applying a rectangular voltage pulse. The amplitude of the voltage pulse is incremented in small steps until the breakdown of the bilayer is obtained. Using such a protocol each bilayer is exposed to a voltage pulse many times and the number of applied voltage pulses is not known in advance. Such a pre-treatment of the lipid bilayer affects its stability and consequently the breakdown voltage of the lipid bilayer.

We suggested a new measurement protocol for breakdown voltage determination. According to our measuring protocol each planar lipid bilayer is exposed to a voltage signal only twice. In the first step bilayer capacitance is determined by a rectangular low voltage signal. The capacitance measurement reveals an intact planar lipid bilayer before inducing its breakdown. In the next step, the planar lipid bilayer breakdown is induced by the linearly rising voltage signal. Different slopes of linear rising signal have been used in our experiments. The breakdown voltage depends on the slope of the linear rising signal. Results show that gently sloping voltage signal electroporates the lipid bilayer at a lower

voltage then steep voltage signal. Linear rising signal with gentle slope can be considered as having longer pre-treatment of the lipid bilayer; thus, the corresponding breakdown voltage is lower. With decreasing the slope of linear rising signal, minimal breakdown voltage for specific lipid bilayer can be determined. Better reproducibility and lower scattering are obtained due to the fact that each bilayer is exposed to electroporation treatment only once. Moreover, minimal breakdown voltage

To determine the viscoelastic properties of planar lipid bilayer, we used the model proposed by Dimitrov et al. Viscoelastic model links capacitance, elastic modulus, viscosity, surface tension, life time and voltage breakdown of planar lipid bilayer. The model has been criticized due to ignorance of the stochastic nature of the process failure when exposed to constant stress. Since the voltage breakdown of the planar bilayer was measured by means of linearly rising voltage signal, the occurrences of random events were significantly reduced. The model fits well enough to the experimental results and gives comparable values of Young's modulus and surface tension to the values listed in the literature.

So far, the results of molecular dynamics and experiments on planar lipid bilayers have not been compared and evaluated. By exposure of planar lipid bilayer to linear rising current signals of different slopes, we were able to detect small voltage drops before planar lipid bilayer breakdown occurred. We related them to pores in planar lipid bilayer. Comparison of experimental results and molecular dynamics simulation gives an estimation of the number and density of the pores in planar lipid bilayer as well as of pore conductivity.

1 Uvod

V živih organizmih imajo membrane celic in celičnih organelov ključno vlogo. Sestavljene so iz različnih lipidnih in beljakovinskih molekul. Naloga celične membrane je vzdrževati kemijsko ravnovesje v celici, ter selektivno prepuščati molekule in ione, ki lahko vstopijo v celico ali izstopijo iz nje [Gennis 1989]. Lipidne molekule so sestavljene iz polarne hidrofilne glave ter nepolarnega hidrofobnega repa. Skupek molekul v vodi tvori energijsko ugodno strukturo tako, da hidrofobni repi nikoli niso izpostavljeni vodnim molekulam. Ravno zaradi teh lastnosti obstaja široka paleta umetnih lipidnih struktur: enoslojev, dvoslojev, večslojev, zaprtih dvoslojev oziroma veziklov in zaprtih enoslojev oziroma micel [Tien in Ottova 2003]. Mnoge lastnosti celične membrane lahko preučujemo tudi na omenjenih strukturah; vezikel, na primer, ohranja geometrijo celice, ravninski lipidni dvosloj, pa lahko ponazarja majhen košček celične membrane.

V zadnjih dvajsetih letih je bilo narejenih veliko študij, v katerih so celično membrano izpostavili električnemu polju [Neumann *et al.* 1999; Chang *et al.* 1992]. Močno električno polje lahko destabilizira celično membrano ter začasno spremeni njeno strukturo. Ključni parameter je z zunanjim električnim poljem vsiljena transmembranska napetost, ki nastane zaradi Maxwell-Wagnerjeve polarizacije. Pod vplivom električnega polja naj bi se lipidne molekule reorientirale in oblikovale vodne pore [Chizmadzev *et al.* 1979]. Le-te povečajo prevodnost membrane ter njeno prepustnost za molekule, ki v običajnem stanju ne bi mogle vstopiti v in preko membrane. Pojav je poznan pod imenom elektroporacija, včasih pa uporabljajo tudi termin elektropermeabilizacija ali dielektrična porušitev celične membrane. Dosežena sprememba prepustnosti membrane je lahko reverzibilna. V tem primeru se celična membrana obnovi in celica preživi. Kadar je sprememba prepustnosti ireverzibilna, celica odmre.

Prvi je o reverzibilni dielektrični porušitvi membrane poročal Stampfli leta 1958 [Stampfli 1958]. Skoraj desetletje kasneje sta Sale in Hamilton poročala o netoplotnem električnem uničenju mikroorganizma z uporabo močnega električnega polja [Sale in Hamilton 1967]. Leta 1972 sta Neumann in Rosenheck pokazala, da električni pulzi spremenijo prepustnost membrane veziklov [Neumann in Rosenheck 1972]. Začetnim pionirskim študijam, so sledila tri pomembna dela, ki so vzpodbudila nadaljnje raziskave na področju elektroporacije. Kot prvi je leta 1982 Neumann s sodelavci dosegel vnos genov v celico z uporabo eksponentno padajoče napetosti nastale pri razelektritvi kondenzatorja [Neumann *et al.* 1982]. Leta 1987 sta Okino in Mohri pokazala vnos molekul v celico z električnimi pulzi v *in vivo* ter *in vitro* pogojih [Okino in Mohri 1987]. Leto dni za tem je rezultate njune študije potrdil Mir s sodelavci [Mir *et al.* 1988]. V začetku je bila večina

poizkusov narejena na posameznih celicah *in vitro*. Manj je bilo znano, da je veliko aplikacij učinkovitih tudi v *in vivo* pogojih. Z uporabo elektroporacije je namreč možno vnesti velike in majhne molekule v celico, v membrano lahko vgradimo proteine, celice lahko zlivamo med seboj. Naštete možnosti so elektroporacijo umestile v uporabo na mnogih področjih kot so biokemija, molekularna biologija in medicina [Kramar in Miklavčič 2003; Kramar in Miklavčič 2005, Kramar *et al.* 2007; Kramar *et al.* 2009; Pakhomov *et al.* 2010].

Pokazali so, da je nastajanje por in učinkovitost elektroporacije odvisna od števila pulzov (N), trajanja posameznega pulza (T), ponavljalne frekvence (f) in napetosti (U) posameznega pulza. Pri uporabi pojava vpeljemo tako imenovan prag poracije. To je napetost, ki jo moramo preseči, če želimo vzpostaviti transport preko celične membrane pri izbranih T, f in N. Pokazali so tudi, da dovedena električna energija kot tudi naboj električnih pulzov nista ključna za razvoj por v membrani, ampak je povezava med U, f, N in T precej bolj kompleksna [Cantella et al. 2001; Maček Lebar in Miklavčič 2001; Miklavčič in Kotnik 2004]. Glede na to ali je elektroporacija reverzibilna ali ireverzibilna ločimo funkcijske oziroma destruktivne aplikacije [Miklavčič in Puc 2006]. Funkcijske aplikacije morajo ohranjati življenjske lastnosti celice, tkiva ali mikroorganizmov. Pri destruktivnih aplikacijah uporabljamo ireverzibilno elektroporacijo. Električni pulzi so namenoma uporabljeni za uničenje celic in mikroorganizmov. Tako se ireverzibilna elektroporacija uporablja za netoplotno konzerviranje hrane in vode, kjer zahtevamo trajno uničenje mikroorganizmov [Teissie *et al.* 2002; Haas in Aturaliye 1999; Rowan *et al.* 2000].

Trenutno najpomembnejša funkcijska aplikacija je vnos majhnih ali velikih molekul v citoplazmo preko membrane [Mir 2001; Gehl 2003; Serša *et al.* 2008]. Elektrokemoterapija je ena od oblik zdravljenja raka, ki temelji na kombinaciji kemoterapije in elektroporacije. Prisotnost električnega pulza ob času, ko koncentracija kemoterapevtika doseže najvišjo vrednost v zunaj celičnem prostoru, poveča transport v notranjost celice, kjer kemoterapevtik učinkuje. Na ta način povečamo učinkovitost kemoterapevtika. Predklinične študije na živalih in klinične študije so pokazale, da elektrokemoterapijo lahko uspešno uporabljamo za lokalno zdravljenje raka [Mir *et al.* 1995; Serša *et al.* 1989; Heller *et al.* 1999]. Z elektroporacijo lahko v celico vnesemo tudi molekule DNK. Postopek se imenuje genska elektrotransfekcija [Mouneimne et al. 1990; Raffy in Teissie 1997]. Zlivanje celic so opazovali med skupki celic v suspenziji [Abidor in Sowers 1992; Sowers 1993, Trontelj *et al.* 2010] ter celo med celicami v tkivu [Mekid in Mir 2000]. Za uspešno fuzijo celic v celični suspenziji, moramo zagotoviti, da sta obe celici dovolj blizu, da se lahko združita. To naprimer lahko zagotovimo z dielektroforezo [Abidor in Sowers 1992]. Pokazali so, da z elektrozlivanjem celic lahko uspešno tvorimo cepiva [Scott-Taylor *et al.* 2000] in protitelesa [Schmidt *et al.* 2001].

Električni impulzi visokih amplitud povzročijo tudi povečanje pretoka ionov in molekul skozi kožo [Prausnitz *et al.* 1993]. Na ta način lahko vnašamo različne zdravilne učinkovine skozi kožo, ki drugače kože ne prehajajo [Vanbever *et al.* 1994]. Princip elektroporacije lahko uporabimo tudi pri vnosu večjih molekul v kožo ali preko kože, kot so na primer nukleotidi [Zewert *et al.* 1995, Pavšelj in Preat 2005].

Elektroporacijo raziskujemo na različnih področjih biološke kompleksnosti: ravninskem lipidnem dvosloju, lipidnih veziklih ter celicah v *in vitro* in *in vivo* pogojih. Raziskave na ravninskih lipidnih dvoslojih so postavile temelje teorije vodnih por, katerih pa kasnejši eksperimenti niso neposredno potrdili niti na lipidnih dvoslojih niti na kompleksnejših modelih [Pavlin *et al.* 2009]. Umetne lipidne strukture so mnogo bolj preproste kot celice zaradi geometrije, sestave in odsotnosti aktivnih procesov. Liposomi ali vezikli s svojo preprostostjo in kroglasto obliko služijo kot dober model celične membrane, ki pa je brez ionskih kanalčkov ali drugih vgrajenih komponent. Geometrijsko drugačen in še bolj preprost model celične membrane je ravninski lipidni dvosloj, s katerim predstavimo košček celične membrane. Njegova prednost je v tem, da je dostopen z obeh strani. Leta 2001 je bila 40. obletnica prve uspešne postavitve ravninskega lipidnega dvosloja kot modela celične membrane [Ottova in Tien 2002]. Vendar se je zgodovina lipidnih dvoslojev začela že mnogo pred tem. Eden prvih mejnikov v zgodovini je bilo leto 1672, ko je Robert Hooke, fizik, ki je dal ime »celici« in je znan predvsem po preučevanju elastičnih lastnosti snovi, opazoval črne lise na milnih mehurčkih in filmih. Raziskovanje umetnih membran je potekalo vzporedno z odkrivanjem lastnosti bioloških celic, odkritjem osmoze in preučevanjem pretoka snovi skozi membrano.

Ravninske lipidne dvosloje običajno pripravimo v posebni komori, ki je sestavljena iz dveh prekatov. Prekata ločuje teflonska folija, v kateri je majhna luknjica s premerom od 0,1 do 1 mm. Na rob luknjice napnemo ravninski lipidni dvosloj z eno od naslednjih metod: metodo barvanja, metodo dvigovanja gladine ali metodo potopitve konice [Smeyers et al. 2003, Erlich 1992].

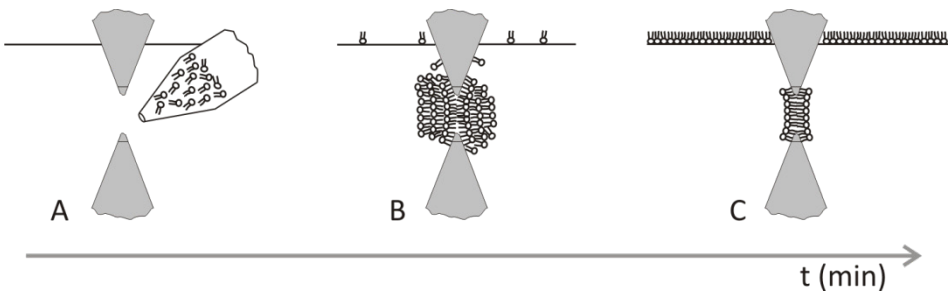

Slika 1. Metoda barvanja. A) Komora z vodo in nanos lipidov na teflonsko folijo, ki deli prekata komore. B) Gmota nanesenih lipidov se enakomerno razporedi po teflonski foliji, odvečni odplavajo na gladino. C) Po določenem času nastane lipidni dvosloj.

Metoda barvanja (*ang. painted bilayer*) ali Muller - Rudinova metoda se je razvila med prvimi [Muller *et al.* 1962]. Vodna raztopina soli je pripravljena v komori, s pipeto pa nanesemo (obarvamo) lipide na teflonsko folijo, ki ločuje prekata komore (slika 1A). V začetku so lipidne molekule združene v veliko gmoto (slika 1B), sčasoma pa se enakomerno porazdelijo po teflonski foliji in na luknjici nastane ravninski lipidni dvosloj (slika 1C).

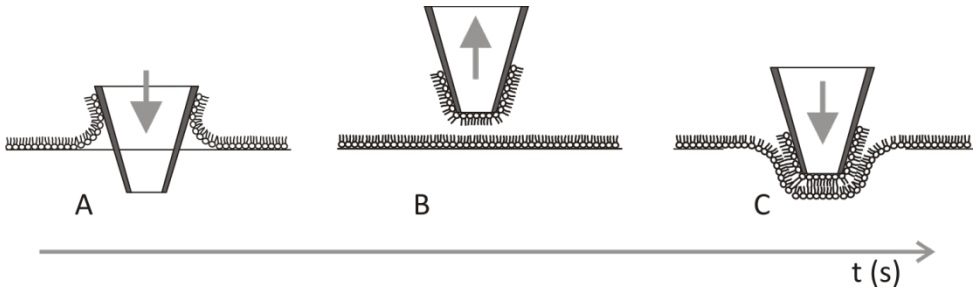

Slika 2. Metoda potopitve konice. A) V kopel potopimo ozko cevko in nanesemo molekule lipidov. B) Cevko dvignemo, C) in jo ponovno potopimo, tako da se na njej tvori ravninski lipidni dvosloj.

Pri metodi potopitve konice (*ang. Tip-Dip bilayer*) potrebujemo kopel, v katero potopimo cevko premera nekaj milimetrov. Na gladino vodne raztopine soli nanesemo lipidne molekule, ki se porazdelijo po celotni gladini in na rob cevke (slika 2A). Ko cevko, dvignemo iz kopeli, na njej nastane lipidni enosloj, nato počakamo nekaj časa, da se molekule lipidov na gladini ponovno razporedijo (slika 2B). Ko cevko ponovno potopimo, nastane na njeni konici ravninski lipidni dvosloj (slika 2C).

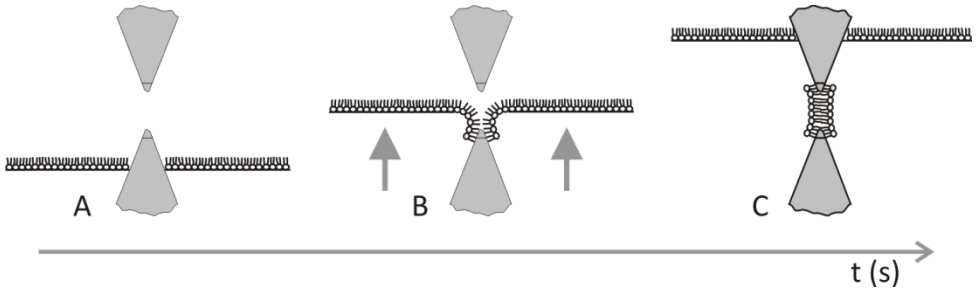

Slika 3. Metoda dviganja gladine. A) Gladino vode postavimo tik pod luknjico v teflonski foliji. Na površino nanesemo lipidne molekule in počakamo, da se porazdelijo enakomerno po gladini. B) V obeh prekatih enakomerno dvignemo gladino vode. C) Na luknjici teflonske folije tvorimo lipidni dvosloj.

Metoda dvigovanja gladine (*ang. folded bilayer*) oziroma Montal - Muellerjeva metoda je ena od najpogosteje uporabljenih metod za preučevanje lipidnih dvoslojev [Montal in Mueller 1972]. Pri tej metodi oba prekata komore napolnimo z vodno raztopino soli pod nivojem luknjice v teflonski foliji. Na gladino obeh prekatov nanesemo lipide in počakamo, da se enakomerno porazdelijo po gladini (slika 3A). Obe gladini nato sočasno dvignemo tako, da je luknjica potopljena v tekočini (slika 3B). Na luknjici v teflonski foliji med dvigovanjem obeh gladin nastane lipidni dvosloj (slika 3C). Prednost te

metode pred metodo barvanja je predvsem v tem, da lahko s spuščanjem in dviganjem gladine v prekatih tvorimo lipidne dvosloje enega za drugim, brez daljšega čakanja.

Ravninski lipidni dvosloj lahko modeliramo s preprostim električnim vezjem (slika 4) in sicer kot vzporedno vezavo upora in kondenzatorja. Ena najpomembnejših in najdlje opazovanih lastnosti ravninskih lipidnih dvoslojev je kapacitivnost. Z merjenjem kapacitivnosti ravninskega lipidnega dvosloja ugotavljamo njegovo kvaliteto. Zgodi se, da se namesto dvosloja lahko tvori večsloj, ki ga prepoznamo po nižji vrednosti kapacitivnosti.

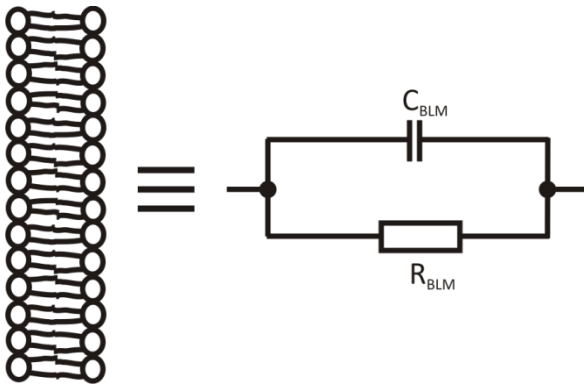

Slika 4. Električni model ravninskega lipidnega dvosloja, ki je sestavljen iz kapacitivnosti (C_{BLM}) in upornosti (R_{BLM}).

Tako so zanimive in največkrat preučevane lastnosti ravninskih lipidnih dvoslojev so kapacitivnost, upornost, debelina, viskoznost, elastičnost in porušitvena napetost (slika 5) [Kramar *et al.* 2010]. Lastnosti ravninskih lipidnih dvoslojev večinoma določamo z meritvijo toka oziroma napetosti preko ravninskega lipidnega dvosloja ali z optičnim opazovanjem, kjer opazujemo odklon žarka ter absorpcijo svetlobe v ravninskem lipidnem dvosloju. Obe vrsti meritev lahko med seboj tudi kombiniramo. Za vzbujanje ravninskih lipidnih dvoslojev so različni avtorji uporabljali tako napetostno [Troiano *et al.* 1998; Sharma *et al.* 1996; Meier *et al.* 2000; Diederich *et al.* 1998; Benz in Janko 1976] kot tokovno [Ridi *et al.* 1998; Robello in Gliozzi 1989; Ridi *et al.* 2000; Genco *et al.* 1993; Kalinowski *et al.* 1998; Koronkiewicz *et al.* 2004] vzbujanje. Pregled vseh sistemov je zbran v poglavju v knjigi, priloga 4 [Kramar *et al.* 2010].

Napetostno vzbujanje ravninskih lipidnih dvoslojev se je zgodovinsko pojavilo pred tokovnim vzbujanjem. Predstavlja neposredno vzpostavitev električnega polja na ravninskem lipidnem dvosloju. Sprva je napetostno vzbujanje najverjetneje posnemalo mirovalno napetost, ki je prisotna na membrani živih celic. Ko vsilimo napetost, je ravninski lipidni dvosloj le-tej izpostavljen praktično v hipu. Nasprotno se pri tokovnem vzbujanju, nosilci nabojev naberejo na eni strani ravninskega lipidnega dvosloja v odvisnosti od vrednosti toka ter postopoma ustvarijo potencialno razliko in s tem napetost na ravninskem lipidnem dvosloju.

V literaturi zasledimo, da so za merjenje električnih lastnosti ravninskih lipidnih dvoslojev uporabljali različne oblike signalov [Troiano *et al.* 1998; Sharma *et al.* 1996; Meier *et al.* 2000; Diederich *et al.* 1998; Benz in Janko 1976; Ridi *et al.* 1998; Robello in Gliozzi 1989; Ridi *et al.* 2000; Genco *et al.* 1993; Kalinowski *et al.* 1998; Koronkiewicz *et al.* 2004]. V večini primerov so uporabili pravokotne pulze širine 10 µs [Troiano *et al.* 1998; Sharma *et al.* 1996; Meier *et al.* 2000; Diederich *et al.* 1998; Benz in Janko 1976; Ridi *et al.* 1998; Robello in Gliozzi 1989; Ridi *et al.* 2000; Genco *et al.* 1993]. Zasledimo tudi uporabo sestavljenega signala iz pravokotnega pulza ter linearno padajočega signala [Sharma *et al.* 1996]. Opisano pa je bil tudi vzbujanje ravninskega lipidnega dvosloja s trikotno obliko signala [Robello in Gliozzi 1989].

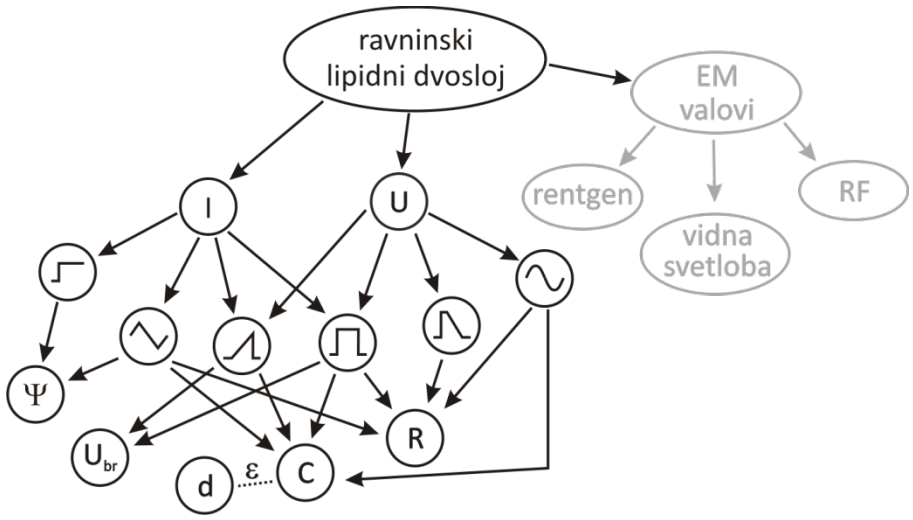

Slika 5. Pregled različnih načinov določanja lastnosti ravninskih lipidnih dvoslojev. *I* je tokovno vzbujanje, *U* napetostno vzbujanje. Oblika signala vzbujanja je narisana v krožcu. S takimi vzbujanji lahko merimo veličine kot so fluktuacije lipidov v membrani (*Ψ*), porušitveno napetost (U_{br}), debelina (*d*), kapacitivnost (*C*) in upornost (*R*) [Kramar *et al.* 2009].

V literaturi zasledimo tri različne metode merjenja kapacitivnosti: merjenje časovne konstante razelektritve ravninskega lipidnega dvosloja, merjenje z izmenično napetostjo sinusne oblike in merjenje s pretvorbo kapacitivnosti v periodo. Pri vseh treh metodah izmerjeno kapacitivnost normiramo na površino lipidnega dvosloja. Normirano kapacitivnost tako lahko primerjamo s poizkusi, narejenimi na različnih sistemih z različnimi površinami ravninskih lipidnih dvoslojev.

Znano je, da je porušitvena napetost odvisna od sestave ravninskega lipidnega dvosloja, sestave in koncentracije okoliškega elektrolita ter od trajanja izpostavitve električnemu polju [Gallucci *et al.* 1996]. Porušitvena napetost ravninskega lipidnega dvosloja je odvisna tudi od trajanja izpostavitve električnemu polju [Troiano *et al.* 1998, Abidor *et al.* 1979]. V teoriji elektromehanike je ravninski lipidni dvosloj predstavljen kot homogen elastični medij, s končno vrednostjo prožnostnega modula [Helfrich 1973]. Ko sila električne kompresije preseže silo elastičnosti, se membrana poruši. Rezultate dobimo ob predpostavki, da za omejene deformacije velja Hookov zakon [Abidor *et al.* 1979].

Najpogosteje uporabljen protokol za merjenje porušitvene napetosti je vzbujanje ravninskega lipidnega dvosloja s pravokotnimi napetostnimi pulzi (slika 6). Trajanje pulza je bilo izbrano med 10 in 100 µs, njegovo amplitudo pa so povečevali po vsakem pulzu, dokler se ravninski lipidni dvosloj ni porušil [Troiano *et al.* 1998]. Z meritvijo porušitvene napetosti na ravninskem lipidnem dvosoju dobimo oceno o njegovi stabilnosti v električnem polju. Napetost prvega pulza je nizka, tako da še ne poruši ravninskega lipidnega dvosloja. Vsak naslednji pulz, ko ravninski lipidni dvosloj še ni porušen, povečamo za izbrani napetostni korak. Amplituda pulza, pri katerem se ravninski lipidni dvosloj poruši, je definirana kot porušitvena napetost ravninskega lipidnega dvosloja [Troiano *et al.* 1998].

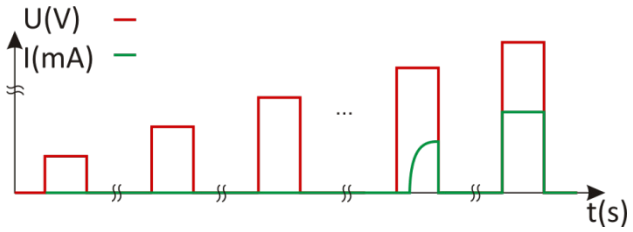

Slika 6. Protokol za določitev porušitvene napetosti ravninskega lipidnega dvosloja.

Pri uporabi takšnega protokola število pulzov, ki jih pritisnemo na ravninski lipidni dvosloj, ni vnaprej znano. Ravno tako ni znano, koliko bo znašal seštevek časov vseh pritisnjenih signalov, ki ga definiramo kot pred-izpostavitev ravninskega lipidnega dvosloja. Čas znotraj pulza, v katerem porušimo ravninski lipidni dvosloj, je abidor s sodelavci definiral kot življenjsko dobo [Abidor *et al.* 1979]. Ugotovil je, da življenjska doba ravninskega lipidnega dvosloja znotraj pravokotnega napetostnega pulza ni enolično določena. Merilni protokol ima tri slabosti, in sicer odvisen je od koraka amplitude, dolžine napetostnega pulza ter pred-izpostavitve ravninskega lipidnega dvosloja. Daljša pred-izpostavitev ravninskega lipidnega dvosloja napetostnemu signalu povzroči nižjo porušitveno napetost [Abidor *et al.* 1979]. Prav tako se zaradi pred-izpostavitve, katero povzročijo zaporedne izpostavitve večjim napetostnim pulzom, ravninski lipidni dvosloj poruši pri nižji napetosti [Troiano *et al.* 1998]. Če je čas med dvema izpostavitvama zadosti dolg, pred-izpostavitev na ravninskem lipidnem dvosloju izzveni in jo obravnavamo, kot da ravninskega lipidnega dvosloja ne bi izpostavili električnemu stresu [Maček Lebar *et al.* 2002].

Dimitrov [Dimitrov 1984] je preučeval povezavo med porušitveno napetostjo in materialnimi lastnostmi ravninskega lipidnega dvosloja. Porušitvena napetost se spreminja glede na strukturo in sestavo ravninskega lipidnega dvosloja. Le-to spreminjamo z dodajanjem različnih kemikalij. Porušitvena napetost ni odvisna od stopnje pH v okoliški raztopini, če je le ta v območju od 5-9. Dimitrov je časovni potek porušitve ravninskega lipidnega dvosloja zaradi električnega polja razdelil na tri stanja:

- zaradi vsiljene napetosti na ravninskem lipidnem dvosloju se poveča nihanje površine membrane;
- reorientacija molekul ustvari deformacije v membrani, kjer se lahko za kratek čas tvorijo vodne pore;
- ekspanzija por privede do mehanske porušitve ravninskega lipidnega dvosloja.

Tokovno vzbujanje se od napetostnega razlikuje v tem, da posredno nadzorujemo pritok nabojev v raztopino. Posledica tega je, da se zaradi visoke upornosti na ravninskem lipidnem dvosloju vzpostavi transmembranska napetost. Pri napetostnem vzbujanju vsilimo napetost, tok ni omejen, njegova amplituda pa je odvisna od upornosti ravninskega lipidnega dvosloja. Ko nastanejo na ravninskem lipidnem dvosloju strukturne spremembe, pore, se pri napetostnem vzbujanju amplituda toka poveča ter dokončno uniči membrano. Pri tokovnem vzbujanju pa ob nastanku por v ravninskem lipidnem dvosloju amplituda transmembranske napetosti pade, s tem pa tudi možnost za porušitev ravninskega lipidnega dvosloja. Na ta način enostavneje opazujemo spremembe prevodnosti na ravninskem lipidnem dvosloju, ki nastajajo zaradi transmembranske napetosti.

Sistemi s tokovnim vzbujanjem so se pojavili že dokaj zgodaj v zgodovini poizkusov na ravninskih lipidnih dvoslojih. Že leta 1972 sta raziskovalca Montal in Mueller opisala sistem, ki ima možnost izbiranja med tokovnim in napetostnim vzbujanjem [Montal in Mueller 1972]. Kmalu zatem leta 1976 je sledil Carius s sodelavci [Carius 1976]. Po več letnem premoru sta Robelo s sodelavci in Kalinowski s sodelavci predstavila dva nova sistema zasnovana s tokovnim vzbujanjem [Robelo in Gliozzi 1989; Kalinowski in Figaszewski 1992]. Opazovala sta spreminjanje napetosti na ravninskem lipidnem dvosloju, ki sta ga povezala z nastajanjem in fluktuacijo por v ravninskem lipidnem dvosloju.

Običajno so ravninski lipidni dvosloj izpostavili konstantnemu toku [Koronkiewicz *et al.* 2004; Kotulska 2007]. Naboj se počasi, v sekundnem območju opazovanja, akumulira na ravninskem lipidnem dvosloju ter gradi napetost. Ko nastane pora ali strukturna sprememba, zaradi povečanja prevodnosti ravninskega lipidnega dvosloja nabrani naboj steče preko pore, amplituda napetosti pa se posledično zmanjša. Zaradi padca napetosti se pora pričenja ožiti, pri tem pa se ponovno prevodnost zmanjša. Naboji se ponovno pričnejo nabirati na ravninskem lipidnem dvosloju, ker vsi ne morejo skozi poro in vrednost napetosti ponovno zraste. Ko preseže nek napetostni prag, se cikel ponovi. Tak ciklični dogodek na ravninskem lipidnem dvosloju so poimenovali fluktuacija pore (slika 7) [Koronkiewicz *et al.* 2004; Kotulska 2007].

Kljub razmeroma široki uporabi elektroporacije v biologiji, biotehnologiji in medicini, nastanek por v celični membrani ob prisotnosti električnega polja še ni docela pojasnjen. Elektroporacijo lahko preučujemo na vseh nivojih biološke kompleksnosti, pa še vedno najdemo različna tolmačenja, ali se tvorijo pore, ali pa gre le za spremembo prepustnosti membrane zaradi drugačnih deformacij v

membrani. Ravno ravninski lipidni dvosloj je sam po sebi enostaven model celične membrane, na katerem pa zelo težko eksperimentalno opazujemo in dokažemo obstoj por ali kakršnih koli drugih deformacij. Teoretični opisi [Neumann *et al.* 1989; Zimmermann 1982; Rols in Teissie 1990; Tsong 1991; Weaver in Chizmadzev 1996] in modeli zgrajeni na osnovi molekularne dinamike [Tarek 2005; Delemotte *et al.* 2008; Tieleman *et al.* 2003; Bockman et al. 2008] sicer podpirajo idejo o nastanku in razvoju por pri izpostavitvi ravninskega lipidnega dvosloja električnemu polju [Tarek 2005; Tieleman *et al.* 2003, Bockman et al. 2008], a še vedno manjkajo neposredne povezave in primerjave z eksperimentalnimi podatki.

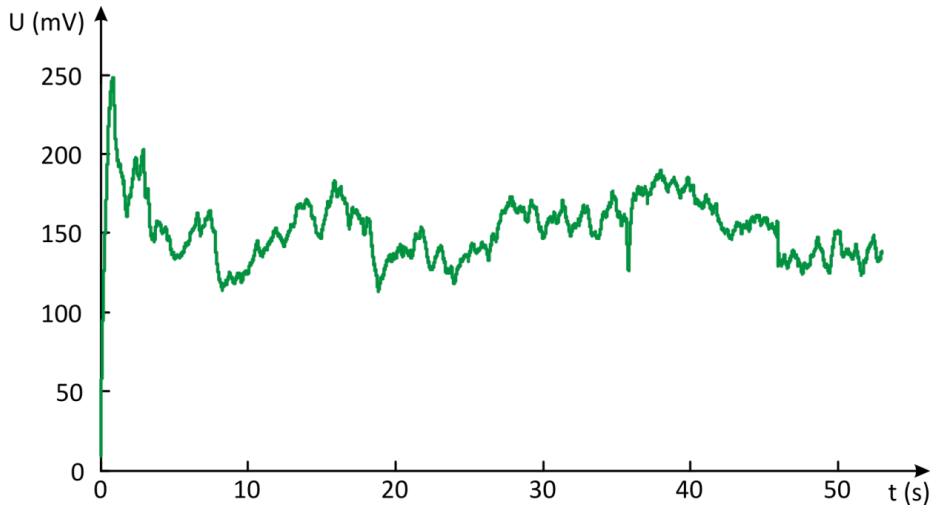

Slika 7. Odziv napetosti na ravninskem lipidnem dvosloju pri konstantnem toku 2nA [Koronkiewicz *et al.* 2004; Kotulska 2007]

V doktorski disertaciji smo se posvetili tudi tem povezavam. Na podlagi rezultatov molekularne dinamike in rezultatov poizkusov na ravninskih lipidnih dvoslojih vzbujanjih z linearno naraščajočim tokovnim signalom smo ocenili prevodnost in gostoto por.

Porušitvena napetost je odvisna od viskoelastičnih lastnosti ravninskega lipidnega dvosloja. Izbrali smo ustrezen model, ki to povezavo predvideva. Viskoelastične lastnosti ravninskega lipidnega dvosloja smo določili iz meritev porušitvene napetosti z linearno naraščajočim napetostnim signalom.

Ker je porušitvena napetost ravninskega lipidnega dvosloja odvisna od časa trajanja posameznega napetostnega pulza ter celotne predhodne izpostavitve, metoda merjenja porušitvene napetosti z napetostnimi pulzi vnaša v merjene rezultate preveliko stohastičnost. Predlagali smo novo metodo določanja porušitvene napetosti ravninskega lipidnega dvosloja z linearno naraščajočim signalom, s katero se izognemo večkratni izpostavitvi in je učinkovitejša od metod, ki so bile uporabljene do sedaj.

2 Materiali in metode

2.1 Priprava ravninskega lipidnega dvosloja

Za postavitev ravninskega lipidnega dvosloja smo uporabili Montal – Muellerjevo metodo [Montal in Mueller 1972]. Oba prekata komore smo napolnili z prevodno raztopino pod nivojem luknjice v teflonski foliji. Na gladino obeh prekatov smo nanesli lipidne molekule. Obe gladini smo sočasno dvigovali in na luknjici v teflonski foliji tvorili ravninski lipidni dvosloj. S spuščanjem in dviganjem gladine prevodne raztopine smo tvorili ravninske lipidne dvosloje brez daljšega čakanja.

Prevodno raztopino smo pripravili iz 0,1 molarne KCl (MERCK, Nemčija) in 0,01 molarne raztopine Hepes (MERCK, Nemčija). Zmešali smo ju v enakem razmerju in jima dodali nekaj kapljic eno molarnega NaOH (MERCK, Nemčija), tako da smo dobili kislost raztopine pH 7,4. Na injekciji smo pritrdili igli premera 0,8 mm. Na igli smo nataknili cevki z zunanjim premerom 2,4 mm in notranjim premerom 0,8 mm. Prek cevk smo vnašali prevodno raztopino v oba prekata komore. Pred priključitvijo smo iz injekcijskih igel in cevk odstranili vse zračne mehurčke.

Za pripravo ravninskih lipidnih dvoslojev smo uporabili POPC (1-pamitoil 2-oleil 3-fosfatidilholin) ter POPS (1-palmitil 2-oleil 3-fosfatidilserin), ki smo ju kupili v prahu (Avanti Polar-Lipids, inc., ZDA). POPC oziroma POPS smo raztopili v mešanici heksana (Riedel-de Haën, Nemčija) in etanola (Riedel-de Haën, Nemčija) v razmerju 9:1. Mešanico heksadekana (MERCK, Nemčija) in etanola v razmerju 3:7 smo uporabili za podporni torus. Kadar smo poizkus pripravljali z mešanico obeh lipidov (POPC in POPS), smo poprej zmešali lipida v želenem razmerju v mikro centrifugirkah s pokrovčkom (Ependorf, Nemčija). S zaprtjem mikro centrifugirke smo omejili izhlapevanje organskega topila iz lipidne mešanice.

Poizkuse smo izvedli s petimi različnimi sestavami ravninskega lipidnega dvosloja, dvema enokomponentnima in tremi dvokomponentnimi. Enokomponentni dvosloji so bili zgrajeni iz ene vrste lipida POPC ali POPS. Dvokomponentni ravninski lipidni dvosloji so bili zgrajeni iz mešanice POPC in POPS v razmerjih 3:1, 1:1 in 1:3. Za vsak ravninski lipidni dvosloj, ki je upoštevan v raziskavi, smo izmerili kapacitivnost in določili porušitveno napetost ter življenjski čas.

Teflonska komora (slika 8-2) je bila sestavljena iz dveh delov. Teflon je omogočal preprosto čiščenje, saj smo komoro med poizkusi hranili v žvepleni kislini (H_2SO_4) (MERCK, Nemčija), ki je odstranila vse ostanke lipidov. Tik pred poizkusom smo vzeli oba prekata komore iz kisline in ju sprali z deionizirano vodo. Med teflonska dela komore smo vstavili teflonsko folijo debeline 25,4 µm (DF100, CHEMFILM), ki je imela majhno luknjico premera $117(1 \pm 0{,}01)$ µm. V vsakem delu komore je vdolbina velikosti

(17,8 × 15,1 × 19,75) mm oziroma 5,3 cm^3. V oba prostora sta bila speljana dodatna kanala premera 0,8 mm, skozi katera smo vbrizgavali prevodno raztopino. Med prekata komore smo namestili tanko folijo, ki je bila pred tem shranjena v kloroformu (Riedel-de Haën, Nemčija). Pri tem smo pazili, da je majhna luknjica čim bolj na sredini zaslonke komore. Če je bila luknjica preveč pri robu odprtine komore, se je zaradi razlike v omočevanju folije in komore ravninski lipidni dvosloj težje tvoril. Oba prekata komore smo stisnili in privili z vijakoma. Prepričali smo se, da je bila luknjica čim bolj na sredini, v nasprotnem primeru smo folijo namestili ponovno. Na vsako stran folije, čim bližje luknjici, smo dodali 1 µl raztopine lipida. Počakali smo, da se je topilo posušilo, nato pa dodali 1,5 µl heksadekana in etanola ter počakali, da se je tudi ta mešanica posušila. Komoro smo pritrdili na palično stojalo in jo postavili pred stereolupo. Skozi stranska kanala smo vstavili cevki s prevodno raztopino KCl. Na komoro smo položili poseben pokrovček, na katerega smo pritrdili elektrode iz Ag-AgCl (IVM, ZDA).

Pri postavitvi elektrod je bilo potrebno paziti, da te niso prekrivale luknjice in da je bila le-ta še vedno vidna skozi stereolupo. Elektrode smo morali vedno vstaviti v komoro pred nanosom lipidnih molekul na površino prevodne raztopine, tako da nismo ”zmotili” lipidne plasti. V prekata komore smo vbrizgali toliko prevodne raztopine, da je gladina segla tik pod rob luknje v komori. V vsak prekat smo kanili po 2 µl lipida oziroma lipidne mešanice. Gladine smo se poizkušali dotakniti le s kapljico, da smo omogočili enostavnejše raztezanje lipidne plasti po gladini prevodne raztopine. Ocenili smo, da so se po dvajsetih minutah lipidi razporedili po gladini.

2.2 Napetostno vzbujanje ravninskega lipidnega dvosloja

2.2.1 Sistem za elektroporacijo ravninskih lipidnih dvoslojev

Sistem za elektroporacijo ravninskih lipidnih dvoslojev je bil sestavljen iz signalnega generatorja, teflonske komore z elektrodama, merilnikov toka in napetosti ter osciloskopa za zajem podatkov [Kramar *et al.* 2009]. Podatke smo shranili v pomnilnik osciloskopa, kasneje pa smo jih analizirali z osebnim računalnikom (slika 8).

Signalni generator (slika 8-1) je omogočal tvorjenje napetostnih signalov poljubnih oblik. Sestavljen je iz krmilnika z mikroprocesorjem MCF5204, modula za tvorjenje signalov ter modula za frekvenčno razširitev. Mikroprocesorski krmilnik smo upravljali z osebnim računalnikom preko RS-232 komunikacije. Prek te komunikacije smo prenesli obliko signala ter ukaze za pred nastavitev izhodnega ojačenja in frekvence. Modul za tvorjenje signalov je spremenil digitalni zapis signala v analogno obliko in ga primerno ojačil. Modul za frekvenčno razširitev nam je omogočil spreminjanje izhodne frekvence signala.

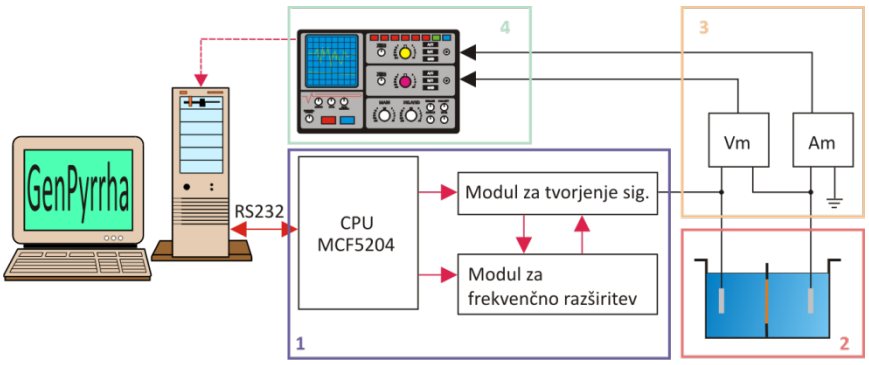

Slika 8. Sistem za elektroporacijo ravninskih lipidnih dvoslojev. (1) Signalni generator sestavljen iz krmilnika z mikroprocesorjem MCF5024 in moduloma za tvorjenje signalov ter frekvenčno razširitev. (2) Teflonska komora za tvorjenje ravninskih lipidnih dvoslojev z dvema Ag-AgCl elektrodama ter prevodno raztopino. (3) Merilnik toka in napetosti. (4) Digitalni osciloskop, za shranjevanje meritev in nadaljnjo obdelavo.

Merilni del sistema (slika 8-3,4) je bil sestavljen iz merilnika toka, diferenčnega merilnika napetosti ter osciloskopa za shranjevanje časovnih potekov obeh količin. Merilnik toka je deloval po principu tokovno napetostnega pretvornika. Napetost na lipidnem dvosloju smo merili z diferenčnim ojačevalnikom LeCroy Instruments 1822. Nastavitve ojačevalnika smo v celoti krmilili z osciloskopom. Njegova dodatna dobra lastnost je bila ta, da smo lahko razliko dveh signalov ojačili tudi za faktor 1000. Časovne poteke toka in napetosti smo shranili z osciloskopom LeCroy Waverunner-2 LT354M. Vzorčna frekvenco smo lahko nastavljali, pasovna širina osciloskopa pa je bila 500 MHz. Na prvem kanalu smo merili signal iz signalnega generatorja. Drugi kanal je bil namenjen opazovanju napetosti diferencialnega ojačevalnika, s četrtim kanalom pa smo merili tok oziroma izhodno napetost tokovnega merilnika. Osciloskop smo nastavili na normalno proženje, na pozitivni prag. Signal smo opazovali z nekaj deset mikrosekundnim pred-proženjem. Merjene signale smo shranili v ANSI tabelo ter jih kasneje analizirali s programskim orodjem Matlab.

2.2.2 Merilni protokol

Merilni protokol je sosledje merjenja kapacitivnosti lipidnega dvosloja ter merjenja porušitvene napetosti lipidnega dvosloja (slika 9). Kapacitivnost in porušitveno napetost smo določili za vsak lipidni dvosloj posebej.

Slika 9. Merilni protokol. Tvorimo ravninski lipidni dvosloj ter izmerimo kapacitivnost C_{BLM}. Podatek o kapacitivnosti odloči, ali je meritev upoštevana v analizi. Na ravninski lipidni dvosloj pritisnemo napetost, ter opazujemo tok. Ob porušitvi ravninskega lipidnega dvosloja tok naraste; odčitamo porušitveno napetost U_{br} in življenjski čas t_{br} ravninskega lipidnega dvosloja.

2.2.3 Porušitvena napetost in življenjska doba ravninskega lipidnega dvosloja ob napetostnem vzbujanju

Porušitveno napetost ravninskega lipidnega dvosloja U_{br} smo določili z linearno naraščajočim signalom. Naklon *k* ter končno napetost linearno naraščajočega signala smo predhodno izbrali. Izbira končne napetosti je morala zagotavljati, da se je ravninski lipidni dvosloj zagotovo porušil. Za določitev porušitvene napetosti ravninskega lipidnega dvosloja smo uporabili sedem različnih naklonov: 4,8 kV/s, 5,5 kV/s, 7,8 kV/s, 11,5 kV/s, 16,7 kV/s, 21,6 kV/s in 48,1 kV/s. Porušitveno napetost U_{br} smo definirali kot napetost ob času t_{br}, ko prične preko ravninskega lipidnega dvosloja teči tok. Čas od začetka dvigovanja vsiljenega napetostnega signala do naraščanja tokovnega signala zaradi procesa porušitve ravninskega lipidnega dvosloja, imenujemo življenjska doba t_{br} (slika 10).

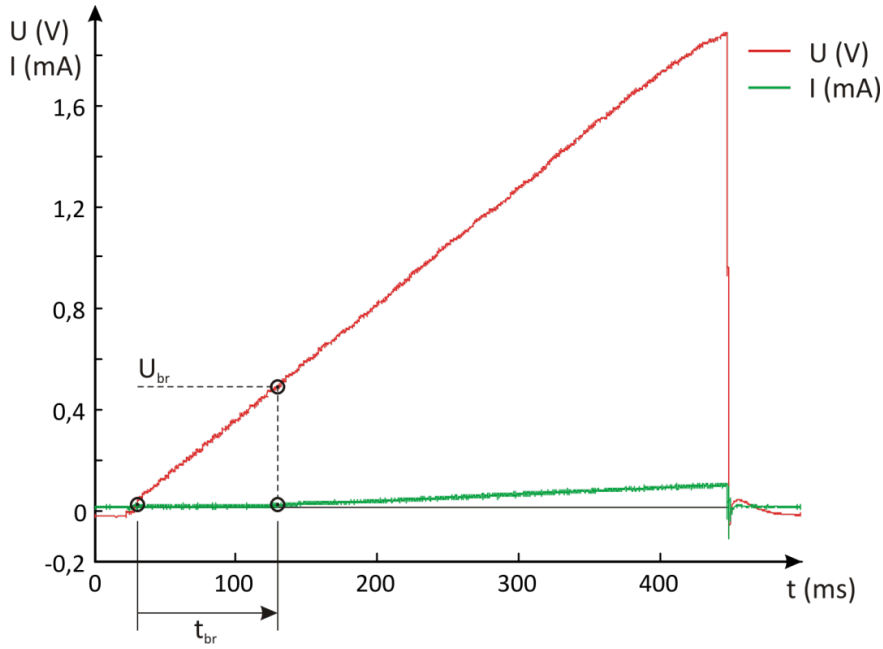

Slika 10. Določitev življenjske dobe in porušitvene napetosti ravninskega lipidnega dvosloja. Rdeč linearno naraščajoči signal predstavlja pritisnjeno napetost. Zelena krivulja kaže potek električnega toka skozi dvosloj. Čas od začetka naraščanja pritisnjene napetosti do pojava toka je definiran kot življenjska doba lipidnega dvosloja t_{br}. Porušitveno napetost U_{br} odčitamo z linearno naraščajočega signala ob času, ko prične teči tok.

Meritev toka in napetosti smo shranili na trdi disk osciloskopa v formatu Matlab. Po končanih poizkusih smo podatke vnesli v okolje Matlab in določili čas začetka naraščanja napetosti in toka. Napisali smo program v Matlab-u, ki je iz izmerjenih signalov toka in napetosti poiskal koleno, točko, ko prične tok naraščati. Algoritem je za iskanje kolena potreboval dve točki. Prvo točko je postavil na začetek merjenega signala, kjer je bila vrednost amplitude toka 0 mA, druga točka pa se je iterativno premikala po signalu. Izračun naklona daljice med začetno točko ter premikajočo se točko je podal, ali je točka že pri kolenu signala. Koleno signala smo določili na podlagi predhodno nastavljene vrednosti naklona. Ker algoritem ni dovolj optimiziran, smo omogočili tudi ročno določanje točke v

kolenu toka. Za vsak izmerjen ravninski lipidni dvosloj smo v tabelo shranili čas kolena napetostnega signala in čas kolena tokovnega signala ter amplitudo napetosti ob tokovnem kolenu. Tabelo smo uporabili pri statistični obdelavi.

2.3 Tokovno vzbujanje ravninskega lipidnega dvosloja

2.3.1 Sistem za opazovanje ravninskih lipidnih dvoslojev s tokovnim vzbujanjem

Pri eksperimentalnem delu smo uporabljali merilni sistem, ki ga je predstavil Kalinowski s sodelavci (slika 11) [Kalinowski in Figazewski 1995(I in II)]. Sistem vsebuje dva modula. Prvi je merilnik kapacitivnosti, ki deluje na osnovi pretvorbe kapacitivnosti v čas [Kalinowski in Figazewski 1995(I)]. Z drugim modulom vzbujamo ravninski lipidni dvosloj s tokom ali napetostjo ter merimo napetost ali tok [Kalinowski in Figazewski 1995(II)]. V naših poizkusih smo z omenjenim sistemom ravninski lipidni dvosloj izpostavili tokovnemu vzbujanju, ter merili napetost. Oba modula lahko krmilimo prek osebnega računalnika [http://pracownicy.uwm.edu.pl/kalinow/ksp/index.html]. Za merjenje smo uporabili štiri elektrode, dve tokovni elektrodi ter dve referenčni elektrodi za merjenje diferenčne napetosti. Uporabili smo enako teflonsko komoro in Ag-AgCl (IVM, ZDA) elektrode kot smo jih uporabljali v poizkusih z napetostnim vzbujanjem.

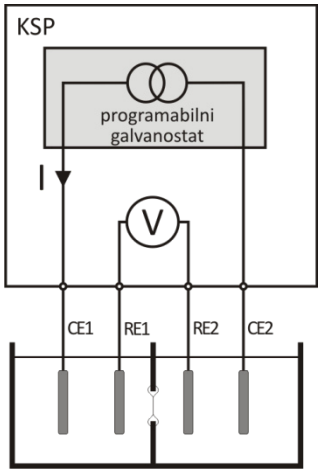

Slika 11. Sistem Kalinowski s sodelavci 1995 [Kalinowski in Figazewski 1995(I in II)]. Tok tvorimo s programirljivim galvanostatom. V komoro tok teče preko tokovnih elektrod CE1 in CE2. Referenčni elektrodi RE1 in RE2 uporabljamo za merjenje diferenčne napetosti na ravninskem lipidnem dvosloju.

2.3.2 Merilni protokol

Merilni protokol je bil sestavljen iz dveh delov: merjenja kapacitivnosti lipidnega dvosloja ter merjenja porušitvene napetosti oziroma porušitvenega toka ravninskega lipidnega dvosloja (slika 12). Kapacitivnost, porušitveno napetost in tok smo določili za vsak lipidni dvosloj posebej. Lipidni dvosloj smo postavili z metodo dviganja gladine (slika 3) [Montal in Mueller 1972].

Slika 12. Merilni protokol. Tvorimo ravninski lipidni dvosloj ter izmerimo kapacitivnost C_{BLM}. Podatek o kapacitivnosti odloči, ali je meritev upoštevana v analizi. Na ravninski lipidni dvosloj pritisnemo tok, ter opazujemo napetost. Ob porušitvi ravninskega lipidnega dvosloja se napetost sesede; odčitamo najvišjo vrednost napetosti in jo definiramo kot porušitvena napetost U_{br}, ob enakem trenutku določimo porušitveni tok I_{br} in življenjski čas t_{br} ravninskega lipidnega dvosloja.

2.3.3 Porušitvena napetost in porušitveni tok ravninskega lipidnega dvosloja ob tokovnem vzbujanju

Ravninski lipidni dvosloj smo vzbujali z linearno naraščajočim tokom ter opazovali napetost, ki se je vzpostavljala na ravninskem lipidnem dvosloju zaradi njegove visoke upornosti (slika 13). Uporabili smo devet različnih naklonov linearno naraščajočih tokovnih signalov: 0,2 µA/s, 0,5 µA/s, 4 µA/s, 8 µA/s, 10 µA/s, in 20 µA/s. Ko je bila na ravninskem lipidnem dvosloju prisotna dovolj velika napetost, se je ravninski lipidni dvosloj porušil. Upornost ravninskega lipidnega dvosloja se je zaradi porušitve zmanjšala, napetost pa se je »sesedla«. Najvišjo točko napetosti smo definirali kot porušitveno napetost ravninskega lipidnega dvosloja U_{br}. Vrednost vzbujalnega linearno naraščajočega toka pa smo definirali kot porušitveni tok I_{br}. Čas od začetka vzbujanja linearno naraščajočega signala do porušitve smo definirali kot življenjsko dobo ravninskega lipidnega dvosloja t_{br}.

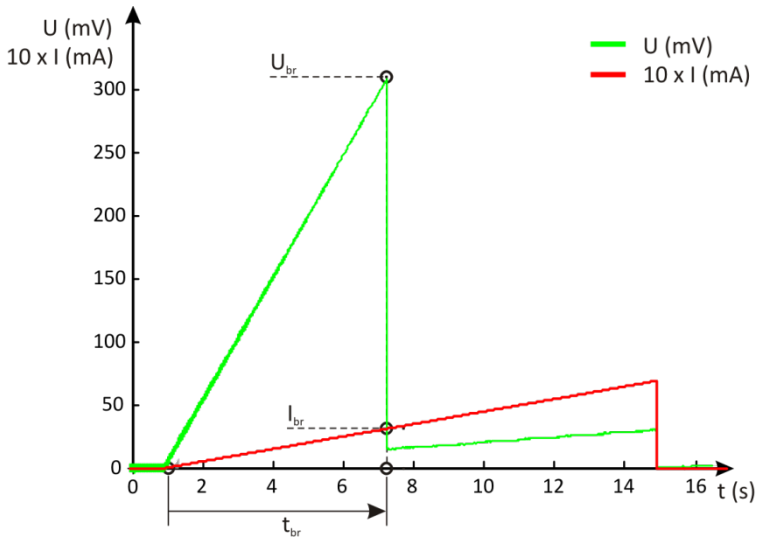

Slika 13. Določanje porušitvene napetosti U_{br}, porušitvenega toka I_{br} in življenjskega časa t_{br} ravninskega lipidnega dvosloja s tokovno naraščajočim signalom.

2.3.4 Opazovanje por v ravninskem lipidnem dvosloju

Ob izpostavitvi ravninskega lipidnega dvosloja linearno naraščajočemu tokovnemu signalu smo med naraščanjem transmembranske napetosti opazili kratkotrajne majhne padce napetosti (slika 14A). Napetost je v trenutku t_{op} padla za vrednost U_p (slika 14B). Predpostavili smo, da padcu napetosti botruje sprememba upornosti oziroma prevodnosti ravninskega lipidnega dvosloja. Na sliki 14C smo upornost membrane predstavili z razmerjem med tokom in napetostjo. Ocenili smo, da so bile v ravninskem lipidnem dvosloju v obdobju, ko se je upornost ravninskega lipidnega dvosloja znižala, prisotne strukturne spremembe ali pore. Čas, ko so bile v ravninskem lipidnem dvosloju prisotne pore smo označili kot t_p. V nekaterih primerih se je vrednost upornosti obnovila na začetno vrednost, v drugih pa se je ravninski lipidni dvosloj porušil. Trenutek obnovitve ravninskega lipidnega dvosloja smo označili s t_{zp}.

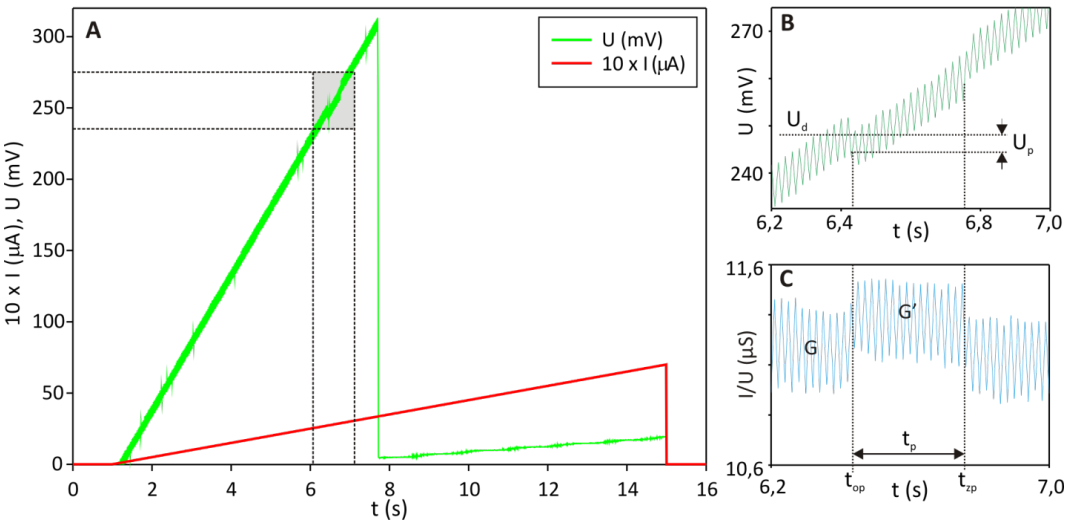

Slika 14. A) Tokovno vzbujanje ravninskega lipidnega dvosloja je predstavljeno z rdečo krivuljo. Napetost na ravninskem lipidnem dvosloju je predstavljena z zeleno krivuljo. Na napetostnem odzivu smo opazili napetostne padce, ki smo jih pripisali strukturnim spremembam oziroma poram v ravninskem lipidnem dvosloju. B) Povečan signal napetosti iz sivega okvirčka. V trenutku t_{op} na ravninskem lipidnem dvosloju pade napetost U_d za vrednost U_p. Pore so odprte čas t_p. Opazimo, da se v trenutku t_{zp} pore najverjetneje zaprejo. C) Z razmerjem toka in napetosti opazujemo krivuljo spremembe prevodnosti, ki jo v delu A opazimo v sivem okvirčku. Prevodnost G ustreza prevodnosti sistema in ravninskega lipidnega dvosloja. V prevodnosti G' je vključena prevodnost por v ravninskem lipidnem dvosloju.

Prevodnost pore smo ocenili v trenutku t_{op}, ko je napetost iz vrednosti U_d padla za vrednost U_p. Trenutek pred padcem lahko izrazimo prevodnost G:

$$G = \frac{I\left(t_{op}^{-}\right)}{U_d}. \tag{1}$$

Takoj, ko pade napetost za vrednost U_p pa imamo novo prevodnost G':

$$G' = \frac{I\left(t_{op}^{+}\right)}{U_d - U_p}. \tag{2}$$

Prevodnost G je skupna prevodnost sistema G_{sis} in ravninskega lipidnega dvosloja G_{BLM}:

$$G = G_{sis} + G_{BLM} = \frac{1}{R_{sis}} + \frac{1}{R_{BLM}}. \tag{3}$$

Ko napetost pade, se v sistemu spremeni prevodnost. Določimo, da se je ta povečala za prevodnost G_p, kar ustreza prevodnosti por(e) v ravninskem lipidnem dvosloju:

$$G' = G_{sis} + G_{BLM} + G_p. \tag{4}$$

Prevodnost por(e) G_p lahko torej ocenimo kar z razliko prevodnosti med G' in G:

$$G_p = G' - G = \frac{I\left(t_{op}^{+}\right)}{U_d - U_p} - \frac{I\left(t_{op}^{-}\right)}{U_d}. \quad (5)$$

Da bi prevodnost zapaženih por ocenili čim bolj natančno, smo uporabili simulacijsko orodje SPICE OPUS [Tuma in Buermen 2009, www.spiceopus.si], kjer smo ravninski lipidni dvosloj ter komoro predstavili z električnim vezjem (slika 15). Upor R_{BLM} je predstavljal upornost ravninskega lipidnega dvosloja, kondenzator C_{BLM} pa kapacitivnost ravninskega lipidnega dvosloja. Upornost in kapacitivnost komore sta predstavljala elementa R_{sis} in C_{sis}. Za vzbujanje smo uporabili tokovni vir I_0 z linearno naraščajočim signalom. Napetostni viri v vezju: V_{CBLM}, V_{RBLM}, V_{Csis}, V_{Rsis} in V_G so bili uporabljeni za merjenje toka prek posameznega elementa. Električnemu vezju smo dodali upor R_p, ki je v vezje priključen prek stikala, katerega smo vključili ob času t_{op} za čas t_p, in tako simulirali pore v ravninskem lipidnem dvosloju (slika 14). Krmiljenje stikala smo izvedli s napetostnim virom V_p, s katerim smo za čas t_p tvorili napetostni pulz, ki je vključil stikalo.

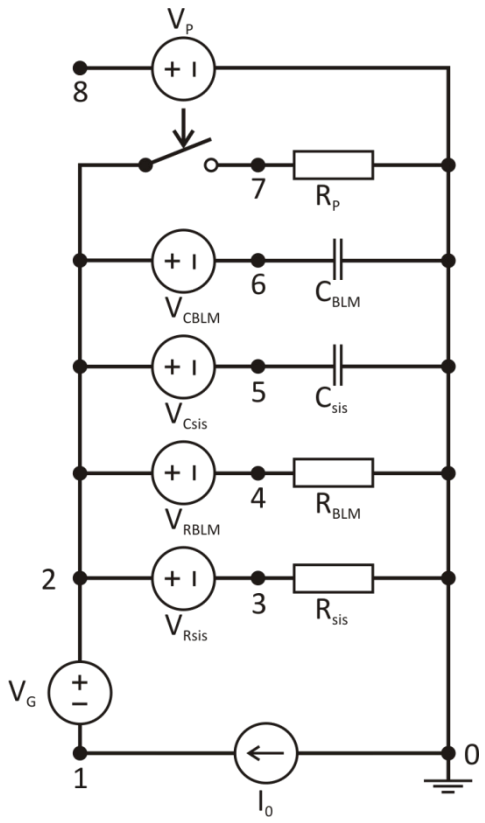

Slika 15. SPICE model ravninskega lipidnega dvosloja. Elementa R_{BLM} in C_{BLM} predstavljata upornost in kapacitivnost ravninskega lipidnega dvosloja. Elementa R_{sis} in C_{sis}, predstavljata komoro. S tokovnim generatorjem I_0 tvorimo linearno naraščajoč tokovni signal. Upornost R_p predstavlja pore v ravninskem lipidnem dvosloju, ki jih priključimo v vezje s stikalom. Stikalo je krmiljeno z napetostnim generatorjem V_p, kjer za čas pore t_p tvorimo napetostni pulz. Napetostne generatorje V_G, V_{Rsis}, V_{Csis}, V_{Csis} in V_{CBLM} nastavimo na napetost 0 V in prek njih merimo tok v posamezno vejo vezja.

Vrednosti elementov v SPICE modelu smo določili z merjenjem ali pa smo jih povzeli iz literature. Kapacitivnost ravninskega lipidnega dvosloja C_{BLM} smo izmerili, upornost ravninskega lipidnega dvosloja R_{BLM} = 10^8 Ω smo povzeli iz literature [Tien in Ottova 2003]. Elementa R_{sis} in C_{sis}, ki predstavljata komoro, smo določili z RLC merilnikom Agilent 4284 A. Med meritvijo ni bilo ravninskega lipidnega dvosloja, gladina vodne raztopine pa je bila pod luknjico. Pri frekvenci 20 Hz smo izmerili R_{sis} = 73 kΩ ter C_{sis} = 400 nF. Eksperimentalno in v modelu smo s tokovnim vzbujanjem pri izbranem naklonu dosegli enak napetostni odziv. Ob napetostnem padcu smo vrednost upora R_p iterativno spreminjali. Ko sta se odziva napetosti eksperimenta in SPICE simulacije ujemala, smo določili upornost oziroma prevodnost por.

2.4 Merjenje kapacitivnosti ravninskega lipidnega dvosloja

Uporabili smo dve različni metodi merjenja kapacitivnosti: merjenje časovne konstante razelektritve ravninskega lipidnega dvosloja in merjenje s pretvorbo kapacitivnosti v periodo. Primerljiv podatek z eksperimenti drugih avtorjev dobimo, ko izračunano kapacitivnost C_{BLM} normiramo na površino A_{BLM} lipidnega dvosloja:

$$c_{BLM} = \frac{C_{BLM}}{A_{BLM}}. \tag{6}$$

Premer luknjice v teflonski foliji je pri naših poizkusih znašal d_{BLM} = 117 µm, zato je površina lipidnega dvosloja A_{BLM} znaša 1,08×10^{-8} m^2.

2.4.1 Merjenje kapacitivnosti s časovno konstanto razelektritve

Ob pregledu literature zasledimo, da je najbolj pogosto uporabljena metoda za merjenje kapacitivnosti ravninskega lipidnega dvosloja prav meritev časovne konstante razelektritve [Troiano *et al.* 1998; Sharma *et al.* 1996; Meier *et al.* 2000; Diederich *et al.* 1998; Benz *et al.* 1976; Wilhelm *et al.* 1993; Benz *et al.* 1979; Kramar *et al.* 2007]. Ravninskemu lipidnemu dvosloju smo vsilili napetostni pulz pravokotne oblike. Naboj *Q*, ki se je pri tem nakopičil v sistemu, je bil $Q(t) = C \cdot u(t)$. Ob koncu pulza smo elektrodo na izhodu generatorja preklopili na upor znane vrednosti. Razelektritev ravninskega lipidnega dvosloja smo opazovali z osciloskopom (slika 16).

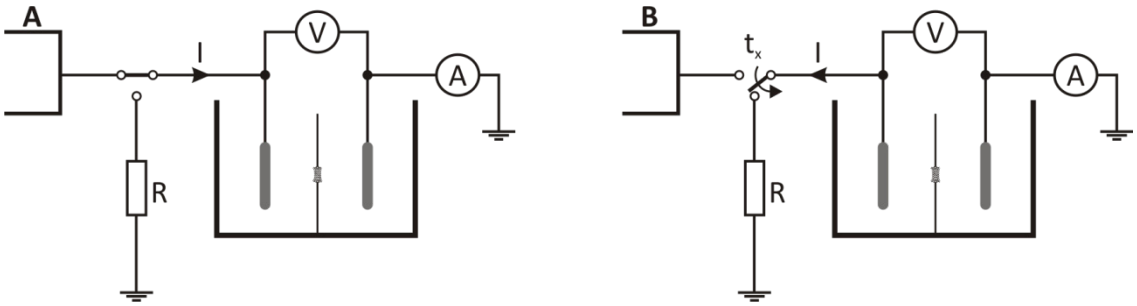

Slika 16. A) Ravninski lipidni dvosloj je izpostavljen napetostnemu pulzu. B) Razelektritev ravninskega lipidnega dvosloja preko znanega upora *R*.

Potek napetosti *u(t)* pri razelektritvi ravninskega lipidnega dvosloja opišemo z enačbo:

$$u(t) = -U_0 e^{-\frac{t}{\tau}}. \tag{7}$$

U_0 je amplituda vsiljene napetosti, τ pa je časovna konstanta sistema, ki je odvisna od kapacitivnosti sistema *C* in upornosti R_{nad}:

$$\tau = R_{nad} \cdot C. \tag{8}$$

Časovno konstanto τ smo določili iz izmerjenega signala v področju razelektritve z uporabo funkcije *nlinfit* v programskem okolju Matlab. Upornost R_{nad} je določena z znanim uporom *R* ter vhodno upornostjo osciloskopa R_{OSC}.

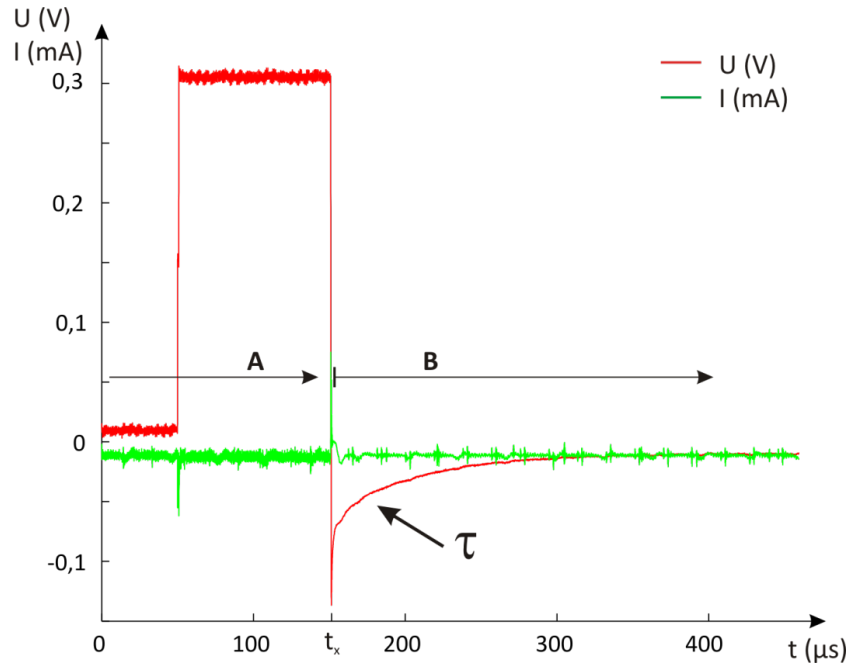

Slika 17. Napetost na ravninskem lipidnem dvosloju pri merjenju kapacitivnosti z metodo razelektritve. Področje A ustreza vezju na sliki 16A, ko na ravninski lipidni dvosloj pritisnemo pravokotni napetostni signal. Ob času t_x preklopimo elektrode na znan upor *R*. Iz eksponentnega odziva s prileganjem eksponentne funkcije določimo časovno konstanto τ.

V trenutku t_x se je naboj, nabran na ravninskem lipidnem dvosloju, razelektril preko upora R in osciloskopa (R_{osc}) (slika 17). Razelektritveni upor R = 1 MΩ in upornost sonde osciloskopa R_{osc} = 1 MΩ sta vezana vzporedno, kar da nadomestno upornost R_{nad} = 500 kΩ (slika 18A). Izračun kapacitivnosti lipidnega dvosloja poenostavi velika upornost ravninskega lipidnega dvosloja (R_{BLM} ~ 10^8 Ω), tako da skupna nadomestna upornost sistema R_{nad} ostane približno 500 Ω, kar je posledica vzporedne vezave R_{nad} in R_{BLM}, kot je prikazano z nadomestnim vezjem na sliki 18B.

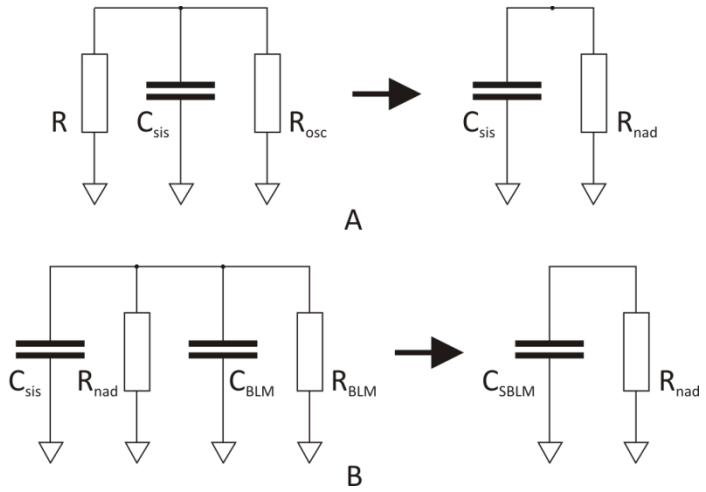

Slika 18. Nadomestni vezji za merjenje kapacitivnosti z metodo razelektritve v dveh korakih. A.) Nadomestno vezje sistema brez ravninskega dvosloja. B.) Nadomestno vezje sistema in ravninskega dvosloja. Pri obeh vezjih upornost ravninskega lipidnega dvosloja lahko zanemarimo, ker je mnogo večja od upornosti sonde osciloskopa in upora preko katerega razelektrimo sistem.

Kapacitivnost lipidnega dvosloja določimo z meritvijo, ki je sestavljena iz dveh delov [Benz *et al.* 1976]. Najprej izmerimo kapacitivnost sistema C_{sis} brez lipidnega dvosloja nato pa kapacitivnost sistema z lipidnim dvoslojem C_{SBLM}. Kapacitivnost ravninskega lipidnega dvosloja C_{BLM} je razlika obeh izmerjenih kapacitivnosti:

$$C_{BLM} = C_{sis} - C_{SBLM}. \tag{9}$$

Da se je lipidna membrana zares tvorila, vidimo iz spremembe poteka razelektritve in nespremenjene amplitude toka. Ob nastopu pulza električni tok ne steče, ker je lipidna membrana skoraj neprepustna za ione. Izračunani kapacitivnosti C_{sis} in C_{SBLM} smo med seboj odšteli (enačba (9)) in dobili oceno kapacitivnosti lipidnega dvosloja C_{BLM}.

2.4.2 Merjenje kapacitivnosti s pretvorbo kapacitivnosti v periodo

Shema merilnega sistema, ki smo ga uporabljali za tovrstno merjenje kapacitivnosti, je predstavljena na sliki 19 [Kalinovski in Figazewski 1992]. Enakomerno naelektrimo lipidni dvosloj do neke napetostne vrednosti. Ko jo presežemo, ravninski lipidni dvosloj praznimo. Periodično polnjenje in

praznjenje ravninskega lipidnega dvosloja da na izhodu vezja pravokoten signal s periodo, ki je odvisna od kapacitivnosti lipidnega dvosloja C_{BLM}.

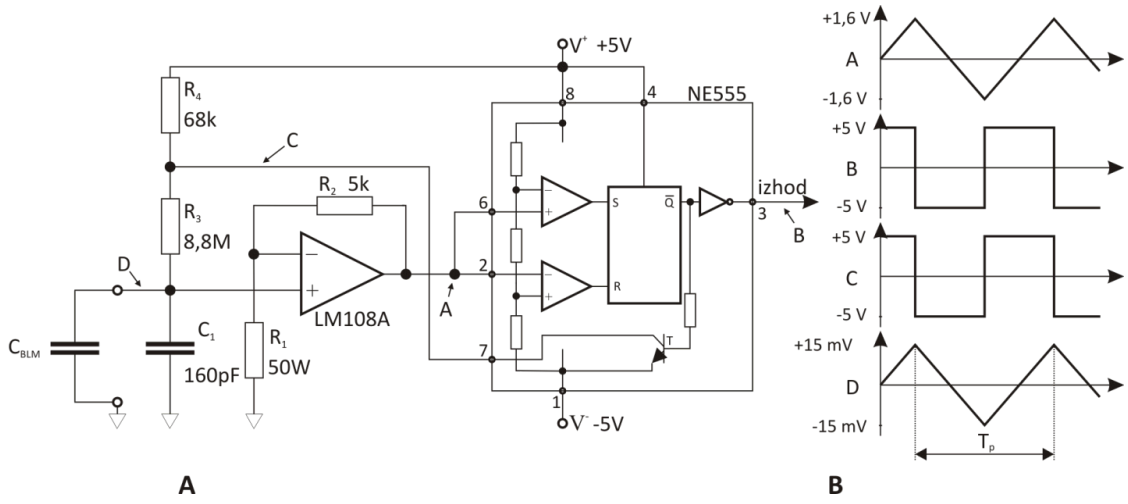

Slika 19. A) Vezje za pretvorbo kapacitivnosti v periodo. B) Potek signalov na posameznih točkah označenih v vezju [Kalinovski in Figazewski 1992].

Kondenzator C_{BLM} na sliki 19 predstavlja kapacitivnost lipidnega dvosloja. Na kondenzatorju merimo napetost v točki *D* in jo ojačimo z operacijskim ojačevalnikom. Ta ima ojačenje *k* določeno z uporoma R_1 in R_2:

$$k = \frac{R_1 + R_2}{R_1}. \tag{10}$$

Izhod ojačevalnika je pripeljan v integrirano vezje NE555, v katerem sta dva napetostna primerjalnika. Vhod prvega je merjena napetost v točki *A*, drugega pa razdeljena napetost, ki gre prek delilnika treh uporov. Glede na nivo napetosti se preklopi izhod RS spominske celice. Izhod iz spominske celice invertiramo. Rezultat je pravokoten signal, kateremu zlahka izmerimo periodo T_p. Napetost na lipidnem dvosloju lahko izrazimo z enačbo:

$$U_{BLM} = \frac{2}{3} V \frac{1}{k} = \frac{2 \cdot V \cdot R_1}{3\left(R_1 + R_2\right)}. \tag{11}$$

Merjenje razdelimo v dve fazi. Prva faza je polnjenje kondenzatorja, kjer teče tok iz napajalnika prek uporov R_4 in R_3 v kondenzator. Tranzistor *T* je zaprt. V drugi fazi se zaradi preklopa RS celice tranzistor *T* odpre in kondenzator C_{BLM} se razelektri. Tok teče prek upora R_3 in tranzistorja *T* v negativni pol napajanja. Zaradi ohranjanja energije velja, da je produkt napajalne napetosti *V* in časa v eni periodi T_p enak:

$$T_p \cdot V = U_{BLM}\left(R_3 + R_4\right)C_{BLM} + U_{BLM} R_3 C_{BLM}. \tag{12}$$

V vezju izberemo simetrično napajanje $V = V^+ = |V^-|$ ter vrednost upora $R_3 \gg R_4$. Iz enačbe (12) izrazimo periodo, pri čemer zanemarimo upornost R_4 (zaradi $R_3 \gg R_4$). Kapacitivnost ravninskega lipidnega dvosloja je torej:

$$C_{BLM} = \frac{V \cdot T_p}{2 \cdot U_{BLM} \cdot R_3} \ . \tag{13}$$

S to merilno metodo smo opazovali spremembo kapacitivnosti v odvisnosti od časa (slika 20). Kapacitivnost smo pričeli meriti, ko je bila gladina prevodne raztopine pod luknjico. Nato smo gladino prevodne raztopine dvignili prek luknjice in postavili ravninski lipidni dvosloj. Sprememba kapacitivnosti ob dvigu gladine prevodne raztopine je bila hipna. Kapacitivnost ravninskega lipidnega dvosloja smo določili z razliko izmerjene vrednosti kapacitivnosti pri spuščeni oziroma dvignjeni gladini. Kapacitivnost izmerjena pri spuščeni gladini prevodne raztopine predstavlja kapacitivnost sistema, kapacitivnost izmerjena pri dvignjeni gladini pa kapacitivnost sistema z ravninskim lipidnim dvoslojem.

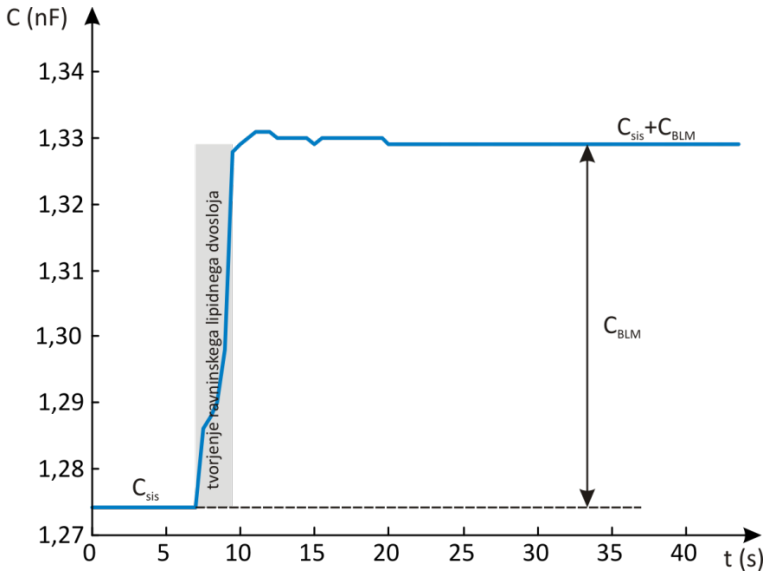

Slika 20. Merjenje kapacitivnosti ravninskega lipidnega dvosloja s pretvorbo v čas. Sivo polje predstavlja čas tvorjenja ravninskega lipidnega dvosloja z Montal-Muellerjevo metodo. Pred tem odčitamo vrednost kapacitivnosti sistema C_{sis}. Ko se ravninski lipidni dvosloj stabilizira, odčitamo vrednost, ki predstavlja seštevek kapacitivnosti sistema C_{sis} in ravninskega lipidnega dvosloja C_{BLM}.

2.5 Statistika

Porušitveno napetost U_{br}, porušitveni tok I_{br}, življenjski čas t_{br} in specifično kapacitivnost c_{BLM} ravninskih lipidnih dvoslojev različnih sestav smo izmerili večkrat. Posamezne skupine meritev smo predstavili s povprečno vrednostjo in standardno deviacijo. Vrednosti, ki so izpolnjevale zahteve po

normalni porazdelitvi vzorcev znotraj skupine in enaki varianci med skupinami, smo statistično primerjali z enosmernim ANOVA testom. Ob ugotovitvi značilne različnosti srednjih vrednosti ($p < 0,05$) med skupinami smo s Tukey-evim testom analizirali statistično značilno različnost med vsemi možnimi pari skupin.

V primeru, ko skupine niso izpolnjevale pogojev za enosmerni ANOVA test, smo uporabili neparametrični Kruskal-Wallis-ov enosmerni test. Pare skupin smo med sabo statistično primerjali z Dunn-ovo metodo.

2.5.1 Določitev porušitvene napetosti ravninskega lipidnega dvosloja

Porušitvena napetost ravninskega lipidnega dvosloja je odvisna od naklona linearno naraščajočega napetostnega signala; bolj ko je strm je napetostni signal, višja napetost je potrebna za porušitev. Da bi opisali omenjeno odvisnost smo na izmerjene vrednosti porušitvene napetosti pri posameznih naklonih linearno naraščajočega napetostnega signala napeli Lapicque-Blair-Hillovo dvoparametersko intenzivnostno časovno krivuljo, ki je najbolj znana relacija za opis pragovnega pojava [Idris in Biktashev 2009]:

$$U = \frac{a}{1 - e^{-t/b}}, \tag{14}$$

pri čemer je U enak porušitveni napetosti U_{br}, ki je bila merjena pri različnih naklonih; t ustreza življenjski dobi ravninskega lipidnega dvosloja t_{br}; konstanti a in b pa sta prosta parametra. Parameter a podaja asimptoto krivulje, ki ustreza minimalni porušitveni napetosti U_{brMIN} za specifičen ravninski lipidni dvosloj. Parameter b določa ukrivljenost krivulje. Zgornjo in spodnjo mejo 95% intervala zaupanja koeficientov a in b, ki smo jih dobili z Matlab-ovo funkcijo *nlinfit*, smo ocenili z Matlab-ovo funkcijo *nlparci* [http://www.mathworks.com/access/helpdesk/help/toolbox/stats/nlparci.html].

Za prileganje viskoelastičnega modela izmerjenim točkam smo uporabili posplošeno nelinearno neanalitično χ^2 funkcijo v programskem okolju Matlab [Bevington in Robinson 1992; Brahms 2008; Press *et al.* 1986]. Za vse regresijske krivulje smo izračunali spodnjo in zgornjo mejo 68% intervala zaupanja. Na slikah smo intervala zaupanja označili s pika-črto krivuljo.

2.6 Simulacije molekularne dinamike

Z besedno zvezo molekularna dinamika poimenujemo posebno obliko računalniške simulacije, ki omogoča spremljanje interakcij med atomi in molekulami v določenem časovnem intervalu na osnovi fizikalnih zakonov. Je specializirana veja molekularnega modeliranja in računalniške simulacije na osnovi statistične mehanike. Rezultat molekularne dinamike je zapis energije ter položaja atomov ali molekul v modelu za posamezen časovni korak. Omogoča nam vpogled v premikanje posameznih

atomov, na način, ki ni mogoč pri laboratorijskih poizkusih. V zadnjih desetletjih je molekularna dinamika močno napredovala z razvojem računalniške strojne opreme. Na področju ravninskih lipidnih dvoslojev so prvi modeli vsebovali preproste strukture obdane z vodnimi molekulami, trajanje opazovanja simulacije pa je bila največ do 8 ps [Kjellander in Marchja 1985]. Z dandanašnjimi modeli lahko zaradi boljše strojne opreme računamo zapletene probleme z veliko atomi oziroma molekulami. Tako nastajajo naprimer tudi modeli ravninskih lipidnih dvoslojev, proteinov vgrajenih v ravninski lipidni dvosloj in veziklov; trajanje opazovanja pa se je podaljšalo tudi nad 10 ns [Marrink *et al.* 2009].

V molekularni dinamiki obravnavamo osnovne gradnike modela na tri načine. V načinu »vsi atomi« (ang. *all atoms*) je v modelu zastopan vsak posamezni atom. V načinu »skupki atomov« (ang. *united atoms*) so določeni atomi združeni v skupine, za katere ni nujno, da so molekule. Na ta način optimiziramo računski čas, ker se skupki atomov navzven obnašajo kot en element. Tretji način je »grobozrnato« računanje; tako da zajamemo v modelu več molekul in jih obravnavamo kot en element (ang *coarse grain*). S to metodo molekule, ki se podobno vedejo, opišemo s samo enim elementom. Ta postopek sicer zmanjša resolucijo, vendar pa je računsko precej manj potraten, kar omogoča daljše časovno opazovanje modelov.

Vse interakcije med gradniki modela, tako intermolekularne kot intramolekularne, so predstavljene z rešitvami harmoničnih funkcij potencialnih energij, ki jih lahko zapišemo na več različnih načinov.

Intramolekularne interakcije povezujejo atome v molekulo, zato so sile med posameznimi atomi velike. Energijski potencial intramolekularnih interakcij zapišemo za vezi med atomi, koti med vezmi atomov ter za dihedralne (torzijske) kote. Le-ti so pomembni zlasti v večjih verižno povezanih atomih, kot je to v lipidni molekuli (slika 21).

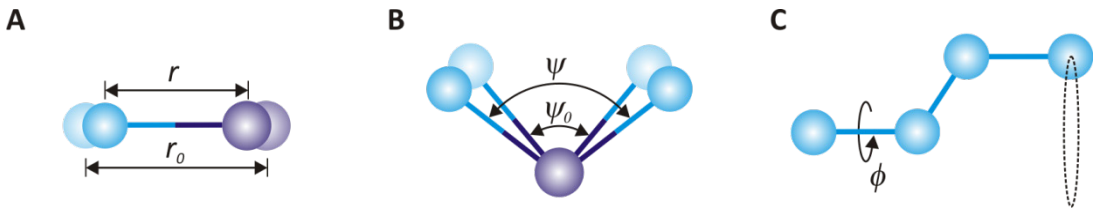

Slika 21. Intramolekularne interakcije med atomi. A) Vez med atomoma, kjer je r_0 razdalja med atomoma v ravnovesnem stanju, r pa trenutna razdalja. B) Kot med vezema dveh sosednjih vezanih atomov, kjer je Ψ_0 kot med vezema v ravnovesnem stanju, Ψ pa trenutni kot. C) Dihedralni kot Φ opisuje premik atomov vezanih v verigi. Na skici je prikazan zasuk ϕ okoli vezi prvega in drugega atoma z leve. Črtkana črta ob zadnjem atomu z leve ponazarja njegovo gibanje.

Energijski potencial vezi v sistemu *E(r)* (slika 21A) opišemo z vsoto razlik med trenutno razdaljo med atomoma *r* in dolžino med atomoma v ravnovesnem stanju r_0, za vse vezane pare atomov:

$$E(r) = \sum_{vezi} k_r (r - r_0)^2, \tag{15}$$

kjer je k_r predstavlja polje sil med dvema atomoma, r trenutno razdaljo med atomoma in r_0 razdaljo med atomoma v ravnovesnem stanju. Za energijski potencial na enem atomu, seštejemo prispevek vseh vezanih atomov.

Energijski potencial kotov med dvema vezema v sistemu $E(\psi)$ (slika 21B) opišemo z vsoto funkcij razlik trenutnega kota ψ in kota v ravnovesnem stanju ψ_0:

$$E(\psi) = \sum_{kotov} k_\psi (\psi - \psi_0)^2, \tag{16}$$

kjer je k_ψ predstavlja amplitudo polje sil med dvema vezema. Za prispevek energijskega potenciala kotov vezi seštejemo prispevek po posameznih kotih.

Energijski potencial vseh dihedralnih kotov v sistemu $E(\phi)$ (slika 21C) opišemo z enačbo:

$$E(\phi) = \sum_{dihed.kotov} k_\phi \left[\cos(n\phi - \phi_0) + 1 \right], \tag{17}$$

kjer je n število vezi v verigi, k_ϕ pa predstavlja polje sil v verigi. Kot ϕ_0 je dihedralni kot v ravnovesnem stanju, ϕ pa trenutni dihedralni kot. Za prispevek energijskega potenciala dihedralnih kotov v verigi seštejemo prispevek po posameznih dihedralnih verigah, ki so pripete na atom.

Vrednosti konstant so bile določene s simulacijo posameznih parov atomov, oziroma z merjenjem strukturnih lastnosti z rentgensko svetlobo [Armen *et al.* 1998] in infra rdečo spektroskopijo [Mendelsohn in Snyder 1996]. Vrednosti teh konstant običajno podajajo razvijalci programske opreme za molekularno dinamiko. Obstaja kar nekaj profilov, kot so na primer AMBER [Pearlman *et al.* 1991], CHARMM [Brooks *et al.* 1983] in GROMOS [Gunsteren in Brendesen 1987], ki se medseboj razlikujejo predvsem po področjih uporabe.

Intermolekularne interakcije povezujejo med seboj molekule in so šibke v primerjavi z intramolekularnimi interakcijami. Za električno nabite atome v sistemu zapišemo Coulombov elektrostatični potencial E_{columb}:

$$E_{columb} = \sum_i \sum_{j<i} \frac{q_i \cdot q_j}{r_{ij}}, \tag{18}$$

kjer sta q_i in q_j naboja atoma v sistemu, r_{ij} pa razdalja med njima Za izračun elektrostatičnega potenciala atoma seštejemo prispevke vseh nabitih atomov v okolici.

Interakcije med ostalimi atomi, ki niso električno nabiti, opisujemo z Van der Waalsovo silo. Silo lahko opišemo z interakcijskim parskim potencialom, ki vsebuje privlačno in odbojno komponento. Obe se spreminjata z razdaljo med atomoma oziroma molekulama. Van der Waalsovo interakcijo modeliramo z uporabo Lennard-Jonesovega potenciala E_{vdw}:

$$E_{vdw} = \sum_{i} \sum_{i<j} w_{ij} \left[\left(\frac{\zeta_{ij}}{r_{ij}} \right)^{12} - \left(\frac{\zeta_{ij}}{r_{ij}} \right)^{6} \right], \tag{19}$$

kjer w_{ij} predstavlja privlačno silo med posameznima atomoma, ζ_{ij} je določen z velikostjo atomov, r_{ij} pa je razdalja med atomi.

Pri modeliranju lahko računamo le z omejenim prostorom, osnovno celico, kjer rob predstavlja konec, ki ga v resnici ni. Zaradi tega se na robu pojavijo nehomogenosti. V izogib temu na robu uporabimo periodične robne pogoje (slika 22). To pomeni, da se interakcije med gradniki na desnem robu preslikajo v levega, iz zgornjega v spodnjega in obratno. Če pogledamo na okoliški prostor iz gradnika v modelu, obravnavamo sistem z neskončno prostornino.

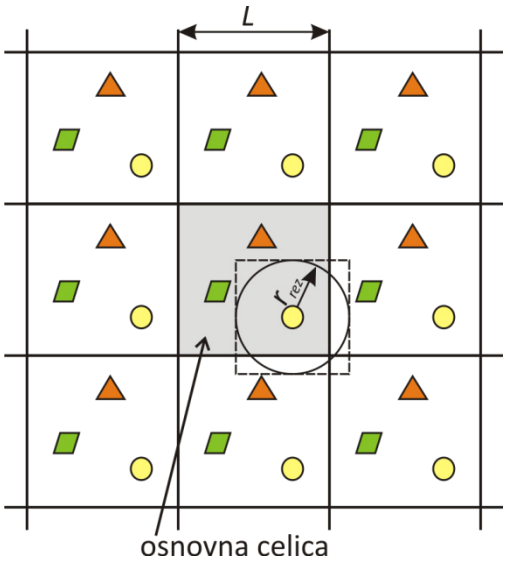

Slika 22. Periodični robni pogoji. V sredini je osnovna celica (*L*x*L*). Zaradi periodičnih robnih pogojev, so enaki gradniki v vseh sosednjih gradnikih. Gradnik na skrajni levi »čuti« gradnike iz skrajne desne. Obravnavanemu gradniku pripišemo vsoto vseh prispevkov intermolekularnih interakcij. Zaradi neskončnega prostora, omejimo prostor, do koder bomo še računali Van der Waalsovo in Coulombovo potencialno energijo.

V periodičnih sistemih računamo prispevek potencialnih energij interakcij med gradniki z Ewaldovo vsoto. Pri tem postopku seštevamo prispevke energij v Fourierevem prostoru. Njegova prednost je izredno hitra konvergenca v primerjavi z realnim prostorom. Vpliv okoliških gradnikov v sistemu na *i*-ti gradnik izračunamo z vsoto energijskih potencialov.

Vrednost prispevkov energijskih potencialov se z oddaljenostjo zmanjšuje. Zaradi »neskončne« prostornine pri računanju vrednosti vsote energijskih potencialov določimo razdaljo, na kateri imajo še vpliv r_{rez}, ki je manjša od velikosti osnovne celice *L*. Pri gradnikih, ki so od obravnavanega gradnika oddaljeni za več kot r_{rez}, vrednost vsote energijskih potencialov postavimo na vrednost nič (slika 23).

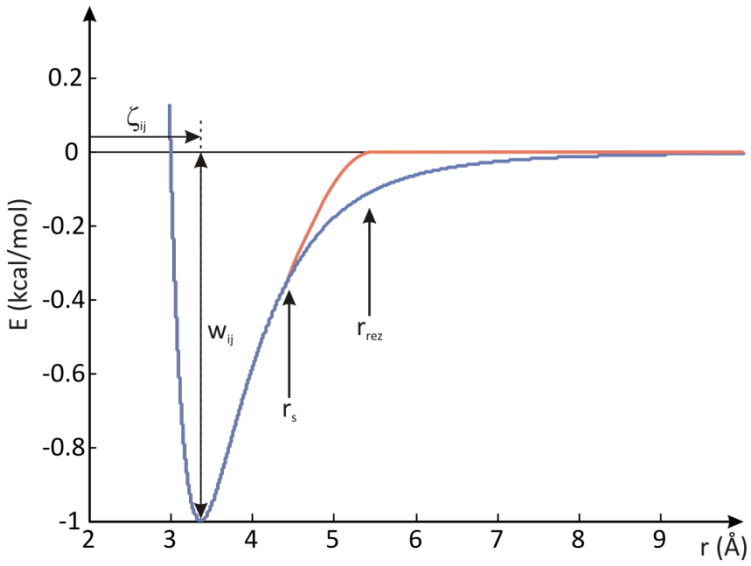

Slika 23. Potek funkcije Lennard-Jonesovega potenciala za zapis Van der Waalsove interakcije med atomi, ki niso vezani z vezjo, kjer w_{ij} predstavlja privlačno silo med posameznima atomoma, ζ_{ij} je določen z velikostjo atomov. Zaradi periodičnih robnih pogojev, moramo določiti razdaljo, kjer bodo imeli gradniki še vpliv na opazovanje r_{rez}. Da preprečimo težave pri odvajanju funkcije se nezveznosti pri rezu znebimo z dodatno preklopno funkcijo ob razdalji r_s ($r_s < r_{rez}$), ki upogne krivuljo pred rezom in jo naredi zvezno.

Osnovni postopek modeliranja z molekularno dinamiko je iterativno premikanje atomov glede na medatomske interakcije (slika 24). Obravnavamo sistem z *N* elementi. Energijski potencial posameznih atomov ali gradnikov izračunamo z vsoto posameznih potencialnih energij, ki delujejo na atome oziroma gradnike *E(r)* (15), *E(ψ)* (16), *E(ϕ)* (17), E_{columb} (18) in E_{vdw} (19):

$$E\left(\vec{r}_1, \vec{r}_2, ..., \vec{r}_N\right) \equiv E\left(\vec{r}^{\,N}\right), \tag{20}$$

kjer je $\vec{r}_i$ koordinata (x,y,z) i-tega atoma oziroma gradnika v modelu.

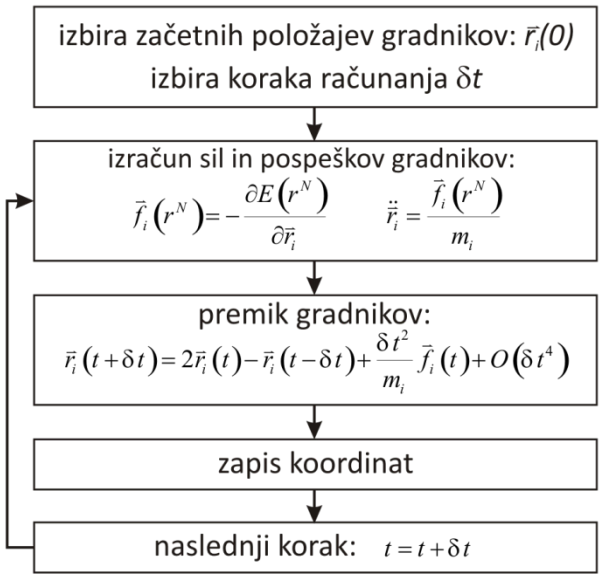

Slika 24. Osnovni postopek računanja v molekularni dinamiki. Iz začetnih položajev gradnikov ter energij med njimi izračunamo silo. Iz izračunane sile in atomske mase lahko izračunamo pospešek gradnika. V naslednjem koraku premaknemo delec ter povečamo čas za izbran interval. Zapišemo nove koordinate premaknjenih gradnikov ter ponovimo računanje.

Za opis gibanja i-tega gradnika rešimo diferencialno enačbo drugega Newtonovega zakona:

$$\vec{f}_i\left(\vec{r}^N\right) = m_i \ddot{\vec{r}}_i \tag{21}$$

kjer je m_i masa *i*-tega gradnika modela $\ddot{\vec{r}}_i$ pa pospešek istega gradnika. Enačbe (21) ne moremo reševati analitično, numerično pa jo lahko enostavno rešimo z Verletovim integracijskim algoritmom [Verlet 1967]:

$$\vec{r}_i(t+\delta t) = 2\vec{r}_i(t) - \vec{r}_i(t-\delta t) + \frac{\delta t^2}{m_i}\vec{f}_i(t) + O\left(\delta t^4\right). \tag{22}$$

Na ta način izračunamo trenutni položaj posameznega gradnika v naslednjem trenutku $t+\delta t$, glede na njegova položaja v predhodnih trenutkih t in $t-\delta t$. Verletov algoritem je izpeljan iz razvoja vektorja položaja gradnika v Taylorjevo vrsto okoli $\vec{r}_i(t)$:

$$\vec{r}_i(t+\delta t) = \vec{r}_i(t) + \delta t\vec{v}_i(t) + \frac{\delta t^2}{2m_i}\vec{f}_i(t) + \frac{\delta t^3}{6}b_i(t) + O\left(\delta t^4\right) \tag{23}$$

$$\vec{r}_i(t-\delta t) = \vec{r}_i(t) - \delta t\vec{v}_i(t) + \frac{\delta t^2}{2m_i}\vec{f}_i(t) - \frac{\delta t^3}{6}b_i(t) + O\left(\delta t^4\right). \tag{24}$$

Z seštevkom enačb (23) in (24) dobimo enačbo (22), ki opisuje premik gradnika. Za spremljanje premikanja gradnikov ne potrebujemo podatka o njihovi hitrosti. Izračune hitrosti potrebujemo pri računanju tlakov in kinetičnih energij v sistemu. V tem primeru lahko enačbi (23) in (24) odštejemo in dobimo enačbo za hitrost:

$$\vec{v}_i(t) = \frac{1}{2\delta t}\left[\vec{r}_i(t+\delta t) - \vec{r}_i(t-\delta t)\right] + O\left(\delta t^3\right). \tag{25}$$

Uporabo enačbe za hitrost moramo prilagoditi stanju v sistemu. V molekularni dinamiki se uporabljajo najpogosteje tri stanja: konstantno število delcev, prostornina ter temperatura (NVT), konstantno število delcev, temperatura ter tlak (NTP) in konstantno število delcev, prostornina in energija (NVE).

V letih razvoja tovrstnega modeliranja je nastala vrsta računalniških programov za računanje in vizualizacijo molekularne dinamike. Na področju modeliranja struktur zgrajenih iz lipidnih molekul, sta najbolj pogosta NAMD [Philips *et al.* 2005] in GROMAX [Lindahl *et al.* 2001]. Ker smo pri delu uporabljali NAMD bodo v naslednjem razdelku uporabljeni formati datotek pripadali temu programu, vendar pa običajno tak tip datotek potrebujemo pri katerem koli računanju z molekularno dinamiko. Prvi korak modeliranja je zapis datotek, v katerih opišemo začetni položaj molekul, začetno energijo med posameznimi gradniki, nastavitvene parametre modela ter velikost prostora v katerem model računamo. Za zagon simulacije računanja potrebujemo datoteke s končnicami: *.pdb, *.psf, *.conf, *.xsc.

Koordinate vseh atomov oziroma gradnikov v modelu podamo v *.pdb datoteki. V tabeli 1 beseda »ATOM« v prvem stolpcu predstavlja ukaz, v naslednjem stolpcu so zaporedne številke atomov oz gradnikov, v našem primeru od 1407 do 1480, kar predstavlja eno lipidno molekulo. S številkami od 1407 do 1448 so predstavljeni gradniki glave lipidnih molekul, ki je predstavljena z vsemi atomi. S številkami 1477 do 1480 so predstavljeni gradniki repov lipidnih molekul, ki so predstavljeni s skupki atomov, saj so vezave vodika in ogljika združene v en gradnik. V tretji koloni so kemijski elementi z indeksi: N-dušik, C-ogljik, H-vodik, O-kisik, P-fosfor. Četrti in zadnji stolpec »POUN« opišeta, katere parametre uporabljamo. V peti koloni, pomeni številka 20 dvajseto lipidno molekulo. Naslednji trije stolpci predstavljajo x, y in z komponento položaja posameznega gradnika $\vec{r}_i(t)$. Deveti in deseti stolpec vsebujeta kota α in β kristalne strukture, ki jih pri modeliranju ravninskih lipidnih dvoslojev nismo uporabljali.

Tabela 1. Levo vsebina datoteke *.PDB, v kateri opišemo položaj atomov v posameznih molekulah v sistemu. Desno Lipidna molekula, ki ustreza opisu na levi stani. Barve posameznih atomov se skladajo z barvami vrstic v katerih so opisani.

```
ATOM   1407  N    POUN  20      28.729  -0.181  31.956  1.00  0.00      POUN
ATOM   1408  C11  POUN  20      28.008   1.099  31.501  1.00  0.00      POUN
ATOM   1409  C12  POUN  20      27.912  -1.370  31.671  1.00  0.00      POUN
ATOM   1410  C13  POUN  20      29.065  -0.026  33.422  1.00  0.00      POUN
ATOM   1411  C14  POUN  20      30.063  -0.316  31.332  1.00  0.00      POUN
ATOM   1412  H11  POUN  20      28.784   1.848  31.566  1.00  0.00      POUN
ATOM   1413  H12  POUN  20      27.128   1.374  32.064  1.00  0.00      POUN
ATOM   1414  H21  POUN  20      28.532  -2.254  31.652  1.00  0.00      POUN
ATOM   1415  H22  POUN  20      27.029  -1.431  32.290  1.00  0.00      POUN
ATOM   1416  H23  POUN  20      27.450  -1.291  30.698  1.00  0.00      POUN
ATOM   1417  H31  POUN  20      28.137  -0.107  33.969  1.00  0.00      POUN
ATOM   1418  H32  POUN  20      29.647  -0.905  33.657  1.00  0.00      POUN
ATOM   1419  H33  POUN  20      29.672   0.859  33.540  1.00  0.00      POUN
ATOM   1420  H41  POUN  20      30.535  -1.260  31.563  1.00  0.00      POUN
ATOM   1421  H42  POUN  20      29.918  -0.432  30.268  1.00  0.00      POUN
ATOM   1422  H43  POUN  20      30.650   0.540  31.629  1.00  0.00      POUN
ATOM   1423  C15  POUN  20      27.493   1.150  29.997  1.00  0.00      POUN
ATOM   1424  H51  POUN  20      26.962   2.122  29.908  1.00  0.00      POUN
ATOM   1425  H52  POUN  20      26.629   0.464  29.869  1.00  0.00      POUN
ATOM   1426  P1   POUN  20      28.715   1.710  27.787  1.00  0.00      POUN
ATOM   1427  O3   POUN  20      30.040   1.270  27.265  1.00  0.00      POUN
ATOM   1428  O4   POUN  20      28.524   3.157  28.059  1.00  0.00      POUN
ATOM   1429  O1   POUN  20      28.535   0.877  29.048  1.00  0.00      POUN
ATOM   1430  O2   POUN  20      27.479   1.066  27.002  1.00  0.00      POUN
ATOM   1431  C1   POUN  20      27.700  -0.113  26.236  1.00  0.00      POUN
ATOM   1432  HA   POUN  20      26.952  -0.889  26.505  1.00  0.00      POUN
ATOM   1433  HB   POUN  20      28.715  -0.562  26.278  1.00  0.00      POUN
ATOM   1434  C2   POUN  20      27.278   0.305  24.774  1.00  0.00      POUN
ATOM   1435  HS   POUN  20      26.295   0.823  24.806  1.00  0.00      POUN
ATOM   1436  O21  POUN  20      27.341  -0.902  23.982  1.00  0.00      POUN
ATOM   1437  C21  POUN  20      26.177  -1.396  23.637  1.00  0.00      POUN
ATOM   1438  O22  POUN  20      25.084  -1.274  24.146  1.00  0.00      POUN
ATOM   1439  C22  POUN  20      26.303  -2.110  22.290  1.00  0.00      POUN
ATOM   1440  H2R  POUN  20      25.280  -2.353  21.930  1.00  0.00      POUN
ATOM   1441  H2S  POUN  20      26.768  -3.093  22.519  1.00  0.00      POUN
ATOM   1442  C3   POUN  20      28.141   1.438  24.153  1.00  0.00      POUN
ATOM   1443  HX   POUN  20      28.171   2.276  24.881  1.00  0.00      POUN
ATOM   1444  HY   POUN  20      29.165   1.006  24.128  1.00  0.00      POUN
ATOM   1445  O31  POUN  20      27.749   1.787  22.817  1.00  0.00      POUN
ATOM   1446  C31  POUN  20      26.959   2.825  22.687  1.00  0.00      POUN
ATOM   1447  O32  POUN  20      26.318   3.310  23.597  1.00  0.00      POUN
ATOM   1448  C32  POUN  20      26.911   3.162  21.181  1.00  0.00      POUN
...
ATOM   1477 C313  POUN  20      28.495   0.602   9.145  1.00  0.00      POUN
ATOM   1478 C314  POUN  20      27.849   0.710   7.691  1.00  0.00      POUN
ATOM   1479 C315  POUN  20      28.915   0.655   6.610  1.00  0.00      POUN
ATOM   1480 C316  POUN  20      28.541   0.753   5.045  1.00  0.00      POUN
```

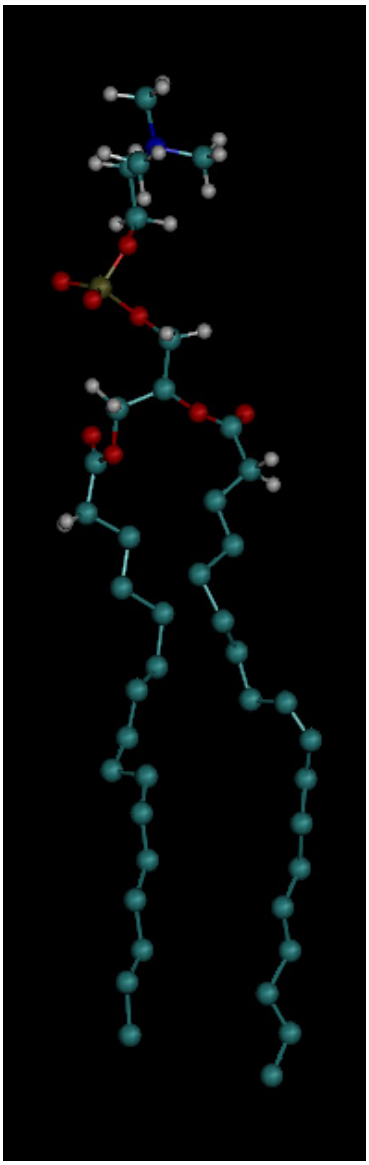

Datoteka *.psf je razdeljena na več odsekov (tabela 2). V prvem delu »!NATOM« imamo za vsak posamezen gradnik, ki je naveden v *.pdb datoteki; podatek o tipu molekule »POUN«, zaporedno številko gradnika, kemijski element, povezavo z sosednjimi elementi. V sedmem stolpcu so navedeni električni naboji gradnikov izraženi z osnovnimi naboji *e*, v osmem pa njihova masa. Ko so vsi gradniki v modelu definirani, se datoteka nadaljuje s poimenovanjem vezi med gradniki »!NBOND«, kotov med vezmi »!NTHETA« in dihedralnih kotov »!NPHI«. Eno vez med dvema gradnikoma predstavljata dve zaporedni številki. Kot med vezema opišemo s tremi zaporednimi številkami, dihedralne kote pa z zaporedjem štirih številk.

Tabela 2. Odseki posameznih delov datoteke *.PSF, v kateri imamo podano povezanost posameznih gradnikov *.PDB datoteke, maso gradnikov in njihov osnovni naboj. Eno vez med dvema gradnikoma predstavljata dve zaporedni številki. Kot med vezema opišemo s tremi zaporednimi številkami, dihedralne kote pa z zaporedjem štirih številk.

65320 !NATOM

1407	POUN	20	POUN	N	NTL	-0.600000	14.0070	0
1408	POUN	20	POUN	C11	CTL2	-0.100000	12.0110	0
1409	POUN	20	POUN	C12	CTL5	-0.350000	12.0110	0
1410	POUN	20	POUN	C13	CTL5	-0.350000	12.0110	0
1411	POUN	20	POUN	C14	CTL5	-0.350000	12.0110	0
1412	POUN	20	POUN	H11	HL	0.250000	1.0080	0
1413	POUN	20	POUN	H12	HL	0.250000	1.0080	0
1414	POUN	20	POUN	H21	HL	0.250000	1.0080	0
1415	POUN	20	POUN	H22	HL	0.250000	1.0080	0

64752 !NBOND: bonds

1407	1408	1407	1409	1407	1410	1407	1411	1408
1412	1408	1413	1408	1423	1409	1414	1409	1415

46256 !NTHETA: angles

1407	1411	1422	1407	1411	1421	1407	1411	1420
1407	1410	1419	1407	1410	1418	1407	1410	1417
1407	1409	1416	1407	1409	1415			

37152 !NPHI: dihedrals

1407	1408	1423	1424	1407	1408	1423	1425	1407
1408	1423	1429	1408	1423	1429	1426	1408	1407
1409	1414	1408	1407	1409	1415			

Za izračun potrebujemo še datoteko topologije molekule, kjer so definirane konstante sil k_r, k_ψ in k_ϕ. V datoteki *.xcs nastavimo začetno velikost prostora, v katerem bo model ravninskega lipidnega dvosloja. Glede na izbiro adiabatnega stanja se lahko velikost prostora tudi spreminja in s tem tudi vrednosti v datoteki *.xcs. Nastavitve računanja modela molekularne dinamike se nahajajo *.conf datoteki. Tu so parametri računanja kot časovni korak računanja, imena vhodnih in izhodnih datotek, adiabatno stanje modela ter nastavitev temperature in tlaka v modelu.

Ko imamo pripravljene vse datoteke, lahko pričnemo z računanjem. Običajno ga izvajamo na več procesorskih super računalnikih, ki se nahajajo v super računalniških centrih. Program za računanje NAMD [http://www.ks.uiuc.edu/Research/namd/] ima vgrajen algoritem, s katerim deli računanje premikanja molekul med posamezne procesorje.

Ob posameznem izvedenem koraku računanja se rezultati koordinat zapišejo v datoteki *.dcd Že med samim računanjem lahko opazujemo kaj se dogaja z modelom, ne da bi računaje prekinili. Vsi podatki se namreč zaporedno v ANSII obliki zapisujejo v datoteko. Odprtje datoteke, nam poda vse izračunane korake do trenutnega stanja, paralelno pa računalnik izračunava nove premike in jih

dodaja v isto datoteko. Gibanje molekul in atomov računanih s programskim paketom NAMD vizualiziramo z VMD programom (slika 25) [http://www.ks.uiuc.edu/Research/vmd/]

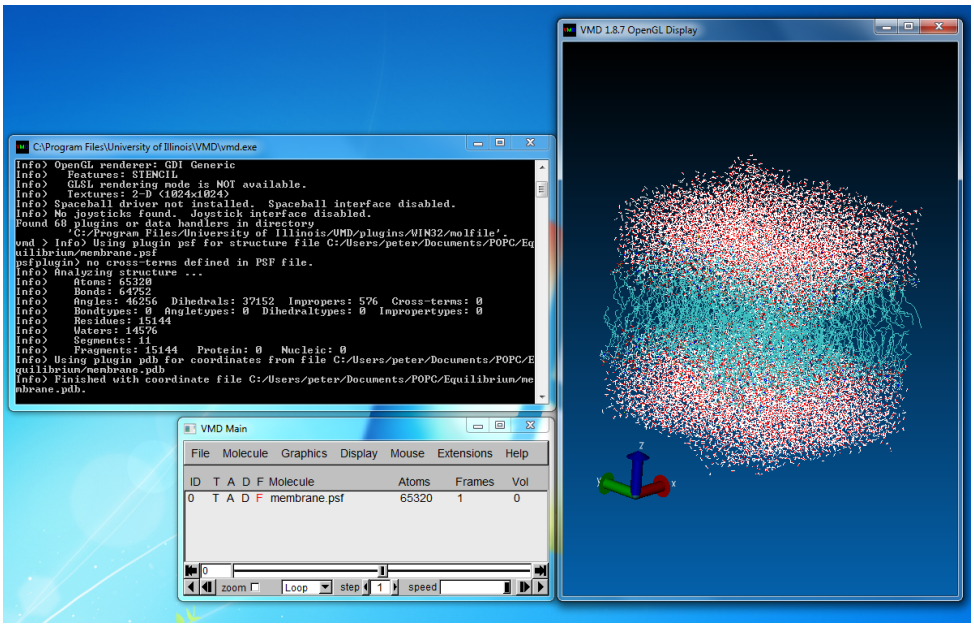

Slika 25. Zaslonski pogled na program VMD (Visual Molecular Dynamics). Razvit na Univerzi Illinois, ZDA.

2.6.1 Gradnja modela ravninskega lipidnega dvosloja

Opis vseh molekul v modelu naredimo v datoteki s končnico *.pdb, ki smo jo predstavili v tabeli 1. Vsaka vrstica vsebuje številko atoma, kemijski element, njegov položaj (x,y,z) ter tip molekule (POUN), v katerem se atomi nahajajo in jo definiramo v topološki datoteki. Lipidno molekulo POPC (1-pamitoil 2-oleoil 3-fosfatidilholin) smo zgradili iz dveh delov. Glavo lipidne molekule smo opisali z vsemi atomi (št.1 do 41). V obeh repih lipidne molekule (št 42 do 73) smo posamezne atome ogljika, ki so imeli nase vezan vodik, združili v en skupek. V datoteki s parametri je tak tip lipidne molekule označen kot POUN.

Če želimo iz lipidne molekule zgraditi ravninski lipidni dvosloj, moramo izvorno kodo lipidne molekule razmnožiti. Ko razmnožujemo izvorno kodo moramo za vsako molekulo napisati novo številko ter spremeniti vrednosti koordinat posameznih atomov. To ponavljamo toliko časa, da zgradimo celoten ravninski lipidni dvosloj. Tak postopek je precej zamuden. Zato lahko uporabimo posebno programsko orodje, ki na osnovi ene molekule zgradi celoten lipidni dvosloj z želeno gostoto lipidnih molekul. Pri našem delu smo uporabili programsko orodje Packmol, ki ga je razvila skupina iz Državne Univerze v Campinasu, Brazilija [Martinez *et al.* 2009]. Z vhodnimi parametri določimo geometrijo ravninskega lipidnega dvosloja ter gostoto lipidnih molekul na površini. Program zgradi ravninski

lipidni dvosloj, ter zapiše *.pdb datoteko. Dobra lastnost programa je, da lipidne molekule med kopiranjem in premikanjem tudi obrača po vzdolžni osi in poizkuša optimizirati njihovo postavitev. V vhodno definicijsko datoteko dodamo tudi molekulo vode in jo glede na želeno gostoto razmnožimo nad in pod ravninskim lipidnim dvoslojem. Ko je model ravninskega lipidnega dvosloja in okoliške raztopine zgrajen (slika 26A), s skripto *psfgen* med posameznimi atomi določimo začetne pospeške, ki so običajno v začetku naključni, in molekulsko maso kemijskih elementov (*.psf datoteka).

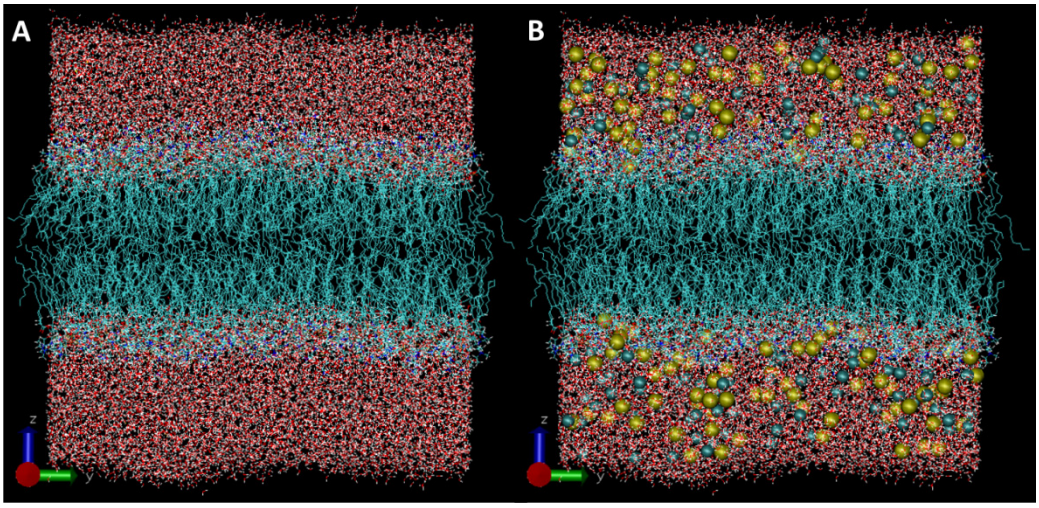

Slika 26. A Model ravninskega lipidnega dvosloja z lipidi in vodo. B Model ravninskega lipidnega dvosloja z vodo in ioni soli natrijevega klorida - Natrija Na^+ in Klora Cl^-.

Ko določimo začeten položaj molekul (*.pdb) in energijo med atomi (*.psf), imamo popoln model. V programu VMD dodamo v raztopino ione v želeni koncentraciji, tako da je raztopina električno nevtralna (slika 26B). Električno nevtralen model prenesemo na super računalnik, kjer zaženemo minimizacijo modela, katere rezultat je ravnovesno stanje gradnikov modela. Pri minimizaciji modela uporabljamo NPT razmere (N – konstantno število gradnikov, P – konstanten tlak, T – konstantna temperatura). Kot rezultat minimizacije modela opazujemo število lipidnih molekul na izbrani površini. Le-ta se od začetka računanja počasi ustali na konstantni vrednosti, ki pa mora biti primerljiva z meritvami z metodo magnetne resonance [Nagle 1993].

Ko je ravninski lipidni dvosloj v ravnovesnem stanju, preizkusimo model še s »toplotnim šokom«. Nastavljeno temperaturo modela povečamo na 350 K in ponovno zaženemo računanje. Vrednost razmerja površine na lipidno molekulo bi se morala povečati. Če je potrebno lahko gretje nadaljujemo na 400 K. Ko sistem postavimo nazaj na temperaturo 300 K, se mora model ravninskega lipidnega dvosloja postaviti nazaj v ravnovesje. Če temu ni tako, moramo preveriti, ali so vhodni parametri modela ustrezni.

Ravninski lipidni dvosloj je dovolj kvaliteten, če je primerljiv z eksperimentalno določenimi podatki iz literature. Izračunani model nato štirikrat preslikamo in prestavimo vzdolž osi x in y, tako da je površina modela štirikrat večja. Pri naših izračunih je bila površina modela ravninskega lipidnega dvosloja 100x100 $Å^2$. Ponovno zaženemo minimizacijo modela z namenom, da dobimo ravnovesje novega sistema. Tako velika površina membrane je primerna za opazovanje različnih pojavov na ravninskem lipidnem dvosloju. Mednje sodi tudi nastajanje por ob izpostavitvi električnemu polju.

2.6.2 Ravninski lipidni dvosloj v električnem polju

Pojav elektroporacije so z modeli molekularne dinamike opisali že mnogi avtorji. Leta 2001 je Tieleman s sodelavci objavil članek, v katerem so avtorji prvič pokazali strukturo pore v ravninskem lipidnem dvosloju [Tieleman *et al.* 2001]. Sledilo mu je več raziskovalcev z velikim številom novih simulacij [Marrink *et al.* 2009]. Vzpostaviti transmembransko napetost na ravninskem lipidnem dvosloju v molekularni dinamiki ni trivialno. Zavedati se moramo, da imamo omejen prostor in periodične robne pogoje. Tielman s sodelavci je predlagal, da bi ob vsak atom pripeli naboj q_i in s tem ustvarili pravokotno silo na ravninski lipidni dvosloj:

$$\vec{F} = q_i \cdot \vec{E} \tag{26}$$

kjer je $\vec{E}$ ustvarjeno zunanje električno polje [Tieleman *et al.* 2003; Tieleman 2004]. Transmembranska napetost na ravninskem lipidnem dvosloju pa je posledica električnega polja:

$$U(L_z) = \left|\vec{E}\right| L_z, \tag{27}$$

kjer je L_z širina modela v *z* smeri.

Sachs s sodelavci je predlagal ionsko neravnovesje v vodni raztopini, ki vzpostavi transmembransko napetost [Sachs *et al.* 2004]. V modelu z ravninskim lipidnim dvoslojem ter ionsko raztopino Na^+ in Cl^- ionov v ravnovesju, prestavimo en ion iz spodnje strani ravninskega lipidnega dvosloja na zgornjo stran. S premikom tvorimo neravnovesje nabojev 2e. Več ionov kot premaknemo, večje je neravnovesje. Toda, če uporabljamo periodične robne pogoje, se prestavljeni ioni »čutijo« med seboj in jih je potrebno razdeliti. Zgraditi je potrebno dvojni lipidni dvosloj in postaviti tri prekate prevodne raztopine ionov (slika 27A). V tem primeru, se zgornji in spodnji prekat med seboj »čutita«, za ionsko ravnovesje je moral biti seštevek nabojev v zgornjem in spodnjem prekatu enak vsoti nabojev v srednjem prekatu [Sachs et al. 2004, Gurtovenko *et al.* 2005, Kandasamy in Larson 2006]. Vendar pa dvojni lipidni dvosloj računanje zelo podaljša, saj imamo število atomov ravninskega lipidnega dvosloja podvojeno. Ta metoda je zato posledično računsko zelo potratna.

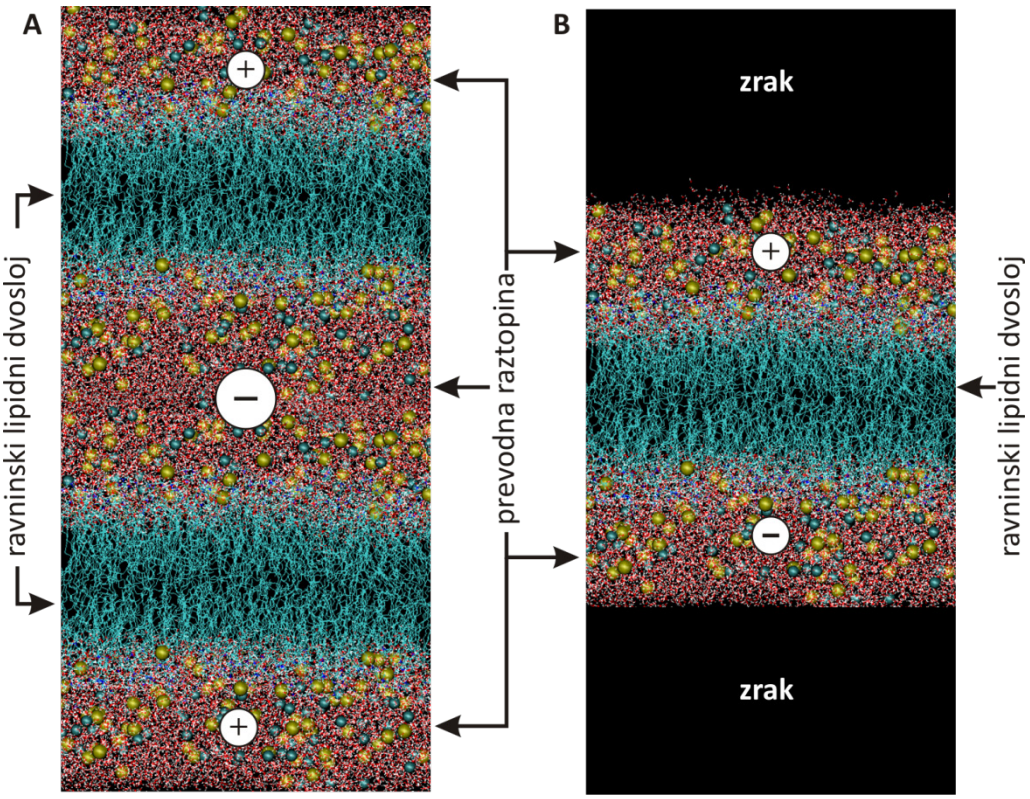

Slika 27. A) Dvojni ravninski lipidni dvosloj. B) Ravninski lipidni dvosloj z dodanim zrakom.

Delemotte s sodelavci je predlagala drugačno metodo vzpostavitve ionskega neravnovesja [Delemotte *et al.* 2008]. Na spodnji in zgornji strani modela so dodali zrak (slika 27B). Kemijsko to ni bil pravi zrak, ampak prazen prostor z definiranim tlakom. Zaradi zraka, se ioni iz spodnje in zgornje vodne raztopine ob periodičnih robnih pogojih niso »čutili«. Računanje je tako mogoče ob prisotnosti enega samega ravninskega lipidnega dvosloja.

Z molekularno dinamiko ravninskih lipidnih dvoslojev pridemo do nekaterih podatkov, ki jih z eksperimenti ne moremo neposredno dokazati. Nastanek pore ob izpostavitvi ravninskega lipidnega dvosloja električnemu polju ter njena struktura sta le dva iz med teh.

2.6.3 Model ravninskega lipidnega dvosloja zgrajen iz lipidnih molekul POPC

Ravninski lipidni dvosloj smo zgradili z lipidov POPC (1-pamitoil 2-oleoil 3-fosfatidilholin). Posamezna molekula POPC vsebuje 79 gradnikov. Glavo lipidne molekule smo sestavili v načinu »vsi atomi«, repe lipidnih molekul pa kot »skupke molekul«. Ravninski lipidni dvosloj smo iz dveh strani obdali s 150 mM raztopino NaCl. Pri minimizaciji ravninskega lipidnega dvosloja smo uporabili 288 lipidnih molekul oziroma 21.024 atomov. Skupaj z vodo in ioni natrija ter klora je model obsegal 65.000 atomov. Ko smo izračunali ravnovesje ravninskega lipidnega dvosloja, smo obstoječ sistem štirikrat povečali, kar naj bi zadostovalo za simulacijo elektroporacije [Delemotte *et al.* 2008]. Novi sistem je vseboval 1.152 lipidnih molekul, 576 v zgornji plasti in 576 v spodnji plasti, 58.304 vodnih molekul,

560 ionov natrija ter 560 atomov klora. Skupaj je sistem obsegal 261.280 atomov. Nad in pod plastjo vode smo dodali plast zraka, tako da se ioni iz spodnje polovice raztopine niso »čutili« v zgornji polovici in obratno (slika 27B). S tako geometrijo smo omogočili, da bomo kljub tri dimenzionalnim periodičnim robnim pogojem ravninski lipidni dvosloj izpostavili ionskemu neravnovesju. Velikost celotnega prostora modela je obsegala (16,8 x 18,3 x 20,1) nm^3. Za minimizacijo sistema in postavitev v ravnovesje smo uporabili NVT pogoje (konstantno število delcev, konstantna prostornina in konstantna temperatura). Pri modeliranju ravninskega lipidnega dvosloja smo morali zaradi zraka v modelu imeti konstanten tlak ene atmosfere (1,01 10^5 Pa). Uporabili smo NPT pogoje (konstantno število delcev, konstanten tlak in konstantna temperatura). Temperatura, pri kateri smo model računali, je bila 300 K.

Napetost na membrani smo vzpostavili z neravnovesjem ionov. Za vsak ion, ki smo ga iz spodnjega sloja vodne raztopine premaknili v zgornji sloj, smo tvorili 2*e* neravnovesja naboja, kjer je *e* osnovni naboj enak 1,602.176.462(63) 10^{-19} As.

Kapacitivnost ravninskega lipidnega dvosloja smo določili iz transmembranske napetosti [Delemotte *et al.* 2008], ki se je vzpostavila zaradi ionskega neravnovesja. Razmerje naboja *Q* zaradi ionskega neravnovesja in transmembranske napetosti ΔV je ustrezalo kapacitivnosti *C* ravninskega lipidnega dvosloja:

$$C = \frac{Q}{\Delta V}. \tag{28}$$

Pri dovolj velikem neravnovesju ionov smo opazili v ravninskem lipidnem dvosloju strukturne spremembe oziroma pore. Preko por je ravninski lipidni dvosloj prepuščal ione. Pretok ionov je ravninski lipidni dvosloj razelektril ter zmanjšal transmembransko napetost, ki je nastala pri postavljanju neravnovesja z ioni. Da bi lahko izmerili prevodnost pore v ravninskem lipidnem dvosloju, smo morali neravnovesje ionov ohranjati. S tem smo obdržali transmembransko napetost. Prehod ionov preko pore v časovnem intervalu je predstavljal tok:

$$I = \frac{dQ}{dt} = \frac{q}{L_z}\frac{dz}{dt}, \tag{29}$$

kjer je *q* linijskaporazdelitev nabojev vzdolž pore in L_z širina modela v *z* smeri.

Prevodnost pore smo definirali kot razmerje med tokom in transmembransko napetostjo:

$$G_P = \frac{I}{\Delta V}. \tag{30}$$

3 Merjenje kapacitivnosti ravninskega lipidnega dvosloja

Za merjenje kapacitivnosti ravninskega lipidnega dvosloja smo uporabljali dve metodi: merjenje časovne konstante razelektritve ravninskega lipidnega dvosloja in merjenje s pretvorbo kapacitivnosti v periodo.

3.1 Merjenje kapacitivnosti s časovno konstanto razelektritve

Ravninske lipidne dvosloje smo tvorili iz molekul lipidov POPC in POPS. Enokomponentni dvosloji so bili zgrajeni iz ene vrste lipida, ali iz POPC ali iz POPS. Dvokomponentni ravninski lipidni dvosloji so bili zgrajeni iz mešanice POPC in POPS v razmerjih 3:1, 1:1 in 1:3. V tabeli 3 so prikazane povprečne vrednosti specifične kapacitivnosti c_{BLM} in število meritev N za posamezno sestavo lipida [Sabotin 2008].

Tabela 3. Povprečne vrednosti specifične kapacitivnosti c_{BLM} in število meritev N za posamezno sestavo ravninskih lipidnih dvoslojev izmerjenih z metodo določanja časovne konstante razelektritve.

Lipidi:	c_{BLM} (μF/cm^2)	N
POPC:POPS = 1:0	0,51±0,17	80
POPC:POPS = 3:1	0,17±0,06	103
POPC:POPS = 1:1	0,31±0,07	60
POPC:POPS = 1:3	0,24±0,14	66
POPC:POPS = 0:1	0,41±0,13	76

Kruskal-Wallisov enosmerni test je pokazal, da obstajajo statistično značilne razlike med srednjimi vrednostmi specifične kapacitivnosti c_{BLM} pri različnih mešanicah lipidov (tabela 3, slika 28).

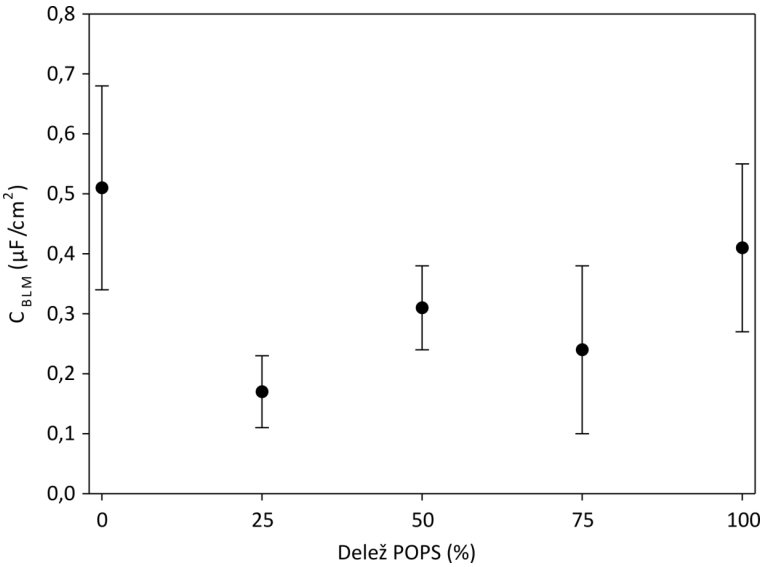

Slika 28. Specifična kapacitivnost c_{BLM} za posamezne mešanice lipidov v odvisnosti od deleža POPS v mešanici. Podane so srednje vrednosti in standardne deviacije.

3.2 Merjenje kapacitivnosti s pretvorbo kapacitivnosti v periodo

Ravninske lipidne dvosloje smo tvorili iz molekul lipidov POPC, POPS ter mešanice POPC:POPS 1:1. V tabeli 4 so prikazane povprečne specifične vrednosti kapacitivnosti c_{BLM} in število meritev *N* ravninskih lipidnih dvoslojev za posamezno sestavo lipidnih molekul.

Tabela 4. Povprečne vrednosti specifične kapacitivnosti c_{BLM} in število meritev *N* za posamezno sestavo ravninskih lipidnih dvoslojev izmerjenih z metodo pretvarjanja kapacitivnosti v periodo.

Lipidi:	c_{BLM} (µF/cm^2)	*N*
POPC:POPS = 1:0	0,51 ± 0,16	58
POPC:POPS = 1:1	0,34 ± 0,17	25
POPC:POPS = 0:1	0,41 ± 0,13	34

Kruskal-Wallisov enosmerni test je pokazal, da obstajajo statistično značilne razlike med srednjimi vrednostmi specifične kapacitivnosti c_{BLM} pri različnih mešanicah lipida (tabeli 4).

3.3 Zaključek

Namen študije je bil preveriti kapacitivnost ravninskih lipidnih dvoslojev z dvema različnima metodama, merjenjem časovne konstante razelektritve in s pretvorbo kapacitivnosti v periodo. Kruskal-Wallisov enosmerni test je pokazal, da ni statistično zančilne razlike med srednjimi vrednostmi specifične kapacitivnosti c_{BLM} pri enakih mešanicah lipida, določena z dvema različnima metoda merjenja.

4 Merjenje porušitvene napetosti ravninskega lipidnega dvosloja z linearno naraščajočim signalom

Ravninske lipidne dvosloje smo izpostavili sedmim različnim naklonom linearno naraščajočih napetostnih signalov. Vrednosti uporabljenih naklonov od najbolj položnega do najbolj strmega so: 4,8 kV/s, 5,5 kV/s, 7,8 kV/s, 11,5 kV/s, 16,7 kV/s, 21,6 kV/s in 48,1 kV/s. Vrednost porušitvene napetosti pri izbranem naklonu vzbujanja smo določili iz povprečja meritev. Pri vsakem naklonu smo opravili vsaj 6 meritev (POPC:POPS 1:1, naklon 16,7 V/ms), a ne več kot 18 meritev (POPC:POPS 0:1, naklon 48,1 V/ms). V naslednjih podpoglavjih so zbrane tabele povprečnih vrednosti in standardnih odklonov za specifično kapacitivnost c_{BLM}, porušitveno napetost U_{br} in življenjsko dobo t_{br} pri posameznem naklonu k napetostnega signala za izbrano sestavo lipida. Podane so tudi tabele statističnih odvisnosti porušitvene napetosti U_{br} med izmerjenimi vrednostmi pri posameznih naklonih k.

4.1 POPC:POPS (1:0)

Povprečna temperatura okolice, pri kateri so bile meritve izvedene, je bila 28,6 °C. Največja relativna napaka meritev je prisotna pri naklonu 5,5 V/ms in znese za porušitveno napetost 9,3%, za življenjsko dobo pa 10,0%. Podatki meritev so zbrani v tabeli 5 in grafično prikazani na sliki 29.

Tabela 5. Povprečne vrednosti specifične kapacitivnosti (c_{BLM}), porušitvene napetosti (U_{br}) in življenjske dobe (t_{br}) ravninskih lipidnih dvoslojev sestavljenih iz 1- palmitil 2 – oleil fosfatidilholina (POPC). V tabeli je zajeto tudi število meritev (N) pri posameznem naklonu (k) linearno naraščajočega napetostnega vzbujanja. Podane so povprečne vrednosti in standardne deviacije.

N	k (kV/s)	c_{BLM} (µF/cm^2)	U_{br} (V)	t_{br} (µs)
17	4,8	0,50 ± 0,12	0,54 ± 0,04	112,92 ± 8,32
16	5,5	0,50 ± 0,14	0,54 ± 0,05	99,24 ± 9,93
16	7,8	0,60 ± 0,22	0,54 ± 0,04	70,74 ± 5,07
12	11,5	0,51 ± 0,11	0,59 ± 0,05	52,25 ± 4,65
12	16,7	0,49 ± 0,09	0,65 ± 0,06	39,38 ± 3,87
17	21,6	0,40 ± 0,1	0,67 ± 0,05	30,50 ± 2,60
16	48,1	0,54 ± 0,10	0,76 ± 0,05	16,76 ± 1,14
POPC:POPS (1:0)				

Z napenjanjem intenzivnostno časovne krivulje (14) na izmerjene vrednosti porušitvenih napetosti pri različnih naklonih (tabela 5) smo ocenili parametra a = 0,56 V in b = 13,43 µs. Parameter a določa asimptotično vrednost porušitvene napetosti za lipidne dvosloje zgrajene iz POPC. Poimenovali smo

jo kot najmanjšo porušitveno napetost U_{brMIN}. Na sliki 29 je označena kot siva črtkana črta. Oceno zaupanja v prosta parametra napete krivulje smo izračunali z Matlab-ovo funkcijo *nlparci*. 95% interval zaupanja za parameter *a* znaša *a* = 0,56 V ± 0,05 V in za parameter *b* = 13.4 µs ± 4.3 µs. Na sliki 29 je pas zaupanja omejen s črnima pika-črta krivuljama.

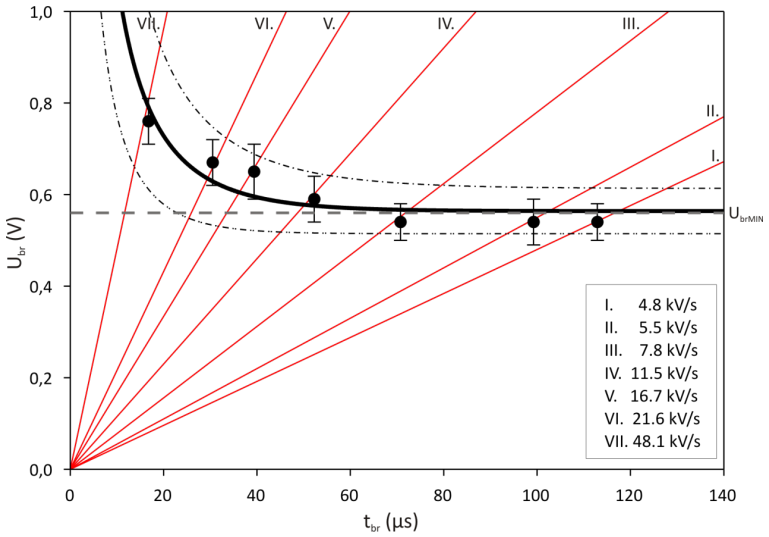

Slika 29. Porušitvena napetost (U_{br}) v odvisnosti od življenjske dobe (t_{br}) ravninskih lipidnih dvoslojev iz 1- palmitil 2 – oleil fosfatidilholina (POPC). Rdeče črte predstavljajo naklone (*k*) linearno naraščajočega napetostnega vzbujanja. Črna krivulja predstavlja napeto krivuljo na izmerjene vrednosti po enačbi (14). 95% interval zaupanja za koeficienta *a* in *b* predstavlja pas med črnima pika-črta krivuljama. Siva črtkana črta je asimptota napete krivulje, ki podaja najmanjšo porušitveno napetost U_{brMIN} = 0,56 V.

Enosmerni ANOVA test porušitvenih napetosti pri različnih naklonih je pokazal statistično različnost srednjih vrednosti U_{br} (p <0,001). Srednje vrednosti izmerjenih porušitvenih napetosti smo med seboj paroma statistično primerjali s Tukey-evim testom (tabela 6).

Tabela 6. Statistična odvisnost porušitvenih napetosti. Statistična odvisnost porušitvenih napetosti U_{br} ravninskih dvoslojev iz POPC med izmerjenimi vrednostmi pri posameznih naklonih *k*. Vrednosti v spodnjem delu tabele predstavljajo verjetnost *p*, da sta srednji vrednosti $U_{br}(k_1)$ in $U_{br}(k_2)$ enaki. Za *p*<0,05 smatramo, da sta vrednosti statistično značilno različni. V zgornjem delu tabele so statistično značilno različne vrednosti označene z 'da' ostale pa z 'ne'.

U_{br} (*k*)	*k=4,8 kV/s*	*k=5,5 kV/s*	*k=7,8 kV/s*	*k=11,5 kV/s*	*k=16,7 kV/s*	*k=21,6 kV/s*	*k=48,1 kV/s*
k=4,8 kV/s		ne	ne	ne	da	da	da
k=5,5 kV/s	1,000		ne	ne	da	da	da
k=7,8 kV/s	1,000	1,000		ne	da	da	da
k=11,5 kV/s	0,085	0,104	0,098		ne	da	da
k=16,7 kV/s	<0,001	<0,001	<0,001	0,159		ne	da
k=21,6 kV/s	<0,001	<0,001	<0,001	0,004	0,920		da
k=48,1 kV/s	<0,001	<0,001	<0,001	<0,001	<0,001	<0,001	

POPC:POPS = 1:0

4.2 POPC:POPS (3:1)

Meritve na ravninskih lipidnih dvoslojih zgrajenih iz mešanice lipidov POPC in POPS v razmerju 3 proti 1 so bile izvedene pri povprečni temperaturi okolice 24,5 °C. Meritev porušitvene napetosti z največjo relativno napako zasledimo pri naklonu 11,5 V/ms in znaša 10,5%. Relativna napaka meritve življenjske dobe pri istem naklonu znaša 9,9%. Podatki meritev so zbrani v tabeli 7 in grafično prikazani na sliki 30.

Tabela 7. Povprečne vrednosti specifične kapacitivnosti (c_{BLM}), porušitvene napetosti (U_{br}) in življenjske dobe (t_{br}) ravninskih lipidnih dvoslojev sestavljenih iz mešanice 1- palmitil 2 – oleil fosfatidilholina (POPC) in 1- palmitil 2 – oleil fosfatidilserina (POPS) v razmerju 3 proti 1. V tabeli je zajeto število meritev (N) pri posameznem naklonu (k) linearno naraščajočega napetostnega vzbujanja. Podane so povprečne vrednosti in standardne deviacije.

N	k (kV/s)	c_{BLM} (µF/cm^2)	U_{br} (V)	t_{br} (µs)
16	4,8	0,22 ± 0,06	0,54 ± 0,05	113,26 ± 9,97
12	5,5	0,20 ± 0,09	0,52 ± 0,04	95,95 ± 6,28
16	7,8	0,18 ± 0,05	0,52 ± 0,05	68,84 ± 6,30
10	11,5	0,19 ± 0,08	0,57 ± 0,06	50,29 ± 5,25
15	16,7	0,22 ± 0,05	0,59 ± 0,05	36,28 ± 2,92
12	21,6	0,22 ± 0,08	0,66 ± 0,03	30,03 ± 1,44
8	48,1	0,18 ± 0,04	0,76 ± 0,04	16,68 ± 0,89
POPC:POPS (3:1)				

Koeficienta krivulje (14) napete na izmerjene porušitvene napetosti (tabela 7) s podanim 95% intervalom zaupanja sta a = 0,54 V ± 0,04 V in b = 14,3 µs ± 3,3 µs. Parameter a je enak »pravi« porušitveni napetosti ravninskega lipidnega dvosloja U_{brMIN} in je na sliki 30 označen s sivo črtkano črto. Črni pika-črta krivulji določata pas zaupanja krivulji, ki jo določata parametra a in b.

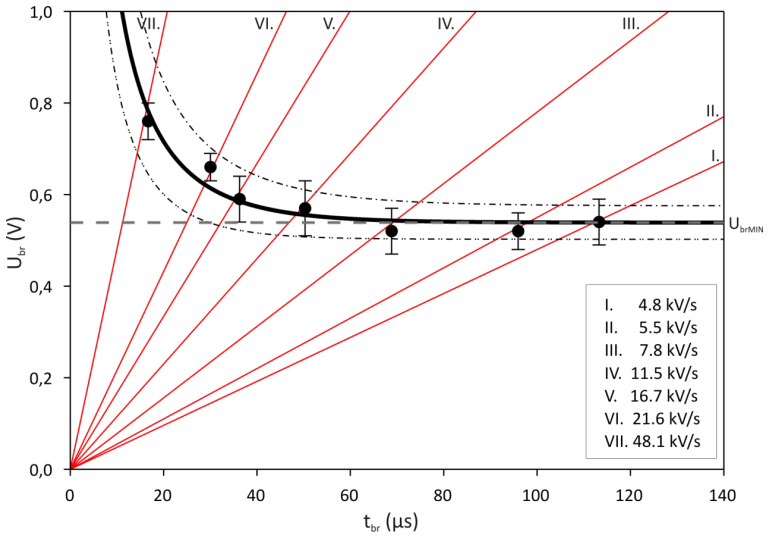

Slika 30. Porušitvena napetost (U_{br}) v odvisnosti od življenjske dobe (t_{br}) ravninskih lipidnih dvoslojev sestavljenih iz mešanice 1- palmitil 2 – oleil fosfatidilholina (POPC) in 1- palmitil 2 – oleil fosfatidilserina (POPS) v razmerju 3 proti 1. Rdeče črte predstavljajo naklone (k) linearno naraščajočega napetostnega vzbujanja. Črna krivulja predstavlja napeto krivuljo na izmerjene vrednosti po enačbi (14). 95% interval zaupanja za koeficienta a in b predstavlja pas med črnima pika-črta krivuljama. Siva črtkana črta je asimptota napete krivulje, ki podaja najmanjšo porušitveno napetost U_{brMIN} = 0,54 V.

Enosmerni ANOVA test je pokazal statistično značilno razliko srednjih vrednosti ($p<0,001$) porušitvenih napetosti določenih pri različnih naklonih vzbujanja. Vse možne pare U_{br} smo med sabo primerjali s Tukey-evim testom (tabela 8).

Tabela 8. Statistična odvisnost porušitvenih napetosti U_{br} ravninskih dvoslojev iz mešanice lipida POPC:POPS = 3:1 med izmerjenimi vrednostmi pri posameznih naklonih k. Vrednosti v spodnjem delu tabele predstavljajo verjetnost p, da sta srednji vrednosti $U_{br}(k_1)$ in $U_{br}(k_2)$ enaki. Za $p<0,05$ smatramo, da sta vrednosti statistično značilno različni. V zgornjem delu tabele so statistično značilno različne vrednosti označene z 'da' ostale pa z 'ne'.

U_{br} (k)	k=4,8 kV/s	k=5,5 kV/s	k=7,8 kV/s	k=11,5 kV/s	k=16,7 kV/s	k=21,6 kV/s	k=48,1 kV/s
k=4,8 kV/s		ne	ne	ne	da	da	da
k=5,5 kV/s	0,916		ne	ne	da	da	da
k=7,8 kV/s	0,945	1,000		ne	da	da	da
k=11,5 kV/s	0,608	0,132	0,133		ne	da	da
k=16,7 kV/s	0,016	<0,001	<0,001	0,834		da	da
k=21,6 kV/s	<0,001	<0,001	<0,001	<0,001	0,004		da
k=48,1 kV/s	<0,001	<0,001	<0,001	<0,001	<0,001	<0,001	

POPC:POPS = 3:1

4.3 POPC:POPS (1:1)

Meritve na ravninskih lipidnih dvoslojih zgrajenih iz mešanice lipidov POPC in POPS v razmerju 1 proti 1 so bile izvedene pri povprečni temperaturi okolice 23,1 °C. Pri naklonu 16,7 V/ms zasledimo največjo relativno napako meritve porušitvene napetosti 10,2% in relativno napako meritev življenjske dobe 10,4%. Podatki meritev so zbrani v tabeli 9 in grafično prikazani na sliki 31.

Tabela 9. Povprečne vrednosti specifične kapacitivnosti (c_{BLM}), porušitvene napetosti (U_{br}) in življenjske dobe (t_{br}) ravninskih lipidnih dvoslojev sestavljenih iz mešanice 1- palmitil 2 – oleil fosfatidilholina (POPC) in 1- palmitil 2 – oleil fosfatidilserina (POPS) v razmerju 1 proti 1. V tabeli je zajeto število meritev (N) pri posameznem naklonu (k) linearno naraščajočega napetostnega vzbujanja. Podane so povprečne vrednosti in standardne deviacije.

N	k (kV/s)	c_{BLM} (µF/cm^2)	U_{br} (V)	t_{br} (µs)
13	4,8	0,36 ± 0,09	0,48 ± 0,03	101,24 ± 7,39
9	5,5	0,38 ± 0,10	0,53 ± 0,05	96,68 ± 9,12
11	7,8	0,42 ± 0,08	0,53 ± 0,04	69,66 ± 4,60
7	11,5	0,35 ± 0,06	0,55 ± 0,04	48,49 ± 3,55
6	16,7	0,37 ± 0,12	0,59 ± 0,06	35,73 ± 3,70
7	21,6	0,34 ± 0,09	0,63 ± 0,05	28,90 ± 2,30
7	48,1	0,42 ± 0,11	0,72 ± 0,03	15,73 ± 0,73
POPC:POPS (1:1)				

Z napenjanjem intenzivnostno časovne krivulje (enačba (14)) na izmerjene vrednosti porušitvenih napetosti pri različnih naklonih (tabela 9) smo ocenili parametra a = 0,56 V in b = 13,43 µs. Parameter a določa asimptotično vrednost najmanjše porušitvene napetosti U_{brMIN}. Na sliki 31 je označena kot siva črtkana črta. Oceno zaupanja v prosta parametra napete krivulje smo izračunali z Matlab-ovo funkcijo *nlparci*. 95% interval zaupanja za parameter a znaša a = 0,56 V ± 0,05 V in za parameter b = 13.4 µs ± 4.3 µs. Na sliki 31 je pas zaupanja omejen s črnima pika-črta krivuljama.

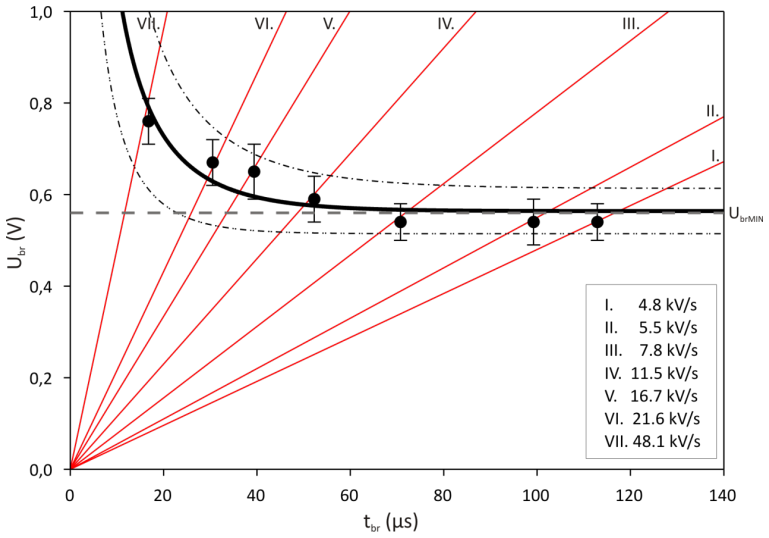

Slika 31. Porušitvena napetost (U_{br}) v odvisnosti od življenjske dobe (t_{br}) ravninskih lipidnih dvoslojev iz 1- palmitil 2 – oleil fosfatidilholina (POPC). Rdeče črte predstavljajo naklone (k) linearno naraščajočega napetostnega vzbujanja. Črna krivulja predstavlja napeto krivuljo na izmerjene vrednosti po enačbi (14). 95% interval zaupanja za koeficienta a in b predstavlja pas med črnima pika-črta krivuljama. Siva črtkana črta je asimptota napete krivulje, ki podaja najmanjšo porušitveno napetost U_{brMIN} = 0,56 V.

Statistično smo srednje vrednosti porušitvenih napetostih preverjali z enosmernim ANOVA testom ($p<0,001$). Statistične primerjave dvojic porušitvene napetosti U_{br} pri različnih naklonih smo izvedli s Tukey-evim testom (tabela 10). Za značilno različne smo imenovali tiste, pri katerih je test hipotezo o enakosti srednjih vrednosti U_{br} zavrgel z verjetnostjo p manjšo od 0,05 ($p<0,05$).

Tabela 10. Statistična odvisnost porušitvenih napetosti U_{br} ravninskih dvoslojev iz mešanice lipida POPC:POPS = 3:1 med izmerjenimi vrednostmi pri posameznih naklonih k. Vrednosti v spodnjem delu tabele predstavljajo verjetnost p, da sta srednji vrednosti $U_{br}(k_1)$ in $U_{br}(k_2)$ enaki. Za $p<0,05$ smatramo, da sta vrednosti statistično značilno različni. V zgornjem delu tabele so statistično značilno različne vrednosti označene z 'da' ostale pa z 'ne'.

U_{br} (k)	k=4,8 kV/s	k=5,5 kV/s	k=7,8 kV/s	k=11,5 kV/s	k=16,7 kV/s	k=21,6 kV/s	k=48,1 kV/s
k=4,8 kV/s		ne	ne	da	da	da	da
k=5,5 kV/s	0,266		ne	ne	ne	da	da
k=7,8 kV/s	0,176	1,000		ne	ne	da	da
k=11,5 kV/s	0,018	0,874	0,881		ne	da	da
k=16,7 kV/s	<0,001	0,119	0,110	0,784		ne	da
k=21,6 kV/s	<0,001	<0,001	<0,001	0,009	0,366		da
k=48,1 kV/s	<0,001	<0,001	<0,001	<0,001	<0,001	0,008	

POPC:POPS = 1:1

4.4 POPC:POPS (1:3)

Meritve na ravninskih lipidnih dvoslojih zgrajenih iz mešanice lipidov POPC in POPS v razmerju 1 proti 3 so bile izvedene pri povprečni temperaturi okolice 26,4 °C. Največja relativna napaka porušitvene napetosti v tej seriji meritev znaša 12,3% pri naklonu vzbujanja 5,5 V/ms. Največjo relativno napako meritve življenjske dobe 12,3% zasledimo pri naklonu 11,5 V/ms. Podatki meritev so zbrani v tabeli 11 in grafično prikazani na sliki 32.

Tabela 11. Povprečne vrednosti specifične kapacitivnosti (c_{BLM}), porušitvene napetosti (U_{br}) in življenjske dobe (t_{br}) ravninskih lipidnih dvoslojev sestavljenih iz mešanice 1- palmitil 2 – oleil fosfatidilholina (POPC) in 1- palmitil 2 – oleil fosfatidilserina (POPS) v razmerju 1 proti 3. V tabeli je zajeto število meritev (N) pri posameznem naklonu (k) linearno naraščajočega napetostnega vzbujanja. Podane so povprečne vrednosti in standardne deviacije.

N	k (kV/s)	c_{BLM} (µF/cm^2)	U_{br} (V)	t_{br} (µs)
14	4,8	0,27 ± 0,18	0,59 ± 0,05	126,02 ± 11,91
11	5,5	0,34 ± 0,16	0,57 ± 0,07	105,58 ± 11,67
12	7,8	0,34 ± 0,16	0,60 ± 0,05	79,34 ± 7,35
10	11,5	0,27 ± 0,14	0,63 ± 0,07	55,80 ± 6,86
8	16,7	0,30 ± 0,14	0,69 ± 0,07	42,73 ± 4,13
11	21,6	0,31 ± 0,19	0,72 ± 0,07	32,98 ± 3,36
9	48,1	0,35 ± 0,19	0,84 ± 0,09	18,51 ± 1,91
POPC:POPS (1:3)				

Koeficienta a = 0,60 V ± 0,04 V in b = 15,5 µs ± 3,8 µs določata potek napete krivulje (enačba (14)) za ravninske lipidne dvosloje zgrajene iz mešanice POPC in POPS v razmerju 1 proti 3. »Prava« porušitvena napetost U_{brMIN} = 0,60V je na sliki 32 prikazana s sivo črtkano črto. Črni pika-črta krivulji določata pas zaupanja krivulji, ki jo določata parametra a in b.

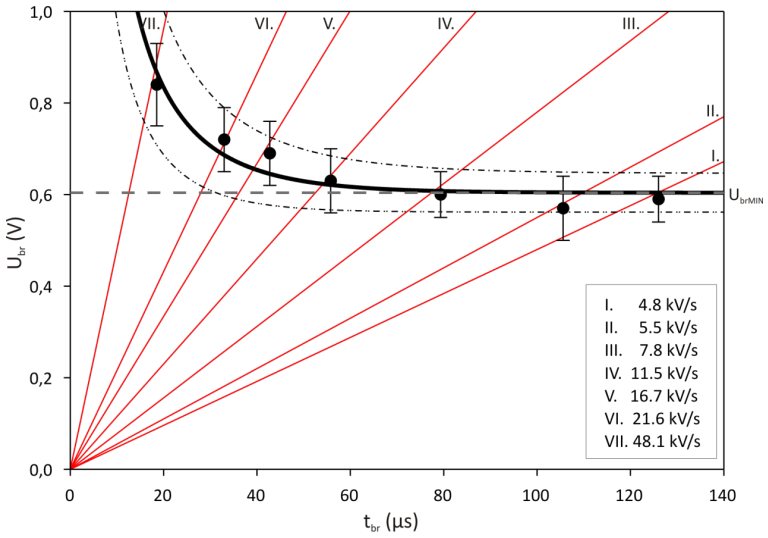

Slika 32. Porušitvena napetost (U_{br}) v odvisnosti od življenjske dobe (t_{br}) ravninskih lipidnih dvoslojev sestavljenih iz mešanice 1- palmitil 2 – oleil fosfatidilholina (POPC) in 1- palmitil 2 – oleil fosfatidilserina (POPS) v razmerju 1 proti 3. Rdeče črte predstavljajo naklone (k) linearno naraščajočega napetostnega vzbujanja. Črna krivulja predstavlja napeto krivuljo na izmerjene vrednosti po enačbi (enačba (14)), črni pika-črta krivulji pa 95% pas zaupanja ocene parametrov krivulje a in b. Siva črtkana črta je asimptota napete krivulje, ki podaja najmanjšo porušitveno napetost U_{brMIN} = 0,60 V.

Porušitvene napetosti pri različnih naklonih se statistično značilno razlikujejo (enosmerni ANOVA test, $p<0,001$). S Tukey-evim testom smo ocenili statistično odvisnost izmerjenih porušitvenih napetosti pri posameznih naklonih (tabela 12).

Tabela 12. Statistična odvisnost porušitvenih napetosti U_{br} ravninskih dvoslojev iz mešanice lipida POPC:POPS = 1:3 med izmerjenimi vrednostmi pri posameznih naklonih k. Vrednosti v spodnjem delu tabele predstavljajo verjetnost p, da sta srednji vrednosti $U_{br}(k_1)$ in $U_{br}(k_2)$ enaki. Za $p<0,05$ smatramo, da sta vrednosti statistično značilno različni. V zgornjem delu tabele so statistično značilno različne vrednosti označene z 'da' ostale pa z 'ne'.

U_{br} (k)	*k=4,8 kV/s*	*k=5,5 kV/s*	*k=7,8 kV/s*	*k=11,5 kV/s*	*k=16,7 kV/s*	*k=21,6 kV/s*	*k=48,1 kV/s*
k=4,8 kV/s		ne	ne	ne	da	da	da
k=5,5 kV/s	0,984		ne	ne	da	da	da
k=7,8 kV/s	1,000	0,952		ne	ne	da	da
k=11,5 kV/s	0,891	0,499	0,964		ne	ne	da
k=16,7 kV/s	0,027	0,005	0,061	0,425		ne	da
k=21,6 kV/s	<0,001	<0,001	0,002	0,052	0,984		da
k=48,1 kV/s	<0,001	<0,001	<0,001	<0,001	<0,001	0,002	

POPC:POPS = 1:3

4.5 POPC:POPS (0:1)

Meritve na ravninskih lipidnih dvoslojih zgrajenih iz lipida POPS so bile izvedene pri povprečni temperaturi okolice 26,1 °C. Največjo relativno napako meritev porušitvene napetosti U_{br} zasledimo pri naklonu 11,5 V/ms in znaša 13,6%. Relativna napaka meritev življenjske dobe t_{br} je največja pri naklonu 7,8 V/ms in znese 13,5%. Podatki meritev so zbrani v tabeli 13 in grafično prikazani na sliki 33.

Tabela 13. Povprečne vrednosti specifične kapacitivnosti (c_{BLM}), porušitvene napetosti (U_{br}) in življenjske dobe (t_{br}) ravninskih lipidnih dvoslojev sestavljenih iz 1- palmitil 2 – oleil fosfatidilserina (POPS). V tabeli je zajeto tudi število meritev (N) pri posameznem naklonu (k) linearno naraščajočega napetostnega vzbujanja. Podane so povprečne vrednosti in standardne deviacije.

N	k (kV/s)	c_{BLM} (µF/cm^2)	U_{br} (V)	t_{br} (µs)
15	4,8	0,43 ± 0,11	0,61 ± 0,04	129,24 ± 7,86
13	5,5	0,53 ± 0,16	0,59 ± 0,05	108,78 ± 8,72
15	7,8	0,48 ± 0,13	0,62 ± 0,08	81,05 ± 10,92
12	11,5	0,53 ± 0,18	0,66 ± 0,09	58,66 ± 7,71
13	16,7	0,47 ± 0,16	0,67 ± 0,05	41,24 ± 3,34
14	21,6	0,50 ± 0,14	0,72 ± 0,06	33,15 ± 2,76
18	48,1	0,44 ± 0,13	0,80 ± 0,04	17,59 ± 0,86
POPC:POPS (0:1)				

Koeficienta eksponentne krivulje (enačba (14)) s 95% intervalom zaupanja sta a = 0,63 V ± 0,04 V in b = 12,2 µs ± 3,5 µs. To pomeni, da je »prava« porušitvena napetost za membrane zgrajene iz POPS U_{brMIN} = 0,63 V in je na sliki 33 prikazana s sivo črtkano črto. Črni pika-črta krivulji določata pas zaupanja krivulji, ki jo določata parametra a in b.

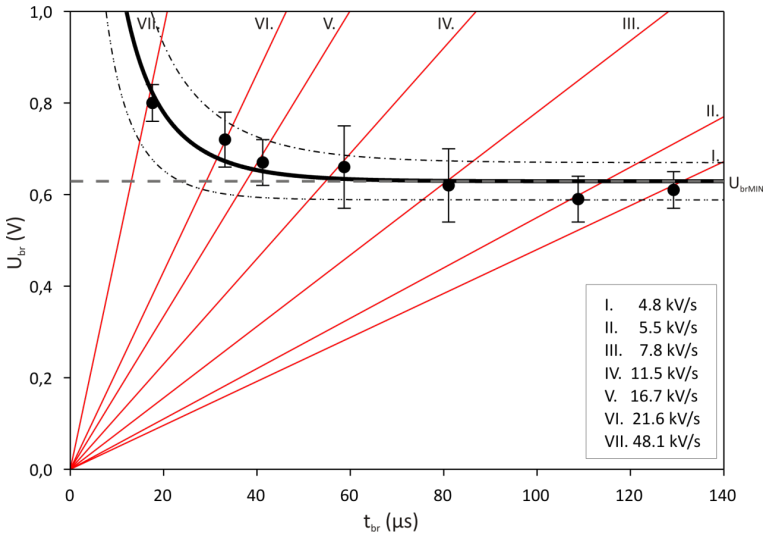

Slika 33. Porušitvena napetost (U_{br}) v odvisnosti od življenjske dobe (t_{br}) ravninskih lipidnih dvoslojev sestavljenih iz 1- palmitil 2 – oleil fosfatidilserina (POPS). Rdeče črte predstavljajo naklone (k) linearno naraščajočega napetostnega vzbujanja. Črna črtasta krivulja predstavlja napeto krivuljo na izmerjene vrednosti po enačbi (14), črni pika-črta krivulji pa 95% pas zaupanja ocene parametrov krivulje a in b. Siva črtkana črta je asimptota napete krivulje, ki podaja najmanjšo porušitveno napetost U_{brMIN} = 0,63 V.

Enosmerna ANOVA statistika pokaže statistično značilno razliko med srednjimi vrednostmi porušitvene napetosti U_{br} pri različnih naklonih vzbujanja (p<0,001). Medsebojne primerjave srednjih vrednosti U_{br} smo opravili s Tukey-evim testom (tabela 14).

Tabela 14. Statistična odvisnost porušitvenih napetosti U_{br} ravninskih dvoslojev iz lipida POPS med izmerjenimi vrednostmi pri posameznih naklonih k. Vrednosti v spodnjem delu tabele predstavljajo verjetnost p, da sta srednji vrednosti $U_{br}(k_1)$ in $U_{br}(k_2)$ enaki. Za p<0,05 smatramo, da sta vrednosti statistično značilno različni. V zgornjem delu tabele so statistično značilno različne vrednosti označene z 'da' ostale pa z 'ne'.

U_{br} (k)	k=4,8 kV/s	k=5,5 kV/s	k=7,8 kV/s	k=11,5 kV/s	k=16,7 kV/s	k=21,6 kV/s	k=48,1 kV/s
k=4,8 kV/s		ne	ne	ne	ne	da	da
k=5,5 kV/s	0,983		ne	ne	da	da	da
k=7,8 kV/s	1,000	0,916		ne	ne	da	da
k=11,5 kV/s	0,267	0,057	0,449		ne	ne	da
k=16,7 kV/s	0,097	0,015	0,200	1,000		ne	da
k=21,6 kV/s	<0,001	<0,001	0,002	0,158	0,320		da
k=48,1 kV/s	<0,001	<0,001	<0,001	<0,001	<0,001	0,006	

POPC:POPS = 1:3

4.6 Primerjava porušitvenih napetosti različnih mešanic ravninskega lipidnega dvosloja

Izmerjene vrednosti porušitvenih napetosti vseh mešanic ravninskih lipidnih dvoslojev smo grafično prikazali na sliki 34.

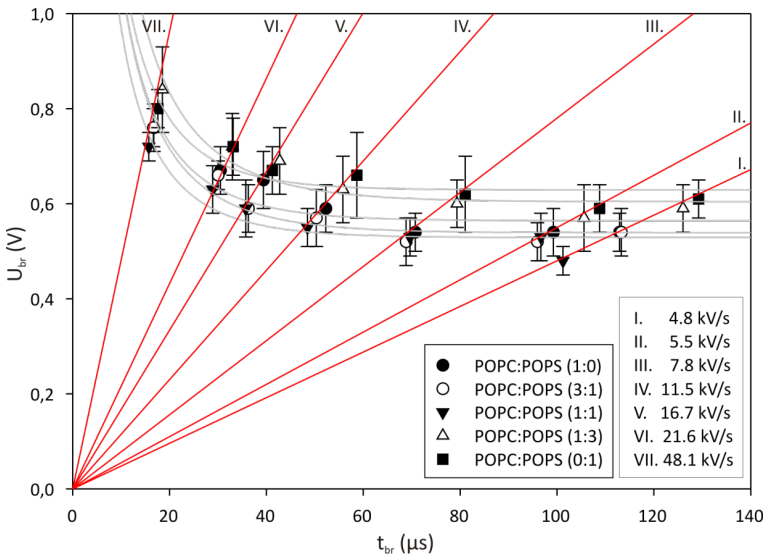

Slika 34. Prikaz porušitvenih napetosti U_{br} v odvisnosti od življenjske dobe t_{br} za vse uporabljene mešanice lipidov (obarvane točke). Rdeče črte predstavljajo naklone (k) linearno naraščajočega napetostnega vzbujanja. Sive polne krivulje predstavljajo podatkom prilagojene funkcijske odvisnosti (enačba (14)) za posamezno mešanico lipida.

Statistično primerjavo porušitvenih napetosti med lipidnimi membranami sestavljenimi samo iz POPC in samo iz POPS smo izvedli s *t-testom* (tabela 15). Vrednosti U_{br} pri naklonih 7,8 kV/s in 11,5 kV/s smo primerjali z Mann-Whitney-evim testom, ker populaciji nista izkazali statistične enakosti varianc, ki jo zahteva *t-test*.

Tabela 15. Statistična primerjava srednjih vrednosti U_{br} pri različnih naklonih k za lipidne dvosloje iz POPC (1-pamitoil 2-oleoil 3-fosfatidilholin) in POPS (1-palmitil 2-oleil 3-fosfatidilserin) s *t-testom*. Vrednosti za k = 7,8 kV/s in k = 11,5 kV/s sta zaradi neizpolnjenega pogoja enakosti varianc primerjani z Mann-Whitney-evim testom.

k	*p*	Stat. različna?
4,8 kV/s	<0,001	da
5,5 kV/s	0,013	da
7,8 kV/s	0,010	da
11,5 kV/s	0,069	ne
16,7 kV/s	0,259	ne
21,6 kV/s	0,010	da
48,1 kV/s	0,025	da

Koeficienti *a* in *b* za vse mešanice so zbrani v tabeli 16 in grafično predstavljeni na sliki 35.

Tabela 16. Parametri krivulje *a* in *b* (enačba (14)) za vse mešanice lipidov.

Lipidi:	parameter *a* (V)	parameter *b* (µs)
POPC:POPS = 1:0	0,56 ± 0,05	13,4 ± 4,3
POPC:POPS = 3:1	0,54 ± 0,04	14,3 ± 3,3
POPC:POPS = 1:1	0,53 ± 0,04	12,7 ± 3,7
POPC:POPS = 1:3	0,60 ± 0,04	15,5 ± 3,8
POPC:POPS = 0:1	0,63 ± 0,04	12,2 ± 3,5

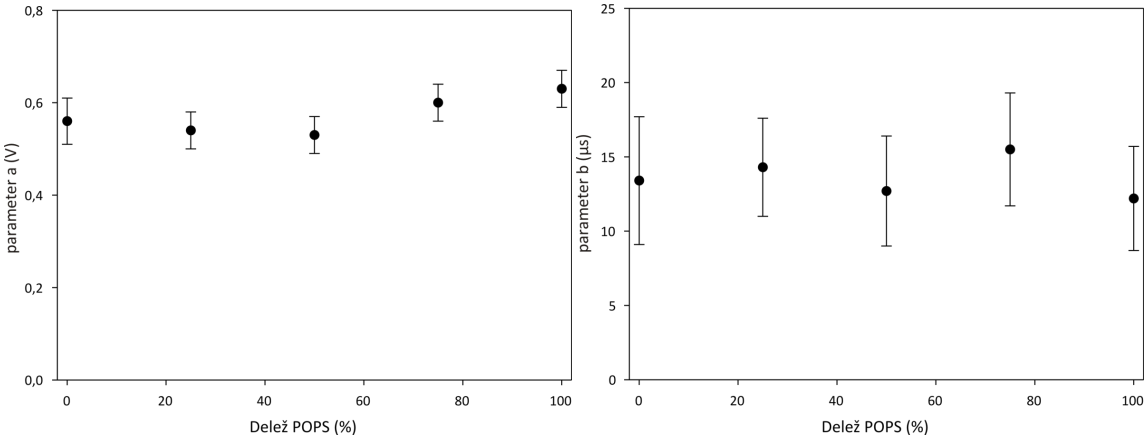

Slika 35. Levo: vrednosti parametra *a* (enačba (14)), ki je enak »pravi« porušitveni napetosti U_{brMIN} v odvisnosti od deleža POPS v mešanici lipida. Področje odstopanja je 95% interval zaupanja. Desno: vrednosti parametra *b* (enačba (14)), ki določa ukrivljenost napete krivulje v odvisnosti od deleža POPS v mešanici lipida. Področje odstopanja je 95% interval zaupanja.

4.7 Zaključki

Kadar raziskujemo metodo elektroporacije v biomedicini in biotehnologiji, je porušitvena napetost ena izmed pomembnejših lastnosti ravninskega lipidnega dvosloja. Ravninski lipidni dvosloj je sicer le preprost model celične membrane, a predvidevamo, da so osnovni principi pojava elektroporacije enaki. Cilj te raziskave je bil poiskati merilni protokol za določitev porušitvene napetosti, s katerim bi se izognili večkratni izpostavitvi ravninskega lipidnega dvosloja električnim pulzom in napetostnemu stresu, ki se pri tem ustvari. Ker je iz literature znano, da prihaja pri izpostavitvah električnim pulzom do velike razpršenosti meritev, si želimo večjo ponovljivost pri določanju življenjske dobe ravninskih lipidnih dvoslojev.

V okviru doktorske disertacije sem želel poiskati metodo, s katero bi omejil vlogo pred-izpostavitve ter zmanjšal naključnost pojava. S predstavljenim merilnim protokolom je ravninski lipidni dvosloj

izpostavljen električnemu stresu le dvakrat. Prvič je izpostavljen električnemu pulzu amplitude 300 mV med merjenjem kapacitivnosti. Z meritvijo kapacitivnosti najlažje kontroliramo kvaliteto ravninskega lipidnega dvosloja. V naslednjem koraku uporabimo linearno naraščajoč napetostni signal ter porušimo ravninski lipidni dvosloj. Trenutek, ko prične skozi ravninski lipidni dvosloj teči tok, določa porušitveno napetost ter življenjsko dobo ravninskega lipidnega dvosloja pri izbranem naklonu linearno naraščajočega napetostnega signala.

Pri poizkusih smo uporabili sedem različnih naklonov linearno naraščajočega napetostnega signala. Za izbiro različnih naklonov smo se odločili na podlagi člankov, ki opisujejo določanje porušitvene napetosti ravninskih lipidnih dvoslojev ter njihovo življenjsko dobo glede na amplitudo pulza [Troiano *et al.* 1998, MačekLebar *et al.* 2002] in vpliva pred-izpostavitve ravninskih lipidnih dvoslojev na življenjsko dobo [Abidor *et al.* 1979]. Naši rezultati kažejo, da sta porušitvena napetost ter življenjska doba ravninskega lipidnega dvosloja funkciji naklona linearno naraščajočega napetostnega signala. Linearno naraščajoča napetost z manjšim naklonom izpostavlja ravninski lipidni dvosloj napetosti dlje časa (daljša pred-izpostavitev), zato je porušitvena napetost nižja kot pri signalih z bolj strmim naklonom. Pri strmem naklonu linearno naraščajočega signala krajšo pred-izpostavitev ravninskega lipidnega dvosloja napetosti. Zaradi krajše pred-izpostavitve ima ravninski lipidni dvosloj višjo porušitveno napetost. Joshi s sodelavci je predstavil teoretični model, v katerem je preučeval nastajanje por v celični membrani v odvisnosti od membranske napetosti ter časa izpostavitve [Joshi in Schoenbach 2000]. S simulacijami sta pokazala, da visokonapetostni pulzi ne povzročijo ireverzibilne poracije na celici, če so le ti dovolj kratki. Leontiadu s sodelavci je z simulacijami pokazal, da je za porušitev ravninskega lipidnega dvosloja potrebno preseči prag [Leontiadu *et al.* 2004]. Zato smo za opis odvisnosti uporabili matematični zapis, ki prag predpostavlja. Asimptota dvo-parametrske krivulje enačbe (14) ustreza porušitveni napetosti specifičnega lipidnega dvosloja. Za ravninske lipidne dvosloje, tvorjene iz lipidnih molekul POPC in POPS, smo izmerili statistično značilne razlike porušitvenih napetosti.

5 Določitev viskoelastičnih lastnosti ravninskega lipidnega dvosloja na podlagi porušitvene napetosti izmerjene z linearno naraščajočim signalom

Mehanske lastnosti ravninskih lipidnih dvoslojev opišemo makroskopsko z uporabo teorije trdnih teles in tekočih kristalov. Helfrich s sodelavci je leta 1973 predlagal teorijo ter možne eksperimente za merjenje elastičnih lastnosti ravninskih lipidnih dvoslojev [Helfrich 1973]. Zaradi anizotropije ravninskega lipidnega dvosloja, je za opis viskoelastičnih lastnosti potrebnih nekaj elastičnih modulov, ki se razlikujejo glede na smer deformacije membrane.

Do sedaj eksperimentalno na ravninskih lipidnih dvoslojih mehanske lastnosti niso bile merjene. Materialne lastnosti lipidnih dvoslojev so določevali na orjaških unilamelarnih veziklih z vzpostavitvijo tlačne razlike [Evans in Needham 1987; Kwok in Evans 1981; Olbrich *et al.* 2000; Rawicz *et al.* 2000; Schneider *et al.* 1984], z magnetno resonanco ter odklonom X-žarkov [Koenig *et al.* 1997]. Meleard s sodelavci je uporabil tehniko video mikroskopije za analizo termičnih nihanj membrane veziklov orjaških unilamelarnih veziklih [Meleard *et al.* 1992]. Genova s sodelavci je z aspiracijo mikropipete na membrani orjaškega unilamelarnega vezikla ustvarjal razliko tlaka, odziv lipidnega dvosloja pa so opazovali z video mikroskopijo [Genova *et al.* 2006]. Na ravninskih lipidnih dvoslojih je Winterhalter s sodelavci ocenil viskoelastične lastnosti brez dodatnega vzbujanja z dinamično svetlobno spektroskopijo [Winterhalter 2000]. Zehl s sodelavci je predstavil Monte Carlo simulacijo za preučevanje fizikalnih lastnosti ravninskih lipidnih dvoslojev [Zehl *et al.* 2006]. Zaradi izredno majhne debeline lipidnega dvosloja ter ekstremno majhnih sprememb debeline ob njegovih deformacijah ne moremo neposredno izmeriti transverzalnega modula elastičnosti. Ocenimo ga lahko preko meritve kapacitivnosti s posebno metodo, ki temelji na merjenju visokih harmonskih frekvenc v amplitudi toka [Hianik 2006].

Sestava ravninskega lipidnega dvosloja vpliva na mehanske lastnosti, kot sta modul elastičnosti ter površinska napetost [Evans in Needham 1987; Rawicz *et al.* 2000; Hianik 2006]. Pri ravninskih lipidnih dvoslojih, zgrajenih iz mešanice lipidnih molekul, privzamemo, da je mešanje lipidov enakomerno. Modul elastičnosti ravninskega lipidnega dvosloja se spreminja ob uporabi različnih topil ter ob dodajanju različnih površinsko aktivnih molekul, kot je na primer holesterol [Evans in Needham 1987; Hianik 2006].

Cilj raziskave je bil določiti mehanske lastnosti ravninskega lipidnega dvosloja. Uporabili smo rezultate meritev, ki so bile opisane v prejšnjem razdelku. Na izmerjene točke porušitvene napetosti

in življenjske dobe posamezne mešanice ravninskega lipidnega dvosloja smo napeli krivuljo modela , ki ga je razvil Dimitrov [Dimitrov 1984]. Model povezuje porušitveno napetost in porušitveni čas ravninskega lipidnega dvosloja, pri čemer upošteva odvisnost teh parametrov od mehanskih lastnosti: Youngovega modula elastičnosti (E), površinske napetosti (σ) in viskoznosti (μ). Glavno vprašanje, ki smo si ga zastavili ob računanju, je bilo ali so iz meritev porušitvene napetosti U_{br} in življenjskega časa t_{br} prek modela dobljene vrednosti Youngovega modula elastičnosti E in površinske napetosti σ primerljive s tistimi, ki so že objavljene v literaturi. Raziskovali smo tudi vpliv mešanice lipidnih molekul na elastičnost in površinsko napetost ravninskega lipidnega dvosloja.

5.1 Viskoelastični model ravninskega lipidnega dvosloja

5.1.1 Predstavitev modela

Predpostavljamo, da je ravninski lipidni dvosloj tanek viskoelastični film sestavljen iz dveh plasti A in B debeline H_A in H_B. Notranji ravnini obeh plasti sta sklenjeni, zunanji pa nihata z amplitudo ζ. Za model veljajo predpostavke, da je amplituda površinskega nihanja plasti A in B (slika 36A) manjša od debeline ravninskega lipidnega dvosloja ($\zeta_{A,B} \ll h$). Odklone površine ravninskega lipidnega dvosloja od mirovne lege H_A oziroma H_B predstavimo s superpozicijo površinskih valov z valovno dolžino λ_n, ki je mnogo daljša od debeline ravninskega lipidnega dvosloja h. Opazovali bomo poljubni površinski val in valovno dolžino izražali z valovnim številom k.

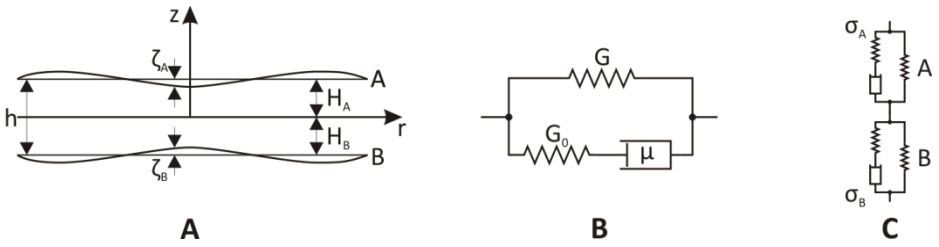

Slika 36. Viskoelastični model ravninskega lipidnega dvosloja. A) Predpostavljamo, da je ravninski lipidni dvosloj sestavljen iz dveh plasti A in B. Debelini posameznih plasti H_A in H_B sta enaki in skupaj znašata h. Amplitude odklonov so ponazorjene z ζ_A in ζ_B. B) Osnovni linearni model trdnega telesa, kjer sta G_0 in G elastična modula, μ pa viskoznost telesa. C) Viskoelastični model ravninskega lipidnega dvosloja predstavljen z osnovnim linearnim modelom trdnega telesa za plast A in B posamezno.

Predpostavimo tudi, da je ravninski lipidni dvosloj nestisljivo telo in se vede kot viskoelastični in izotropni material predstavljen z osnovnim linearnim modelom trdnega telesa (slika 36B), kjer G in G_0 predstavljata elastična modula, μ pa viskoznost telesa. Deformacijo ravninskega lipidnega dvosloja povzroči tlak, ki ga ustvarimo s pritisnjeno napetostjo U na ravninski lipidni dvosloj. Gostoto električne energije na ravninskem lipidnem dvosloju izrazimo z enačbo:

$$\Pi = \Pi_{el} = -\varepsilon_m \varepsilon_0 \frac{U^2}{2h^2}. \qquad (31)$$

Z odvajanjem gostote električne energije po debelini ravninskega lipidnega dvosloja *h* dobimo tlak na ravninskem lipidnem dvosloju, ki ga povzroči zunanja napetost:

$$\Pi' = \frac{d\Pi}{dh} = \varepsilon_m \varepsilon_0 \frac{U^2}{h^3}. \tag{32}$$

Predpostavimo tudi, da so tangencialne komponente površinske napetosti izredno majhne in da jih lahko zanemarimo. Površinsko napetost ravninskega lipidnega dvosloja predstavimo z dvema vzporednima vzmetema A in B plasti (slika 36C):

$$\overline{\sigma} = \frac{\sigma_A \cdot \sigma_B}{\sigma_A + \sigma_B}. \tag{33}$$

Nihanje zgornje ζ_A in spodnje ζ_B plasti ravninskega lipidnega dvosloja opisuje kompleksni parameter ω:

$$\omega = \beta + i\gamma\,, \tag{34}$$

kjer realni del β določa odmik ravninskega lipidnega dvosloja od osnovne ravnine, imaginarni del γ pa nihanje ravninskega lipidnega dvosloja. Vrednost koeficienta β nam predstavlja stanja ravninskega lipidnega dvosloja:

- $\beta > 0$ na ravninskem lipidnem dvosloju se pojavijo motnje, poviša se upognjenost membrane in posledično porušitev ravninskega lipidnega dvosloja,
- $\beta = 0$ ravninski lipidni dvosloj je labilno stabilen,
- $\beta < 0$ ravninski lipidni dvosloj je stabilen.

Poljubno obliko lahko opišemo kot superpozicijo valov, ki jih okarakterizirajo valovna števila *k*. Valovno število *k*, ki ustreza labilni stabilnosti imenujemo kritično valovno število k_c. Običajno so valovi *k* manjši od k_c, kar pomeni, da je ravninski lipidni dvosloj stabilen. Poleg teh valov imamo opravka še z dominantnim valom, določenim z valovnim številom k_d, pri katerih ima β maksimum. Ti valovi povzročijo, da se memrbrana poruši. Čas porušitve τ je obratno sorazmeren koeficientu β [Dimitrov 1984]:

$$\tau \approx \frac{1}{\beta} \tag{35}$$

$$\mathrm{Re}(\omega)=\beta=\frac{12G+h^3k^3\left(\bar{\sigma}k^2-\Pi'\right)}{12\mu\left(1+\frac{G}{G_0}\right)+\frac{\mu h^3k^2\left(\bar{\sigma}k^2-\Pi'\right)}{G_0}}. \tag{36}$$

Vpeljemo poenostavitve viskoelastičnega modela [Dimitrov 1984]:

1. $G_0=\infty$
2. $\sigma_A=\sigma_B=\sigma \Rightarrow$ simetrična membrana $\Rightarrow \bar{\sigma}=\frac{\sigma}{2}$

V osnovno enačbo (36) vnesemo naštete predpostavke modela:

$$\begin{aligned}
\beta &= -\frac{12G+h^3k^2\left(\bar{\sigma}k^2-\Pi'\right)}{12\mu\left(1+\frac{G}{G_0}\right)+\frac{\mu h^3k^2\left(\bar{\sigma}k^2-\Pi'\right)}{G_0}} \\
&= -\frac{12G+h^3k^2\left(\bar{\sigma}k^2-\Pi'\right)}{\frac{12\mu G_0+12\mu G+\mu h^3k^2\left(\bar{\sigma}k^2-\Pi'\right)}{G_0}} \\
&= -\frac{G_0\left[12G+h^3k^2\left(\bar{\sigma}k^2-\varepsilon_m\varepsilon_0\frac{U^2}{h^3}\right)\right]}{12\mu G_0+12\mu G+\mu h^3k^2\left(\bar{\sigma}k^2-\varepsilon_m\varepsilon_0\frac{U^2}{h^3}\right)} \\
&= -\frac{G_0\left[12G+h^3k^4\bar{\sigma}-k^2\varepsilon_m\varepsilon_0U^2\right]}{12\mu G_0+12\mu G+\mu h^3k^4\bar{\sigma}-\mu k^2\varepsilon_m\varepsilon_0U^2} \\
&= -\frac{12G+h^3k^4\bar{\sigma}-k^2\varepsilon_m\varepsilon_0U^2}{12\mu+\underbrace{12\mu\frac{G}{G_0}}_{\Rightarrow 0}+\underbrace{\frac{\mu h^3k^4\bar{\sigma}}{G_0}}_{\Rightarrow 0}-\underbrace{\frac{\mu k^2\varepsilon_m\varepsilon_0U^2}{G_0}}_{\Rightarrow 0}}
\end{aligned} \tag{37}$$

Zaradi prve predpostavke, kjer smo določili, da obravnavamo Kelvinovo telo ($G_0 = \infty$), so zadnji trije členi v imenovalcu enaki nič. Sledi,

$$\begin{aligned}
\beta &= -\frac{G}{\mu}-\frac{h^3\bar{\sigma}k^4}{12\mu}+\frac{\varepsilon_m\varepsilon_0k^2U^2}{12\mu} \\
&= -\frac{G}{\mu}-\frac{h^3\frac{\sigma}{2}k^4}{12\mu}+\frac{\varepsilon_m\varepsilon_0k^2U^2}{12\mu} \\
&= -\frac{G}{\mu}-\frac{h^3\sigma k^4}{24\mu}+\frac{\varepsilon_m\varepsilon_0k^2U^2}{12\mu}.
\end{aligned} \tag{38}$$

Porušitev membrane pričakujemo pri največji vrednosti koeficienta β, pri katerem je $k = k_d$. V tem primeru ravninski lipidni dvosloj najbolj zaniha in je verjetnost porušitve največja:

$$\left.\frac{\partial\beta}{\partial k}\right|_{k=k_d} = 0\,. \tag{39}$$

Poiščemo odvod rastnega koeficienta β po valovnem številu:

$$\frac{\partial\beta}{\partial k} = \frac{\partial}{\partial k}\left(-\frac{G}{\mu} - \frac{h^3\sigma}{24\mu}k^4 + \frac{\varepsilon_m\varepsilon_0U^2}{12\mu}k^2\right) = -\frac{h^3\sigma}{6\mu}k^3 + \frac{\varepsilon_m\varepsilon_0U^2}{6\mu}k \tag{40}$$

in izpolnimo enačbo (39):

$$\begin{aligned} -\frac{h^3\sigma}{6\mu}k_d^3 + \frac{\varepsilon_m\varepsilon_0U^2}{6\mu}k_d &= 0 \\ \frac{\varepsilon_m\varepsilon_0U^2}{\cancel{6\mu}} &= \frac{h^3\sigma}{\cancel{6\mu}}k_d^2,\ k_d \neq 0 \\ k_d^2 &= \frac{\varepsilon_m\varepsilon_0U^2}{h^3\sigma}. \end{aligned} \tag{41}$$

Vrednost k_d vstavimo v enačbo (38):

$$\begin{aligned} \beta_d &= \beta\left(k = k_d\right) \\ &= -\frac{G}{\mu} - \frac{h^3\sigma}{24\mu}\cdot\frac{\varepsilon_m^2\varepsilon_0^2U^4}{h^6\sigma^2} + \frac{\varepsilon_m\varepsilon_0U^2}{12\mu}\cdot\frac{\varepsilon_m\varepsilon_0U^2}{h^3\sigma} \\ &= -\frac{G}{\mu} - \frac{\varepsilon_m^2\varepsilon_0^2U^4}{24\mu h^3\sigma} + \frac{\varepsilon_m^2\varepsilon_0^2U^4}{12\mu h^3\sigma} \\ &= -\frac{G}{\mu} + \frac{\varepsilon_m^2\varepsilon_0^2U^4}{24\mu h^3\sigma} \\ &= \frac{\varepsilon_m^2\varepsilon_0^2U^4 - 24Gh^3\sigma}{24\mu h^3\sigma} \end{aligned} \tag{42}$$

Rezultat ustreza dominantnemu koeficientu β_d. Z upoštevanjem enačbe (35) dobimo enačbo za življenjski čas ravninskega lipidnega dvosloja:

$$\tau \approx \frac{1}{\beta_d} \approx \frac{24\mu h^3\sigma}{\varepsilon_m^2\varepsilon_0^2U^4 - 24Gh^3\sigma} \approx \frac{\frac{\mu}{G}}{\left(\frac{\varepsilon_m^2\varepsilon_0^2U^4}{24Gh^3\sigma} - 1\right)}. \tag{43}$$

Da se znebimo znaka približno, privzamemo sorazmernostno konstanto α. Funkcijo naravnega logaritma vpeljemo iz predpostavke, da je sistemu lastno nihanje zaradi Bravnovega gibanja $\zeta_0 \ll h$, v nasprotnem primeru pa bo življenjski čas enak nič.

$$\alpha \doteq \ln\left(\frac{h}{2\zeta_0}\right). \tag{44}$$

Enačbo (43) zapišemo:

$$\tau = \alpha \frac{\frac{\mu}{G}}{\left(\frac{\varepsilon_m^2 \varepsilon_0^2 U^4}{24Gh^3\sigma} - 1\right)} \tag{45}$$

Posledice:

I. Porušitvena napetost U_c pri $\tau \to \infty$

Iz enačbe (45) izpostavimo napetost:

$$\begin{aligned}
&\tau\left(\frac{\varepsilon_m^2 \varepsilon_0^2 U^4}{24Gh^3\sigma} - 1\right) = \alpha\frac{\mu}{G} \\
&\frac{\varepsilon_m^2 \varepsilon_0^2 U^4}{24Gh^3\sigma} - 1 = \frac{\alpha\mu}{G\tau} \Big/ 24Gh^3\sigma \\
&\varepsilon_m^2 \varepsilon_0^2 U^4 - 24Gh^3\sigma = \frac{\alpha\mu}{G\tau} 24Gh^3\sigma \\
&U^4 = \frac{1}{\varepsilon_m^2 \varepsilon_0^2}\left[24Gh^3\sigma\left(1 + \frac{\alpha\mu}{G\tau}\right)\right]
\end{aligned} \tag{46}$$

In dobimo končno enačbo:

$$U = \sqrt[4]{\frac{1}{\varepsilon_m^2 \varepsilon_0^2}\left[24Gh^3\sigma\left(1 + \frac{\alpha\mu}{G\tau}\right)\right]}. \tag{47}$$

Poglejmo enačbo(46), v primeru ko se parameter $\tau \to \infty$:

$$\lim_{\tau\to\infty} U = U_c$$
$$\lim_{\tau\to\infty} U = \lim_{\tau\to\infty} \sqrt[4]{\frac{1}{\varepsilon_m^2\varepsilon_0^2}\left[24Gh^3\sigma\left(1+\underbrace{\frac{\alpha\mu}{G\tau}}_{=0}\right)\right]} \tag{48}$$
$$U_c = \sqrt[4]{\frac{24Gh^3\sigma}{\varepsilon_m^2\varepsilon_0^2}},$$

oziroma

$$U_c^2 = \frac{2h}{\varepsilon_m\varepsilon_0}\sqrt{6\sigma Gh} \tag{49}$$

II. Z naraščajočo napetostjo se čas potreben za porušitev ravninskega lipidnega dvosloja τ zmanjšuje.

Enačbo (45) preoblikujemo

$$\frac{\tau G}{\alpha\mu} = \left[\frac{\varepsilon_m^2\varepsilon_0^2U^4}{24Gh^3\sigma} - 1\right]^{-1} \tag{50}$$

In naredimo substitucijo spremenljivk

$$\begin{aligned}\overline{\tau} &= \frac{G}{\alpha\mu}\tau \\ \overline{U}^4 &= \frac{\varepsilon_m^2\varepsilon_0^2U^4}{24Gh^3\sigma}.\end{aligned} \tag{51}$$

Dobimo enačbo:

$$\begin{aligned}\overline{\tau} &= \left[\overline{U}^4 - 1\right]^{-1} \\ \overline{\tau}^{-1} &= \overline{U}^4 - 1 \\ \overline{U}^4 &= \overline{\tau}^{-1} + 1 \\ \overline{U} &= \sqrt[4]{\overline{\tau}^{-1}+1} \Rightarrow \overline{U} = \sqrt[4]{1+10^{-\log(\tau)}}\end{aligned} \tag{52}$$

Upoštevajmo še, da je Youngov modul elastičnosti zaradi obravnavanja nestisljivega telesa enak $E = 3 \cdot G$ [Dimitrov 1984] ter ga vstavimo v enačbo (49)

$$U_c^2 = \frac{2h}{\varepsilon_m \varepsilon_0} \sqrt{2\sigma Eh} = \frac{Eh^2}{\varepsilon_m \varepsilon_0} \sqrt{\frac{8\sigma}{Eh}}. \tag{53}$$

5.1.2 Uporaba modela

V splošni enačbi viskoelastičnega modela (47) je zapisana relacija med porušitveno napetostjo U in življenjskim časom τ ravninskega lipidnega dvosloja. Privzamemo, da se vsi ostali parametri v enačbi ne spreminjajo, zato lahko zapišemo enačbo:

$$U = \sqrt[4]{a_D + \frac{b_D}{\tau}}, \tag{54}$$

kjer parametra a_D in b_D ustrezata

$$\begin{aligned} a_D &= U_c^4 = \frac{8h^2}{\varepsilon_m^2 \varepsilon_0^2} \sigma Eh \\ b_D &= \frac{24h^3 \sigma \alpha \mu}{\varepsilon_m^2 \varepsilon_0^2}. \end{aligned} \tag{55}$$

Specifično kapacitivnost ravninskega lipidnega dvosloja izrazimo kot

$$c_{BLM} = \frac{\varepsilon_m \varepsilon_0}{h} \tag{56}$$

In jo lahko vstavimo v enačbi (55) za izračun parametrov a_D in b_D:

$$\begin{aligned} a_D &= \frac{8}{c_{BLM}^2} \sigma Eh \\ b_D &= \frac{24}{c_{BLM}^2} h \sigma \alpha \mu \end{aligned} \tag{57}$$

Krivuljo (54) smo napeli na rezultate meritev porušitvene napetosti ravninskega lipidnega dvosloja z linearno naraščajočim signalom predstavljene v poglavju 4, kjer nam U predstavlja porušitveno napetost U_{br}, τ pa življenjski čas ravninskega lipidnega dvosloja t_{br}. Iz parametrov a_D in b_D smo izračunali Youngov modul elastičnosti (E) in površinsko napetosti (σ) ravninskega lipidnega dvosloja.

Preostale parametre smo privzeli po Dimitrovu [Dimitrov 1984]. Sorazmernostna konstanta osnovnih fluktuacij α = 2, viskoznost μ = 6 Ns/m2 in debelina ravninskega lipidnega dvosloja h = 3,5 nm.

Iz meritev porušitvene napetosti v poglavju 4 smo podali rezultate za specifično kapacitivnost c_{BLM}, porušitveno napetost U_{br} in življenjski čas t_{br} ravninskih lipidnih dvoslojev zgrajenih iz POPC (1-pamitoil 2-oleoil 3-fosfatidilholin), POPS (1-palmitil 2-oleil 3-fosfatidilserin) in mešanic POPC in POPS v petih različnih razmerjih (1:0, 3:1, 1:1, 1:3 in 0:1). Z uporabo viskoelastičnega modela opisanega v poglavju 5.1.1 smo določili Youngov modul elastičnosti (E) in površinske napetosti (σ) ravninskega lipidnega dvosloja za posamezno mešanico lipidov.

5.1.3 POPC:POPS (1:0)

Za ravninske lipidne dvosloje zgrajene izključno iz POPC molekul smo naredili 106 uspešnih poizkusov. Njihova povprečna vrednost specifične kapacitivnosti je bila 0,51 ± 0,07 µF/cm^2. Na povprečne vrednosti izmerjenih porušitvenih napetosti U_{br} pri posameznem naklonu k smo napeli viskoelastični model ravninskega lipidnega dvosloja (enačba (54)). Iz parametrov modela a_D = (3,20 ± 1,37) 10^{-2} V^4 ter b_D = 5,0 ± 0,8 V^{4}µs smo izračunali Youngov modul elastičnosti E = 23,09 ± 0,37 N/cm^2 ter površinsko napetost σ = (12,90 ± 3,50)·10^{-5} J/m^2 (slika 37).

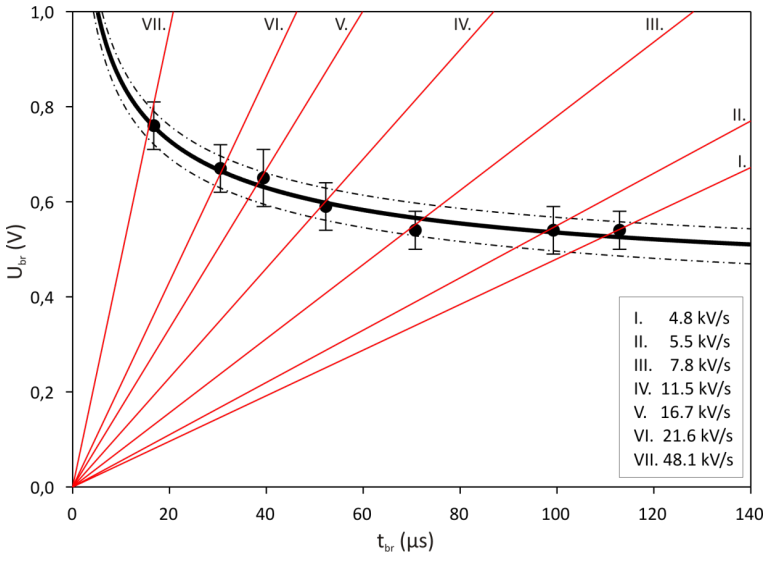

Slika 37. Porušitvena napetost (U_{br}) v odvisnosti od življenjske dobe (t_{br}) ravninskih lipidnih dvoslojev iz 1-palmitil 2–oleil 3-fosfatidilholina (POPC). Rdeče črte predstavljajo naklone (k) linearno naraščajočega napetostnega vzbujanja. Črna krivulja predstavlja napeto krivuljo na izmerjene vrednosti po enačbi (54). Pas med črnima pika-črta krivuljama predstavlja 68% interval zaupanja za koeficienta a_D in b_D.

5.1.4 POPC:POPS (3:1)

Za ravninske lipidne dvosloje zgrajene iz mešanice POPC in POPS v razmerju 3:1 smo naredili 89 uspešnih poizkusov. Njihova povprečna vrednost kapacitivnosti je bila 0,17 ± 0,06 μF/cm^2. Na povprečne vrednosti izmerjenih porušitvenih napetosti U_{br} pri posameznem naklonu k smo napeli viskoelastični model ravninskega lipidnega dvosloja (enačba (54)). Iz parametrov modela a_D = (2,33 ± 0,75) 10^{-2} V^4 ter b_D = 4,8 ± 0,6 V^{4}μs smo izračunali Youngov modul elastičnosti E = 17,61 ± 0,21 N/cm^2 ter površinsko napetost σ = (12,90 ± 3,50)·10^{-5} J/m^2 (slika 38).

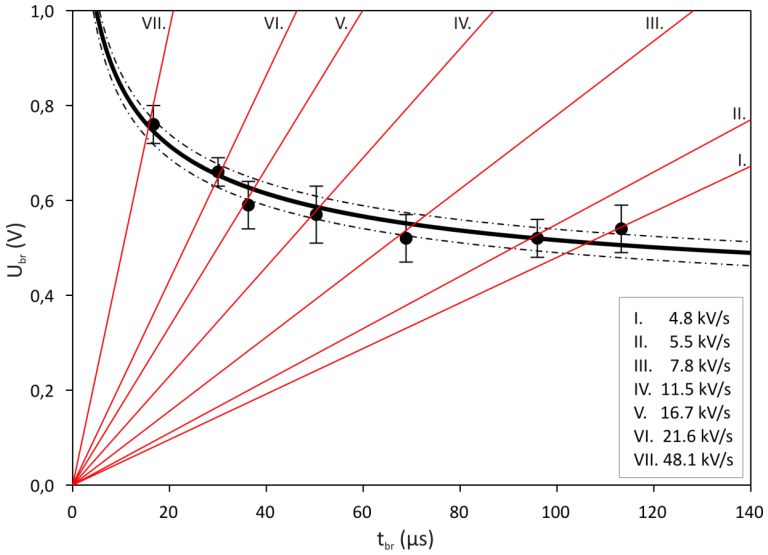

Slika 38. Porušitvena napetost (U_{br}) v odvisnosti od življenjske dobe (t_{br}) ravninskih lipidnih dvoslojev sestavljenih iz mešanice 1-palmitil 2–oleil 3-fosfatidilholina (POPC) in 1-palmitil 2–oleil fosfatidilserina (POPS) v razmerju 3 proti 1. Rdeče črte predstavljajo naklone (k) linearno naraščajočega napetostnega vzbujanja. Črna krivulja predstavlja napeto krivuljo na izmerjene vrednosti po enačbi (54). Pas med črnima pika-črta krivuljama predstavlja 68% interval zaupanja za koeficienta a_D in b_D.

5.1.5 POPC:POPS (1:1)

Za ravninske lipidne dvosloje zgrajene iz mešanice POPC in POPS v razmerju 1:1 smo naredili 60 uspešnih poizkusov. Njihova povprečna vrednost kapacitivnosti je bila 0,31 ± 0,07 μF/cm^2. Na povprečne vrednosti izmerjenih porušitvenih napetosti U_{br} pri posameznem naklonu k smo napeli viskoelastični model ravninskega lipidnega dvosloja (enačba (54)). Iz parametrov modela a_D = (1,99 ± 0,64) 10^{-2} V^4 ter b_D = 3,9 ± 0,5 V^{4}μs smo izračunali Youngov modul elastičnosti E = 18,48 ± 0,24 N/cm^2 ter površinsko napetost σ = (3,69 ± 1,67)·10^{-5} J/m^2 (slika 39).

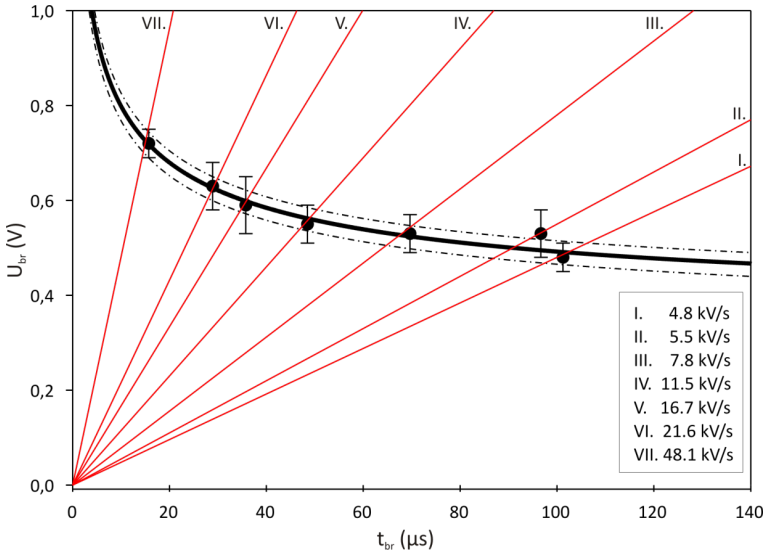

Slika 39. Porušitvena napetost (U_{br}) v odvisnosti od življenjske dobe (t_{br}) ravninskih lipidnih dvoslojev sestavljenih iz mešanice 1-palmitil 2–oleil fosfatidilholina (POPC) in 1-palmitil 2–oleil fosfatidilserina (POPS) v razmerju 1 proti 1. Rdeče črte predstavljajo naklone (k) linearno naraščajočega napetostnega vzbujanja. Črna krivulja predstavlja napeto krivuljo na izmerjene vrednosti po enačbi (54). Pas med črnima pika-črta krivuljama predstavlja 68% interval zaupanja za koeficienta a_D in b_D.

5.1.6 POPC:POPS (1:3)

Za ravninske lipidne dvosloje zgrajene iz mešanice POPC in POPS v razmerju 1:3 smo naredili 75 uspešnih poizkusov. Njihova povprečna vrednost kapacitivnosti je bila 0,24 ± 0,14 μF/cm^2. Na povprečne vrednosti izmerjenih porušitvenih napetosti U_{br} pri posameznem naklonu k smo napeli viskoelastični model ravninskega lipidnega dvosloja (enačba (54)). Iz parametrov modela a_D = (4,70 ± 1,06) 10^{-2} V^4 ter b_D = 7,4 ± 1,5 V^{4}μs smo izračunali Youngov modul elastičnosti E = 22,90 ± 0,28 N/cm^2 ter površinsko napetost σ = (4,22 ± 4,92)·10^{-5} J/m^2 (slika 40).

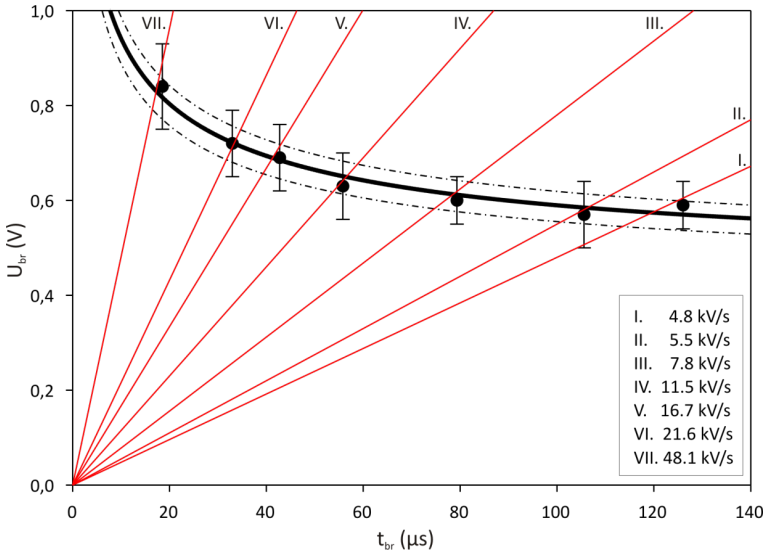

Slika 40. Porušitvena napetost (U_{br}) v odvisnosti od življenjske dobe (t_{br}) ravninskih lipidnih dvoslojev sestavljenih iz mešanice 1-palmitil 2–oleil fosfatidilholina (POPC) in 1-palmitil 2–oleil fosfatidilserina (POPS) v razmerju 1 proti 3. Rdeče črte predstavljajo naklone (k) linearno naraščajočega napetostnega vzbujanja. Črna krivulja predstavlja napeto krivuljo na izmerjene vrednosti po enačbi (54). Pas med črnima pika-črta krivuljama predstavlja 68% interval zaupanja za koeficienta a_D in b_D.

5.1.7 POPC:POPS (0:1)

Za ravninske lipidne dvosloje zgrajene izključno iz POPS molekul smo naredili 106 uspešnih poizkusov. Njihova povprečna vrednost kapacitivnosti je bila 0,41 ± 0,13 μF/cm^2. Na povprečne vrednosti izmerjenih porušitvenih napetosti U_{br} pri posameznem naklonu k smo napeli viskoelastični model ravninskega lipidnega dvosloja (enačba (54)). Iz parametrov modela a_D = (8,36 ± 2,14) 10^{-2} V^4 ter b_D = 5,6 ± 1,1 V^{4}μs smo izračunali Youngov modul elastičnosti E = 53,37 ± 0,65 N/cm^2 ter površinsko napetost σ = (9,41 ± 0,60)·10^{-5} J/m^2 (slika 41).

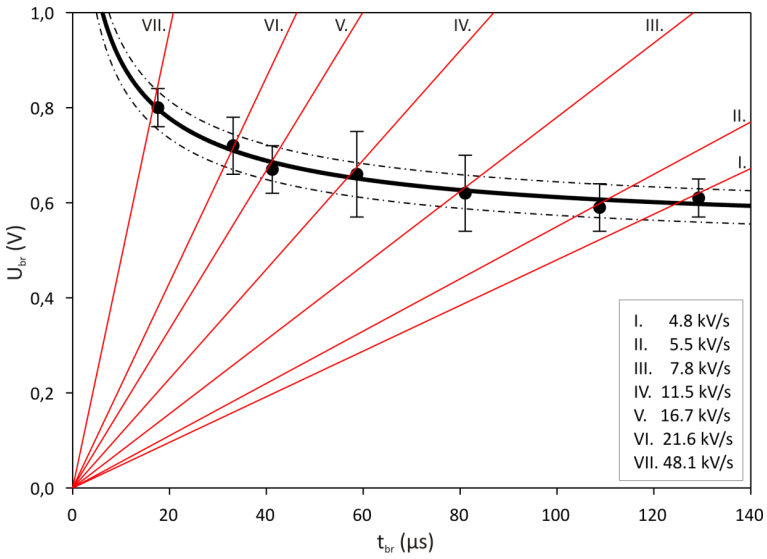

Slika 41. Porušitvena napetost (U_{br}) v odvisnosti od življenjske dobe (t_{br}) ravninskih lipidnih dvoslojev sestavljenih iz 1-palmitil 2–oleil fosfatidilserina (POPS). Rdeče črte predstavljajo naklone (k) linearno naraščajočega napetostnega vzbujanja. Črna krivulja predstavlja napeto krivuljo na izmerjene vrednosti po enačbi (54). Pas med črnima pika-črta krivuljama predstavlja 68% interval zaupanja za koeficienta a_D in b_D.

5.1.8 Primerjava mešanic

Parametra krivulje (enačba (54)) a_D in b_D, izmerjena specifična kapacitivnost c_{BLM} ravninskega lipidnega dvosloja ter izračunani vrednosti Youngov modul elastičnosti (E) in površinske napetosti (σ) so za vse obravnavane sestave ravninskih lipidnih dvoslojev podani v tabeli 17 ter prikazani na sliki 42.

Tabela 17. Zbrane vrednosti parametrov a_D in b_D, izmerjena specifična kapacitivnost c_{BLM} ravninskega lipidnega dvosloja ter izračunane vrednosti elastičnosti E in površinske napetosti σ, ravninskih lipidnih dvoslojev zgrajenih iz različnih koncentracij lipidov POPC in POPS.

POPC:POPS	N	a_D (10^{-2} V^4)	b_D (V^{4}µs)	c_{BLM} (µF/cm^2)	E (N/cm^2)	σ (10^{-5} J/m^2)
1:0	106	3,20 ± 1,37	5,0 ± 0,8	0,51 ± 0,17	23,09 ± 0,37	12,90 ± 3,50
3:1	89	2,33 ± 0,75	4,8 ± 0,6	0,17 ± 0,06	17,61 ± 0,21	1,37 ± 0,96
1:1	60	1,99 ± 0,64	3,9 ± 0,5	0,31 ± 0,07	18,48 ± 0,24	3,69 ± 1,67
1:3	75	4,70 ± 1,06	7,4 ± 1,5	0,24 ± 0,14	22,90 ± 0,28	4,22 ± 4,92
0:1	100	8,36 ± 2,14	5,6 ± 1,1	0,41 ± 0,13	53,37 ± 0,65	9,41 ± 0,60

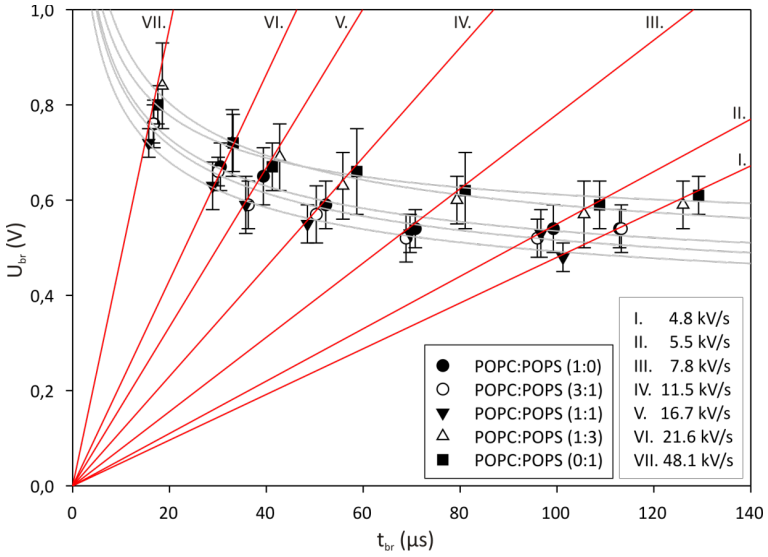

Slika 42. Prikaz porušitvenih napetosti U_{br} v odvisnosti od življenjske dobe t_{br} za vse uporabljene mešanice lipidov (obarvane točke). Rdeče črte predstavljajo naklone (k) linearno naraščajočega napetostnega vzbujanja. Sive polne krivulje predstavljajo podatkom prilagojene funkcijske odvisnosti viskoelastičnega modela (enačba (54)) za posamezno mešanico lipida.

Na sliki 43 sta predstavljena parametra a_D in b_D določena iz podatkov porušitvenih napetosti prilagojenih na viskoelastični model ter izračunan Yungov modul elastičnosti ter površinska napetost ravninskega lipidnega dvosloja za različne mešanice. Enokomponentni ravninski lipidni dvosloji

zgrajeni iz molekul POPS imajo značilno večji Youngov modul elastičnosti *E*. Ravninski lipidni dvosloji zgrajeni iz POPC lipidnih molekul dosežejo višjo površinsko napetost *σ* ob porušitvi.

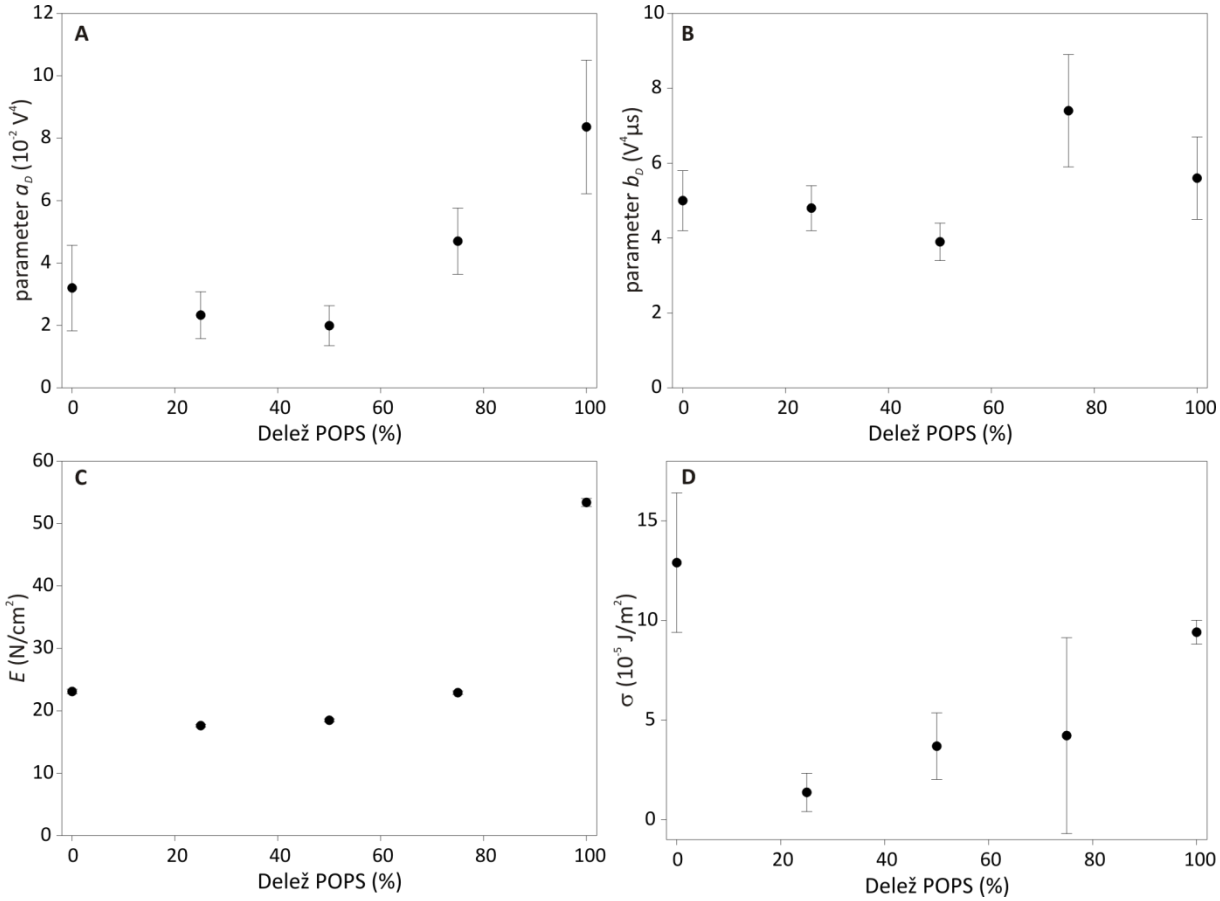

Slika 43. Zgoraj: parametera a_D (A) in b_D (B) izračunana iz viskoelastičnega modela napetega na na rezultate merjenja porušitvene napetosti pri različnih mešanicah POPC in POPS ravninskih lipidnih dvoslojih. Spodaj: Youngov modul elastičnosti *E* (C) in površinska napetost *σ* (D) na ravninskem lipidnem dvosloju izračunana iz parametrov a_D in b_D.

5.2 Zaključki

Za določitev Youngovega modula elastičnosti *E* in površinske napetosti *σ* ravninskega lipidnega dvosloja smo uporabili viskoelastični model ravninskega lipidnega dvosloja, ki ga je opisal Dimitrov [Dimitrov 1984]. Model povezuje kapacitivnost, Youngov modul elastičnosti, viskoznost, površinsko napetost, življenjski dobo in porušitveno napetost ravninskega lipidnega dvosloja. V preteklosti so bile modelu očitane pomanjkljivosti, ker ne upošteva stohastične narave procesa porušitve ob izpostavitvi konstantni napetosti [Weaver in Chizmadzev 1996; Chen *et al.* 2006]. Z merjenjem porušitvene napetosti ravninskega dvosloja z uporabo linearno naraščajočega signala, močno zmanjšamo naključnost porušitve ravninskega lipidnega dvosloja. Povezali smo eksperimentalne rezultate porušitvene napetosti ter življenjske dobe z viskoelastičnimi lastnostmi ravninskih lipidnih

dvoslojev ter izračunali vrednosti Youngovega modula elastičnosti in površinske napetosti ravninskega lipidnega dvosloja.

Izračunane vrednosti površinske napetosti ravninskega lipidnega dvosloja ob porušitvi smo primerjali s tistimi, ki so jih objavili drugi avtorji. Izmerjene vrednosti površinske napetosti (σ) merjene na velikih unilamelarnih veziklih se nahajajo med 0,01 in 25 10^{-3} J/m^2; odvisno od sestave membrane [Evans in Needham 1987; Olbrich *et al.* 2000; Dimitrov 1984; Bloom *et al.* 1991, Hallett *et al.* 1993; Mui *et al.* 1993; Needham *et al.* 1988]. Do sedaj eksperimentalno na ravninskih lipidnih dvoslojih nobena od mehanskih lastnosti ni bila merjena. Naši rezultati površinske napetosti se skladajo s podatki za velike unilamelarne vezikle iz literature, čeprav moramo poudariti, da imajo ocene precej velika stresanja, še posebej pri mešanicah POPC:POPS 3:1 in 1:3. Eden od možnih razlogov je lahko izbrana vrednost debeline (h) ravninskega lipidnega dvosloja, ki ni natančno določena za vsak ravninski lipidni dvosloj posamezne mešanice. Električno polje v ravninskem lipidnem dvosloju povzroči lateralni stres, ki neposredno vpliva na površinsko napetost ter igra pomembno vlogo pri postavitvi lipidnih glavic ter nastajanju por v ravninskih lipidnih dvoslojih [Lewis 2003].

V naši raziskavi so bili ravninski lipidni dvosloji sestavljeni z dveh različnih lipidnih molekul. Lipidna molekula POPS (1-palmitil 2-oleil 3-fosfatidilserin) ima negativno nabito glavico, lipidna molekula POPC (1-pamitoil 2-oleoil 3-fosfatidilholin) pa ima elektrostatično nevtralno glavico. Zaradi odbojnih elektrostatičnih sil med lipidnimi molekulami smo pri ravninskih lipidnih dvoslojih sestavljenih iz POPS lipidnih molekul, pričakovali nižje porušitvene napetosti (U_{br}) ter posledično tudi nižje vrednosti elastičnega modula (E) ter površinske napetosti (σ). Vendar pa smo izmerili za POPS ravninski lipidni dvosloj najvišje vrednosti porušitvene napetosti. V primeru veziklov je eden od ključnih napovednikov membranske trdnosti elastični modul ukrivljenosti vezikla [Evans *et al.* 2003]. V našem primeru je bil ocenjen modul elastičnosti (E) za ravninske lipidne dvosloje zgrajene iz POPS statistično značilno višji kot iz POPC. To ni bila le posledica višje porušitvene napetosti, ampak tudi ostalih parametrov, ki nastopajo v modelu viskoelastičnosti Dimitrova. Meier s sodelavci je iz izsledkov svojih raziskav zaključil, da je porušitvena napetost in posledično stabilnost ravninskega lipidnega dvosloja neodvisna od polarizacije glavic lipidnih molekul [Meier *et al.* 2000]. Tudi njihove meritve porušitvene napetosti so pokazale, da imajo ravninski lipidni dvosloji zgrajeni iz POPS lipidnih molekul nekoliko višjo vrednost kot ravninski lipidni dvosloji zgrajeni iz POPC lipidnih molekul. O podobnih rezultatih je poročal Winterhalter s sodelavci. V njihovi raziskavi so določali stabilnost ravninskih lipidnih dvoslojev za električno nabite (PS) ter električno nevtralne (PC) skupine glavic [Winterhalter 2000].

V podporo našim rezultatom je tudi simulacija z molekularno dinamiko, ki jo je opravil Pandit s sodelavci [Pandit2003]. Simulirali so ravninski lipidni dvosloj zgrajen iz dipalmitoilphosphatidilcholina

(DPPC) in dipalmitoilphosphatidilserina (DPPS). Čeprav so lipidne molekule druge vrste, pa lahko zaradi enako nabitih glavic PC in PS potegnemo paralelo z našo študijo. Iz rezultatov simulacij so ugotovili, da posamezna molekula DPPC v ravninskem lipidnem dvosloju predstavlja povezavo z dvema sosednjima lipidnima molekulama, DPPS molekula pa s štirimi sosednjimi molekulami. Več kot je povezav s sosednjimi molekulami, bolj je stabilna struktura ravninskega lipidnega dvosloja. To pa je lahko tudi razlaga zakaj so porušitvene napetosti ravninskih lipidnih dvoslojov zgrajenih iz POPS lipidnih molekul višje.

Za ravninske lipidne dvosloje zgrajene iz mešanic molekul POPC in POPS so bile vrednosti izmerjene porušitvene napetosti (U_{br}) ter ocenjene vrednosti Youngovega elastičnega modula (E) in površinske napetosti (σ), v območju kot za ravninski lipidni dvosloj zgrajen iz izključno POPC molekul. Na podlagi teh ugotovitev lahko zaključimo, da so mehanske lastnosti pri dvo komponentnih ravninskih lipidnih dvoslojih določene z manj stabilno molekulo - v našem primeru je to POPC.

6 Dinamični model ravninskega lipidnega dvosloja

Če želimo ravninski lipidni dvosloj izpostaviti električnemu polju v modelu molekularne dinamike, moramo v modelu nastaviti primerne kemijske procese. Do sedaj so raziskovalci pokazali, da pripis sil na posamezen atom v sistemu [Tieleman *et al.* 2003; Tarek 2005], ali pa ustvarjanje ionskega neravnovesja [Gurtavenko *et al.* 2008; Delemotte *et al.* 2008] na ravninskem lipidnem dvosloju, ustvari električno polje preko membrane. Če je bilo ustvarjeno električno polje dovolj veliko, so opazili nastanek pore v ravninskem lipidnem dvosloju.

Tudi pri poizkusih z ravninskimi lipidnimi dvosloji so do sedaj že opazili strukturne spremembe v ravninskem lipidnem dvosloju ob izpostavitvi ravninskega lipidnega dvosloja tokovnemu [Koronkiewicz *et al.* 2004, Kotulska 2007] ali napetostnemu vzbujanju [Melikov *et al.* 2001]. Ravninski lipidni dvosloj so v preteklosti izpostavili konstantnemu toku, ter opazovali spremembe v napetosti. Fluktuacije so običajno pripisali eni veliki pori, ki se širi in oži. Do sedaj rezultati med molekularno dinamiko in poizkusi na ravninskih lipidnih dvoslojih še niso bili primerjani in ovrednoteni.

V naših poizkusih smo uporabili linearno naraščajoč tokovni signal različnih naklonov. Z linearno naraščajočim tokovnim signalom smo se želeli znebiti preštevilnemu odpiranju in zapiranju por v ravninskem lipidnem dvosloju ter doseči čimprejšnje porušenje ravninskega lipidnega dvosloja. Strukturne spremembe, ki smo jih opazili pred porušitvijo ravninskega lipidnega dvosloja, smo ovrednotili s prevodnostjo in jih primerjali s prevodnostjo izračunano na eni sami pori v modelu molekularne dinamike. Iz teh podatkov smo ocenili gostoto por v ravninskem lipidnem dvosloju.

6.1 Molekularna dinamika

Model ravninskega lipidnega dvosloja je bil zgrajen iz POPC lipidnih molekul, ki je bila predstavljena z združenimi atomi. Glava lipidne molekule je bila opisana z vsemi atomi, repi pa so bili opisani kot skupek molekul. Z modelom ravninskega lipidnega dvosloja smo zajeli v povprečju površino 100x100 $Å^2$. Kapacitivnost modela ravninskega lipidnega dvosloja smo normirali z velikostjo modela. Specifična kapacitivnost je znašala 0,85 $\mu F/cm^2$.

Pri vzpostavitvi ravninskega lipidnega dvosloja ionskemu neravnovesju Q = 8e smo opazili nastajanje pore (slika 44). Simulacija obsega časovni interval 30 ns. Po 10 ns so vodne molekule začele vdirati v ravninski lipidni dvosloj (slika 44b). Ioni v tem trenutku še niso potovali preko membrane, lipidne molekule pa so se reorganizirale v energijsko ugodnejšo strukturo. Reorganizacija lipidnih molekul je omogočila še večji prodor vode in pa prehod ionov preko pore (slika 44c)

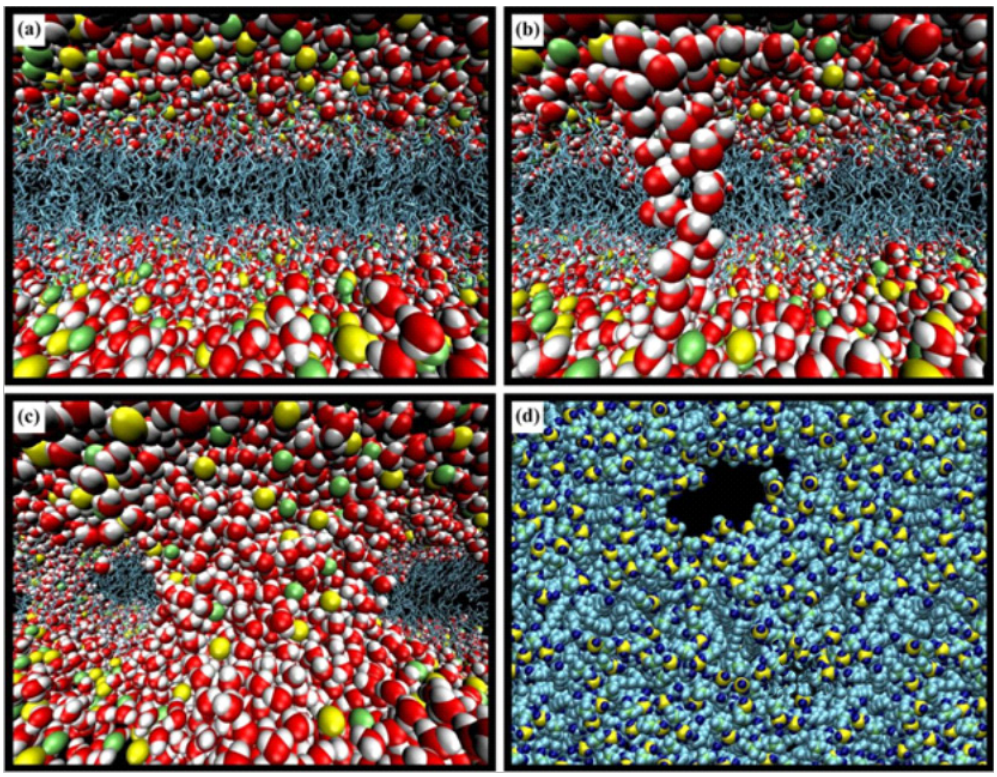

Slika 44. Nastanek pore v ravninskem lipidnem dvosloju v molekularni dinamiki. (a) Ravninski lipidni dvosloj smo izpostavili ionskemu neravnovesju. (b) Po 10 ns so vodne molekule pričele vdirati v ravninski lipidni dvosloj. (c) Lipidne molekule so zavzele energijsko ugodno strukturo in tvorile poro v ravninskem lipidnem dvosloju. Ioni, predstavljeni z rumenimi in zelenimi kroglicami so prehajali peko pore. (d) Pogled na ravninski lipidni dvosloj z vrha ob odsotnosti vodnih in ionskih molekul. Struktura pore je dobro vidna.

Naboj na ravninskem lipidnem dvosloju ob nastanku pore je Q = 1,28 10^{-18} As. Če naboj normiramo na površino ravninskega lipidnega dvosloja, imamo površinski naboj σ = 1,28 µAs/cm^2. Za izračun prevodnosti pore v ravninskem lipidnem dvosloju izrazimo linijski naboj vzdolž pore $q = Q/L_z$ = 64 pAs/m Na ravninskem lipidnem dvosloju se je vzpostavila napetost 1 V. Prevodnost pore smo ocenili na 160 pS. Če jo normiramo na površino ravninskega lipidnega dvosloja v modelu, je prevodnost 160 S/cm^2.

6.2 Tokovno vzbujanje ravninskega lipidnega dvosloja

Ker smo želeli primerjati poizkuse z simulacijami molekularne dinamike smo zaradi narave modela uporabili tokovno vzbujanje. Ravninski lipidni dvosloj zgrajen iz POPC (1-pamitoil 2-oleoil 3-fosfatidilholin) lipidnih molekul smo izpostavili linearno naraščajočim tokovnim signalom z nakloni k_I od 0,2 do 20 µA/s (tabela 18). Povprečna temperatura, pri kateri so bile meritve izvedene, je bila 22°C.

Zgradili smo 61 ravninskih lipidnih dvoslojev. Od teh jih je bilo v obdelavo vključenih 58. Njihova povprečna kapacitivnost je bila C_{BLM} = 57 ± 17 pF. Izmerjeno kapacitivnost smo normirali na površino luknjice v teflonski foliji oziroma površino ravninskega lipidnega dvosloja. Specifična kapacitivnost je

c_{BLM} = 0,51 ± 0,16 µF/cm^2. Izmerjene napetosti U_{br} (slika 45) in tokovi I_{br}, (slika 46) ob porušitvi ravninskega lipidnega dvosloja se niso statistično razlikovali med seboj. Porušitvena napetost U_{br} vseh meritev je bila 308 ± 77 mV. Povprečni porušitveni tok vseh meritev je znašal 3,5 ± 1,2 µA.

Tabela 18. Vrednosti porušitvenih napetosti U_{br}, porušitvenih tokov I_{br} in življenjskih časov t_{br} POPC ravninskih lipidnih dvoslojev vzbujanih z linearno naraščajočim tokom naklonov k_I. Za posamezni naklon je podana tudi povprečna kapacitivnost ravninskega lipidnega dvosloja C_{BLM}. Z N pa je označeno število meritev, ki so bila opravljena pri posameznem naklonu k_I.

k_I (µA/s)	N	U_{br} (mV)	I_{br} (µA)	t_{br} (s)	c_{BLM} (µF/cm^2)
0,2	9	333 ± 95	3,5 ± 1,0	17,68 ± 4,91	0,51 ± 0,09
0,5	13	313 ± 59	3,4 ± 0,6	6,78 ± 1,25	0,50 ± 0,09
4	5	324 ± 10	3,4 ± 0,1	0,87 ± 0,04	0,47 ± 0,08
8	5	316 ± 7	3,4 ± 0,1	0,43 ± 0,02	0,45 ± 0,06
10	6	325 ± 18	3,4 ± 0,2	0,35 ± 0,02	0,55 ± 0,05
20	8	339 ± 22	3,7 ± 0,3	0,18 ± 0,01	0,52 ± 0,07

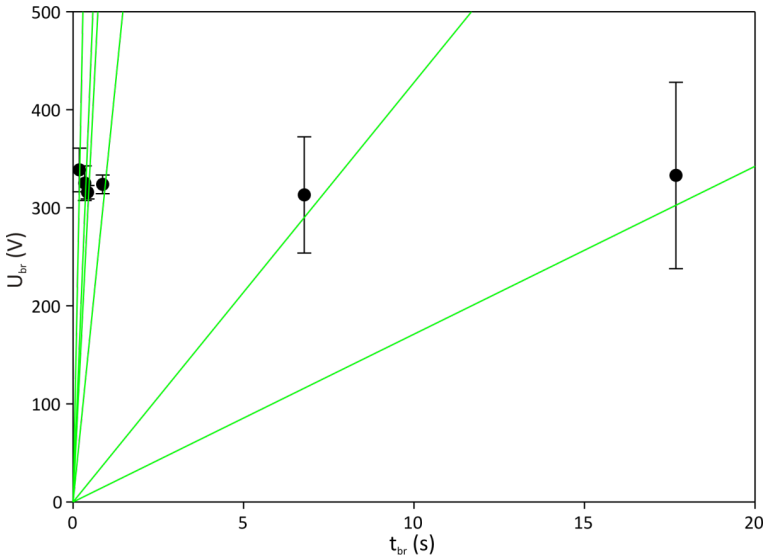

Slika 45. Izmerjene vrednosti porušitvene napetosti pri vzbujanju z linearno naraščajočim tokovnim signalom.

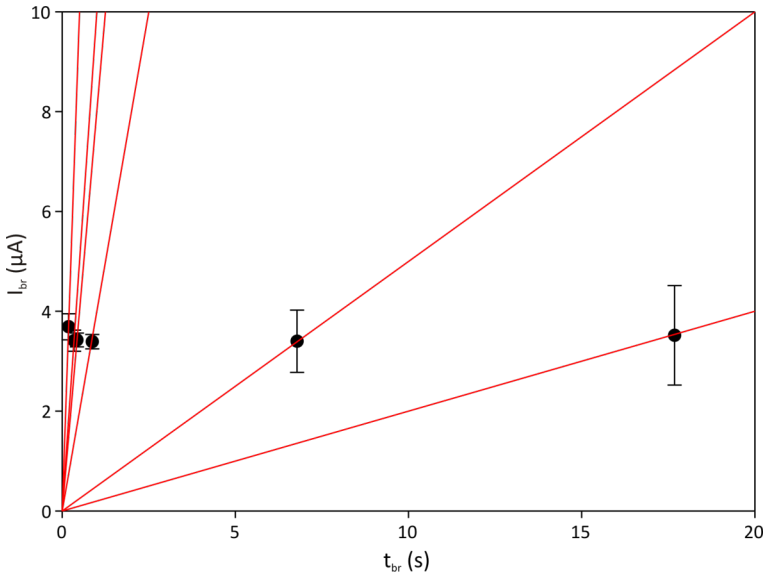

Slika 46. Porušitveni tokovi izmerjeni pri linearno naraščajočem tokovnem vzbujanju. Rdeče črte predstavljajo vzbujalni signal.

6.3 Opazovanje por v ravninskem lipidnem dvosloju

V statistično obdelavo smo vključili 58 ravninskih lipidnih dvoslojev. Ob vzbujanju ravninskega lipidnega dvosloja z linearno naraščajočim tokom smo na merjeni napetosti pri sedemindvajsetih primerih opazili padec napetosti potem pa skok napetosti pred porušitvijo ravninskega lipidnega dvosloja, ko se je napetost sesedla. V nekaterih primerih je bilo padcev napetosti na enem ravninskem lipidnem dvosloju več. V končni analizi smo vedno upoštevali le prvi padec napetosti. Napetost, pri kateri smo opazili prvi padec napetosti na ravninskem lipidnem dvosloju je bila povprečno U_d = 255 ± 87 mV. Pri teh vzorcih je bila porušitvena napetost ravninskega lipidnega dvosloja U_{br} = 331 ± 77 mV. Vsiljeni tok ob prvem pojavu padca napetosti je povprečno znašal $I(t_{op})$ = 2,7 ± 0,8 µA. Porušitveni tok ravninskih lipidnih dvoslojev je znašal I_{br} = 4,0 ± 1,7 µA. Če ravninske lipidne dvosloje, pri katerih so nastali padci napetosti razdelimo po naklonih linearno naraščajočih tokovnih signalov ugotovimo, da so v vseh primerih porušitvene napetosti U_{br} statistično značilno višje od napetosti U_d, kjer smo izmerili padce napetosti (slika 47).

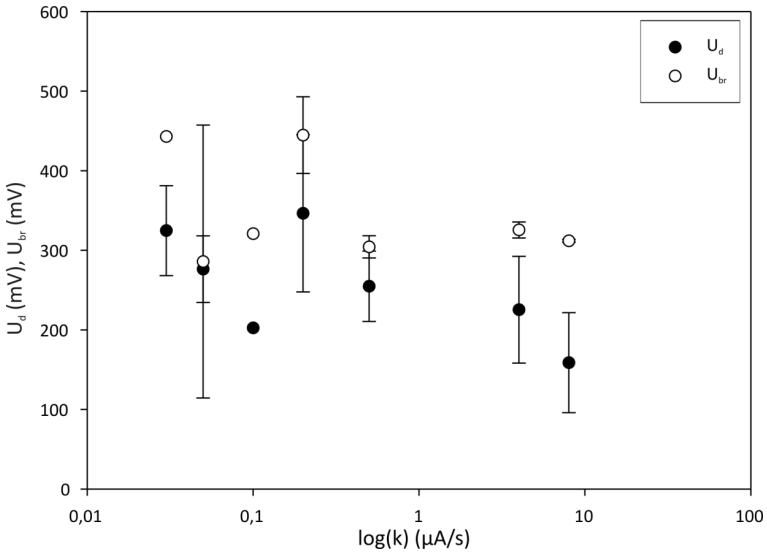

Slika 47. Primerjava porušitvenih napetosti U_{br} ter napetosti U_d ob katerih so se pojavile prve strukturne spremembe, pore v ravninskem lipidnem dvosloju, po posameznih naklonih linearno naraščajočega tokovnega signala.

Padce napetosti smo sicer opazili na mnogih ravninskih lipidnih dvoslojih pri različnih naklonih linearno naraščajočega tokovnega signala. A ker se v vseh primerih niso pojavili smo odstotni delež padcev napetosti na ravninskem lipidnem dvosloju pri posameznem naklonu zbrali v tabeli 19. Zaradi majhnega števila ponovitev, ne moremo z gotovostjo trditi, da je opazovanje padcev napetosti lažje pri položnejšem naklonu linearno naraščajočega tokovnega signala. Pri meritvah z zelo nizkimi nakloni (*), smo zaradi omejitve sistema uporabili trapezni signal. Z gotovostjo pa lahko trdimo, da pri strmi rampi ne moremo več opazovati padcev napetosti, ker prehitro dosežemo porušitev ravninskega lipidnega dvosloja (slika 48).

Tabela 19. Odstotni delež padcev napetosti na ravninskem lipidnem dvosloju pri posameznem naklonu k linearno naraščajočega toka, kjer N predstavlja število vseh meritev, N_d pa število meritev, kjer smo opazili padce napetosti. Pri naklonih ozačenih z zvezdico (*) smo zaradi omejitve sistema uporabili trapezni signal.

k (µA/s)	N	N_d	delež (%)
0,03*	3	3	100
0,05*	5	4	80
0,1*	4	1	25
0,2	9	3	33,33
0,5	13	10	76,92
4	5	4	80
8	5	2	40
10	6	0	0
20	8	0	0

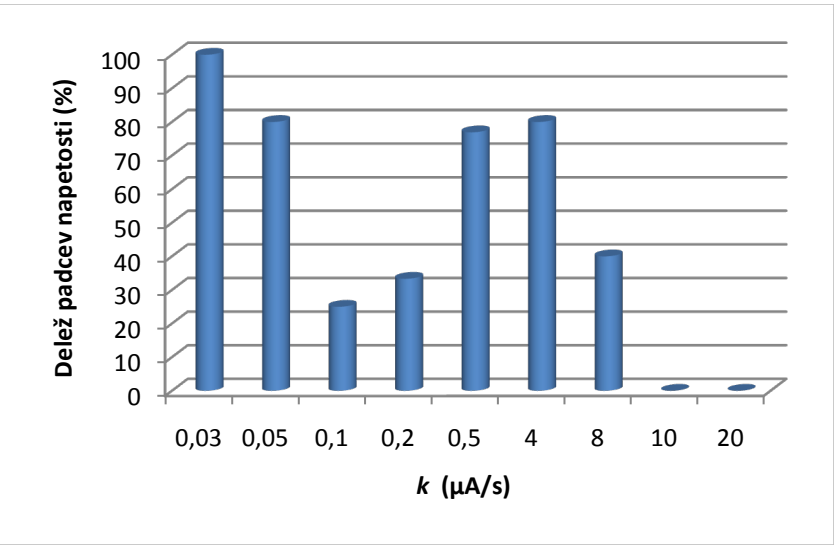

Slika 48. Odstotni delež padcev napetosti na ravninskem lipidnem dvosloju pri posameznem naklonu *k* linearno naraščajočega toka.

Padce napetosti ob tokovnem vzbujanju z linearno naraščajočim tokom lahko razumemo kot nastanek strukturnih sprememb oziroma por v ravninskem lipidnem dvosloju. Na sedemindvajsetih ravninskeh lipidnih dvoslojih smo opazili 40 različnih strukturnih sprememb. Povprečna vrednost prevodnosti opaženih strukturnih sprememb G_p je bila 0,23 ± 0,15 µS. Za prevodnosti vseh por v ravninskem lipidnem dvosloju smo pripravili histogram (slika 49). Ocenili smo, da je najvišji modus por pri $G_{p,hist}$ = 100 nS.

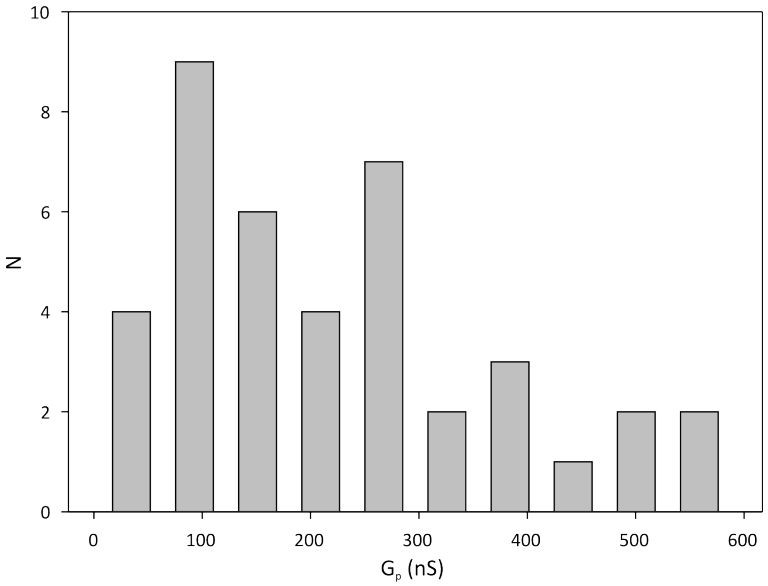

Slika 49. Histogram porazdelitve prevodnosti strukturnih sprememb v ravninskem lipidnem dvosloju ob posameznih padcih napetosti.

6.4 Zaključki

V tabeli 20 smo zbrali vrednosti specifične kapacitivnosti c_{BLM}, prevodnosti pore G_P in napetosti U_p, ko so se pore pričele pojavljati, dobljene z modelom molekularne dinamike oziroma s poizkusi.

Tabela 20. Vrednosti specifične kapacitivnosti c_{BLM}, prevodnosti por G_P in napetosti U_p, ko so se pričele pojavljati pore, dobljene z modelom molekularne dinamike oziroma s poizkusi. Uporabili smo lipidne molekule POPC. V modelu molekularne dinamike je stranica modela velikosti *L, d* pa je premer luknjice na katero smo v poizkusih napenjali ravninski lipidni dvosloj. Površina ravninskega lipidnega dvosloja je A_{BLM}. Kapacitivnost ravninskega lipidnega dvosloja normirana na površino je c_{BLM}. Prevodnost por v ravninskem lipidnem dvosloju smo označili z G_p. Pri molekularni dinamiki je G_p ocenjen za eno poro, pri poizkusih pa gre za hkraten nastanek večih por, modus prevodnosti por pa smo ocenili iz histograma.

	Molekularna dinamika	Eksperimenti
Lipidi	POPC	POPC
L / d	10 nm	117 µm
A_{BLM}	$1\ 10^{-16}$ m^2	$1{,}08\ 10^{-8}$ m^2
c_{BLM}	0,85 µF/cm^2	0,51 ± 0,16 µF/cm^2
G_p	160 pS	100 nS
U_p	1 V	257 ± 85 mV

Ideja o vzbujanju ravninskega lipidnega dvosloja s tokovnim signalom ni nova [Carius 1976]. Ob izpostavitvi ravninskega lipidnega dvosloja konstantnemu toku, so avtorji opazovali spremembe v napetosti na ravninskem lipidnem dvosloju. Napetostne spremembe so običajno pripisali eni veliki pori, ki se širi in oži; zaradi nizkih vrednosti tokov in napetosti pa so fluktuacije velikosti pore v ravninskem lipidnem dvosloju lahko opazovali tudi do nekaj ur [Kotulska 2007]. Do sedaj rezultati med molekularno dinamiko in poizkusi na ravninskih lipidnih dvoslojih še niso bili primerjani in ovrednoteni. V naših poizkusih smo uporabili linearno naraščajoče tokovne signale različnih naklonov. Z linearno naraščajočim tokovnim signalom smo se želeli izogniti dlje trajajočemu odpiranju in zapiranju por v ravninskem lipidnem dvosloju ter doseči čimprejšnje porušenje ravninskega lipidnega dvosloja.

Iz simulacij molekularne dinamike smo prevodnost ene pore ocenili na 160 pS. Pri poizkusih smo opazili, da se največkrat pojavi sprememba prevodnosti 100 nS, kar pomeni, da je v ravninskem lipidnem dvosloju nastalo večje število por N_p. Število por izračunamo iz razmerja med spremembo prevodnosti izmerjeno med poizkusi ter prevodnostjo ene pore določene iz modela molekularne dinamike:

$$N_p = \frac{G_{p,hist}}{G_{p,MD}} = \frac{100\ \mathrm{nS}}{160\ \mathrm{pS}} = 625. \tag{58}$$

Če predpostavimo, da so pore na ravninskem lipidnem dvosloju porazdeljene enakomerno, je gostota por ρ_p:

$$\rho_p = \frac{N_p}{A_{BLM}} = \frac{625}{1{,}08 \cdot 10^{-8}\ \mathrm{m}^2} = 578 \cdot 10^8\ 1/\mathrm{m}^2\,. \tag{59}$$

Posamezna pora torej v povprečju nastane na površini A_p:

$$A_p = \frac{1}{\rho_p} = 17{,}28\ \mu\mathrm{m}^2\,. \tag{60}$$

Izkaže se, da bi moral ravninski lipidni dvosloj modeliran v molekularni dinamiki imeti stranico večjo od 4,16 µm x 4,16 µm, če bi želeli v modelu opazovati več kot eno poro. Tako velikega ravninskega lipidnega dvosloja pa si pri trenutni računalniški moči še ne moremo privoščiti.

7 Razprava

Ravninski lipidni dvosloj je sicer le preprost model celične membrane, a predvidevamo, da so osnovni principi pojava elektroporacije enaki kot na celični membrani. Njegova prednost je v tem, da je med poizkusi dostopen z obeh strani. Ob izpostavitvi ravninskega lipidnega dvosloja električnemu polju vsilimo na njem transmembransko napetost, ki nastane zaradi Maxwell-Wagnerjeve polarizacije. Pod vplivom električnega polja se lipidne molekule reorientirajo, tako da se poveča prevodnost ravninskega lipidnega dvosloja. Pravimo, da v ravninskem lipidnem dvosloju nastanejo pore. Kadar je električno polje na ravninskem lipidnem dvosloju dovolj majhno, da se ravninski lipidni dvosloj ne poruši, govorimo o reverzibilni elektroporaciji. Ko z vrednostjo električnega polja presežemo prag določene vrednosti, se ravninski lipidni dvosloj poruši; takrat govorimo o ireverzibilni elektroporaciji.

Ravninske lipidne dvosloje smo tvorili iz 1-palmitil 2-oleil fosfatidilholin-a (POPC) in 1-palmitil 2-oleil fosfatidilserin-a (POPS). Po atomski zgradbi sta si ti dve molekuli lipida zelo podobni. Razlikujeta se samo po alkoholu vezanem na fosfat, torej po polarni glavici. V primeru POPC je alkohol holin, ki v kompleksu s fosfatom izkazuje dipolno nabitost (zwitterion). To pomeni da je polarna glavica nabita s pozitivnim in negativnim nabojem kar pogojuje električno nevtralnost lipidne glavice. Pri POPS pa je alkohol serin, ki v kompleksu s fosfatom izkazuje negativno nabitost polarne glavice lipida [Diederich *et al.* 1998].

Ravninski lipidni dvosloj v električnem polju lahko modeliramo s preprostim RC vezjem. Ravno zato je ena od najdlje opazovanih lastnosti ravninskih lipidnih dvoslojev kapacitivnost, ki govori o njegovi kvaliteti. V okviru študije smo preverili kapacitivnost ravninskih lipidnih dvoslojev z dvema različnima metodama, merjenjem časovne konstante in s pretvorbo kapacitivnosti v periodo. Kruskal-Wallisov enosmerni test je pokazal, da ni statistično značilne razlike med srednjimi vrednostmi specifične kapacitivnosti določene z eno ali drugo metodo pri enakih mešanicah lipida.

Kadar raziskujemo metodo elektroporacije v biomedicini in biotehnologiji, je porušitvena napetost ena izmed pomembnejših lastnosti ravninskega lipidnega dvosloja. Porušitvena napetost je vrednost napetosti, pri kateri se ravninski lipidni dvosloj poruši. Za merjenje porušitvene napetosti so najpogosteje uporabljali pravokotne napetostne pulze; amplitudo pulzov so povečevali v majhnih korakih vse dotlej, ko se je ravninski lipidni dvosloj porušil. Amplituda napetostnega pulza, kjer se je ravninski lipidni dvosloj porušil, je bila določena kot porušitvena napetost ravninskega lipidnega dvosloja. Pri uporabi tega protokola ne vemo v naprej, kolikokrat bomo morali izpostaviti ravninski lipidni dvosloj napetosti, da se bo le-ta porušil. Ravninski lipidni dvosloj je izpostavljen napetosti večkrat ter ob različnih časovnih intervalih. Taka pred-izpostavitev vpliva na stabilnost, posledično pa

tudi na porušitveno napetost ravninskega lipidnega dvosloja [Abidor *et al.* 1979]. Abidor s sodelavci je v svojem delu opisal veliko naključnost v življenjskem času ravninskega lipidnega dvosloja znotraj pulza ob porušitvi [Abidor *et al.* 1979].

Cilj raziskave v okviru doktorske disertacije je bil poiskati merilni protokol za določitev porušitvene napetosti, s katerim bi se izognili večkratni in predvsem nedoločeni izpostavitvi ravninskega lipidnega dvosloja električnim pulzom in napetostnemu stresu, ki se pri tem ustvari. Ker je iz literature znano, da prihaja pri izpostavitvah električnim pulzom do velike razpršenosti meritev, smo si želeli večje ponovljivosti pri določanju porušitvene napetosti in življenjske dobe ravninskih lipidnih dvoslojev. Izoblikovali smo merilno metodo, s katero smo omejili pred-izpostavitev ravninskega lipidnega dvosloja napetostnemu stresu, in zmanjšali naključnost življenjske dobe ravninskega lipidnega dvosloja. Z novim merilnim protokolom je ravninski lipidni dvosloj izpostavljen napetostnemu stresu le dvakrat. Prvič je izpostavljen električnemu pulzu amplitude 300 mV med merjenjem kapacitivnosti. V naslednjem koraku za porušitev raninskega lipidnega dvosloja uporabimo linearno naraščajoč napetostni signal. Trenutek, ko začne skozi ravninski lipidni dvosloj teči tok, določa porušitveno napetost ter življenjsko dobo ravninskega lipidnega dvosloja ob izbranem naklonu napetostnega signala.

Pri poizkusih smo uporabili sedem različnih naklonov linearno naraščajočega napetostnega signala. Za izbiro različnih naklonov smo se odločili na podlagi člankov, ki opisujejo določanje porušitvene napetosti ravninskih lipidnih dvoslojev ter njihovo življenjsko dobo glede na amplitudo pulza [Troiano *et al.* 1998, Maček Lebar *et al.* 2002] in vpliva pred-izpostavitve ravninskih lipidnih dvoslojev na življenjsko dobo [Abidor *et al.* 1979]. Naši rezultati kažejo, da sta porušitvena napetost ter življenjski čas ravninskega lipidnega dvosloja odvisna od naklona linearno naraščajočega napetostnega signala. Linearno naraščajoča napetost z manjšim naklonom izpostavlja ravninski lipidni dvosloj napetosti dlje časa (daljša pred-izpostavitev), zato je porušitvena napetost nižja kot pri signalih z bolj strmim naklonom. Joshi s sodelavci je predstavil teoretični model, v katerem je preučeval nastajanje pore v celični membrani v odvisnosti od membranske napetosti ter časa izpostavitve [Joshi in Schoenbach 2000]. S simulacijami so pokazali, da visokonapetostni pulzi ne povzročijo ireverzibilne poracije na celici, če so le ti dovolj kratki. V našem primeru imamo pri strmem naklonu linearno naraščajočega signala krajšo pred-izpostavitev ravninskega lipidnega dvosloja napetosti. Zaradi krajše pred-izpostavitve ima ravninski lipidni dvosloj višjo porušitveno napetost. Rezultati so v skladu z modelom Joshija s sodelavci, ki trdijo, da se bo membrana porušila, če je pri določeni velikosti pore na membrani še vedno prisotna napetost [Joshi in Schoenbach 2000].

Asimptota intenzivnostno časovne krivulje nas v svoji limiti vodi proti vrednosti, ki ustreza najnižji porušitveni napetosti ravninskega lipidnega dvosloja U_{brMIN}. Evans s sodelavci je namesto ravninskega lipidnega dvosloja opazoval lipidne vezikle, vzbujanje z električnim poljem pa je zamenjal s mehanskim vzbujanjem s tlakom [Evans *et al.* 2003]. Tlak so ustvarjali s pipeto, ki je srkala membrano vezikla v svojo notranjost. Tlak srkanja so nadzorovali in ga linearno povečevali. Pri počasnem naraščanju tlaka se je membrana vezikla porušila pri nižjem tlaku, kot če so tlak povečevali hitro. Opazimo analogijo rezultatov, le vzbujanje je v opisanem primeru »mehansko« v našem pa »električno«. Pri položnem linearno naraščajočem signalu je porušitvena napetost nižja. Pri strmem naklonu linearno naraščajočega signala pa je porušitvena napetost višja. Tudi Tieleman s sodelavci, ki je z računalniško simulacijo modeliral mehanski stres in vpliv električnega polja na lipidni dvosloj, je prišel do enakih zaključkov; večja hitrost povečevanja električne ali pa mehanske obremenitve membrane, ki se kaže v strmini naklona linearne funkcije obremenitve, je povzročila poracijo dvosloja pri višjih nateznih napetostih na membrani [Tieleman *et al.* 2003]. Podobnost ugotovitev z našimi rezultati nakazuje na podoben fizikalni proces porušitve lipidnega dvosloja neglede na to ali je vzbujanje električnega ali pa mehanskega izvora.

Diederich s sodelavci je določila porušitveno napetost membran zgrajenih iz POPC in POPS pri različnih koncentracijah okoliške vodne raztopine KCl z metodo razelektritve naboja (ang. charge pulse) [Diederich *et al.* 1998]. Za POPC so izmerili porušitvene napetosti med 400 mV do 455 mV, odvisno od koncentracije elektrolita. Za POPS so izmerili vrednosti med 410 mV do 480 mV v odvisnosti od koncentracije okoliškega elektrolita. Ugotovili so, da se porušitvena napetost membrane za obe vrsti lipida poveča v elektrolitu z višjo koncentracijo raztopljenega KCl. Avtorji o pH vrednosti vodnega medija ne poročajo, vendar je znano, da vodna raztopina KCl izkazuje rahlo kisel pH. V članku zasledimo, da je bila posamezna membrana pred porušitvijo izpostavljena od 20 do 200 pulzom. Vrednosti porušitvenih napetosti so za približno 100 mV nižje od vrednosti, ki smo jih izmerili v naših poizkusih, kar je lahko posledica večkratne pred-izpostavitve lipidnih dvoslojev. Z novim protokolom določimo porušitveno napetost in življenjsko dobo ravninskega lipidnega dvosloja s povprečno relativno napako 3,5%, kar je ponovljivo pri vseh naklonih *k*.

Primerjava izmerjenih porušitvenih napetosti za membrane sestavljene samo iz POPC in samo iz POPS pokaže statistično značilno razliko v višini porušitvene napetosti v odvisnosti od sestave lipida pri petih od sedmih uporabljenih naklonov *k*. Polarna glavica lipida POPS je negativno nabita. V strukturi lipidnega dvosloja se polarne glavice lipida orientirajo v smeri vodnega medija. Zaradi naboja glavic iste polaritete prihaja med njimi do odbojne elektrostatične sile zaradi česar bi pričakovali manjšo stabilnost in nižjo porušitveno napetost membran zgrajenih iz POPS v primerjavi z membranami iz POPC. Polarna glavica lipida POPC je fosfatidilholin (PC), ki zaradi dipolne nabitosti navzven izkazuje

električno nevtralnost in ne povzroča elektrostatičnih odbojnih sil med polarnimi glavicami. Odbojno silo med polarnimi glavicami POPS zmanjša prisotnost ionov v vodni raztopini, ki delno nevtralizirajo jakost električnega polja med glavicami. Diederich in sodelavci so po Gouy-Chapman-ovi teoriji izračunali, da so odbojne sile med polarnimi glavicami fosfatidilserina (PS) tako velike, da v koncentraciji vodnega medija manjši od 100 mM enovalentnih ionov ne bi bilo mogoče tvoriti stabilnega vezikla [Diederich *et al.* 1998]. Kljub temu so uspešno tvorili lipidni dvosloj v mnogo nižji, 10 mM vodni koncentraciji KCl. Iz njihovih rezultatov je razvidno, da je pri vodnem mediju 2 M KCl porušitvena napetost za POPC 455 mV, za POPS pa presenetljivo nekoliko višja 480 mV. Tudi v našem primeru smo izmerili višjo porušitveno napetost pri lipidnih dvoslojih zgrajenih iz POPS (630 mV) v primerjavi s tistimi zgrajenimi iz POPC (560 mV).

V naši raziskavi smo tvorili tudi ravninske lipidne dvosloje z mešanjem lipidnih molekul POPC in POPS v različnih razmerjih. Iz teh rezultatov je razvidno, da se porušitvene napetosti nahajajo v bližini oziroma med vrednostmi, ki smo jih izmerili za enokomponentne ravninske lipidne dvosloje. Organizacijo mešanice lipidov v lipidnem dvosloju opisuje raziskava Huanga in Feigenson-a [Huang in Feigenson 1993]. S simulacijo PS in PC binarnih lipidnih mešanic po metodi Monte Carlo so proučevali razporeditev lipidov v enosloj. Model temelji na izračunu presežne energije mešanja (ang. *excess energy of mixing*), ki je upošteval elektrostatične odnose med polarnimi glavicami, in prosti parameter, v katerega so zajeli vse ostale neidealne interakcije med molekulami lipidov. Rezultati simulacije pri mešanju lipidov PC in PS v razmerju 1:1 so pokazali, da se lipidi organizirajo v domene (ang. *clusters*) istovrstnega lipida. Omenjeno konfiguracijo avtorji predpostavijo kot zelo verjetno tudi v bioloških membranah, kjer je prisoten pojav neidealnega mešanja lipidov. Podobno razporeditev binarne mešanice lipidov POPC in POPS v razmerju 4:1 zasledimo v članku Kastl-ove in sodelavcev [Kastl *et al.* 2006]. Raziskovalci poročajo o domenah (zaključenih področjih) POPS molekul znotraj bolj zastopanih POPC molekul. Iz teh podatkov sklepamo, da sta se pri naših poskusih z mešanicami lipidov oba enosloja membrane organizirala v obliko enokomponentnih domen na površini membrane. Ob tej predpostavki je zelo verjetna tudi asimetrija sestave ravninskega lipidnega dvosloja v obeh plasteh. Genco s sodelavci je izvedel poskuse na asimetričnih ravninskih lipidnih dvoslojih, ki jih je vzbujal z električnim tokom [Genco *et al.* 1993]. Asimetrijo membrane so dosegli z različnima sestavama enoslojev. Ena stran lipidnega dvosloja je bila zgrajena izključno iz fosfatidilserina, druga pa iz mešanice fosfatidilholina in holesterola v razmerju 4:1. Raziskava je pokazala, da se zaradi negativno nabitih polarnih glavic PS vzpostavi električno polje znotraj ravninskega lipidnega dovosloja, ki zniža kritično transmembransko napetost. Znižanja porušitvene napetosti membran sestavljenih iz mešanice POPC in POPS ne zaznamo. Omenjeni pojav pa bi bil možna razlaga za podobnost izmerjenih minimalnih porušitvenih napetosti U_{brMIN} pri sestavi dvoslojev

iz mešanic POPC:POPS v razmerjih 1:0, 3:1 in 1:1. Iz podatkov za minimalno porušitveno napetost U_{brMIN} = 0,56 V pri enokomponentni sestavi dvosloja iz POPC in U_{brMIN} = 0,63 V pri enokomponentni sestavi dvosloja iz POPS bi namreč pričakovali, da se bodo minimalne porušitvene napetosti lipidnih dvoslojev mešane sestave linearno razporedile med njima.

Porušitvena napetost je med drugim odvisna od viskoelastičnih lastnosti ravninskega lipidnega dvosloja [Evans *et al.* 2003]. V doktorski disertaciji smo preučevali, ali lahko z merjenjem električnih lastnosti ravninskega lipidnega dvosloja sklepamo kakšne so njegove viskoelastične lastnosti, saj je metod za merjenje le-teh malo. Dimitrov je zgradil teoretični model na osnovi viskoelastičnih lastnosti ravninskega lipidnega dvosloja ter izračunal kritično napetost, kjer se le-ta poruši [Dimitrov 1984]. Predvideva minimalno potrebno napetost za porušitev ravninskega lipidnega dvosloja pri dolgih električnih pulzih. Troiano s sodelavci je model ocenil kot neustrezen, ker ne upošteva naključnosti pojava porušitve ravninskega lipidnega dvosloja [Troiano *et al.* 1998].

Z uporabo linearno naraščajočega signala izbranih naklonov, smo zmanjšali standardno deviacijo porušitvene napetosti in življenjskega časa ravninskega lipidnega dvosloja lipida na 10% ali manj. Ravno ponovljivost meritev porušitvene napetosti in življenjskega časa omogočata uporabo viskoelastičnega modela Dimitrova za oceno Youngovega elastičnega modula (E) ter površinske napetosti (σ) ravninskega lipidnega dvosloja.

Youngov modul elastičnosti ravninskega lipidnega dvosloja (E) lahko določimo le z vzbujanjem na mehanski ali električni način. Hianik je Youngov modul elastičnosti modul izmeril z izpostavitvijo ravninskega lipidnega dvosloja izmeničnemu električnemu polju ter merjenjem višjih harmonskih komponent transmembranskega toka, ki so prehajale preko membrane [Hianik 2006]. Za ravninske lipidne dvosloje sestavljene iz jajčnega fosfatidilholina (egg-PC) so izmerili Youngov modul elastičnosti modul v intervalu od 10^5 Pa (10 N/cm^2) pri nižjih frekvencah, do 10^7 Pa (10^3 N/cm^2) pri višjih frekvencah (~ 2 kHz). Pri svojih raziskavah je Hianik opazoval tudi vpliv različnih topil na Youngovem modulu elastičnosti (E). Za topila s krajšimi hidrokarbonskimi vezmi (n-heptan, n-dekan) so bile vrednosti Youngovega modula elastičnosti primerljive z zgoraj navedenimi, pri topilih z daljšimi hidrokarbonskimi vezmi (n-heksadekan) pa so bile vrednosti dvakratne. V naši raziskavi smo za topilo uporabili n-heksan. Izračunane vrednosti Youngovega modula elastičnosti (E) ravninskega lipidnega dvosloja so primerljive vrednostim raziskave Hianik-a pri nižjih frekvencah in uporabi topil z manjšo hidrokarbonsko verigo.

Cilj naše raziskave je bil določiti mehanske lastnosti ravninskega lipidnega dvosloja kot sta Youngov modul elastičnosti (E) in površinska napetost (σ) iz izmerjenih vrednosti porušitvene napetosti (U_{br}) ter napovednega viskoelastičnega modela Dimitrova. Protokol meritve viskoelastičnih lastnosti

ravninskega lipidnega dvosloja je časovno potraten. Predvsem zaradi razloga, da je potrebno porušitveno napetost (U_{br}) in življenjski čas (t_{br}) meriti pri različnih naklonih linearno naraščajočega signala. Ne glede na to slabost, pa so vrednosti Youngovega modula elastičnosti (E) in površinske napetosti (σ) določene s predlagano metodo primerljive z rezultati drugih metod, ki so objavljeni v literaturi za meritve na velikih unilamelarnih veziklih.

Izpostavitev ravninskega lipidnega dvosloja električnemu polju povzroči v njem strukturne spremembe imenovane pore, ki pa jih eksperimentalno zelo težko opazujemo in dokažemo njihov obstoj. Na podlagi rezultatov molekularne dinamike in rezultatov poizkusov na ravninskih lipidnih dvoslojih vzbujanih z linearno naraščajočim tokovnim signalom smo ocenili prevodnost in gostoto por.

Ideja o vzbujanju ravninskega lipidnega dvosloja s tokovnim signalom ni nova [Carius 1976]. Ob izpostavitvi ravninskega lipidnega dvosloja konstantnemu toku, so avtorji opazovali spremembe v napetosti na ravninskem lipidnem dvosloju. Predpostavili so, da so napetostne spremembe posledica nastanka ene velike pore, ki se širi in oži; zaradi nizkih vrednosti tokov in napetosti pa so fluktuacije velikosti pore v ravninskem lipidnem dvosloju opazovali lahko tudi več ur [Kotulska 2007]. Do sedaj rezultati med molekularno dinamiko in poizkusi na ravninskih lipidnih dvoslojih še niso bili primerjani in ovrednoteni. V naših poizkusih smo uporabili linearno naraščajoče tokovne signale različnih naklonov. Z linearno naraščajočim tokovnim signalom smo se želeli izogniti dlje trajajočemu odpiranju in zapiranju por v ravninskem lipidnem dvosloju ter doseči čimprejšnje porušenje ravninskega lipidnega dvosloja.

Neposredno primerjavo med ravninskim lipidnim dvoslojem zgrajenim eksperimentalno ter modelom v molekularni dinamiki lahko naredimo le z ovrednotenjem specifične kapacitivnosti. Razlike med površinami, na katere normiramo kapacitivnost so izredno velike in pri tem lahko pride do večjih odstopanj. Iz simulacij molekularne dinamike smo ocenili kapacitivnost ravninskega lipidnega dvosloja z razmerjem neravnovesja nabojev ter transmembranske napetosti, ki je znašala 0,85 $\mu F/cm^2$. Eksperimentalno smo kapacitivnost za ravninski lipidni dvosloj zgrajen iz POPC lipidnih molekul izmerili 0,51 ± 0,16 $\mu F/cm^2$. Tudi napetosti, kjer opazimo v ravninskem lipidnem dvosloju strukturne spremembe, primerjamo le v območju meritve. Ravno tako sta oceni prevodnosti neko povprečno stanje sistema, ki pa še ni nujno vsakokrat ponovljivo. Kljub tem dejstvom lahko rezultate simulacij molekularne dinamike in poizkusov povežemo ter ocenimo dogajanje na ravninskem lipidnem dvosloju ob izpostavitvi električnemu polju.

Ob izpostavitvi ravninskega lipidnega dvosloja linearno naraščajočemu tokovnemu signalu smo med naraščanjem transmembranske napetosti opazili kratkotrajne majhne padce napetosti. Predpostavili

smo, da padcem napetosti botruje povečanje prevodnosti ravninskega lipidnega dvosloja. Ocenili smo, da so bile v ravninskem lipidnem dvosloju v obdobju, ko se je prevodnost ravninskega lipidnega dvosloja povečala, prisotne strukturne spremembe oziroma pore. Iz simulacij molekularne dinamike smo prevodnost posamezne pore ocenili na 160 pS. Pri poizkusih smo opazili, da se največkrat pojavi sprememba prevodnosti 100 nS, kar pomeni, da je v ravninskem lipidnem dvosloju nastalo večje število por. Število por izračunano iz spremembe prevodnosti izmerjene med poizkusi ter prevodnostjo ene pore določene iz modela molekularne dinamike znaša 625. Ocenili smo, da je gostota por v ravninskem lipidnem dvosloju 578 10^8 $1/m^2$. Območje na ravninskem lipidnem dvosloju, kjer nastane le ena pora je 17,28 μm^2. Iz tega sledi, da je razdalja med dvema porama v ravninskem lipidnem dvosloju približno 4,16 µm. Ob predstavitvi rezultatov molekularne dinamike običajno predstavijo le eno samo poro v ravninskem lipidnem dvosloju. Če bi želeli modelirati več por bi moral biti model ravninskega dvosloja večji od 17,28 μm^2. To pomeni, da bi morala biti površina ravninskega dvosloja vsaj 10^4 večja. Tako velikega ravninskega lipidnega dvosloja pa si pri trenutni računalniški moči še ne moremo privoščiti.

Na področju modeliranja molekularne dinamike bi bilo v prihodnosti zanimivo preizkusiti, kako nastajajo strukturne spremembe oziroma pore v ravninskih lipidnih dvoslojih sestavljenih z različnih lipidnih molekul, predvsem POPS molekul, za katere vemo da imajo v glavici lipida dodan negativen naboj. Ravno tako bi bilo možno ravninski lipidni dvosloj v modelu izpostaviti tlačni razliki ter opazovati viskoelastične lastnosti in jih primerjati z vrednostmi elastičnosti in površinske napetosti izraženih iz porušitvene napetosti in življenjskega časa.

8 Izvirni prispevki k znanosti

Merjenje porušitvene napetosti ravninskega lipidnega dvosloja z linearno naraščajočim signalom

Ker je porušitvena napetost ravninskega lipidnega dvosloja odvisna od časa trajanja posameznega napetostnega pulza ter predhodne izpostavitve, metoda merjenja porušitvene napetosti z napetostnimi pulzi vnaša v merjene rezultate preveliko stresanje rezultatov. Predlagali smo novo metodo določanja porušitvene napetosti ravninskega lipidnega dvosloja z linearno naraščajočim signalom, s katero se izognemo večkratni izpostavitvi in zmanjša stresanje rezultatov v primerjavi z metodami, ki so bile uporabljene do sedaj.

Določitev viskoelastičnih lastnosti ravninskega lipidnega dvosloja na podlagi porušitvene napetosti izmerjene z linearno naraščajočim signalom

Porušitvena napetost je odvisna od viskoelastičnih lastnosti ravninskega lipidnega dvosloja. Izbrali smo ustrezen model, ki to povezavo predvideva. Ker so z uporabo linearno naraščajočega signala rezultati porušitvenih napetosti ter življenskih časov bolj ponovljivi, jih lahko uporabimo tudi za izračun viskoelastičnih lastnosti. Viskoelastične lastnosti ravninskega lipidnega dvosloja smo določili iz meritev porušitvene napetosti z linearno naraščajočim napetostnim signalom.

Ocena prevodnosti in gostote por v ravninskem lipidnem dvosloju

Izpostavitev ravninskega lipidnega dvosloja električnemu polju povzroči v njem strukturne spremembe imenovane pore, ki pa jih eksperimentalno zelo težko opazujemo in dokažemo njihov obstoj. Na podlagi primerjave rezultatov molekularne dinamike in rezultatov poizkusov na ravninskih lipidnih dvoslojih vzbujanih z linearno naraščajočim tokovnim signalom smo ocenili prevodnost posamezne pore in gostoto por.

9 Literatura

I.G. Abidor, V.B. Arakelyan, L.V. Chernomordik, Y.A. Chizmadzhev, V.F. Pastushenko, M.R. Tarasevich, Electric breakdown of bilayer membranes: I. The main experimental facts and their qualitative discussion, *Bioelectrochem. Bioenerg*. 6 (1979) 37-52.

I.G. Abidor, A.E. Sowers, Kinetics and mechanism of cell membrane electrofusion, *Biophysical Journal* 61 (1992) 1557–1569.

R.S. Armen, O.D. Uitto S.E. Feller, Phospholipid Component Volumes: Determination and Application to Bilayer Structure Calculations, *Biophisical Journal* 75 (1998) 734-744.

R. Benz, K. Janko, Voltage-induced capacitance relaxation of lipid bilayer membranes; effects on membrane composition, *Biochimica et Biophysica Acta* 455 (1976) 721-738.

R. Benz, F. Beckers, U. Zimmermann, Reversible Electrical Breakdown of Lipid Bilayer Membranes: A Charge-Pulse Relaxation Study, *Journal of Membrane Biology* 48 (1979) 181-204.

P. R. Bevington and D. K. Robinson, *Data Reduction and Error Analysis for the Physical Sciences*. New York, USA, McGraw-Hill, 1992.

R.A. Böckmann, S.W.I. Siu, S. Leis, B.L. de Groot, S. Kakorin, E. Neumann, H. Grubmüller, Kinetics, Statistics, and Energetics of Lipid Membrane Electroporation Studied by Molecular Dynamics Simulations, *Biophysical Journal* 95 (2008) 1837-1850.

N. Brahms, *Generalized Nonlinear Non-analytic Chi-Square Fitting*: Matlab Central, 2008.

M. Bloom, E. Evans, and O. G. Mouritsen, Physical-Properties Of The Fluid Lipid-Bilayer Component Of Cell-Membranes - A Perspective, *Quarterly Reviews of Biophysics* 24 (1991) 293-397.

N. Brahms, Generalized Nonlinear Non-analytic Chi-Square Fitting: Matlab Central, 2008.

B. R. Brooks, R. E. Bruccoleri, B. D. Olafson, D. J. States, S. Swaminathan, and M. Karplus, CHARMM: A Program for Macromolecular Energy, Minimization, and Dynamics Calculations, *Journal of Computational Chemistry* 4 (1983) 187-217.

P.J. Canatella, J.F. Karr, J. A. Petros, and M.R. Prausnitz.,Quantitative Study of Electroporation-Mediated Molecular Uptake and Cell Viability, *Biophisical Journal* 80 (2001) 755-764.

W. Carius, Voltage dependence of bilayer membrane capacitance Harmonic response to ac excitation with dc bias, *Journal of colloid and interface science* 57 (1976) 301-307.

D.C. Chang, B.M. Chassey, J.A. Saunders, A.E. Sowers, *Guide to electroporation and electrofusion*, Academic Press, New York, 1992.

C. Chen, S.W. Smye, M.P. Robinson, J.A. Evans, Membrane electroporation theories: a review. *Medical & Biological Engineering & Computing* 44(1-2) (2006) 5-14.

Y.A. Chizmadzev, V.B. Arakelyan, V.F. Pastushenko, 248 – Electric Breakdown of Bilayer Lipid Membranes III. Analysis of Possible Mechanisms of Defect Origination, *Bioelectrochem. Bioenerg*. 6 (1979) 63-70.

L. Delemotte, F. Dehez, W. Treptow, M. Tarek, Modeling Membranes under a Transmembrane Potential, *The Journal of Physical Chemistry B*, 112(18) (2008) 5547-5550.

A. Diederich, G. Bahr, M. Winterhalter, Influence of surface charges on the rapture of black lipid membranes, *Physical Review E* 58 (1998) 4883-4889.

D.S. Dimitrov, Electric field-induced breakdown of lipid bilayer and cell membranes: a thin viscoelastic film model, *Journal of Membrane Biology* 78 (1984) 53-60.

B.E.Ehrlich, Incorporation of Ion Channels in Planar Lipid Bilayers: How to Make Bilayers Work for You, In *The Heart and Cardiovascular System*, (Ed. H.A.Fozzard et al.) pp. 551-560, Raven Press, New York 1992.

E. Evans and D. Needham, Physical-properties of surfactant bilayer-membranes - thermal transitions, elasticity, rigidity, cohesion, and colloidal interactions, *Journal of Physical Chemistry* 91 (1987) 4219-4228.

Evans, V. Heinrich, F. Ludwig, and W. Rawicz, Dynamic Tension Spectroscopy and Strength of Biomembranes, *Biophysical Journal* 85 (2003) 2342-2350.

E. Gallucci, S. Micelli, G. Monticelli, Pore Formation in Lipid Bilayer Membranes Made of Phosphatidylinositol and Oxidized Cholesterol Followed by Means of Alternating Current, Biophisical Journal 71 (1996) 824-831.

J. Gehl, Review: Electroporation: theory and methods, perspectives for drug delivery, gene therapy and research, *Acta Physiologica Scandinavica* 177 (2003) 437-447.

I. Genco, A. Gliozzi, A. Relini, M. Robello, E. Scalas, Electroporation in symmetric and asymmetric membranes, *Biochimica et Biophysica Acta* 1149 (1993) 10-18.

J. Genova, A. Zheliaskova, and M. D. Mitov, The influence of sucrose on the elasticity of SOPC lipid membrane studied by the analysis of thermally induced shape fluctuations, *Colloids And Surfaces A-Physicochemical And Engineering Aspects* 282 (2006) 420-422.

R.B. Gennis, Biomembranes, *Molecular structure and function, Springer*, New York, 1989.

W.F. van Gunsteren, H.J.C. Brendesen, Groningen Molecular Simulation (GROMOS) Library Manual (Bimos, Groningen,1987).

A.A. Gurtovenko, M. Miettinen, M. Karttunen, I. Vattulainen, Effect of Monovalent Salt on Catonic Lipid Membranes As Revealed by Molecular Dynamics Simulations, *The Journal of Physical Chemistry B* 109 (2005) 21126-21134

C. N. Haas, D. N. Aturaliye, Kinetics of electroporationassisted chlorination of giardia muris. *Water Research* 33 (1999) 1761–1766.

F. R. Hallett, J. Marsh, B. G. Nickel, and J. M. Wood, Mechanical-Properties Of Vesicles .2. A Model For Osmotic Swelling And Lysis, *Biophysical Journal* 64 (1993) 435-442.

W. Helfrich, Elastic Properties of Lipid Bilayers: Theory and Possible Experiments, *Zeitschrift Fur Naturforschung C-A Journal Of Biosciences, C* 28 (1973) 693-703.

R. Heller, R. Gilbert, M. J. Jaroszeski, Clinical application of electrochemotherapy, *Advanced Drug Delivery Reviews* 35 (1999) 119–129.

T. Hianik, Structure and physical properties of biomembranes and model membranes, *Acta Physica Slovaca* 56 (2006) 687-806.

J. Huang, G.W. Feigenson, Monte Carlo simulation of lipid mixtures: Finding phase separation, *Biophysical Journal* 65, 5, (1993) 1788-1794.

I. Idris in V.N. Biktashev, Analytical Approach to Initiation of Propagating Fronts, *Physical Review Letters* 101 (2008) 244101.

R.P. Joshi, K.H. Schoenbach, Electroporation dynamics in biological cells subjected to ultrafast electrical pulses: A numerical simulation study, *Physical Review E* 62 (2000) 1025–1033.

S. Kalinowski, Z. Figaszewski, A new system for bilayer lipid membrane capacitance measurements: method, apparatus and applications, *Biochimica et Biophysica Acta* 1112 (1992) 57-66.

S. Kalinowski, Z. Figaszewski, A four-electrode system for measurement of bilayer lipid membrane capacitance, *Measurement Science and Technology* 6 (1995) 1034-1049.

S. Kalinowski, Z. Figaszewski, A four-electrode potentiostat-galvanostat for studies of bilayer lipid membranes, *Measurement Science and Technology* 6 (1995) 1050-1055.

S.Kalinowski, G.Ibron, K.Bryl, Z.Figaszewski, Chronopotentiometric studies of electroporation of bilayer lipid membranes, *Biochimica et Biophysica Acta* 1396 (1998), 204-212.

S.K. Kandasamy, R.G. Larson, Cation and anion transport trough hydrophilic pores in lipid bilayers, *The Journal of Chemical Physics* 125 (2006) 074901(1-9)

K. Kastl, M. Menke, E. Lüthgens, S.βFaV. Gerke, A. Janshoff, C. Steinem, Partially reversible adsorption of annexin A1 on POPC/POPS bilayers investigated by QCM measurements, SFM, and DMC simulations, *European Journal of Chemical Biology (ChemBioChem)* 7 (2006) 106-115.

R. Kjellander, S. Marchja, Perturbation of hydrogen bonding in water near polar surfaces, *Chemical Physics Letters* 120 (1985) 393-396.

B. W. Koenig, H. H. Strey, and K. Gawrisch, Membrane lateral compressibility determined by NMR and X-ray diffraction: Effect of acyl chain polyunsaturation, *Biophysical Journal* 73 (1997) 1954-1966.

S. Koronkiewicz, S. Kalinowski, K. Bryl, Programmable chronopotentiometry as a tool for the study of electroporation and resealing of pores in bilayer lipid membranes, *Biochimica et Biophysica Acta* 1561 (2004) 222-229.

M. Kotulska, Natural fluctuations of an electropore show fractional Levy stable motion, *Biophysical journal* 92 ˙(2007) 2412-2421.

P. Kramar (ur.), D. Miklavčič (ur.), *Electroporation based technologies and treatments: proceedings of the international scientific workshop and postgraduate course*. Ljubljana: Faculty of Electrical Engineering, 2003.

P. Kramar (ur.), D. Miklavčič (ur.), *Electroporation based technologies and treatments: proceedings of the international scientific workshop and postgraduate course*, November 14-20, 2005, Ljubljana, Slovenia. 1. izd. Ljubljana: Fakulteta za elektrotehniko, 2005.

P. Kramar (ur.), D. Miklavčič (ur.), L. Mir (ur.). *Electroporation based technologies and treatments: proceedings of the international scientific workshop and postgraduate course*, November 11-17, 2007, Ljubljana, Slovenia. 1. izd. Ljubljana: Fakulteta za elektrotehniko, 2007

P. Kramar, D. Miklavčič, A. Maček-Lebar, Determination of the lipid bilayer breakdown voltage by means of a linear rising signal, *Bioelectrochemistry* 70 (2007) 23-27.

P. Kramar (ur.), D. Miklavčič (ur.), L. Mir (ur.). *Electroporation based technologies and treatments: proceedings of the international scientific workshop and postgraduate course*, November 15-22, 2009, Ljubljana, Slovenia. 1. izd. Ljubljana: Fakulteta za elektrotehniko, 2009

P. Kramar, D. Miklavčič, A. Maček-Lebar, A system for the determination of planar lipid membrane voltage and its applications, *IEEE transactions of nanobioscience* 8 (2009) 132-138.

P. Kramar, D. Miklavčič, M. Kotulska, A. Maček Lebar, Voltage and current clamp methods for determination of planar lipid bilayer properties, In *Advances in planar lipid bilayer and liposomes, 11*, Editor: Aleš Iglič, *2010*.

R. Kwok in E. Evans, Thermoelasticity of large lecithin bilayer vesicles, *Biophysical Journal* 35, (1981) 637-652.

H. Leontiadou, A.E. Mark, S.J. Marrink, Molecular Dynamics Simulations of Hydrophilic Pores in Lipid Bilayers, *Biophisical Journal* 86 (2004) 2156-2164.

T. J. Lewis, A model for bilayer membrane electroporation based on resultant electromechanical stress, *IEEE Transactions on Dielectrics and Electrical Insulation* 10 (2003) 769-777.

E. Lindahl and B. Hess and D. van der Spoel: GROMACS 3.0, A package for molecular simulation and trajectory analysis, *Journal of Molecular Modeling* 7 (2001) 306-317.

A. Maček-Lebar, D. Miklavčič, Cell electropermeabilization to small molecules in vitro: control by pulse parameters, *Radiology and Oncology* 35 (2001) 193-202.

A. Maček Lebar, G.C. Troiano, L. Tung, D. Miklavčič, Inter-pulse interval between rectangular voltage pulses affects electroporation threshold of artificial lipid bilayers, *IEEE Transaction on Nanobioscience* 1 (2002) 116-120.

S.J. Marrink, A.H. de Vries, D.P. Tieleman, Lipids on the move: Simulations of membrane pores, domains, stalks and curves, *Biochimica et Biophysica Acta* 1788 (2009) 149-168.

L Martinez, R Andrade, EG Birgin, JM Martinez, Packmol: A package for building initial configurations for molecular dynamics simulations. *Journal of Computational Chemistry* 30 (2009) 2157-2164.

W. Meier, A. Graff, A. Diederich, M. Winterhalter, Stabilization of planar lipid membranes: A stratified layer approach, *Physical Chemistry Chemical Physics* 2 (2000) 4559-4562.

H. Mekid, L.M. Mir, In vivo cell electrofusion, *Biochimica et Biophysica Acta* 1524 (2000) 118–130.

P. Meleard, J. F. Faucon, M. D. Mitov, and P. Bothorel, Pulsed-light microscopy applied to the measurement of the bending elasticity of giant liposomes, *Europhysics Letters* 19, (1992) 267-271.

K. C. Melikov, V. A. Frolov, A. Shcherbakov, A. V. Samsonov, Y. A. Chizmadzhev, L. V. Chernomordik, Voltage-Induced Nonconductive Pre-Pores and Metastable Single Pores in Unmodified Planar Lipid Bilayer, *Biophisical Journal* 80 (2001) 1829-1836.

R. Mendelsohn, G.R. Snyder, Infrared spectroscopic determination of conformational disorder and microphase separation in phospholipid acyl chains, in Biological Membranes: *A molecular Perspective from Computation and Experiment*, ed. K.M. Merz, B. Roux (Birkhauser, Boston 1996) pp. 145-174.

D. Miklavčič, T. Kotnik, Electroporation for electrochemotherapy and gene therapy, in:P.J. Rosch, M.S. Markov (Eds.), *Bioelectromagnetic Medicine*, Marcel Dekker, New York, 2004, pp. 637-656.

D. Miklavčič, M. Puc, Electroporation, *Wiley Encyclopedia of Biomedical Engineering*, John Wiley & Sons, New York, 2006.

L.M. Mir, H. Banoun, C. Paoletti, Introduction of definite amounts of nonpermeant molecules into living cells after electropermeabilization: direct access to the cytosol, *Experimental Cell Research* 175 (1988) 15–25.

L. M. Mir, Therapeutic perspectives of in vivo cell electropermeabilization, *Bioelectrochemistry* 53 (2001) 1–10.

L. M. Mir, S. Orlowski, J. Belehradek, J. Teissie, M. P. Rols, G. Serša, D. Miklavčič, R. Gilbert, R. Heller, Biomedical applications of electric pulses with special emphases on antitumor electrochemotherapy, *Bioelectrochemistry and Bioenergetics* 38 (1995) 203–207.

M. Montal, P. Mueller, Formation of bimolecular membranes from lipid monolayers and a study of their electrical properties, *Proceedings of the National Academy of Sciences* 69 (1972) 3561-3566.

Y Mouneimne, P.F. Tosi, R. Barhoumi, C. Nicolau, Electroinsertion of full length recombinant CD4 into red blood cell membrane, *Biochimica et Biophysica Acta* 1027 (1990) 53–58.

P. Mueller, D.O. Rudin, H.T. Tien, W.C. Wescott, Reconstitution of a cell membrane structure in vitro and its transformation into an excitable system, *Nature* 194 (1962) 979–980.

B. L. S. Mui, P. R. Cullis, E. A. Evans, and T. D. Madden, Osmotic Properties Of Large Unilamellar Vesicles Prepared By Extrusion, *Biophysical Journal* 64 (1993) 443-453.

J.F. Nagle, Area/lipid of bilayers from NMR, *Biophisical Journal*, 64 (1993) 1476-1481.

D. Needham, T. J. McIntosh, and E. Evans, Thermomechanical And Transition Properties Of Dimyristoylphosphatidylcholine Cholesterol Bilayers, *Biochemistry* 27 (1988) 4668-4673.

E. Neumann, K. Rosenheck, Permeability changes induced by electric impulses in vesicular membranes, *Journal of Membrane Biology* 10 (1972) 279-290.

E. Neumann, M.S. Ridder, Y. Wang, P. H. Hofschneider, Gene transfer into mouse lyoma cells by electroporation in high electric fields. *The EMBO Journal* 1 (1982) 841–845.

E. Neumann, A. Sowers, C. Jordan, *Electroporation and electrofusion in cell biology*, Plenum, New York, 1989.

E.Neumann, S.Kakorin, K.Toensing, Funadamentals of electroporative delivery of drugs and genes, *Bioelectrochemistry and Bioenergetics* 48 (1999) 3–16.

M. Okino, H. Mohri, Effects of high-voltage electrical impulse and an anticancer drug on in vivo growing tumors, *Japanese Journal of Cancer Research* 78 (1987) 1319–1321.

K. Olbrich, W. Rawicz, D. Needham, and E. Evans, Water permeability and mechanical strength of polyunsaturated lipid bilayers, *Biophysical Journal* 79 (2000) 321-327.

A.L. Ottova, H.T. Tien, The 40th anniversary of bilayer lipid membrane research, *Bioelectrochemistry* 56, (2002) 171-173.

A.G. Pakhomov, D. Miklavčič, M.S. Markov (uredniki), *Advanced Electroporation Techniques in Biology and Medicine*, CRC Press, Boca Raton, 2010.

S.A. Pandit, D. Bostick, and M.L. Berkowitz, Mixed Bilayer Dipalmitoylphosphatidylcholine and Dipalmitoylphosphatidylserine: Lipid Complexation, Ion Bonding, and Electrostatics, *Biophysical Journal* 85 (2003) 3120-3131.

M. Pavlin, T. Kotnik, D. Miklavčič, P. Kramar, A. Maček Lebar, Electroporation of Planar Lipid Bilayers and Membranes. In *Advances in Planar Lipid Bilayers and Liposomes* 6, (2008) 165-226. Academic Press.

N. Pavšelj, V. Préat, DNA electrotransfer into the skin using a combination of one high- and one low-voltage pulse, *Journal of Controlled Release* 106, (2005) 407-415.

D.A. Pearlman, D.A. Case, J.C. Caldwell, G.L. Seibel, U.C. Singh, P. Weiner, P.A. Kollman, *AMBER 4.0* (University of California, San Francisco, 1991).

J.C. Phillips, R. Braun, W. Wang, J. Gumbart, E. Tajkhorshid, E. Villa, C. Chipot, R.D. Skeel, L. Kale, K. Schulten, Scalable molecular dynamics with NAMD, *Journal of Computational Chemistry*, 26 2005 1781-1802.

M.R. Prausnitz, V.G. Bose, R. Langer, J.C. Weaver, Electroporation of mammalian skin: A mechanism to enhance transdermal drug delivery, *Proceedings of the National Academy of Sciences* 90 (1993) 10504–10508.

W. H. Press, B. P. Flannery, S. A. Teukolsky, and W. T. Vetterling, Numerical Recipes; *The Art of Scientific Computing,* Cambridge University, 1986.

S Raffy, J Teissie, Electroinsertion of glycophorin A in interdigitation-fusion giant unilamellar lipid vesicles, *The Journal of Biological Chemistry* 272 (1997) 25524–25530.

W. Rawicz, K. C. Olbrich, T. McIntosh, D. Needham, and E. Evans, Effect of chain length and unsaturation on elasticity of lipid bilayers, *Biophysical Journal* 79 (2000) 328-339.

A. Ridi, E. Scalas, M. Robello, A. Gliozzi, Linear response of a fluctuating lipid bilayer, *Thin Solid Films* 327-329 (1998) 796-799.

A. Ridi, E. Scalas, A. Gliozzi, Noise measurements in bilayer lipid membranes during electroporation, *The European Physical Journal E* 2 (2000) 161-168.

M. Robello, A. Gliozzi, Conductance transition induced by an electric field in lipid bilayers, *Biochimica et Biophysica Acta* 982 (1989) 173-176.

M.P. Rols, J. Teissié, Electropermeabilization of mammalian cells. quantitative analysis of the phenomenon, *Biophisical Journal* 58 (1990) 1089-1098.

N. J. Rowan, S. J. MacGregor, J. G. Anderson, R. A. Fouracre, O. Farish, Pulsed electric field inactivation of diarrhoeagenic Bacillus cereus through irreversible electroporation, *Letters in Applied Microbiology* 31 (2000) 110–114.

I. Sabotin, *Porušitvena napetost dvokomponentnega ravninskega lipidnega dvosloja*, Diplomsko delo univerzitetnega študija, Univerza v Ljubljani, Fakulteta za elektrotehniko 2008.

J.N. Sachs, P.S. Crozier, T.B. Woolf, Atomistic simulations of biologically realistic transmembrane potential gradients, *Journal of Chemical Physics* 121 (2004) 22 10847-10851.

A.J.H. Sale, A. Hamilton, Effects of high electric fields on microorganisms: I. Killing of bacteria and yeasts. *Biochimica et Biophysica Acta*, 148 (1967) 781-788.

E. Schmidt, U. Leinfelder, P. Gessner, D. Zillikens, E.B. Brocker, U. Zimmermann, CD19+ B lymphocytes are the major source of human antibody-secreting hybridomas generated by electrofusion, *Journal of Immunological Methods* 255 (2001) 93–102.

M. B. Schneider, J. T. Jenkins, and W. W. Webb, Thermal fluctuations of large cylindrical phospholipid-vesicles, *Biophysical Journal* 45 (1984) 891-899.

T.H. Scott-Taylor, R. Pettengell, I. Clarke, G. Stuhler, M.C. La Barthe, P. Walden, A.G. Dalgleish,. Human tumour and dendritic cell hybrids generated by electrofusion: potential for cancer vaccines, *Biochimica et Biophysica Acta* 1500 (2000) 265–267.

G. Serša, D Miklavčič, M Čemažar, Z Rudolf, G Pucihar, M Snoj, Electrochemotherapy in treatment of tumours. *European Journal of Surgical Oncology* 34 (2008) 232-240.

G. Serša, B. Stabuc, M Čemazar, B Jančar, D. Miklavčič, Z Rudolf, Electrochemotherapy with cisplatin: Potentiation of local cisplatin antitumour effectiveness by application of electric pulses in cancer patients. *European Journal of Cancer* 34(8) (1989) 1213-1218.

V. Sharma, K. Uma Maheswari, J. C. Murphy, L. Tung, Poloxamer 188 Decreases Susceptibility of Artificial Lipid Membranes to Electroporation, *Biophisical Journal* 71 (1996) 3229-3241.

M.Smeyers, M.Leonetti, E.Goormaghtigh, F.Homble, Structure and function of plant membrane ion channels reconstituted in planar lipid bilayers, In *Planar Lipid Bilayers (BLMs) and their Applications*. (Ed. H.T.Tien, A.Ottova-Leitmannova) pp. 449-478, Elsevier, New York 2003.

A.E. Sowers, Membrane electrofusion: a paradigm for study of membrane fusion mechanisms, *Methods in Enzymology* 220 (1993) 196–211.

R. Stampfli, Reversible electrical breakdown of the excitable membrane of a Ranvier node, *An Acad Brasil Ciens* 30 (1958) 57-63.

M Tarek, Membrane electroporation: A molecular dynamics simulation. *Biophysical Journal* 88(6) (2005) 4045-4053.

J. Teissie, N. Eynard, M.C. Vernhes, A. Benichou, V. Ganeva, B. Galutzov, P.A. Cabanes, Recent biotechnological developments of electropulsation. A prospective review, *Bioelectrochemistry* 55 (2002) 107–112.

D.P. Tieleman, H.J. Berendsen, M.S. Sansom, Voltage-dependent insertion of alamethicin at phospholipid/water and octane/water interfaces, *Biophysical Journal* 80(1) (2001) 331–346.

D.P. Tieleman, H. Leontiadou, A.E. Mark, S.J. Marrink, Simulation of pore formation in lipid bilayers by mechanical stress and electric fields. *Journal of the American Chemical Society* 125 (21) (2003) 6382-6383.

D.P. Tieleman The molecular basis of electroporation, *BMC Biochemistry* 5:10 (2004).

H.T.Tien, A.Ottova, The lipid bilayer concept: Experimental realization and current applications, In *Planar lipid bilayers (BLMs) and their applications*, (Ed. H.T.Tien, A.Ottova-Leitmannova) pp. 1-74, Elsevier, New York 2003.

G.C. Troiano, L. Tung, V. Sharma, K.J. Stebe, The Reduction in Electroporation Voltages by the Addition of Surfactant to Planar Lipid Bilayer, *Biophisical Journal* 75 (1998) 880-888.

K. Trontelj, M. Ušaj, D. Miklavčič, Cell electrofusion visualized with fluorescence micro-scopy (Video Article), *Journal of Visual Experiments*, 41 (2010) 1991.

T.Y. Tsong, Electroporation of cell membranes, *Biophisical Journal* 60 (1991) 297-306.

T. Tuma, A. Buermen, *Circuit Simulation with SPICE OPUS, Theory and Practice*, Series: Modeling and Simulation in Science, Engineering and Technology, Springer 2009.

R. Vanbever, N. Lecouturier, V. Preat, Transdermal delivery of metoprolol by electroporation, *Pharmacological Research* 11 (1994) 1657–1662.

L. Verlet, Computer experiments on clasical fluids. I. Thermodynamical properties if Lennard-Jones molecules, *Physical Review Letters* 195 (1976) 98.103.

J.C. Weaver, Y.A. Chizmadzhev, Theory of electroporation: a review, *Bioelectrochemistry and Bioenergetics* 41 (1996) 135-160.

C. Wilhelm, M. Winterhalter, U. Zimmermann, R. Benz, Kinetics o pore size during irreversible electrical breakdown of lipid bilayer membranes, *Biophisical Journal* 64 (1993) 121-128.

M. Winterhalter, Black lipid membranes, *Current Opinion in Colloid & Interface Science* 5, (2000) 250-255.

T. Zehl, M. Wahab, H. J. Mogel, and P. Schiller, Monte Carlo simulations of self-assembled surfactant aggregates, *Langmuir* 22 (2006) 2523-2527.

T.E. Zewert, U. Pliquett, R. Langer, J. C. Weaver, Transport of DNA antisense oligonucleotides across human skin by electroporation, *Biochemical and Biophysical Research Communications* 212 (1995) 286–292.

U. Zimmermann, Electric Field-mediated Fusion and Related Electrical Phenomena, *Biochimica et Biophysica Acta* 694 (1982) 227-277.

Spletni viri

http://www.ks.uiuc.edu/Research/namd/ 20.5.2010.

http://www.ks.uiuc.edu/Research/vmd/ 20.5.2010.

http://pracownicy.uwm.edu.pl/kalinow/ksp/index.html 20.5.2010.

http://www.spiceopus.si 20.5.2010.

http://www.mathworks.com/access/helpdesk/help/toolbox/stats/nlparci.html 20.5.2010.

Izjava

Izjavljam, da sem doktorsko disertacijo izdelal samostojno, pod mentorstvom doc. dr.Alenke Maček Lebar. Pomoč drugih sodelavcev sem navedel v zahvali.

Peter Kramar

Dodatek

K doktorski disertaciji sem dodal štiri objavljene članke in eno poglavje. V priloženih delih sem prvi ali vodilni avtor in so relevantni raziskavam navedenim v doktorski disertaciji:

1. P. Kramar, D. Miklavčič, A. Maček-Lebar, Determination of the lipid bilayer breakdown voltage by means of a linear rising signal, *Bioelectrochemistry* 70 (2007) 23-27.
2. P. Kramar, D. Miklavčič, A. Maček-Lebar, A system for the determination of planar lipid membrane voltage and its applications, *IEEE Transactions of Nanobioscience* 8 (2009) 132-138.
3. I. Sabotin, A. Maček Lebar, D. Miklavčič, Measurement protocol for Planar Lipid Bilayer Viscoelastic Properties, *IEEE Transactions on Dielectrics and Electrical Insulation* 16(5) (2009) 1237-1242.
4. P. Kramar, D. Miklavčič, A. Maček Lebar, Merjenje lastnosti ravninskih lipidnih dvoslojev, *Elektrotehniški vestnik* 76(5) (2009) 293-298.
5. P. Kramar, D. Miklavčič, M. Kotulska, A. Maček Lebar, Voltage and current clamp methods for determination of planar lipid bilayer properties, In *Advances in planar lipid bilayer and liposomes, 11*; Urednik: Aleš Iglič, 2010.

Članek 1

Determination of the lipid bilayer breakdown voltage by means of linear rising signal

Peter Kramar, Damijan Miklavčič, Alenka Maček Lebar

Objavljen v: Bioelectrochemistry 70 (2007) 23-27

Available online at www.sciencedirect.com
ScienceDirect
Bioelectrochemistry 70 (2007) 23–27
Bioelectrochemistry
www.elsevier.com/locate/bioelechem

Determination of the lipid bilayer breakdown voltage by means of linear rising signal

P. Kramar, D. Miklavcic, A. Macek Lebar *

Faculty of Electrical Engineering, University of Ljubljana, SI-1000 Ljubljana, Slovenia

Received 1 June 2005
Available online 5 April 2006

Abstract

Electroporation is characterized by formation of structural changes within the cell membrane, which are caused by the presence of electrical field. It is believed that "pores" are mostly formed in lipid bilayer structure; if so, planar lipid bilayer represents a suitable model for experimental and theoretical studies of cell membrane electroporation. The breakdown voltage of the lipid bilayer is usually determined by repeatedly applying a rectangular voltage pulse. The amplitude of the voltage pulse is incremented in small steps until the breakdown of the bilayer is obtained. Using such a protocol each bilayer is exposed to a voltage pulse many times and the number of applied voltage pulses is not known in advance. Such a pre-treatment of the lipid bilayer affects its stability and consequently the breakdown voltage of the lipid bilayer. The aim of this study is to examine an alternative approach for determination of the lipid bilayer breakdown voltage by linear rising voltage signal.

Different slopes of linear rising signal have been used in our experiments (POPC lipids; folding method for forming in the salt solution of 100 mM KCl). The breakdown voltage depends on the slope of the linear rising signal. Results show that gently sloping voltage signal electroporates the lipid bilayer at a lower voltage then steep voltage signal. Linear rising signal with gentle slope can be considered as having longer pre-treatment of the lipid bilayer; thus, the corresponding breakdown voltage is lower. With decreasing the slope of linear rising signal, minimal breakdown voltage for specific lipid bilayer can be determined.

Based on our results, we suggest determination of lipid bilayer breakdown voltage by linear rising signal. Better reproducibility and lower scattering are obtained due to the fact that each bilayer is exposed to electroporation treatment only once. Moreover, minimal breakdown voltage for specific lipid bilayer can be determined.

Keywords: Lipid bilayer; Linear rising signal; Capacitance; Breakdown voltage

1. Introduction

Electroporation is characterized by a formation of structural changes within the cell membrane, which are caused by the presence of electric field. These changes, named "pores", increase the plasma membrane permeability, and enable ions and molecules to enter the cell [1]. Reversible electroporation is used to introduce various substances into the cell and has many practical applications like gene therapy, transdermal drug delivery and electrochemotherapy [2–5]. If cell membrane collapses due to too high electric field, the electroporation becomes irreversible. This form of the phenomenon can be used for liquid food and water conservation [6,7]. The applicability of electroporation is broad: from biotechnology and biology to medicine. Each application has its own optimal electrical parameters [8], which has to be determined beforehand [9].

It is stipulated that pores are mostly formed by rearranging of lipid molecules in lipid bilayer structure; if so, planar lipid bilayer is a good model for experimental and theoretical studies [10]. The planar lipid bilayer can be considered as a small part of total cell membrane. Lipid bilayer as an artificial model of the cell membrane can be made of only one type of lipid molecules, their mixtures or even lipids and proteins [11]. Lipid bilayers of different compositions have different electrical properties that are, due to their influence on membrane stability in electric field, important for the use of electroporation.

Planar lipid bilayer stability in an electric field and consequently the voltage that cause bilayer rapture is one of the most

* Corresponding author. Tel.: +386 1 4768 770; fax: +386 1 4264 658.
E-mail address: alenka@lbk.fe.uni-lj.si (A.M. Lebar).

1567-5394/$ - see front matter © 2006 Elsevier B.V. All rights reserved.
doi:10.1016/j.bioelechem.2006.03.022

important properties of planar lipid bilayers. The breakdown voltage of the lipid bilayer is usually determined by a rectangular voltage pulse. The amplitude of the voltage pulse is incremented in small steps until the breakdown of the bilayer is obtained [12]. Using such a protocol, the number of applied voltage pulses is not known in advance and each bilayer is exposed to voltage stress many times. Such a pre-treatment of the lipid bilayer affects its stability and consequently the determined breakdown voltage of the lipid bilayer [13]. In this study, another approach for the breakdown voltage determination is suggested: using linear rising signal, the breakdown voltage is determined by a single voltage exposure.

2. Materials and methods

2.1. Electrical setup

Our system for following up electroporation of planar lipid bilayers consists of a signal generator, a Teflon chamber and a device, which is used for measurements of membrane current and voltage (Fig. 1).

Signal generator is a voltage generator of an arbitrary type that provides voltage amplitudes from −5 V to +5 V. It is controlled by costume written software (Genpyrrha), specially designed for drawing the voltage signal that is used for membrane electroporation. The last but not least part of the signal generator is an analogue switch. The switch disconnects the output of the signal generator and switches to the 1 MΩ resistor. The switch is fast, it turns off the signal generator in 2 ns. In this way, a system discharge voltage is measured and consequently the capacitance of the lipid bilayer.

Two Ag-AgCl electrodes, one on each side of the planar lipid bilayer, were plunged into the salt solution. Transmembrane voltage was measured via a LeCroy differential amplifier 1822. The same electrodes were used to measure transmembrane current. Both signals were stored in oscilloscope LeCroy Waverunner-2 354 M in Matlab format. All the signals were processed offline. Chamber is made out of Teflon. It consists of two cubed reservoirs with volume of 5.3 cm^3 each. In the hole between two reservoirs, a thin Teflon sheet with a round hole

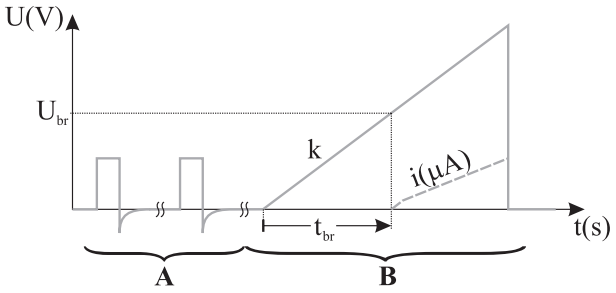

Fig. 2. Measurement protocol: (A) capacitance measurement of lipid bilayer was measured in two steps. In the first step, we measured capacitance of the electronic system without lipid bilayer. Second step was measuring capacitance of electronic system with lipid bilayer and salt solution. (B) Voltage breakdown measurement with linear rising signal.

(105 μm diameter) is inserted. Lipid bilayer is formed by the Montal-Muller method [14].

2.2. Chemical setup

The salt solution was prepared of 0.1 molar KCl and 0.01 molar Hepes in the same proportion. Some droplets of one molar NaOH were added to obtain pH 4.7. The lipids were prepared from POPC (1-pamitol, 2-oleiol phosphatdiholin) in powder form (Avanti Polar-Lipids Inc. ZDA). The POPC was melted in solution of hexane and ethanol in ratio 9:1. The mixture of hexadecane and pentane in ratio 3:7 was used for torus forming.

2.3. Measurement protocol

Measurement protocol consisted of two parts: capacitance measurement (Fig. 2A) and lipid bilayer breakdown voltage measurement (Fig. 2B). Capacitance and the breakdown voltage were determined for each lipid bilayer.

The capacitance of lipid bilayer was measured in two steps (Fig. 2). In the first step, we measured capacitance of the electronic system without lipid bilayer (C_{SYS}). The resistance of oscilloscope probes (1 MΩ) and the special resistor (1 MΩ) were

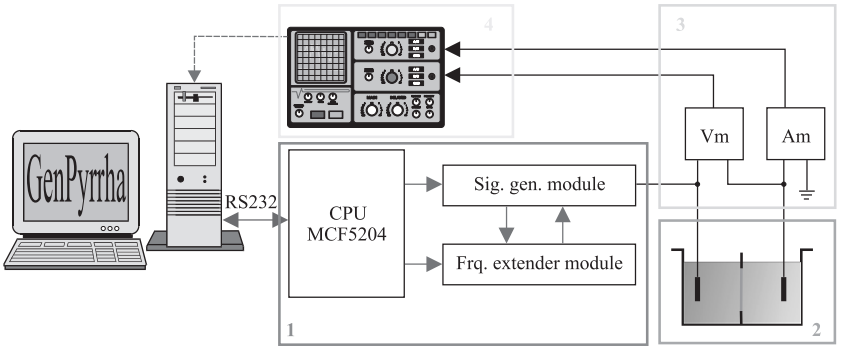

Fig. 1. System for electroporation of planar lipid bilayer. (1) The microprocessor board with MCF5024 processor and two modules. One module generates arbitrary signals and the other that is realized in Xillinx is used for frequency extension. (2) Chamber for forming lipid bilayers and two Ag-AgCl electrodes. (3) Modules for current and voltage amplification. (4) Digital oscilloscope for data storing.

connected in parallel as shown on Fig. 3A. Therefore, the resistance R_{SYS} was approximately 500 kΩ. By finding the time constant τ_{SYS} of the voltage discharge the capacitance C_{SYS} was determined considering the relation

$$C_{SYS} = \frac{\tau_{SYS}}{R_{SYS}}. \quad (1)$$

Second step was measuring capacitance of electronic system with lipid bilayer and salt solution (C_{SBLM}) (Fig. 3B). Equivalent resistor (R_{SYS}) was still 500 kΩ, because the resistance of the lipid bilayer was greater than 10^8 Ω [15].

By finding the time constant τ_{SBLM} of the voltage discharge, the capacitance C_{SBLM} was determined

$$C_{SBLM} = \frac{\tau_{SBLM}}{R_{SBLM}}. \quad (2)$$

The capacitance of lipid bilayer was obtained as a difference between C_{SYS} and C_{SBLM}:

$$C_{BLM} = C_{CYS} - C_{SBLM}. \quad (3)$$

The specific membrane capacitance (c) was obtained by dividing C_{BLM} by the bilayer surface area.

We determined breakdown voltage (U_{br}) of the lipid bilayer by the linear rising signal. The slope of the linear rising signal (k) and the peak voltage of the signal has to be selected in advance. Six different slopes were selected. Breakdown voltage was defined as the voltage at the moment t_{br} when sudden increase of transmembrane current was observed. Time of breakdown t_{br} was defined as a lifetime of the lipid bilayer at a chosen slope of the linear rising signal (Fig. 2).

2.4. Statistics

To compare breakdown voltages and specific membrane capacitances of the lipid bilayers exposed to voltage signals of different slopes (k) Kruskal–Wallis, one-way analysis of variance on ranks test was used. All pairwise multiple comparisons were made by Tukey's test. Descriptive statistics include mean value and standard deviation.

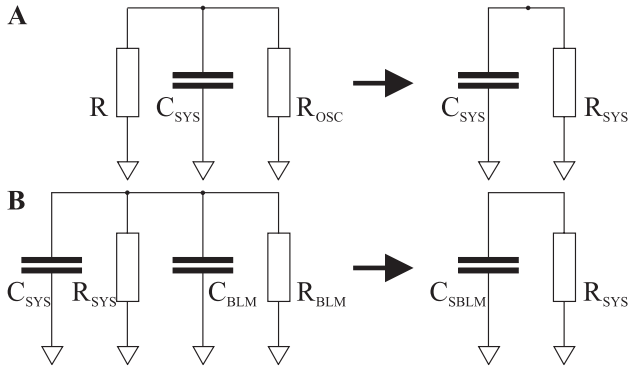

Fig. 3. Electric circuits: (A) system without lipid bilayer and salt solution; (B) system with planar lipid bilayer and salt solution.

Table 1
Specific membrane capacitances (c), breakdown voltages (U_{br}) and lifetimes (t_{br}) for lipid bilayers exposed to linear rising voltage signals of different slopes (k)

N	k (kV/s)	c (μF/cm^2)	U_{br} (V)	t_{br} (μs)
18	4.8	0.5±0.1	0.51±0.02	104±4
6	5.5	0.5±0.1	0.48±0.01	86±3
4	7.8	0.6±0.1	0.49±0.01	61±2
3	16.7	–	0.57±0.01	34±1
5	21.6	0.4±0.1	0.59±0.02	27±1
3	48.1	–	0.74±0.02	15±1

Values given are mean±standard deviation. Number of measurements N in each experimental group is given in the first column.

Using nonlinear regression, a two-parameter curve was fitted to the data

$$U = \frac{a}{1 - e^{-t/b}}, \quad (4)$$

where U was U_{br} measured at different slopes, t was corresponding t_{br}, and a and b are two parameters. Parameter a is an asymptote of the curve, which corresponds to minimal breakdown voltage U_{brMIN} for specific bilayer. Parameter b governs the inclination of the curve.

3. Results

Mean specific membrane capacitances (c) and mean breakdown voltages (U_{br}) of the lipid bilayers with their standard deviations for six different slopes (k) are given in Table 1. Specific membrane capacitances of membranes exposed to linear rising signal of different slopes (k) were in the same range; no statistically significant difference was obtained between different experimental groups. The c for all bilayers included in the study was measured to be 0.5±0.1 μF/cm^2.

Breakdown voltage U_{br} increased with increasing slope of the linear rising voltage signal. U_{br} measured at slope 4.8 kV/s is not statistically different from U_{br} measured at slope 5.5 kV/s

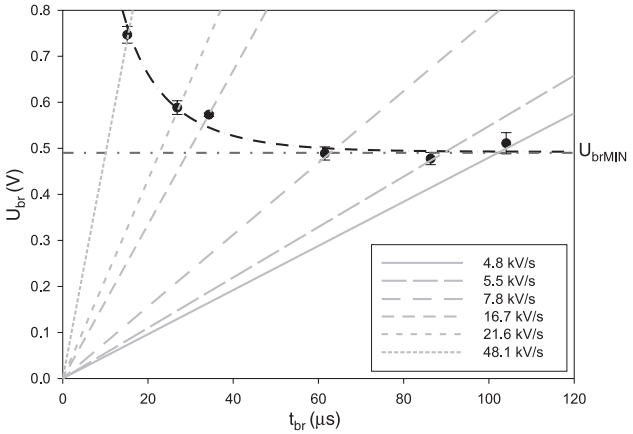

Fig. 4. The breakdown voltage (U_{br}) (black dots) of lipid bilayers as a function of lifetime t_{br}. The gray lines on the figure show six different slopes (k) of applied liner rising voltage signal. Black dashed curve represents two parameters equation fitted to data (Eq. (4)). An asymptote of the curve (a) with the value of 0.49 V corresponds to minimal breakdown voltage U_{brMIN} for lipid bilayers made of POPC.

($p=0.009$) and it is not statistically different from U_{br} measured at slope 7.8 kV/s ($p=0.305$). U_{br} measured at slope 5.5 kV/s is not statistically different from U_{br} measured at slope 7.8 kV/s ($p=0.941$). Also U_{br} measured at slopes 16.7 kV/s and 21.6 kV/s are not statistically different ($p=0.872$). All other pairwise multiple comparisons exhibited $p<0.001$; these means that U_{br} of all other experimental groups differ significantly.

The data are also presented in graphical form (Fig. 4). The parameters a and b of the curve (4) are 0.49 V and 14.77 μs, respectively. An asymptote of the curve (a) with the value of 0.49 V is considered as minimal breakdown voltage U_{brMIN} for lipid bilayers made of POPC.

4. Discussion

Breakdown voltage is one of the most important properties of a lipid bilayer when biomedical and biotechnological applications of electroporation are under consideration. Although planar lipid bilayer differs in a number of characteristics from the biological membrane, it is believed that general picture of the electroporation is the same [16]. The aim of this study was to present a different measuring protocol for determination of the lipid bilayer breakdown voltage, which would avoid multiple exposure of the lipid bilayer to a voltage stress.

According to our measuring protocol, each lipid bilayer is exposed to voltage signal only twice. First bilayer capacitance is determined by a rectangular voltage signal of 0.30 V. Capacitance measurement reveals an intact lipid bilayer before inducing its breakdown. In the next step, lipid bilayer breakdown is induced by linear rising voltage signal.

Evans et al. used similar approach in their experiments on lipid vesicles [17]. They applied tension at different loading rates and they found out that tension needed for membrane rupture increases with increasing loading rate. These results are in line with the results of our study, with different stimulating signal. On the other hand, Satkauskas et al. compared effectiveness of different electrochemotherapy protocols in vivo on mice [18]. They used different durations and amplitudes of rectangular voltage pulses and observed nonlinear dependence between amplitude (strength) and duration of the signal for the same electrochemotherapy effectiveness.

In our study, we selected six different slopes of linear rising voltage signal due to already known experimental evidence that lipid bilayer lifetime is dependent on the applied voltage [12,19] and that the lipid bilayer breakdown voltage is dependent on the lipid bilayer pre-treatment [13]. Our results show that lifetime of lipid bilayer depends on the slope of linear rising voltage signal and that also the breakdown voltage is a function of the slope of the linear rising voltage signal; it increases with increasing slope. This is comparable to results obtained by Evans et al. [17]. According to theoretical model proposed by Joshi and Schoenbach [20], the pore generation rate depends exponentially on the membrane voltage; therefore, in the case of steep voltage signal, breakdown voltage was achieved after shorter pre-treatment. On the other hand, also because of shorter pre-treatment of the lipid bilayer in the case of steep voltage signal the corresponding breakdown voltage was higher. Strength-duration two-parameter curve (Eq. (4)) was fitted to experimental data and an asymptote corresponded to minimal breakdown voltage U_{brMIN} of specific lipid bilayer (POPC).

Troiano et al. [12] have used the same lipids (POPC) in their experimental studies. With considerably long rectangular voltage pulses (10 s), they had detected breakdown voltage of 0.17 V. This value however is much lower then the U_{brMIN} obtained in our study (0.49 V). Because the entire pre-treatment (number of applied voltage pulses) of the lipid bilayers in their experiments is not known, it is possible that much low breakdown voltage was detected.

Based on our results, we suggest determination of lipid bilayer breakdown voltage by linear rising signal. Better reproducibility and lower scattering are obtained due to fact that each bilayer is exposed to electroporation treatment only once. Moreover, minimal breakdown voltage for specific lipid bilayer can be determined.

References

[1] E. Neumann, S. Kakorin, K. Toensing, Funadamentals of electroporative delivery of drugs and genes, Bioelectrochemistry and Bioenergetics 48 (1999) 3–16.
[2] A.R. Dent, V. Preat, Transdermal delivery of timol by electroporation through human skin, Journal of Controlled Release 88 (2003) 253–262.
[3] D. Ferber, Gene therapy: safer and virus-free? Science 294 (2001) 1638–1642.
[4] L.M. Mir, S. Orlowski, Mechanisms of electrochemotherapy, Advanced Drug Delivery Reviews 35 (1999) 107–118.
[5] M. Cemazar, I. Wilson, G.U. Dachs, G.M. Tozer, G. Sersa, Direct visualisation of electroporation-assisted in vivo gene delivery to tumors using interval microscopy—spatial and time dependent distribution, BMC Cancer 4 (2001) 81–87.
[6] G.W. Gould, Biodeterioration of foods and an overview of preservation in the food and dairy industries, International Biodeterioration & Biodegradation 36 (1995) 267–277.
[7] M.C. Vernhes, A. Benichou, P. Pernin, P.A. Cabanes, J. Teissie, Elimination of free-living amoebae in fresh water with pulsed electric fields, Water Research 36 (2002) 3429–3438.
[8] M. Puc, S. Corovic, K. Flisar, M. Petkovsek, J. Nastran, D. Miklavcic, Techniques of signal generation required for electropermeabilisation. Survey of electropermeabilisation devices, Bioelectrochemistry 64 (2004) 113–124.
[9] A. Macek Lebar, G. Sersa, S. Kranjc, A. Groselj, D. Miklavcic, Optimisation of pulse parameters in vitro for in vivo electrochemotherapy, Anticancer Research 22 (2002) 1731–1736.
[10] M. Fosnaric, V. Kralj-Iglic, K. Bohinc, A. Iglic, S. May, Stabilization of pores in lipid bilayers by anisotropic inclusions, Journal of Physical Chemistry. B 107 (2003) 12519–12526.
[11] H.T. Tien, A. Ottova, Planar lipid bilayers (BLMs) and their applications, Elsevier, New York, 2003, Ch. The Lipid Bilayer Concept: Experimental Realization and Current Applications, pp. 1–74.
[12] G.C. Troiano, L. Tung, V. Sharma, K.J. Stebe, The reduction in electroporation voltages by the addition of surfactant to planar lipid bilayer, Biophysical Journal 75 (1998) 880–888.
[13] I.G. Abidor, V.B. Arakelyan, L.V. Chernomordik, Y.A. Chizmadzhev, V.F. Pastushenko, M.R. Tarasevich, 246-electric breakdown of bilayer lipid membranes: i. The main experimental facts and their qualitative discussion, Bioelectrochemistry and Bioenergetics 6 (1979) 37–52.
[14] M. Montal, P. Muller, Formation of bimolecular membranes from lipid monolayers and study their electrical properties, Proceedings of the National Academy of Sciences of the United States of America 69 (1972) 3561–3566.
[15] H.T. Tien, Bilayer Lipid Membranes (BLM), Marcel Dekker, inc., New York, 1974.

[16] M. Tarek, Membrane electroporation: a molecular dynamics simulation, Biophysical Journal 88 (2005) 4045–4053.
[17] E. Evans, V. Heinrich, F. Ludwig, W. Rawicz, Dynamics tension spectroscopy and strength of biomembranes, Biophysical Journal 85 (2003) 2342–2350.
[18] S. Satkauskas, D. Batiuskaite, S. Salomskaite-Davalgiene, M.S. Venslauskas, Effectivness of tumor electrochemotherapy as a function of electric pulse strength duration, Bioelectrochemistry 65 (2005) 105–111.
[19] A. Macek Lebar, G.C. Troiano, L. Tung, D. Miklavcic, Inter-pulse interval between rectangular voltage pulses affects electroporation threshold of artificial lipid bilayers, IEEE Transactions on Nanobioscience 1 (3) (2002) 116–120.
[20] R.P. Joshi, K.H. Schoenbach, Electroporation dynamics in biological cells subjected to ultrafast electrical pulses: a numerical simulation study, Physical Review E 62 (2000) 1025–1033.

Članek 2

A System for the Determination of Planar Lipid Bilayer Breakdown Voltage and Its Applications

Peter Kramar, Damijan Miklavčič in Alenka Maček Lebar

Objavljen v: IEEE Transations on nanobioscience 8 (2009) 132-138

A System for the Determination of Planar Lipid Bilayer Breakdown Voltage and Its Applications

Peter Kramar, Damijan Miklavčič, and Alenka Maček Lebar*

***Abstract*—In this paper, we focus on measurement principles used in electroporation studies on planar lipid bilayers. In particular, we point out the voltage-clamp measurement principle that has great importance when the breakdown voltage of a planar lipid bilayer is under consideration; however, it is also appropriate for the determination of other planar lipid bilayer electrical properties such as resistance and capacitance. A new experimental system that is based on the voltage-clamp measurement principle is described. With the use of a generator that can generate arbitrary-type signals, many specific shapes of a voltage signal could be generated, and therefore, the experimental system is appropriate for a broad spectrum of measurements.**

***Index Terms*—Biomechanics, capacitance measurement, dielectric breakdown, electric field effects, isoelectric phenomena.**

I. Introduction

ELECTROPORATION is characterized by the formation of structural changes within the cell plasma membrane, which are caused by the presence of an electric field. These changes, most often described as "pores," are estimated to be in the order of 1–10 nm, increase the plasma membrane permeability, and enable transport of ions and molecules across the plasma membrane [1]. Electroporation is either reversible or irreversible. Reversible electroporation is used to introduce various substances into the cell and has practical applications in medicine, biology, and biotechnology, such as gene therapy, transdermal drug delivery, and electrochemotherapy [2]–[5]. If the cell membrane does not reseal due to a very high electric field, the electroporation is irreversible. Irreversible electroporation was suggested for liquid food and water conservation [6], [7], and tissue ablation [8], [9]. The applicability of electroporation is broad: from biotechnology and biology to medicine. The exact molecular mechanisms of the phenomenon are still not fully elucidated; however, it is believed that "pores" in the cell membrane are mostly formed by the rearrangement of lipid molecules. Therefore, artificial lipid bilayer structures in the form of planar lipid bilayers or lipid bilayer vesicles can be used as a model for experimental [10], [11] and theoretical studies of electroporation [12].

Lipid bilayer structures can be made of one type of lipid molecules or their mixtures. In more complex forms, they can be composed of different lipids and proteins [13]. Lipid bilayer composition drives events during the electroporation process and determines the electrical properties of a lipid bilayer structure. According to the broadly used electric circuit model of the lipid bilayer, which consists of resistance (R) and capacitance (C) in parallel, resistance and capacitance are the most often measured electrical properties of the lipid bilayer. From the electroporation point of view also, the breakdown voltage (U_{br}), i.e., the transmembrane voltage at which the lipid bilayer brakes, and the mass flux (Ψ) through the lipid bilayer are important.

Synthetic liposomes and vesicles are natural models, which mimic the geometry and topology of cell membranes. In some recent papers, it was reported that the field induces elongation of vesicles in the direction of the applied field prior to electroporation [10], and that the average rate of radius growth of the reversible pores is about five orders of magnitude smaller than that of irreversible electropores in planar lipid membranes of similar phospholipids [11].

But if the planar lipid bilayer is considered as a small fraction of the total cell membrane, it represents the simplest model for experimental studies of electroporation; especially because it is accessible from both sides.

Two measurement principles of planar lipid bilayer's properties are mainly used: the voltage-clamp method [14]–[25] and the current-clamp method [26]–[37]. In addition, due to the steadily growing use of wireless communication systems, application of electromagnetic waves is their alternative (see Fig. 1). By using different shapes of signals and frequencies, planar lipid bilayer's properties such as resistance, capacitance, thickness, voltage breakdown, and mass flux can be measured.

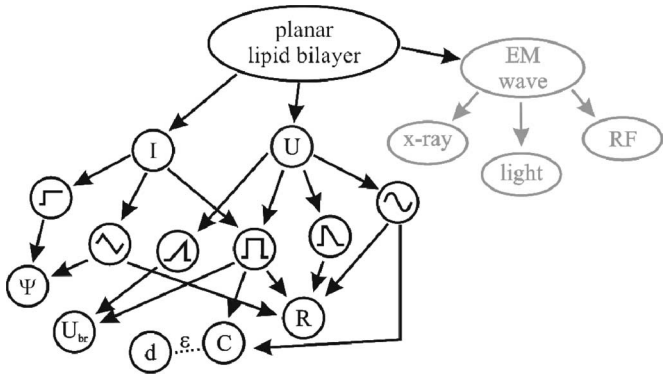

Fig. 1. Electrical properties of a planar lipid bilayer: resistance (R), capacitance (C), thickness (d), voltage breakdown (U_{br}), and mass flux (Ψ); these are measured with the application of current (I) signal and voltage (U) signal of diverse shapes. Application of electromagnetic waves is an alternative.

Manuscript received March 14, 2008. Current version published July 31, 2009. This work was supported by the Slovenian Research Agency under Grant P2-0249. *Asterisk indicates corresponding author.*

P. Kramar and D. Miklavčič are with the Faculty of Electrical Engineering, University of Ljubljana, Ljubljana SI-1000, Slovenia (e-mail: peter.kramar@fe.uni-lj.si; damijan.miklavcic@fe.uni-lj.si).

*A. M. Lebar is with the Faculty of Electrical Engineering, University of Ljubljana, Ljubljana SI-1000, Slovenia (e-mail: alenka.maceklebar@fe.uni-lj.si).

Digital Object Identifier 10.1109/TNB.2009.2022834

In the voltage-clamp method, the voltage signal is applied to the lipid bilayer. The simplest as well as the most often used shape of the voltage signal is a square voltage pulse [14], [18], but other shapes have also been used [15], [21], [38], [39]. Some experiments were done by using two sinus-shaped voltage signals: the first with a low frequency and large amplitude, and the second with a high frequency and low amplitude that was added to the first one. In this way, lipid bilayer conductance and capacitance were determined at the same time [37].

In the current-clamp method, the current is applied to the lipid bilayer. Usually, this method is appropriate for measuring the resistance of lipid bilayer and the mass flow. It is believed that during these kinds of measurements, the lipid bilayer is more stable due to less voltage stress [27], [30]; therefore, small changes in the membrane structure can also be observed. Scalas *et al.* [31], for example, reported on the time course of voltage fluctuations that followed an increase of the membrane conductance due to the opening and closing of hydrophilic pores [28], [31], [40].

Under current-clamp conditions, the transmembrane voltage increases slowly; therefore, stable pores could be formed [27], [29], [32], [41]. The creation of the first pore in the planar lipid bilayer causes a fast reduction in transmembrane voltage, which decreases the probability of next pore creation [27]. Because the pore size is voltage dependent, the pore size decreases. As a consequence, the transmembrane voltage and the pore size increase again. These fluctuations of transmembrane voltage and pore size allow for maintenance of the electroporated planar lipid bilayer. Therefore, such experimental conditions are extremely useful for investigations of membrane organization at the molecular level.

Combination of electrical recording techniques with different kinds of high-frequency electromagnetic fields offers additional insights. For structure elucidation of lipid–water mesophases, small- and wide-angle X-ray scattering methods were used [42]. Hanyu *et al.* [43] presented an experimental system that allows measurement of current (function) and fluorescence emission (structural change) of an ion channel in the planar lipid bilayer while the membrane potential is controlled like functional relationships between the planar lipid bilayer and membrane interacting peptides. Rapid and reversible changes in photoresponsive planar lipid bilayer's electrical properties when irradiated with light were studied by Yamaguchi and Nakanishi [44]. Planar lipid bilayers have also been exposed to an RF field of about 900 MHz according to GSM standards, and the authors reported that temperature oscillations due to the pulsed RF fields are too small to influence planar lipid bilayer's low-frequency behavior [45].

In this paper, we focus on the voltage-clamp measurement principle. We explain advantages and disadvantages of this method and describe its measuring system requirements. We present a new measuring system that has broad applicability; the new system allows generation of arbitrary waveforms, and therefore, many existing experimental procedures can be repeated and completely new measurements can be planned.

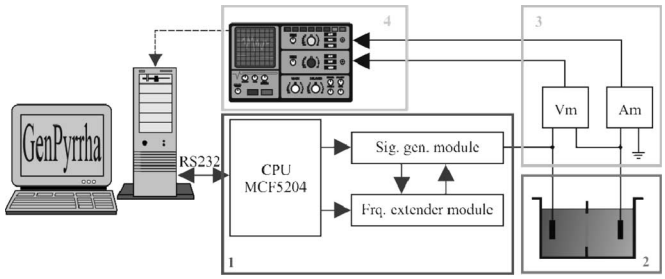

Fig. 2. Experimental system: 1) microprocessor board with MCF5024 processor and two modules. The signal generator module generates arbitrary signals. The frequency extender module is realized in the programmable integrated circuit (FPGA) and is used for frequency extension; 2) chamber for forming planar lipid bilayer and two Ag–AgCl electrodes; 3) modules for current and voltage amplification; 4) oscilloscope for data collection and storage.

II. Experimental System

The system consists of a signal generator, a Teflon chamber where the planar lipid bilayer is prepared, a device for voltage and current measurement and storage. Fig. 2 presents a typical structure of the experimental system: a signal generator (see Fig. 2-1), a chamber for forming planar lipid bilayers and electrodes (see Fig. 2-2), voltage and current amplifiers (see Fig. 2-3), and an oscilloscope for data storage (see Fig. 2-4).

A. Signal Generator

Signal generator is a generator of an arbitrary type. It provides voltage amplitudes from -5 to $+5$ V. It is controlled by custom-designed software, specially designed for drawing the arbitrary voltage signals that are used for membrane electroporation. In the program, the gain of the output amplifier and the way of triggering can be selected as single, continuous, or burst type. The signal can be either monopolar or bipolar, and a different number of pulses can be generated. The last but not least part of the signal generator is an analog switch. The switch disconnects the output of the signal generator and switches one electrode to the 1-MΩ resistor. The switch is fast: it turns off the signal generator in 2 ns. In this way, the system discharge voltage, as well as the capacitance of the lipid bilayer, is measured. The signal time resolution is 860 ns or 1.17 MHz; however, lower and higher frequencies can also be obtained.

For higher frequencies applications, a special circuit for frequency extensions that consists of a programmable integrated circuit [field-programmable gate array (FPGA)] is added. The highest sampling frequency is 33 MHz. Lower frequencies can be selected by inner decades that are programmed in the programmable integrated circuit and separated by a 7-bit binary counter.

B. Voltage and Current Amplification, and Storage

Two Ag–AgCl electrodes (IVM, USA), one on each side of the planar lipid bilayer, are immersed into a salt solution. The transmembrane voltage is measured by LeCroy differential amplifier 1822. The same electrodes are also used to measure the transmembrane current. An electronic circuit transforms the

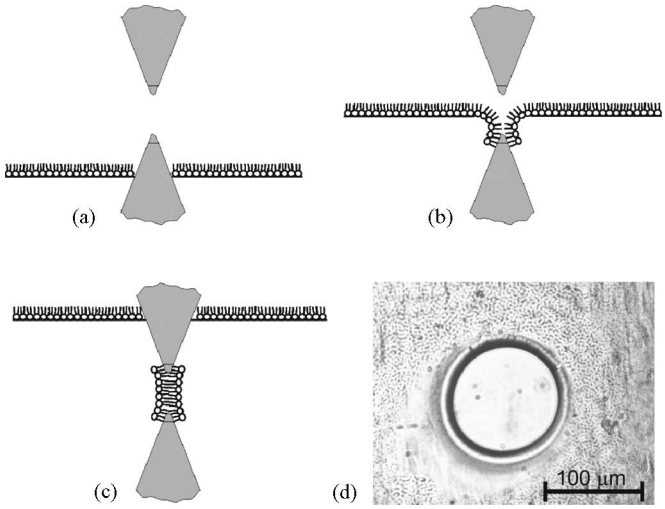

Fig. 3. Montal–Müeller method for planar lipid bilayer formation [46]. (a) Layer of lipid molecules on the salt solution. (b) Level of the salt solution is slowly raised above the hole. (c) Planar lipid bilayer is made on the hole. (d) Round hole in a Teflon sheet made by electrical discharge. The image of the hole was captured by Olympus DP 10 Camera and Olympus DP soft programme through Olympus CK 40 microscope at the 20× magnification. The diameter of the hole (105 μm) was determined by Olympus DP-soft programme measuring tools.

transmembrane current into voltage, so that 1 V corresponds to 1 mA of a transmembrane current.

Both signals are stored by the oscilloscope LeCroy Waverunner-2 354M in the MATLAB format. All sampled signals are analyzed in MATLAB software after experiments.

C. Chamber

The chamber is made of Teflon. Teflon is highly resistant to chemicals, and therefore, it may be cleaned with aggressive chemicals such as sulfuric acid (H_2SO_4). Between experiments the chamber is soaked in H_2SO_4. The chamber consists of two parts; each part is a cubed reservoir with a volume of 5.3 cm^3. Between the reservoirs a 25.40-μm-thin Teflon sheet is inserted. A round hole [see Fig. 3(d)] was made in the Teflon sheet by electrical discharge. The diameter of the hole was measured (105 μm) and the area of the hole was calculated (8.66 nm^2). The lipid bilayer is formed on the hole by a folding method given by Montal and Müeller [see Fig. 3(a)–(c)] [46]. This method was selected due to its fast rebuilding ability of a planar lipid bilayer after each breakdown. The membrane was assumed to span 90% of the area of the hole, while the remaining 10% is occupied by the torus of solvent that supports the membrane.

The salt solution is poured in both reservoirs through special channels. The channels have a diameter of 0.8 mm and lies below 50° with respect to the bottom of the reservoirs. Through each channel, a pipeline is inserted into each reservoir. The level of salt solution in the reservoir is regulated by using a syringe filled with salt solution, which is attached to the outer side of the pipeline.

TABLE I
SPECIFIC MEMBRANE CAPACITANCES

Lipid mixtures	C (μF/CM^2)	N
POPC	0.5±0.1	33
POPC+1μM $C_{12}E_8$	0.21±0.02	37
POPS:POPC (3:7)	0.29±0.07	42

Specific membrane capacitances (C) that have been measured for three lipid mixtures. Values given are mean ± standard deviation. The number of measurements (N) in each experimental group is given in the third column.

D. Chemicals

The results presented in this paper were obtained by chemicals described in this section. Our experiments were done using the salt solution prepared of 0.1 molar KCl (MERCK, Germany) and 0.01 molar 4-(2-hydroxyethyl)-1-piperazineethanesulfonic acid (Hepes) (MERCK, Germany) in the same proportion. Some droplets of 1 molar NaOH (MERCK, Germany) were added to obtain a pH value of 7.4.

Synthetic lipids 1-palmitoyl-2-oleoyl-*sn*-glycero-3-phosphocholine (POPC) and 1-palmitoyl-2-oleoyl-*sn*-glycero-3-[phospho-L-serine] (POPS) were used in our experiments. Both are common parts of experimental structures (lipid bilayers and vesicles) and mimic at least one important constituent of the cell membrane—glycerophospholipids. They were obtained in powder form (Avanti Polar Lipids, Inc., ZDA), and melted in the solution of hexane and ethanol (Riedel-de Haën, Germany) in a ratio of 9:1. Octaethyleneglycol mono-*n*-dodecyl ether ($C_{12}E_8$) was obtained in crystal form (Fluka, Switzerland). The mixture of hexadecane and pentane (Merck, Germany) in a ratio of 3:7 was used for torus forming.

III. MEASUREMENT PRINCIPLES AND PROPERTIES OF PLANAR LIPID BILAYERS

The system described has been tested with different experimental protocols. Some of them were already proposed by other authors. We have determined the capacitance of lipid bilayers [18] and the breakdown voltage of planar lipid bilayers using rectangular pulses [14], [21], [24] as well as linear rising signals [38].

A. Capacitance of Lipid Bilayer

The capacitance (C) is a parameter that is considered to be the best tool for probing the stability and formal goodness of planar lipid bilayers. Using the system described, C is determined by the discharge method [18]. The data measured for each planar lipid bilayer mixture are presented in Table I.

B. Conductance During Electroporation

Resistance (R) or conductance (G) as an electrical property of planar lipid bilayers can be measured only during the application of voltage or current signals. Measurement of the current requires high sensitivity in the range of nanoamperes.

When a rectangular voltage pulse of a high amplitude is applied on the planar lipid bilayer, electroporation occurs and the conductance of the lipid bilayer increases considerably (see

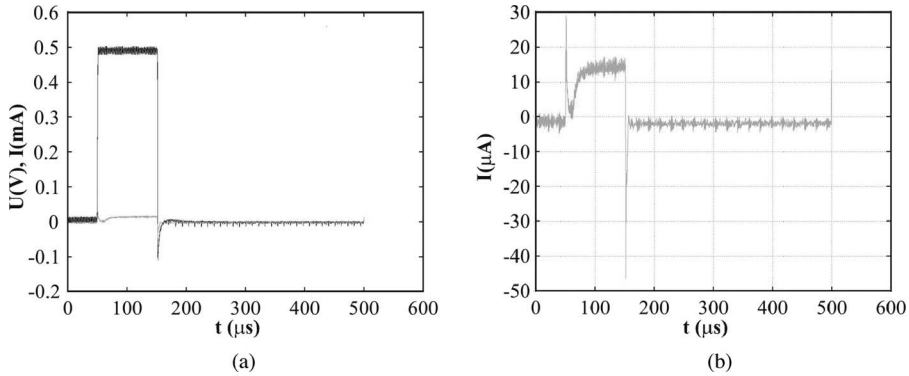

Fig. 4. Electroporation of the planar lipid bilayer. (a) Applied square signal and measured transmembrane current. (b) Enlargement of the transmembrane current during the voltage pulse.

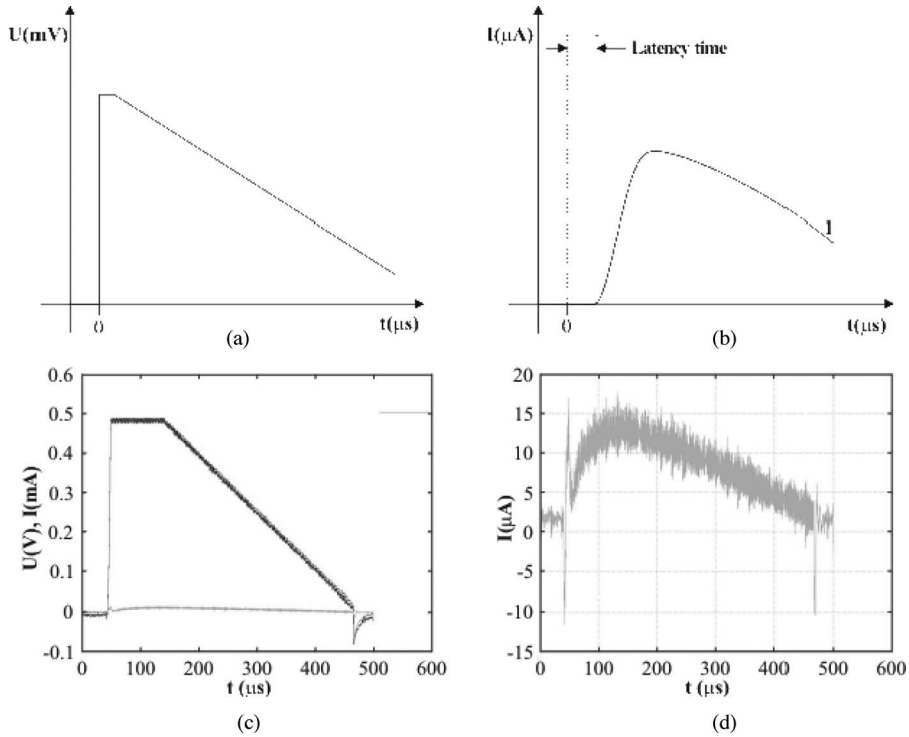

Fig. 5. (a) Voltage signal composed of an initial rectangular pulse and a negative slope ramp [15]. (b) Transmembrane current. *I* is a typical trace of the transmembrane current during the electroporation. (c) and (d) Corresponding results of our experiments.

Fig. 4). Consequently, current through the planar lipid bilayer also increases by several orders of magnitude, as shown in Fig. 4. Due to the constant voltage amplitude during the pulse, the dynamic conductance [$G(t)$] is determined by

$$G(t) = \frac{i(t)}{u(t)} \tag{1}$$

where $i(t)$ is the current measured through the planar lipid bilayer and $u(t)$ is the applied voltage.

Sharma *et al.* have used a special waveform for measuring the dynamic conductance of the lipid bilayer during the electroporation [15]. The applied signal is composed of an initial rectangular pulse and a negative-sloped ramp. Such a pulse protocol allows longer measurement of membrane conductance. Due to the fact that with the system described in this paper an arbitrary shape of the voltage signal can be provided to the electrodes, our system is applicable for such measurements also (see Fig. 5).

C. Breakdown Voltage of the Planar Lipid Bilayer

Breakdown voltage ($U_{\rm br}$) is one of the most important properties of a lipid bilayer when biomedical and biotechnological applications of electroporation are under consideration.

Mostly, the breakdown voltage of the planar lipid bilayer is determined by applying a rectangular voltage pulse (10 μs–10 s). The amplitude of the voltage pulse is incremented in small steps until the breakdown of the bilayer is reached [14]. First, the voltage pulse charges up the planar lipid bilayer. Above the critical voltage ($U_{\rm br}$), defects are caused in the planar lipid bilayer

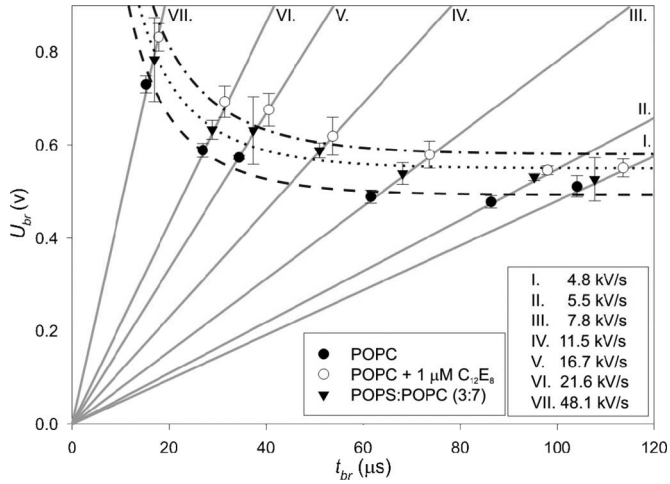

Fig. 6. Breakdown voltage ($U_{\rm br}$) (dots) of planar lipid bilayers with different chemical composition as a function of lifetime $t_{\rm br}$. The gray lines show seven different slopes of the applied linear rising voltage signal. Dash, dotted, and dash-dotted curves represent a two-parameter curve fitted to data (2).

allowing an increase of the transmembrane current. Usually, the membrane collapses thereafter.

Using the rectangular voltage pulse measuring protocol, the number of applied voltage pulses is not known in advance and each planar lipid bilayer is exposed to a voltage stress many times. Such a pretreatment of the planar lipid bilayer affects its stability and consequently the determined breakdown voltage of the planar lipid bilayer [24]. Another approach for the breakdown voltage determination was suggested by our group [38]. Using a linear rising signal, the breakdown voltage of each planar lipid bilayer is determined by a single voltage exposure.

The slope of the linear rising signal and the peak voltage of the signal have to be selected in advance. Breakdown voltage is defined as the voltage at the moment $t_{\rm br}$ when a sudden increase of the transmembrane current is observed. Time $t_{\rm br}$ was defined as the lifetime of the planar lipid bilayer at a chosen slope of the linear rising signal (see Fig. 6). Due to the already known experimental evidence that the planar lipid bilayer lifetime depends on the applied voltage [14], [47] and the planar lipid bilayer breakdown voltage depends on the planar lipid bilayer pretreatment [24], $U_{\rm br}$ and $t_{\rm br}$ were measured at six or seven different slopes. Indeed, the lifetime of the planar lipid bilayer depends on the slope of the linear rising voltage signal, and also the breakdown voltage is a function of the slope of the linear rising voltage signal; it increases with the increasing slope. Therefore, using nonlinear regression, a two-parameter curve was fitted to the data,

$$U = \frac{a}{1 - e^{-t/b}} \tag{2}$$

where U is the $U_{\rm br}$ measured at different slopes, t is the corresponding $t_{\rm br}$, and a and b are the parameters. Parameter a is an asymptote of the curve that corresponds to minimal breakdown voltage $U_{\rm brMIN}$ for a specific planar lipid bilayer chemical composition. Parameter b governs the inclination of the curve.

The results obtained with the described measuring protocol are presented in Fig. 6. $U_{\rm br}$ and $t_{\rm br}$ of POPC, POPC + 1 μM $C_{12}E_8$, and POPS:POPC (3:7) planar lipid bilayers have been measured, and $U_{\rm brMIN}$ for each planar lipid bilayer chemical composition has been calculated: $U_{\rm brMIN}$ is 0.49, 0.58, and 0.55 V, respectively.

IV. Discussion

In this paper, we focused on measurement principles used in electroporation studies on planar lipid bilayers. We pointed out the voltage-clamp measurement principle that has great importance when the breakdown voltage of planar lipid bilayers is under consideration; however, it is also appropriate for the determination of other planar lipid bilayer electrical properties such as resistance and capacitance. A new experimental system that is based on the voltage-clamp measurement principle was described. Due to the signal generator of an arbitrary pulse shape, many special shapes of the voltage signal could be generated, and therefore, the experimental system is appropriate for a broad spectrum of measurements. Values of planar lipid bilayer capacitance, dynamic conductance during irreversible breakdown of the planar lipid bilayer, and lipid bilayer breakdown voltage are given.

The most common and simple method for measuring planar lipid bilayer capacitance is the discharge pulse method, which was described in detail by Sharma *et al.* [15], and Benz and Janko [18]. The method is easily applied using the described system. Due to the fact that the capacitance of the planar lipid bilayer depends on the bilayer composition as well as on the concentration of the salt solution [39], many different values can be found in scientific papers [48]; the results given in Table I are in line with previous measurements of planar lipid bilayer capacitance. The voltage-clamp method has also been used by Gallucci *et al.*, who have described a measurement system where two sinus signals with frequencies 1 Hz and 1 kHz are mixed and applied to the planar lipid bilayer. The amplitude and phase of both signals govern the planar lipid bilayer capacitance and resistance simultaneously [39]. Such continuous monitoring of *C* may prove useful in tracking planar lipid bilayer electrical properties that depend on the lipid composition and incorporated nonphospholipids substances. This method allows measuring of electrical properties of nonpermeabilized planar lipid bilayers and during the process of defect formation—electroporation. Capacitance of a planar lipid bilayer can also be determined by a triangular voltage signal [26] that is controlled by the regulation system that includes a charged planar lipid bilayer as a part. In this way, the period of the triangular voltage signal is related to the capacitance of the planar lipid bilayer.

Conductance measurements were presented by tracking dynamic conductance during the irreversible breakdown of the planar lipid bilayer (see Fig. 4). Measurement of fluctuation and transient pores in the planar lipid bilayer requires high-sensitivity current measurements in the range of nanoamperes. Melikov *et al.* [22] monitored fluctuations in the planar lipid bilayer conductance induced by applying a voltage step of sufficiently high amplitude. They demonstrated that the amplitude of fluctuations varied in a rather broad interval (form 150 to

1500 pS), and they related it to the formation of local conductive defects—hydrophilic pores.

Breakdown voltage ($U_{\rm br}$) is one of the most important properties of a lipid bilayer when biomedical and biotechnological applications of electroporation are under consideration. $U_{\rm br}$ depends on the composition of the planar lipid bilayer, i.e., the type of lipid hydrophilic chain and nonphospholipid substances. By a rectangular voltage pulse, $U_{\rm br}$ of planar lipid bilayers made of many different compositions was determined [48]. Meier *et al.* have reported that palmitoyl–oleoyl (PO) membranes require $\sim$100 mV smaller breakdown voltages compared to diphytanoyl (DPh) membranes [16]. Incorporation of nonphospholipid substances into planar lipid bilayers changes $U_{\rm br}$ as well. The effect is a consequence of the surfactant molecular shape acting to change the spontaneous curvature of the membrane, which is especially important during the defects formation process [12], [49], [50].

$U_{\rm br}$ has been measured either by the voltage-clamp or the current-clamp method using a rectangular, triangular, or step shape of the signal (see Fig. 1). However, voltage-clamp methods provide great stress to the planar lipid bilayer and hence, are not appropriate for observation of small defects—pores in the membrane structure. Namely, the strong electric field caused by the applied voltage usually generates a diverse population of pores in the planar lipid bilayer [22] and eventually planar lipid bilayer destruction. By means of a linear rising signal, $U_{\rm br}$ is determined by single voltage exposure that applies lower voltage stress on the planar lipid bilayer than during the pulse measuring protocol.

Therefore, the new experimental system, which is based on the voltage-clamp measurement principle and allows generation of arbitrary waveforms, can be a great contribution to the planning of new experimental procedures and makes it easier to perform the existing procedures.

REFERENCES

[1] E. Neumann, S. Kakorin, and K. Toensig, "Fundamentals of electroporative delivery of drugs and genes," *Bioelectrochem. Bioenerg.*, vol. 48, pp. 3–16, 1999.

[2] M. Cemazar, D. Miklavcic, L. M. Mir, J. Belehradek Jr., M. Bonnay, D. Fourcault, and G. Sersa, "Electrochemotherapy of tumours resistant to cisplatin: A study in a murine tumour model," *Eur. J. Cancer*, vol. 37, pp. 1166–1172, 2001.

[3] A. R. Denet and V. Preat, "Transdermal delivery of timolol by electroporation through human skin," *J. Controlled Release*, vol. 88, pp. 253–262, 2003.

[4] D. Ferber, "Gene therapy. Safer and virus-free?," *Science*, vol. 294, pp. 1638–1642, 2001.

[5] L. M. Mir and S. Orlowski, "Mechanisms of electrochemotherapy," *Adv. Drug Del. Rev.*, vol. 35, pp. 107–118, 1999.

[6] M. C. Vernhes, A. Benichou, P. Pernin, P. A. Cabanes, and J. Teissie, "Elimination of free-living amoebae in fresh water with pulsed electric fields," *Water Res.*, vol. 36, pp. 3429–3438, 2002.

[7] G. W. Gould, "Biodeterioration of foods and an overview of preservation in the food and dairy industries," *Int. Biodeter. Biodegrad.*, vol. 34, pp. 267–277, 1995.

[8] B. Rubinsky, G. Onik, and P. Mikus, "Irreversible electroporation: A new ablation modality-clinical implications," *Technol. Cancer Res. Treatment*, vol. 6, pp. 37–48, 2007.

[9] R. V. Davalos, L. M. Mir, and B. Rubinsky, "Tissue ablation with irreversible electroporation," *Ann. Biomed. Eng.*, vol. 33, pp. 223–231, 2005.

[10] N. Asgharian and Z. A. Schelly, "Electric field-induced transient birefringence and light scattering of synthetic liposomes," *Biochim. Biophys. Acta*, vol. 1418, pp. 295–306, 1999.

[11] N. M. Correa and Z. A. Schelly, "Electroporation of unilamellar vesicles studied by using a pore-mediated electron-transfer reaction," *Langmuir*, vol. 14, pp. 5802–5805, 1998.

[12] M. Fošnarič, V. Kralj-Iglič, K. Bohinc, A. Iglič, and S. May, "Stabilisation of pores in lipid bilayers by anisotropic inclusions," *J. Phys. Chem. B*, vol. 107, pp. 12519–12526, 2003.

[13] H. T. Tien and A. L. Ottova, "The lipid bilayer concept and its experimental realisation: From soap bubbles, kitchens sink, to bilayer lipid membranes," *J. Membrane Sci.*, vol. 189, pp. 83–117, 2001.

[14] G. C. Troiano, L. Tung, V. Sharma, and K. J. Stebe, "The reduction in electroporation voltages by the addition of surfactant to planar lipid bilayer," *Biophys. J.*, vol. 75, pp. 880–888, 1998.

[15] V. Sharma, K. U. Maheswari, J. C. Murphy, and L. Tung, "Poloxamer 188 decreases susceptibility of artificial lipid membranes to electroporation," *Biophys. J.*, vol. 71, pp. 3229–3241, 1996.

[16] W. Meier, A. Graff, A. Diederich, and M. Winterhalter, "Stabilization of planar lipid membranes: A stratified layer approach," *Phys. Chem. Chem. Phys.*, vol. 2, pp. 4559–4562, 2000.

[17] A. Diederich, G. Bahr, and M. Winterhalter, "Influence of surface charges on the rapture of black lipid membranes," *Phys. Rev. E*, vol. 58, pp. 4883–4889, 1998.

[18] R. Benz and K. Janko, "Voltage-induced capacitance relaxation of lipid bilayer membranes; effects on membrane composition," *Biochim Biophys. Acta*, vol. 455, pp. 721–738, 1976.

[19] J. Vargas, J. M. Alarcon, and E. Rojas, "Displacement currents associated with the insertion of alzheimer disease amyloid (beta)-peptide into planar bilayer membranes," *Biophys. J.*, vol. 79, pp. 934–944, 2000.

[20] C. Wilhelm, M. Winterhalter, U. Zimmermann, and R. Benz, "Kinetics of pore size during irreversible electrical breakdown of lipid bilayer membranes," *Biophys. J.*, vol. 64, pp. 121–128, 1993.

[21] R. Benz, F. Beckers, and U. Zimmermann, "Reversible electrical breakdown of lipid bilayer membranes: A charge–pulse relaxation study," *J. Membrane Biol.*, vol. 48, pp. 181–204, 1979.

[22] K. C. Melikov, V. A. Frolov, A. Shcherbakov, A. V. Samsonov, Y. A. Chizmadzhev, and L. V. Chernomordik, "Voltage-induced nonconductive pre-pores and metastable single pores in unmodified planar lipid bilayer," *Biophys. J.*, vol. 80, pp. 1829–1836, 2001.

[23] R. W. Glaser, S. L. Leikin, L. V. Chernomordik, V. F. Pastushenko, and A. I. Sokirko, "Reversible electrical breakdown of lipid bilayers: Formation and evolution of pores," *Biochim. Biophys. Acta*, vol. 940, pp. 275–287, 1988.

[24] I. G. Abidor, V. B. Arakelyan, L. V. Chernomordik, Y. A. Chizmadzhev, V. F. Pastushenko, and M. R. Tarasevich, "246—Electric breakdown of bilayer lipid membranes I. The main experimental facts and their qualitative discussion," *Bioelectrochem. Bioenerg.*, vol. 6, pp. 37–52, 1979.

[25] A. N. Chanturiya, "Detection of transient capacitance increase associated with channel formation in lipid bilayers," *Biochim. Biophys. Acta*, vol. 1026, pp. 248–250, 1990.

[26] S. Kalinowski and Z. Figaszewski, "A new system for bilayer lipid membrane capacitance measurements: Method, apparatus and applications," *Biochim. Biophys. Acta*, vol. 1112, pp. 57–66, 1992.

[27] S. Koronkiewicz, S. Kalinowski, and K. Bryl, "Programmable chronopotentiometry as a tool for the study of electroporation and resealing of pores in bilayer lipid membranes," *Biochim. Biophys. Acta*, vol. 1561, pp. 222–229, 2002.

[28] A. Ridi, E. Scalas, M. Robello, and A. Gliozzi, "Linear response of a fluctuating lipid bilayer," *Thin Solid Films*, vol. 327–329, pp. 796–799, 1998.

[29] M. Robello and A. Gliozzi, "Conductance transition induced by an electric field in lipid bilayers," *Biochim. Biophys. Acta*, vol. 982, pp. 173–176, 1989.

[30] A. Ridi, E. Scalas, and A. Gliozzi, "Noise measurements in bilayer lipid membranes during electroporation," *Eur. Phys. J. E*, vol. 2, pp. 161–168, 2000.

[31] E. Scalas, A. Ridi, M. Robello, and A. Gliozzi, "Flicker noise in bilayer lipid membranes," *Europhys. Lett.*, vol. 43, pp. 101–105, 1998.

[32] I. Genco, A. Gliozzi, A. Relini, M. Robello, and E. Scalas, "Electroporation in symmetric and asymmetric membranes," *Biochim. Biophys. Acta*, vol. 1149, pp. 10–18, 1993.

[33] E. Pescio, A. Ridi, and A. Gliozzi, "A picoampere current generator for membrane electroporation," *Rev. Sci. Instrum.*, vol. 71, pp. 1740–1744, 2000.

[34] M. Robello, M. Fresia, L. Maga, A. Grasso, and S. Ciani, "Permeation of divalent cations through (alpha)-latrotoxin channels in lipid bilayers: Steady-state current–voltage relationship," *J. Membrane Biol.*, vol. 95, pp. 55–62, 1987.
[35] S. Kalinowski and Z. Figaszewski, "A four-electrode system for measurement of bilayer lipid membrane capacitance," *Meas. Sci. Technol*, vol. 6, pp. 1034–1049, 1995.
[36] S. Kalinowski and Z. Figaszewski, "A four-electrode potentiostat–galvanostat for studies of bilayer lipid membranes," *Meas. Sci. Technol.*, vol. 6, pp. 1050–1055, 1995.
[37] S. Micelli, E. Gallucci, and V. Ricciarelli, "Studies of mitochondrial porin incorporation parameters and voltage-gated mechanism with different black lipid membranes," *Bioelectrochemistry*, vol. 52, pp. 63–75, 2000.
[38] P. Kramar, D. Miklavčič, and A. M. Lebar, "Determination of lipid bilayer breakdown voltage by means of linear rising signal," *Bioelectrochemistry*, vol. 70, pp. 23–27, 2007.
[39] E. Gallucci, S. Micelli, and G. Monticelli, "Pore formation in lipid bilayer membranes made of phosphatidylinositol and oxidized cholesterol followed by means of alternating current," *Biophys. J.*, vol. 71, pp. 824–831, 1996.
[40] S. Kalinowski, G. Ibron, K. Bryl, and Z. Figaszewski, "Chronopotentiometric studies of electroporation of bilayer lipid membranes," *Biochim. Biophys. Acta*, vol. 1396, pp. 204–212, 1998.
[41] S. Koronkiewicz, S. Kalinowski, and K. Bryl, "Programmable chronopotentiometry as a tool for the study of electroporation and resealing of pores in bilayer lipid membranes," *Biochim. Biophys. Acta*, vol. 1561, pp. 222–229, 2004.
[42] A. Blume, "Lipids," in *Bioelectrochemistry of Membranes*, D. Waltz, J. Teissié, and G. Milazzo, Eds. Basel, Switzerland: Birkhauser, 2004, pp. 24–61.
[43] Y. Hanyu, T. Yamada, and G. Matsumoto, "Simultaneous measurement of spectroscopic and physiological signals from a planar bilayer system: Detecting voltage-dependent movement of a membrane-incorporated peptide," *Biochemistry*, vol. 37, pp. 15376–15382, 1998.
[44] H. Yamaguchi and H. Nakanishi, "Characterization of the preparation process and photochemical control of electrical properties of bilayer lipid membranes containing azobenzene chromophores," *Biochim. Biophys. Acta*, vol. 1148, pp. 179–184, 1993.
[45] T. F. Eibert, M. Alaydrus, F. Wiczewski, and V. W. Hansen, "Electromagnetic and thermal analysis for lipid bilayer membranes exposed to RF fields," *Trans. Biomed. Eng.*, vol. 46, pp. 1013–1021, 1999.
[46] M. Montal and P. Müeller, "Formation of bimolecular membranes from lipid monolayers and study their electrical properties," *Proc. Nat. Academy Sci. USA*, vol. 69, pp. 3561–3566, 1972.
[47] A. Maček-Lebar, G. C. Troiano, L. Tung, and D. Miklavčič, "Inter-pulse interval between rectangular voltage pulses affects electroporation threshold of artificial lipid bilayers," *IEEE Trans. Nanobiosci.*, vol. 1, no. 3, pp. 116–120, Sep. 2002.
[48] M. Pavlin, T. Kotnik, D. Miklavčič, P. Kramar, and A. M. Lebar, "Electroporation of planar lipid bilayers and membranes," in *Advances in Planar Lipid Bilayers and Liposomes,* vol. 6, A. L. Liu, Ed. Amsterdam, The Netherlands: Elsevier, 2008, pp. 165–226.
[49] B. Babnik, D. Miklavčič, M. Kandušer, H. Hagerstrand, V. Kralj-Iglič, and A. Iglič, "Shape transformation and burst of giant POPC unilamellar liposomes modulated by non-ionic detergent C12E8," *Chem. Phys. Lipids*, vol. 125, pp. 123–138, 2003.
[50] B. Mavcic, B. Babnik, A. Iglic, M. Kanduser, T. Slivnik, and V. Kralj-Iglic, "Shape transformation of giant phospholipid vesicles at high concentrations of C12E8," *Bioelectrochemistry*, vol. 63, pp. 183–187, 2004.

Peter Kramar was born in Kranj, Slovenia, in 1977. He received the B.Sc. and M.Sc. degrees in electrical engineering from the Faculty of Electrical Engineering, University of Ljubljana, Ljubljana, Slovenija, in 2003 and 2005, respectively.

He is currently a Teaching Assistant with the University of Ljubljana. His current research interests include electroporation of planar lipid bilayers.

Damijan Miklavčič was born in Ljubljana, Slovenia, in 1963. He received the Ph.D. degree in electrical engineering from the University of Ljubljana, Ljubljana.

He is currently a Professor with the Faculty of Electrical Engineering, University of Ljubljana, where he is also the Head of the Laboratory of Biocybernetics, and is actively engaged in the field of biomedical engineering. His current research interests include electroporation-assisted drug and gene delivery, including cancer treatment by means of electrochemotherapy, tissue oxygenation, and modeling.

Alenka Maček Lebar was born in Ljubljana, Slovenia, in 1967. She received the M.Sc. and Ph.D. degrees in electrical engineering from the University of Ljubljana, Ljubljana, in 1995 and 1999, respectively.

She is currently an Assistant Professor with the Faculty of Electrical Engineering, University of Ljubljana. Her current research interests include the biomedical engineering field, especially the field of electroporation.

Članek 3

Measurement protocol for Planar Lipid Bilayer Viscoelastic Properties

Izidor Sabotin, Alenka Maček Lebar, Damijan Miklavčič in Peter Kramar

Objavljen v: IEEE Transactions on Dielectrics and Electrical Insulation 16(5) (2009) 1237-1242

Measurement Protocol for Planar Lipid Bilayer Viscoelastic Properties

Izidor Sabotin, Alenka Maček Lebar, Damijan Miklavčič and **Peter Kramar**
University of Ljubljana, Faculty of Electrical Engineering
Tržaška 25
Ljubljana, SI-1000, Slovenija

ABSTRACT

This paper describes how to estimate planar lipid bilayer's elasticity module E and surface tension σ by means of measuring its breakdown voltage and using Dimitrov's viscoelastic model of electric field-induced breakdown of lipid bilayers. Planar lipid bilayers (BLMs) were made of two components: 1-palmitoyl 2-oleoyl phosphatidylcholine (POPC) and 1-palmitoyl 2-oleoyl phosphatidylserine (POPS) in five different compositions. Folding method for forming planar lipid bilayers in the salt solution of 100 mM KCl was used. Breakdown voltages U_{br} and membrane life times t_{br} were measured by means of applying linear rising voltage signals of seven different slopes. Specific capacitances c_{BLM} of bilayers were measured with charge pulse method. Then Dimitrov's viscoelastic model was fitted to measured data allowing for estimation of elasticity module and surface tension of the lipid bilayer. Our results show that one-component bilayers composed from POPS were more stable and thus having higher breakdown voltages and elasticity moduli then bilayers composed of POPC. Surface tension values were similar regardless of the membrane composition. Values of the elasticity (E) and surface tension (σ) are comparable to those published in the literature. We conclude that the protocol used, though time consuming, is an alternative to other methods used for determination of bilayer's mechanical properties.

Index Terms — **Bioelectric phenomena, biomechanics, dielectric breakdown, capacitance measurement, electric field effects, electromechanical effects, membranes.**

1 INTRODUCTION

BIOLOGICAL membranes play a crucial role in living organisms. They are soft condensed matter structures that envelope the cells and their inner organelles. Biological membranes maintain relevant concentration gradients by acting as selective filters for ions and molecules. Besides their passive role, they also host a number of metabolic and biosynthetic activities [1].

Lipid bilayers are important constituents of living cell. This fact provokes a serious interest towards the study of the mechanical properties of membranes and the influence of different lipid bilayer compositions on these properties. Artificially built planar lipid bilayer is considered as a small fraction of total cell membrane, it represents the simplest model for experimental studies of membrane properties; especially because it is accessible from both sides. Latter fact makes the planar lipid bilayer especially suitable for experiments that apply electric voltage or current to the membrane and measure its response. The idea of applying voltage to lipid structures in order to determine their properties is almost a hundred years old [2]. In 1920s physicist Fricke measured the electrical response of a red blood cell suspension as a function of frequency. He proposed a model for a biological membrane with electrically equivalent circuit comprising of a resistor and a capacitor connected in parallel. Using the equation for the parallel plate capacitor he estimated the dielectric constant (ε) and thickness (h) of the membrane.

The interaction of electric fields with biological membranes and pure phospholipid bilayers has been extensively studied in the last decades [3, 4]. Strong external electric field can destabilizes membranes and induce changes in their structure. The key parameter is the induced-transmembrane voltage generated by an external electric field due to the difference in the electric properties of the membrane and the external medium, known as Maxwell–Wagner polarization. According to the most widely accepted theory the lipids in the membrane are rearranged to form aqueous pores. This increases the conductivity of the membrane and its permeability to water-soluble molecules which are otherwise deprived of membrane transport mechanisms. This phenomenon is known as electroporation, sometimes referred to also as dielectric breakdown or electropermeabilization of membranes.

Manuscript received on 27 February 2009, in final form 22 June 2009.

The stability of planar lipid bilayer is determined by the breakdown voltage which is one of the most important properties of artificial bilayers in studying electroporation. The breakdown voltage of the lipid bilayer is usually determined by a rectangular voltage pulse. The amplitude of the voltage pulse is incremented in small steps until the breakdown of the bilayer is obtained [5]. With this protocol the number of applied voltage pulses is not known in advance and each bilayer is exposed to voltage stress many times. Such a pretreatment of the lipid bilayer affects its stability and consequently the determined breakdown voltage of the lipid bilayer [6]. To avoid this inconsistency we have suggested an approach using linear rising voltage signal [7] that allows the breakdown voltage determination in a single exposure to voltage.

A macroscopic approach using the theory of elasticity of solid bodies and liquid crystals can be applied to describe mechanical properties of lipid bilayers. In 1973 Helfrich proposed a theory and possible experiments of measurement elastic properties on planar lipid bilayers [8]. As the anisotropy of lipid bilayers is clearly expressed several elasticity modules are required to describe its viscoelastic properties. Depending on the directions of the membrane deformation we distinguish volume compressibility, area compressibility, unilateral extension along membrane plane and transversal compression.

Experimentally, the material properties of bilayers have been determined using, for example, micropipette pressurization of giant bilayer vesicles [9-13] and with nuclear magnetic resonance and x-ray diffraction [14]. Analysis of the thermal fluctuations of giant vesicles using video-microscopy techniques were used by Meleard et al [15]. Lipid bilayer mechanical properties were commonly measured on giant unilamelar vesicles. Pressure was applied on a membrane with micropipette aspiration method; the properties were measured by means of video microscopy [16]. On planar lipid bilayer Winterhalter et al reports that dynamics light scattering allows to quantify viscoelastic properties in non-pertubative way. Zehl et al presented Monte Carlo simulations for investigation of the self assembly and physical properties of aggregated structures involved in a model system [17].

Transversal elasticity modulus cannot be measured directly due to small thickness of the membrane and extremely small changes of the thickness upon deformation [18]. It can be estimated through capacitance measurement with a special electrostriction method which is based on measurements of the amplitude of higher current harmonics.

It is known, that the composition of the bilayers influences its mechanical properties such as elasticity modulus and surface tension [9, 12, 18]. If the monolayer is composed of the mixture of different phospholipids, then depending on the structure of phospholipids the monolayer could be more or less densely packed. It is also known that elasticity modulus is dependent on solvent used for preparation of planar lipid bilayers and on addition of different surface active chemicals (e.g. cholesterol) [9, 18].

In our study, we measured the breakdown voltage of planar lipid bilayers of five different compositions by means of linear rising voltage. The aim of the study was to estimate the planar lipid bilayer mechanical properties such as transversal elasticity and surface tension by means of measured planar lipid bilayer electrical properties and a viscoelastic predictive model. The main question that we addressed was how comparable are the estimated mechanical properties obtained from predictive model to reports by other researches. Influence of planar lipid bilayer composition on elasticity (E) and surface tension (σ) of planar lipid bilayer was also investigated. Proposed protocol, though time consuming, is an alternative approach to investigation of mechanical properties of planar lipid bilayers.

2 MATERIALS AND METHODS

2.1 ELECTRICAL SETUP

Our system for following up electroporation of planar lipid bilayers consists of a signal generator, a Teflon chamber and a device, which is used for measurements of transmembrane current and voltage (Figure 1). Signal generator is a voltage generator of an arbitrary type that provides voltage amplitudes from −5 V to +5 V. It is controlled by costume written software (Genpyrrha), specially designed for drawing the voltage signal that is used for membrane electroporation. Part of the signal generator is also a fast analogue switch. The switch disconnects the output of the signal generator and switches to the 1 MΩ resistor in 2 ns. In this way, a system discharge voltage is measured and consequently the capacitance of the lipid bilayer. Two Ag-AgCl electrodes, one on each side of the planar lipid bilayer, were immersed into the salt solution. Transmembrane voltage was measured via a LeCroy differential amplifier 1822. The same electrodes were used to measure transmembrane current. Both signals were stored in oscilloscope LeCroy Waverunner-2 354 M in Matlab format. All the signals were processed offline.

Chamber is made of Teflon. It consists of two cubed reservoirs with volume of 5.3 cm^3 each. In the hole between two reservoirs, a thin Teflon sheet with a round hole (117 μm in diameter) was inserted. Lipid bilayer is formed by the Montal-Muller method.

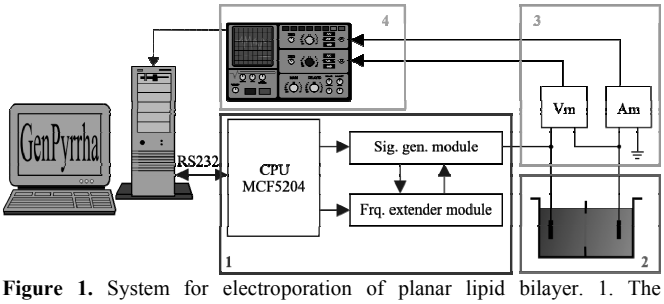

Figure 1. System for electroporation of planar lipid bilayer. 1. The microprocessor board with MCF5204 processor and two modules. One module generates arbitrary signals and the other that is realized in Xillinx, is used for frequency extension. 2. Chamber for forming lipid bilayers and two Ag-AgCl electrodes. 3. Modules for current and voltage amplification. 4. Digital oscilloscope for data storage [7].

2.2 CHEMICAL SETUP

The salt solution was prepared of 0.1M KCl and 0.01M Hepes in the same proportion. Some droplets of 1M NaOH were added to obtain pH 7.4. The lipids were prepared from POPC (1-pamitoyl 2-oleoyl phosphatidylcholine) and POPS (1-pamitoyl 2-oleoyl phosphatidylserine) in powder form (Avanti Polar-Lipids Inc. ZDA). Lipids were melted in solution of hexane and ethanol in ratio 9:1. The mixture of hexadecane and pentane in ratio 3:7 was used for torus forming. When preparing two-component bilayers both species of lipids were mixed together in appropriate ratio in small plastic tube before they were applied. Five different compositions of lipids were used. Two of them were made exclusively of one component. Two-component bilayers were made of mixture of POPC and POPS in three different ratios: 3:1, 1:1 and 1:3.

2.3 MEASUREMENT PROTOCOL

Measurement protocol consisted of two parts: capacitance measurement (Figure 2A) and lipid bilayer breakdown voltage measurement (Figure 2B). Capacitance and the breakdown voltage were determined for each lipid bilayer. The capacitance of lipid bilayer was measured with discharge method as previously described [7]. The membrane capacitance (C_{BLM}) was normalised to the surface area of the orifice for comparison with other studies (c_{BLM}).

We determined breakdown voltage (U_{br}) of the lipid bilayer by the linear rising signal. The slope of the linear rising signal (k) and the peak voltage of the signal has to be selected in advance. Seven different slopes were selected. Breakdown voltage was defined as the voltage at the moment t_{br} when sudden increase of transmembrane current was observed. Time of breakdown t_{br} was defined as a lifetime of the lipid bilayer at a chosen slope of the linear rising signal [7]

2.4 STATISTICS

To compare breakdown voltages and specific membrane capacitances of the lipid bilayers exposed to voltage signals of different slopes (*k*) one way ANOVA test was used. All pairwise multiple comparisons were made by Tukey's test. When statistically analyzing data of bilayers composed of POPS exclusively Kruskal-Wallis one-way analysis of variance on ranks test was used, as the population did not fulfil all the requirements for one way ANOVA test i.e. the equality of variance between the compared populations. Pairwise multiple comparisons were performed by Dunn's method.

When comparing the mean breakdown voltages at the same slopes (*k*) between one component lipid bilayers unpaired t-test was used. As the variances of mean breakdown voltages at slopes *k=7.8 kV/s* and *k=11.5 kV/s* were statistically different, the comparisons were made with Mann-Whitney's test. We rejected the null hypothesis of analyses if the p-value of the test was less than 0.05 ($p < 0.05$) regardless of the test used.

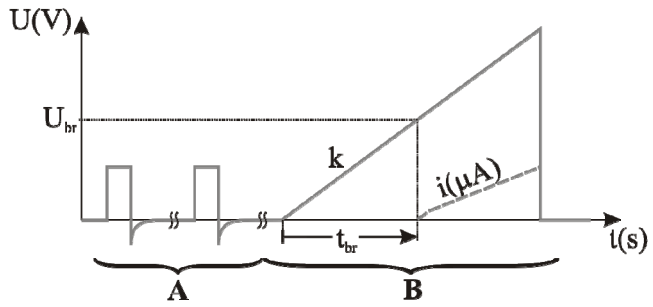

Figure 2. Measurement protocol: A) capacitance measurement of lipid bilayer was measured in two steps. In the first step we measured capacitance of the electronic system without lipid bilayer. Second step was measuring capacitance of electronic system with lipid bilayer and salt solution. B) voltage breakdown measurement with linear rising signal [7].

2.5 DETERMINATION OF ELASTICITY AND SURFACE TENSION

For determination of viscoelastic properties we used the model of Dimitrov [19]. The model considers the lipid bilayer as a thin viscoelastic film with fluctuating surfaces, bounded by two semi-infinitive bulk phases. The assumption that the membrane behaves as a viscoelastic, isotropic material, represented as a standard solid model, composed of a Kelvin body in series with a linear spring, is made. Originally, this model predicts the critical voltage (U_c) and critical time (t_c) needed to collapse a membrane at applied voltage. In our study critical voltage corresponds to breakdown voltage (U_{br}) and critical time to life time (t_{br}) of planar lipid bilayer. The parameters of model are Young's transversal elasticity modulus (E), surface tension (σ), viscosity (μ), thickness of the membrane (h) and permittivity of membrane (ε_m). If the bilayer's life time limits to infinity, the model of Dimitrov yields:

$$U_c = \sqrt[4]{\frac{8\mathrm{E}\cdot\sigma\cdot h^3}{\varepsilon_m^2\varepsilon_0^2}} \tag{1}$$

In our experimental protocol (Figure 2) planar lipid bilayer lifetime (t_{br}) is measured and can not be infinitive. Therefore generic model equation that still contains (t_{br}) is more adequate [19]:

$$U_{br} = \sqrt[4]{\frac{1}{\varepsilon_m^2\varepsilon_0^2}\left[8Eh^3\sigma\left(1+\frac{3\alpha\mu}{Et_{br}}\right)\right]}\,. \tag{2}$$

In equation (2) we consider:

$$c = \frac{\varepsilon_m\varepsilon_0}{h} \tag{3}$$

$$a = \frac{8}{c^2}\sigma\mathrm{E}\mathrm{h} \tag{4}$$

$$b = \frac{24}{c^2}\mathrm{h}\sigma\alpha\mu \tag{5}$$

Where *c* corresponds to planar lipid bilayer capacitance normalized with the surface area c_{BLM}.

Equation (2) can be written as:

$$U_{br} = \sqrt[4]{a + \frac{b}{t_{br}}} \tag{6}$$

Using nonlinear regression, the viscoelastic model in equation 6 was fitted to the data by Generalized Nonlinear Non-analytic Chi-Square Fitting function in Matlab [20-22]. Parameters *a* and *b*, which are obtained trough fitting, served to calculate Young's elasticity modulus (E) and surface tension (σ) of planar lipid bilayer according to following two equations derived from (3,4,5):

$$E = 3\frac{a}{b}\alpha\mu \tag{7}$$

$$\sigma = \frac{bc^2}{24\alpha\mu h} \tag{8}$$

Specific capacitance (c_{BLM}) has been measured and can be used in a model. Other parameters such as thickness (h = 3.5 nm), viscosity (μ = 6 Ns/m^2) and α = 2 were used in calculation according to the reference [19].

3 RESULTS

We measured specific capacitance (c_{BLM}), life time (t_{br}) and breakdown voltages (U_{br}) for five different planar lipid bilayer compositions. By means of viscoelastic model we estimated transversal elasticity (E) and surface tension (σ) of planar lipid bilayer. All measured data are in agreement with our previously published data [7]. Fitted parameters (a) and (b), measured capacitance c_{BLM}, and calculated elasticity (E) and surface tension (σ) data with their standard deviation are collected in Table 1. For all regression curves in Figure 3 the 68% confidence interval of the fit upper and lower border has been plotted by dot-dashed curves.

Table 1. Fitted parameters (a) and (b), measured capacitance (c_{BLM},) and calculated Elasticity (E) and Surface tension (σ) for five different planar lipid bilayer compositions are gathered in table with their standard deviation.

Mixture	**a**	**b**	$\mathbf{c_{BLM}}$	**E**	**σ**
POPC:POPS	10^{-2} V^4	V^{4}μs	μF/cm^2	N/cm^2	10^{-5} J/m^2
1:0 (n = 106)	3.20 ± 1.37	5.0 ± 0.8	0.51 ± 0.07	23.09 ± 0.37	12.90 ± 3.50
3:1 (n = 89)	2.33 ± 0.75	4.8 ± 0.6	0.17 ± 0.06	17.61 ± 0.21	1.37 ± 0.96
1:1 (n = 60)	1.99 ± 0.64	3.9 ± 0.5	0.31 ± 0.07	18.48 ± 0.24	3.69 ± 1.67
1:3 (n = 75)	4.70 ± 1.06	7.4 ± 1.5	0.24 ± 0.14	22.90 ± 0.28	4.22 ± 4.92
0:1 (n = 100)	8.36 ± 2.14	5.6 ± 1.1	0.41 ± 0.13	53.37 ± 0.65	9.41 ± 0.60

For membranes composed exclusively of POPC (n = 106) membranes were included and mean c_{BLM} value with standard deviation was measured to be 0.51 ± 0.07 μF/cm^2. U_{br} increased with increasing steepness (k) of the voltage applied as seen in Figure 3 at POPC:POPS = 1:0. Pairwise statistical comparison of the mean U_{br} were made. In general, mean U_{br} at steeper slopes of linear rising voltage applied were statistically significantly higher from mean U_{br} at less steep voltage ramps applied. U_{br} at k = 48.1 kV/s was statistically significantly higher than U_{br} measured at the rest of applied slopes of voltage signal. At k = 21.6 kV/s U_{br} was statistically significantly higher from U_{br} at slopes k = 11.5 kV/s or less and at k = 16.7 kV/s U_{br} was statistically significantly higher from U_{br} at slopes k = 7.8 kV/s or less. Mean U_{br} values at slopes k = 4.8 kV/s, k = 7.8 kV/s and k = 7.8 kV/s showed no statistical difference. Similar statistical analysis was performed for mean breakdown voltages for all membrane compositions and similar statistical results, with respect to the voltage signal slopes were obtained irrespective of the membrane composition. From the fitted Dimitrov model function to the mean breakdown voltages we obtained the elasticity modulus E and surface tension σ for lipid membranes composed of POPC. We estimated the elasticity modulus to be 23.09 ± 0.37 N/cm^2 and surface tension (12.90 ± 3.50)x10^{-5} J/m^2.

For membranes composed of POPS exclusively (n = 100) membranes were included in defining mean c_{BLM}, t_{br} and U_{br} values. Mean specific capacitance c_{BLM} was measured to be 0.41 ± 0.13 μF/cm^2. A trend of increasing U_{br} with respect to steeper applied voltage slopes is seen in Figure 3 at POPC:POPS = 0:1. Between one component lipid bilayers i.e. membranes composed of POPC and POPS exclusively, statistical analysis of mean U_{br} values at same voltage slopes applied was made. Mean U_{br} values at slopes k = 4.8 kV/s, k = 5.5 kV/s, k = 7.8 kV/s, k = 21.6 kV/s, k = 48.1 kV/s measured on lipid bilayers composed of POPS were significantly higher from mean U_{br} values measured on membranes composed of POPC only. At slopes k = 11.5 kV/s and k = 16.7 kV/s no statistical difference was observed as the probability values for rejection of the null hypothesis were p = 0.069 and p = 0.259 respectively. The estimated elasticity modulus E for bilayers composed of POPS was 53.37 ± 0.65 N/cm^2 and the surface tension was evaluated to (9.41 ± 0.60)x10^{-5} J/m^2.

For membranes composed of POPC:POPS = 3:1 (n = 89) membranes were used in the analysis. Measured c_{BLM} was 0.17 ± 0.06 μF/cm^2. A trend of increasing U_{br} with respect to steeper applied voltage slopes is seen in Figure 3 at POPC:POPS = 3:1. The estimated elasticity module was 17.61 ± 0.21 N/cm^2 and surface tension was (1.37 ± 0.96)x10^{-5} J/m^2.

For membranes composed of POPC:POPS mixed in 1:1 (n = 60) membranes were included in the analysis. The mean specific capacitance c_{BLM} was 0.31 ± 0.07 μF/cm^2. Distinctive U_{br} dependence on the linear rising voltage applied is seen in Figure 3 at POPC:POPS = 1:1. The estimated elasticity module was 18.48 ± 0.24 N/cm^2 and surface tension was (3.69 ± 1.67)x10^{-5} J/m^2 respectively.

For membranes composed of POPC:POPS = 1:3 (n = 75) membranes were used in the analysis. Measured c_{BLM} was 0.24 ± 0.14 μF/cm^2. A trend of increasing U_{br} with respect to steeper applied voltage slopes is seen in Figure 3 at POPC:POPS = 1:3. We estimated elasticity E to 22.90 ± 0.28 N/cm^2 and surface tension σ to (4.22 ± 4.92)x10^{-5} J/m^2.

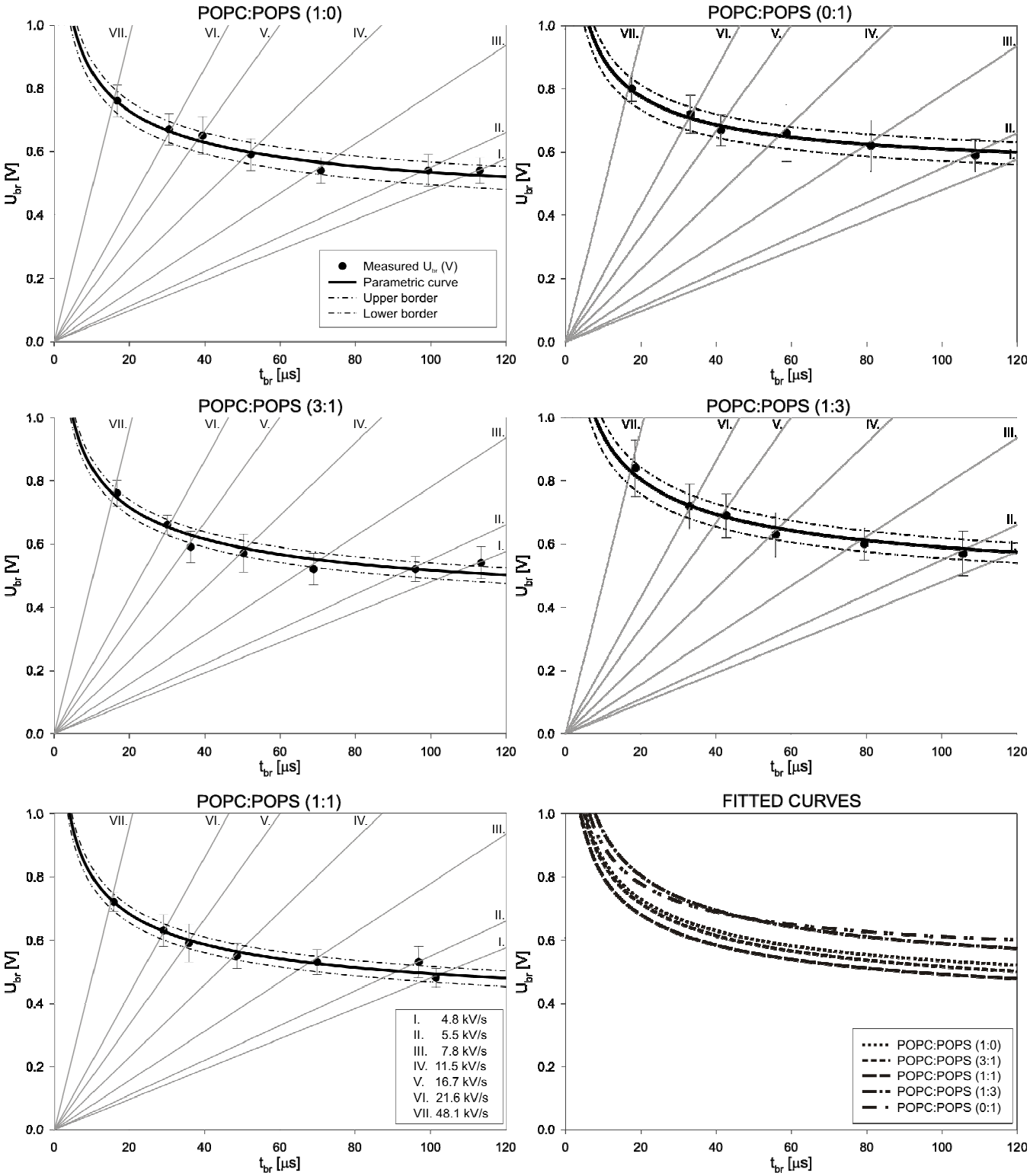

Figure 3. Dependence of the membrane breakdown voltage U_{br} and life time t_{br} on steepness of the applied linear rising voltage. All seven slopes used are denoted with roman numbers and plotted in gray color. The error bars in U_{br} measurements represent standard deviation of the data. Composition of the membrane experimented on denotes the title of the graphs meaning the volumetric ratio of the two lipids used (1-pamitoyl 2-oleoyl phosphatidylcholine POPC and 1-pamitoyl 2-oleoyl phosphatidylserine POPS). The black solid line represents the fitted Dimitrov model function on the data measured. Corresponding dash-doted lines represent the 68% confidence interval of the fit (upper border and lower border). Fits for all compositions are plotted on the graph in bottom-right corner.

4 DISCUSION

The breakdown voltage of planar lipid bilayers of five different compositions were measured by means of linear rising voltage. The aim of the study was to estimate the planar lipid bilayer mechanical properties such as transversal elasticity and surface tension by means of measured planar lipid bilayer electric properties and a predictive model.

Dimitrov's viscoelastic model of electric field-induced breakdown voltage of lipid bilayers predicts a dependence on electric pulse length to the electroporation thresholds of the electromechanical theory [19]. Originally it predicted a minimum critical voltage, for which the membrane becomes unstable at long pulse durations. Troiano et al. reported that this model did not fit to their measured data. The breakdown voltage of the lipid bilayer in their experiments was however determined by repeatedly applying a rectangular voltage pulse; the amplitude of the voltage pulse was incremented in small steps until the breakdown of the bilayer was obtained [5]. Using such a protocol the number of applied voltage pulses is not known in advance and each bilayer is exposed to voltage stress several and different times. Such a pretreatment of the lipid bilayer most probably affects its stability and consequently the determined breakdown voltage of the lipid bilayer [6]. By using a linear rising voltage signal, as we proposed in our previous study, we avoid this inconsistency. The breakdown of planar lipid bilayer is forced in a single voltage exposure. As a result of this protocol standard deviation of bilayer's life-time t_{br} at particular voltage slope was reduced to 10% or less. When a rectangular pulses are used, the bilayer breaks down at a random life time during the pulse. The consistency of t_{br} measuremnt enabled us to use generic model of Dimitrov in order to estimate bilayer's elasticity modulus (E) and surface tension (σ).

Lipid bilayers have been shown to rupture at surface tensions in a range from ~0.01 to 25 10^{-3} J/m^2 depending on the lipid composition [9, 11, 19, 23-26]. Our results are within this interval though it has to be stressed out that uncertainty of our estimation is rather high, especially in the case of 3:1 and 1:3 mixtures. One of the reasons for that could be also the selected value of the thickness (h) which is not exactly determined for each lipid composition. On the other hand, it has been argued [27] that the electric field causes a lateral stress in the membrane that directly influences the interfacial tension and therefore has a dominant role in determining headgroup packing and pore formation.

Transversal elasticity of a planar lipid bilayer can be determined only by stressing the membrane in some way. Hianik measured the elasticity of planar lipid bilayer with electrostriction method based on measurement of the amplitude of higher current harmonics [18]. For a bilayer composed of eggPC a transversal elasticity modulus measured was on the interval from 10^5 Pa (10 N/cm^2) at lower frequencies to 10^7 Pa (10^3 N/cm^2) at higher frequencies (~ 2 kHz). He also observed the dependence of E on various solvent used. For solvents with shorter hydrocarbon chains (n-heptan, n-decane) elasticity values as mentioned above were measured, but for solvents with longer hydrocarbon chains (n-hexadecan), two orders of magnitude higher values of elasticity were reported. We used n-hexan and thus our determined elasticity moduli are comparable with Hianik's results at low frequencies using solvents with shorter hydrocarbon chains.

The bilayers were composed of two lipid species that are present in biological membranes. A lipid molecule of POPS has negatively charged headgroup while a molecule of POPC has electrostatically neutral headgroup (zwitterion). Lower breakdown voltages and consequently lower elasticity modulus and surface tension were expected for POPS bilayers due to repulsive electrostatic forces between the lipid molecules. On the contrary higher breakdown voltages for bilayers composed of POPS were measured. The elastic bending moduli of vesicles is one of the key predictors of membrane strength [28]. In our case estimated elasticity module for POPS was higher than that of POPC planar lipid bilayers. This is not only a consequence of higher breakdown voltage but also the result of other parameters of Dimitrov's viscoelastic model. Maier et al. concluded that breakdown voltage and consequently membrane stability is independent of the polarization of headgroups of lipids [29]. Similar to our results they measured the breakdown voltage for bilayers composed of POPS to be about the same, or slightly higher than breakdown voltages of POPC membranes. Similar Winterhalter et al. reports that the stability of the membrane was the same for lipids with charged (PS) and uncharged (PC) headgroups [30].

Another report that supports our findings comes from MD simulations performed by Pandit el al. [31]. They simulated a lipid bilayer composed of Dipalmitoylphosphatidylcholine (DPPC) and Dipalmitoylphosphatidylserine (DPPS). As the polar headgroups of the lipids under investigation were the same as ours we can draw parallels between their and our conclusions. They discovered that a single molecule of DPPC in the bilayers prefers complexation with two other lipids, whereas DPPS molecule prefers complexation with four. As complexation with more molecules means more stabile bilayer structure, the reason why the POPS bilayers are more stabile can be explained.

When two component lipid bilayers were investigated measured U_{br} and estimated E and σ were in the range of obtained values for pure POPC bilayers. This brings us to the conclusion, that the two-component bilayer's mechanical properties are predominantly determined by the least stable component – in our case this is the POPC.

5 CONCLUSION

The aim of our study was to estimate the planar lipid bilayer mechanical properties such as elasticity and surface tension by means of measured planar lipid bilayer electric properties using a viscoelastic predictive model. The protocol of the measurement of viscoelastic properties is time consuming due to the fact that planar lipid bilayer breakdown voltage and life time have to be measured at several steepnesses of linear rising signal. Nevertheless, the values of the transversal elasticity (E) and surface tension (σ) obtained with our method are comparable with previously published results in literature obtained with other methods. We also found that POPS lipids form stronger bilayers in comparison to POPC and have higher elasticity modulus. Furthermore this is reflected in two-component bilayer's mechanical properties which are dominantly determined by the least stable component.

ACKNOWLEDGMENT

This study was supported by the Slovenian Research Agency – Research Programme: Electroporation-Based Technologies

and Treatments. The experimental work was performed in the laboratories of the Infrastructure Programme: Network of research infrastructure centers at University of Ljubljana.

REFERENCES

[1] R. B. Gennis, *Biomembranes, Molecular Structure and Function*. New York: Springer, 1989.

[2] H. T. Tien and A. L. Ottova, "The lipid bilayer concept and its experimental realization: from soap bubbles, kitchen sink, to bilayer lipid membranes", J. Membrane Sci., Vol. 189, pp. 83-117, 2001.

[3] D. C. Chang, B. M. Chassey, J. A. Saunders, and A. E. Sowers, *Guide to Electroporation and Electrofusion*. New York, USA, Academic Press, 1992.

[4] E. Neumann, A. E. Sowers, and C. A. Jordan, *Electroporation and Electrofusion in Cell Biology*. New York, USA, Plenum, 1989.

[5] G. C. Troiano, L. Tung, V. Sharma, and K. J. Stebe, "The reduction in electroporation voltages by the addition of a surfactant to planar lipid bilayers", Biophysical J., Vol. 75, pp. 880-888, 1998.

[6] I.G. Abidor, V.B. Arakelyan, L.V. Chernomordik, Yu.A. Chizmadzhev, V.F. Pastushenko and M.R. Tarasevich, "264 - Electric Breakdown of Bilayer Lipid Membranes I. The Main Experimental Facts and Their Qualitative Discussion", Bioelectrochemistry and Bioenergetics, Vol. 6, pp. 37-52, 1979.

[7] P. Kramar, D. Miklavčič, and A. M. Lebar, "Determination of the lipid bilayer breakdown voltage by means of linear rising signal", Bioelectrochemistry, Vol. 70, pp. 23-27, 2007.

[8] W. Helfrich, "Elastic Properties Of Lipid Bilayers - Theory And Possible Experiments", Zeitschrift Fur Naturforschung C-A Journal Of Biosciences, Vol. C 28, pp. 693-703, 1973.

[9] E. Evans and D. Needham, "Physical-properties of surfactant bilayer-membranes - thermal transitions, elasticity, rigidity, cohesion, and colloidal interactions", J. Phys. Chem., Vol. 91, pp. 4219-4228, 1987.

[10] R. Kwok and E. Evans, "Thermoelasticity of large lecithin bilayer vesicles", Biophysical J., Vol. 35, pp. 637-652, 1981.

[11] K. Olbrich, W. Rawicz, D. Needham, and E. Evans, "Water permeability and mechanical strength of polyunsaturated lipid bilayers", Biophysical J., Vol. 79, pp. 321-327, 2000.

[12] W. Rawicz, K. C. Olbrich, T. McIntosh, D. Needham, and E. Evans, "Effect of chain length and unsaturation on elasticity of lipid bilayers", Biophysical J., Vol. 79, pp. 328-339, 2000.

[13] M. B. Schneider, J. T. Jenkins, and W. W. Webb, "Thermal fluctuations of large cylindrical phospholipid-vesicles", Biophysical J., Vol. 45, pp. 891-899, 1984.

[14] B. W. Koenig, H. H. Strey, and K. Gawrisch, "Membrane lateral compressibility determined by NMR and X-ray diffraction: Effect of acyl chain polyunsaturation", Biophysical J., Vol. 73, pp. 1954-1966, 1997.

[15] P. Meleard, J. F. Faucon, M. D. Mitov, and P. Bothorel, "Pulsed-light microscopy applied to the measurement of the bending elasticity of giant liposomes", Europhysics Letters, Vol. 19, pp. 267-271, 1992.

[16] J. Genova, A. Zheliaskova, and M. D. Mitov, "The influence of sucrose on the elasticity of SOPC lipid membrane studied by the analysis of thermally induced shape fluctuations", Colloids And Surfaces A-Physicochemical And Engineering Aspects, Vol. 282, pp. 420-422, 2006.

[17] T. Zehl, M. Wahab, H. J. Mogel, and P. Schiller, "Monte Carlo simulations of self-assembled surfactant aggregates", LANGMUIR, Vol. 22, pp. 2523-2527, 2006.

[18] T. Hianik, "Structure and physical properties of biomembranes and model membranes", Acta Physica Slovaca, Vol. 56, pp. 687-806, 2006.

[19] D. S. Dimitrov, "Electric field-induced breakdown of lipid bilayers and cell-membranes - a thin viscoelastic film model", J. Membrane Biology, Vol. 78, pp. 53-60, 1984.

[20] P. R. Bevington and D. K. Robinson, *Data Reduction and Error Analysis for the Physical Sciences*. New York, USA, McGraw-Hill, 1992.

[21] N. Brahms, *Generalized Nonlinear Non-analytic Chi-Square Fitting*: Matlab Central, 2008.

[22] W. H. Press, B. P. Flannery, S. A. Teukolsky, and W. T. Vetterling, *Numerical Recipes; The Art of Scientific Computing*: Cambridge University, 1986.

[23] M. Bloom, E. Evans, and O. G. Mouritsen, "Physical-Properties Of The Fluid Lipid-Bilayer Component Of Cell-Membranes - A Perspective", Quarterly Reviews of Biophysics, Vol. 24, pp. 293-397, 1991.

[24] F. R. Hallett, J. Marsh, B. G. Nickel, and J. M. Wood, "Mechanical-Properties Of Vesicles .2. A Model For Osmotic Swelling And Lysis", Biophysical J., Vol. 64, pp. 435-442, 1993.

[25] B. L. S. Mui, P. R. Cullis, E. A. Evans, and T. D. Madden, "Osmotic Properties Of Large Unilamellar Vesicles Prepared By Extrusion," Biophysical J., Vol. 64, pp. 443-453, 1993.

[26] D. Needham, T. J. McIntosh, and E. Evans, "Thermomechanical And Transition Properties Of Dimyristoylphosphatidylcholine Cholesterol Bilayers", Biochemistry, Vol. 27, pp. 4668-4673, 1988.

[27] T. J. Lewis, "A model for bilayer membrane electroporation based on resultant electromechanical stress", IEEE Trans. Dielectr.Electr. Insul., Vol. 10, pp. 769-777, 2003.

[28] E. Evans, V. Heinrich, F. Ludwig, and W. Rawicz, "Dynamic Tension Spectroscopy and Strength of Biomembranes", Biophysical J., Vol. 85, pp. 2342-2350, 2003.

[29] W. Meier, A. Graff, A. Diederich, and M. Winterhalter, "Stabilization of planar lipid membranes: A stratified layer approach", *Physical* Chemistry Chemical Phys., Vol. 2, pp. 4559-4562, 2000.

[30] M. Winterhalter, "Black lipid membranes", Current Opinion in Colloid & Interface Sci., Vol. 5, pp. 250-255, 2000.

[31] S. A. Pandit, D. Bostick, and M. L. Berkowitz, "Mixed Bilayer Dipalmitoylphosphatidylcholine and Dipalmitoylphosphatidylserine: Lipid Complexation, Ion Bonding, and Electrostatics", Biophysical J., Vol. 85, pp. 3120-3131, 2003.

Izidor Sabotin was born in Murska Sobota, Slovenia in 1981. He received the B.Sc. degree from the Faculty of Electrical Engineering, University of Ljubljana, Slovenia in 2008. Currently he works as a researcher at the Faculty of Mechanical Engineering in Ljubljana. His field of research is microtechnologies and its manufacturing processes in connection with microfluidic devices and biomedical engineering, especially in the field of electroporation.

Alenka Maček Lebar was born in 1967 in Ljubljana, Slovenia. She received the M.Sc. and Ph.D. degrees in electrical engineering from the University of Ljubljana, Ljubljana, Slovenia, in 1995 and 1999, respectively. She is an Assistant Professor on the Faculty of Electrical Engineering, University of Ljubljana. Her main research is directed toward the biomedical engineering field, especially in the field of electroporation.

Damijan Miklavčič was born in Ljubljana, Slovenia, in 1963. He received the Ph.D. degree in electrical engineering from the University of Ljubljana, Ljubljana. He is currently a Professor with the Faculty of Electrical Engineering and the Head of the Laboratory of Biocybernetics, University of Ljubljana. He is active in the field of biomedical engineering. His research interest in the last years focuses on electroporation-assisted drug and gene delivery, including cancer treatment by means of electrochemotherapy, tissue oxygenation, and modeling.

Peter Kramar was born in Kranj, Slovenia in 1977. He received the B.Sc. degree from the Electrical Engineering, University of Ljubljana, Faculty of Electrical Engineering, Ljubljana, Slovenija in 2003, and the M.Sc. degree in 2005. He is a teaching assistant at University of Ljubljana, His main research area is electroporation of planar lipid bilayers.

Članek 4

Merjenje lastnosti ravninskih lipidnih dvoslojev

Peter Kramar, Damijan Miklavčič, Alenka Maček Lebar

Objavljen v: Elektrotehniški vestnik 76(5) (2009) 293-298

Elektrotehniški vestnik 76(5): 293–298, 2009
Electrotechnical Review, Ljubljana, Slovenija

Merjenje lastnosti ravninskih lipidnih dvoslojev

Peter Kramar, Damijan Miklavčič, Alenka Maček Lebar

Univerza v Ljubljani, Fakulteta za elektrotehniko, Tržaška 25, 1000 Ljubljana, Slovenija
E-pošta: peter.kramar@fe.uni-lj.si

Povzetek. Lipidne molekule so v naravi glavni sestavni del celične membrane. Sestavljene so iz polarne hidrofilne glave in nepolarnega hidrofobnega repa. Zato skupek molekul v vodi lahko tvori energijsko ugodne strukture. Ena takih je ravninski lipidni dvosloj, ki ga z obeh strani obdaja raztopina soli. V raztopino zlahka vstavimo elektrode ter ravninski lipidni dvosloj vzbujamo s tokovnim ali napetostnim signalom poljubne oblike in merimo odziv, ki ga vzbujani signal povzroči.
Lastnosti, ki jih na ta način na ravninskem lipidnem dvosloju opazujemo, so: kapacitivnost, debelina, upornost oziroma prevodnost, pretok snovi in porušitvena napetost. Vsaka od naštetih lastnosti zahteva svoj način merjenja. Kadar raziskujemo pojav elektroporacije v biomedicini in biotehnologiji, je porušitvena napetost ena izmed ključnih lastnosti ravninskega lipidnega dvosloja. Znano je, da je porušitvena napetost odvisna od sestave ravninskega lipidnega dvosloja in koncentracije okoliškega elektrolita ter od trajanja izpostavitve električnemu polju.

V članku predstavljamo osnovne principe merjenja naštetih lastnosti ravninskih lipidnih dvoslojev.

Ključne besede: ravninski lipidni dvosloj, merilni sistemi, kapacitivnost, prevodnost

Measurement of planar lipid bilayer Properties

Extended abstract. Lipid molecules are an important part of the cell membrane. They are composed of polar hydrophobic heads and nonpolar hydrophilic tails. Due to their physical properties and simplicity they can form a wide constituent of self assembly systems such as: monolayer, bilayer, vesicles and micelles. We studied a planar lipid bilayer surrounded by a water solution from both sides.

The properties studied on the planar lipid bilayer were: capacity, thickness, conductivity, resistivity, fluctuations and voltage breakdown. Each property required its own measurement method. The signal used was the voltage or current clamp.

The voltage breakdown is one of the most important properties when studying the phenomena of electroporation in biomedicine and biotechnology. It has been known that the breakdown voltage depends on the lipid membrane composition, ionic bath solution, amplitude and electric field exposure duration.

In most cases, the breakdown voltage of the planar lipid bilayer is determined by applying a rectangular voltage pulse. The amplitude of the voltage pulse is incremented in small steps until the breakdown of the bilayer is obtained. Using the rectangular voltage pulse measuring protocol, the number of applied voltage pulses is not known in advance and each planar lipid bilayer is exposed to a voltage stress many times. Such a pre-treatment of the planar lipid bilayer affects its stability and consequently the determined breakdown voltage of the planar lipid bilayer. Another approach to the breakdown voltage determination was suggested by our group. Using a linear rising signal, the breakdown voltage of each planar lipid bilayer is determined by a single voltage exposure [20,21].

Key words: planar lipid bilayer, property measurement, capacity, permeability

Prejet 27. oktober, 2009
Odobren 9. november, 2009

1 Uvod

Lipidne molekule so glavni sestavni del celične membrane tako rastlinskih kot živalskih celic. Sestavljene so iz polarne hidrofilne glave in nepolarnega hidrofobnega repa. Zato skupek molekul v vodi tvori energijsko ugodno strukturo tako, da nepolarni hidrofobni repi nikoli niso izpostavljeni vodnim molekulam. Prav ta lastnost in njihova preprostost jim omogočata uporabnost na različnih področjih, kot so biologija, kemija, fizika in medicina. Široko paleto lipidnih struktur: enoslojev, dvoslojev, večslojev, zaprtih dvoslojev oziroma veziklov in zaprtih enoslojev oziroma micel lahko tvorimo v različnih okoljih [1].

Osnovna struktura celične membrane in membran celičnih organel je lipidni dvosloj. Ker je notranjost celice težko dosegljiva, je lastnosti njene membrane zapleteno meriti. Umeten lipidni dvosloj je sicer preprost, a velikokrat zadovoljiv model celične membrane. Tvorimo lahko vezikle ali liposome, kjer je oblika strukture podobna celici, zgradba membrane pa zelo poenostavljena. Druga možnost je ravninski lipidni dvosloj, ki si ga lahko predstavljamo kot majhen delček celične membrane. Poglavitna prednost takšnega ravninskega lipidnega dvosloja je, da je med merjenjem dostopen z obeh strani [2].

Ravninske lipidne dvosloje ponavadi pripravimo v posebni komori, ki je sestavljena iz dveh prekatov. Prekata ločuje teflonska folija, v kateri je luknjica s premerom od 0,1 do 1 mm. Na luknjici tvorimo ravninski

lipidni dvosloj z eno od naslednjih metod: metodo barvanja, metodo dvigovanja gladine ali metodo potopitve konice [3, 4].

Metoda barvanja (*ang. painted bilayer*) ali Mueller-Rudinova metoda je bila razvita med prvimi [5]. Vodna raztopina je pripravljena v komori, s pipeto pa nanesemo lipide na teflonsko folijo, ki ločuje oba prekata komore (slika 1A). V začetku so lipidne molekule združene v veliko gmoto (slika 1B). Sčasoma odvečni lipidi odplavajo na gladino in na luknjici nastane ravninski lipidni dvosloj (slika 1C).

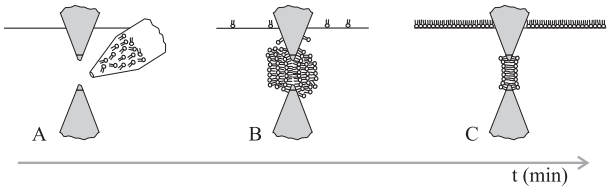

Slika 1. Metoda barvanja [5]. A) Komora z vodo in nanos lipidov na teflonsko folijo, ki deli prekata komore. B) Gmota nanesenih lipidov se enakomerno razporedi po teflonski foliji, odvečni lipidi odplavajo na gladino. C) Po določenem času nastane lipidni dvosloj.
Figure 1. Painted planar lipid bilayer method [5]. A) The chamber is filled with a water solution. Lipids are painted on a teflon sheet. B) A cluster of painted lipid molecules is slowly spread on a teflon sheet, excess lipids go to a water solution surface. C) After some time, a planar lipid bilayer is formed.

Pri metodi potopitve konice (*ang. Tip-Dip bilayer*) potrebujemo kopel, v katero potopimo ozko cevko [6]. Na gladino nanesemo lipidne molekule, ki se porazdelijo po celotni gladini in na rob cevke (slika 2A). Ko cevko vzamemo iz kopeli, se na njej nabere lipidni enosloj (slika 2A). Cevko dvignemo nad gladino in počakamo, da se molekule lipidov ponovno razporedijo (slika 2B). Ko cevko ponovno potopimo, nastane na njeni konici ravninski lipidni dvosloj (slika 2C).

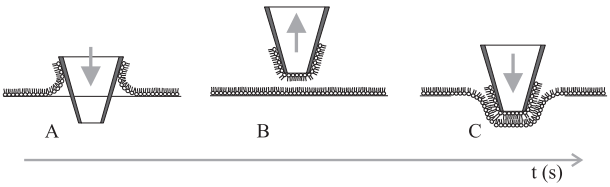

Slika 2. Metoda potopitve konice [6]. A) V kopel potopimo ozko cevko in nanesemo molekule lipidov. B) Cevko dvignemo, C) in jo ponovno potopimo, tako da se na njej tvori ravninski lipidni dvosloj.
Figure 2. Tip-Dip method [6]. A) When a small pipeline is inserted into the bath of a salt solution lipid molecules are added on the surface of the solution. B) The pipeline is lifted out of the bath solution. C) Insertion of the pipeline back to the bath solution forms the planar lipid bilayer on the edge of the pipeline.

Metoda dvigovanja gladine (*ang. folded bilayer*) oziroma Montal-Muellerjeva metoda je ena najpogosteje uporabljenih metod za proučevanje ravninskih lipidnih dvoslojev [7]. Oba prekata komore napolnimo z vodo pod nivojem luknjice v teflonski foliji. Na gladino obeh prekatov nanesemo lipide in počakamo, da se enakomerno porazdelijo po gladini (slika 3A). Obe gladini nato sočasno dvignemo (slika 3B). Na luknjici v teflonski foliji nastane ravninski lipidni dvosloj (slika 3C). Prednost te metode pred metodo barvanja je predvsem v tem, da brez daljšega čakanja, s spuščanjem in dviganjem gladine v prekatih tvorimo ravninske lipidne dvosloje večkrat zapored drugega za drugim.

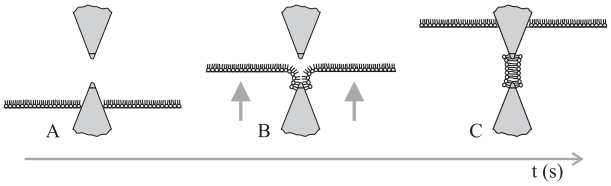

Slika 3. Metoda dviganja gladine [7]. A) Gladino vode postavimo tik pod luknjico v teflonski foliji. Na površino nanesemo lipidne molekule in počakamo, da se porazdelijo enakomerno po gladini. B) V obeh prekatih enakomerno dvignemo gladino vode. C) Na luknjici teflonske folije tvorimo ravninski lipidni dvosloj.
Figure 3. Folded planar lipid bilayer method [7]. A) A layer of lipid molecules on the surface of a salt solution. B) The levels of the salt solution are slowly rised above the hole. C) A planar lipid bilayer is formed on the hole.

Lastnosti lipidnih dvoslojev, kot so prevodnost, kapacitivnost, porušitvena napetost ali debelina, večinoma določamo z meritvijo toka oziroma napetosti prek lipidnega dvosloja ali z optičnim opazovanjem, kjer opazujemo odklon žarka ter absorpcijo svetlobe v lipidnem dvosloju. Električne in optične meritve lahko med seboj tudi kombiniramo.

Omenjene meritve so osnova za opazovanje tako enostavnih lipidnih dvoslojev kot tudi dvoslojev, ki smo jim dodali različne molekule ter jim tako spremenili eno ali več lastnosti [8, 9]. Sestavo lipidnega dvosloja lahko poljubno spreminjamo in jo s tem približamo sestavi prave celične membrane [1]. Tako lahko na preprostem modelu proučujemo, kako na celično membrano vplivajo elektromagnetna valovanja [10]. Lipidne dvosloje lahko uporabljamo tudi kot preprost model tankih plasti [11].

V nadaljevanju se bomo osredinili na opazovanje lipidnih dvoslojev in določanje njihovih lastnosti na podlagi meritev napetosti in toka. Lipidni dvosloj namreč lahko predstavimo s preprostim električnim vezjem; vzporedno vezavo kondenzatorja in upora. Napetostno ali tokovno vzbujanje takega preprostega vezja je lahko osnova za izračun vrednosti elementov, ki določajo lastnosti lipidnega dvosloja. Opisali bomo merjenje kapacitivnosti, upornosti in porušitvene napetosti ravninskega lipidnega dvosloja. Posamezne veličine namreč lahko merimo na različne načine, s kombiniranjem meritev pa se znanje o določenem ravninskem lipidnem dvosloju še dopolnjuje. Natančneje se bomo seznanili z napetostnim in tokovnim vzbujanjem ravninskih lipidnih dvoslojev. Opisali bomo

oblike signalov, ki jih uporabljamo pri posameznem vzbujanju, ter katere lastnosti lahko z njimi opazujemo (slika 4).

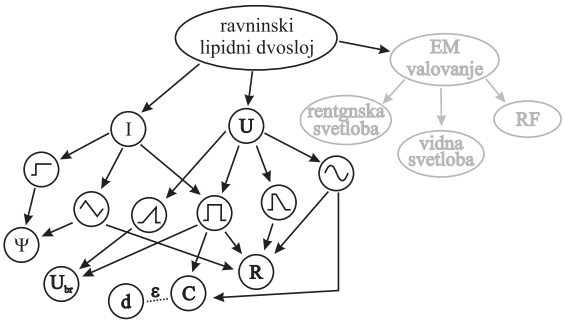

Slika 4. Pregled različnih načinov določanja lastnosti ravninskih lipidnih dvoslojev. Z I je označeno tokovno vzbujanje, z U napetostno vzbujanje. Oblika signala vzbujanja je narisana v krožcu. S takimi vzbujanji lahko merimo veličine, kot so nihanje lipidov v membrani (ψ), porušitveno napetost (U_{br}), debelina (d), kapacitivnost (C) in upornost (R).
Figure 4. Review of the planar lipid bilayer properties measurements. I represents the current clamp and U the voltage clamp. The shape of the clamping signal is drawn in the circle. We can directly or indirectly measure: lipid fluctuations (ψ), voltage breakdown (U_{br}), thickness (d), capacitance (C) and resistance (R)

2 Kapacitivnost (C)

V literaturi zasledimo tri različne metode merjenja kapacitivnosti: merjenje časovne konstante razelektritve ravninskega lipidnega dvosloja, merjenje z izmenično napetostjo sinusne oblike in merjenje s pretvorbo kapacitivnosti v frekvenco. Pri vseh treh metodah izmerjeno kapacitivnost normiramo na površino lipidnega dvosloja. Normirano kapacitivnost tako lahko primerjamo s poizkusi, narejenimi na različnih sistemih z različnimi površinami ravninskih lipidnih dvoslojev.

Najpogosteje kapacitivnost merimo z določitvijo časovne konstante razelektritve ravninskega lipidnega dvosloja [12]. Ravninskemu lipidnemu dvosloju vsilimo napetost izbrane velikosti. Pri tem se na ravninskem lipidnem dvosloju nabere naboj. Ko je impulza konec, ravninski lipidni dvosloj razelektrimo prek upora znane vrednosti. Razelektritev ravninskega lipidnega dvosloja lahko opazujemo kar z osciloskopom (slika 5).

Napetost pri razelektritvi na ravninskem lipidnem dvosloju $u(t)$ lahko opišemo kot:

$$u(t) = U_0 e^{-\frac{t}{\tau}}. \tag{1}$$

U_0 je amplituda vsiljene napetosti; τ časovna konstanta, ki je odvisna od kapacitivnosti (C) in upornosti (R) ravninskega lipidnega dvosloja in merilnega sistema,

$$\tau = R \cdot C. \tag{2}$$

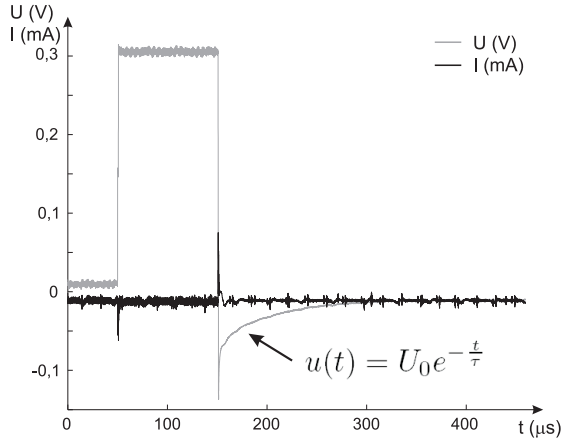

Slika 5. Napetost na ravninskem lipidnem dvosloju pri merjenju kapacitivnosti z metodo razelektritve.
Figure 5. Voltage on a planar lipid bilayer during capacitance measurement made by using the discharge method.

Če poznamo upornost sistema in je ta veliko manjša od upornosti ravninskega lipidnega dvosloja ($\sim 10^8\ \Omega$) [1], lahko kapacitivnost ravninskega lipidnega dvosloja določimo z meritvijo, ki je sestavljena iz dveh delov. Najprej izmerimo kapacitivnost sistema brez ravninskega lipidnega dvosloja (C_{sis}), v drugem delu pa kapacitivnost sistema z lipidnim dvoslojem (C_{SBLM}). Predpostavimo lahko, da je kapacitivnost ravninskega lipidnega dvosloja (C_{BLM}) razlika obeh izmerjenih kapacitivnosti:

$$C_{BLM} = C_{sis} - C_{SBLM}. \tag{3}$$

Metoda razelektritve ravninskega lipidnega dvosloja je najpogosteje uporabljena zato, ker je njena izvedba preprosta; potrebujemo le napetostni vir, hitro stikalo ter spominski osciloskop za opazovanje razelektritve ravninskega lipidnega dvosloja.

Zasledimo tudi merilno metodo, v okviru katere vrednost kapacitivnosti pretvorimo v čas [13]. Enakomerno naelektrimo lipidni dvosloj do neke napetostne vrednosti, ko jo presežemo, ravninski lipidni dvosloj praznimo. Periodično polnjenje in praznjenje C_{BLM} da na izhodu vezja pravokotni signal s periodo, ki je odvisna od kapacitivnosti lipidnega dvosloja (slika 6).

Kondenzator C_{BLM} na sliki 6 predstavlja kapacitivnost lipidnega dvosloja. Na kondenzatorju merimo napetost v točki D in jo ojačimo z operacijskim ojačevalnikom. Ta ima ojačenje k določeno z uporoma R_1 in R_2:

$$k = \frac{R_1 + R_2}{R_1}. \tag{4}$$

Izhod ojačevalnika je pripeljan v integrirano vezje NE555, v katerem sta dva napetostna primerjalnika. Vhod prvega je merjena napetost v točki A, drugega pa razdeljena napetost, ki gre prek delilnika treh uporov.

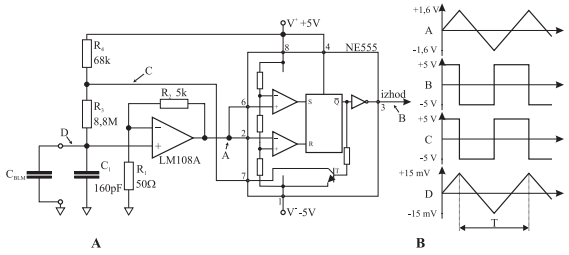

Slika 6. A) Vezje za transformacijo kapacitivnosti v periodo. B) Potek signalov na posamezni točki v vezju [13].
Figure 6. A) Capacitance to the time transformation circuit. B) Voltage signal on selected points of the signal [13].

Glede na nivo napetosti se preklopi izhod RS spominske celice. Izhod iz celice invertiramo, rezultat pa je pravokotni signal, kateremu zlahka izmerimo periodo T_p. Napetost na lipidnem dvosloju lahko izrazimo z enačbo:

$$U_{BLM} = \frac{2}{3} V \frac{1}{k} = \frac{2 \cdot V \cdot R_1}{3\,(R_1 + R_2)}. \tag{5}$$

Merjenje razdelimo v dve fazi. Prva faza je polnjenje kondenzatorja, kjer teče tok iz napajalnika prek uporov R4 in R3 v kondenzator. Tranzistor T je zaprt. V drugi fazi se zaradi preklopa RS celice tranzistor T odpre in kondenzator C_{BLM} se razelektri. Tok teče prek upora R3 in tranzistorja T v negativni pol napajanja. Zaradi ohranjanja energije velja, da je produkt napajalne napetosti (V) in časa v eni periodi T_p enak:

$$T_p \cdot V = U_{BLM}\,(R_3 + R_4)\,C_{BLM} + U_{BLM} R_3 C_{BLM}. \tag{6}$$

V vezju izberemo simetrično napajanje $V = V^+ = |V^-|$ ter vrednost upora $R_3 \gg R_4$. Iz enačbe (6) izrazimo periodo, pri čemer zanemarimo upornost R_4 (zaradi $R_3 \gg R_4$). Kapacitivnost ravninskega lipidnega dvosloja je torej:

$$C_{BLM} = \frac{V T_p}{2 U_{BLM} R_3}. \tag{7}$$

Kapacitivnost ravninskega lipidnega dvosloja merimo tudi z uporabo izmenične napetosti [14]. Usmerjena izhodna napetost se spreminja v odvisnosti od vrednosti kapacitivnosti ravninskega lipidnega dvosloja. Merilni sistem je treba najprej umeriti na spektru znanih kapacitivnosti, da določimo parametre parabolične krivulje, kateri sledi odvisnost. Na omenjeni način lahko sočasno merimo tudi upornost ravninskega lipidnega dvosloja.

3 Upornost (R) oziroma prevodnost (G)

Upornost (R) oziroma prevodnost (G) lipidnih dvslojev ponavadi opišemo z razmerjem izmerjenega in vzbujalnega signala. Kadar vzbujamo lipidni dvosloj z napetostjo, lahko z opazovanjem toka neposredno opazujemo prevodnost. Nasprotno je pri tokovnem vzbujanju, ko opazujemo upornost ravninskega lipidnega dvosloja z merjenjem napetosti. Ustrezno razmerje obeh signalov podaja upornost ravninskega lipidnega dvosloja, ki je praviloma izredno velika (reda $10^8\ \Omega$).

Pri metodi, ko ravninski lipidni dvosloj vzbujamo s sinusnim signalom poljubne amplitude (0,1 - 1,5 V) in frekvenco 1 Hz, merimo upornost in kapacitivnost sočasno. Temu signalu prištejemo še sinusni signal amplitude 2 mV in frekvence 1 kHz [14]. Z 1 kHz signalom merimo kapacitivnost, kot smo opisali v razdelku o merjenju kapacitivnosti. Nadomestno vezje za tak sistem vidimo na sliki 7. Zapišemo napetostni enačbi za realni

$$V_1 \cos(\varphi - \varphi_1) + V_{BLM} \cos(\varphi_{BLM} - \varphi) = V_S \tag{8}$$

in imaginarni del napetosti

$$V_1 \sin(\varphi - \varphi_1) = V_{BLM} \sin(\varphi_{BLM} - \varphi). \tag{9}$$

Iz kapacitivnosti ravninskega lipidnega dvosloja in znanega toka lahko izračunamo fazni kot φ_{BLM} na lipidnem dvosloju z enačbo:

$$\omega C_{BLM} V_{BLM} = I \sin \varphi_{BLM}, \tag{10}$$

pri čemer znani tok izrazimo z uporom R_1 in kondenzatorjem C_1:

$$I = V_1 \sqrt{(\omega C_1)^2 + \left(\frac{1}{R_1}\right)^2}. \tag{11}$$

Z vsemi tremi enačbami lahko izračunamo še napetost na lipidnem dvosloju V_{BLM} in fazni kot φ celotnega sistema. Prevodnost na lipidnem dvosloju izračunamo iz relacije:

$$G_{BLM} V_{BLM} = I \cos \varphi. \tag{12}$$

Taka metoda merjenja nam omogoča sočasno spremljanje kapacitivnosti in upornosti; tudi med spreminjanjem lastnosti lipidnega dvosloja.

4 Porušitvena napetost lipidnega dvosloja (V_C)

Pod vplivom električnega polja tako v celični kot tudi v umetni membrani nastanejo strukturne spremembe – pore, ki omogočajo transport ionov in molekul skozi ravninski lipidni dvosloj. Natančni mehanizmi nastajanja por, njihova velikost, struktura in stabilnost niso v celoti poznani [15]. V zadnjem času v literaturi najdemo molekularne modele, ki nakazujejo dinamično nastajanje por in s tem delno pojasnjujejo tudi mehanizme nastajanja [16,17]. Z meritvijo porušitvene napetosti dobimo

podatek o trdnosti in stabilnosti ravninskega lipidnega dvosloja. Porušitveno napetost ponavadi merimo tako, da opazujemo tok ob pravokotnih napetostnih pulzih, ki jih dovedemo na ravninski lipidni dvosloj. Amplitudo napetostnih pulzov povečujemo, dokler ne zaznamo povečanja električnega toka (slika 8). Električni tok je znak, da je ravninski lipidni dvosloj porušen. Amplitudo napetostnega pulza, s katerim smo ravninski lipidni dvosloj porušili, imenujemo porušitvena napetost [8]. Pri tako zasnovani meritvi je izmerjena porušitvena napetost odvisna od trajanja pulza in od časa predhodnih izpostavitev ravninskega lipidnega dvosloja električnemu polju [18,19], ki pa ga vnaprej ne poznamo.

Zato smo predlagali novo metodo določanja porušitvene napetosti, ki bi bila predvsem preprosteja in učinkoviteja od tistih, ki so jih uporabljali do zdaj [20]. Porušitveno napetost ravninskega lipidnega dvosloja določimo z linearno naraščajočim napetostnim signalom (slika 9). Naklon in končno napetost linearno naraščajočega signala je treba prej izbrati. Izbira končne napetosti mora zagotavljati, da se bo ravninski lipidni dvosloj zagotovo porušil. Izkazalo se je, da je metoda odlična [20]. Z različnimi nakloni linearno naraščajočih signalov lahko določimo celo prag porušitvene napetosti za izbrani lipidni dvosloj – to je napetost, pri kateri se ravninski lipidni dvosloj poruši, če ji je izpostavljen daljši čas. Med meritvijo je ravninski lipidni dvosloj izpostavljen napetostnemu signalu le enkrat, tako se izognemo vplivu večkratne izpostavitve ter zmanjšamo stresanje vrednosti izmerjene porušitvene napetosti [20].

5 Sklep

Ravninski lipidni dvosloj je preprost model celične membrane. Njegova poglavitna prednost je dostopnost z obeh strani. Zasnova modela omogoča preprosto spreminjanje kemijske strukture ravninskega lipidnega dvosloja in merjenje njegovih lastnosti: kapacitivnosti, upornosti in porušitvene napetosti.

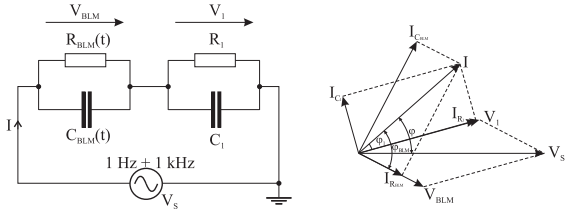

Slika 7. Nadomestno vezje sistema in kazalčni diagram za merjnje električnih lastnosti ravninskih lipidnih dvoslojev s sinusnim vzbujanjem [14].
Figure 7. Substitute circuit of the system and vector diagram for measuring electrical properties of planar lipid bilayers with a sinus signal [14].

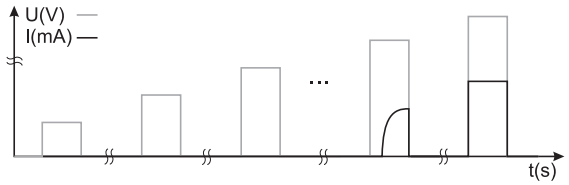

Slika 8. Določitev porušitvene napetosti ravninskega lipidnega dvosloja.
Figure 8. Planar lipid bilayer breakdown determination.

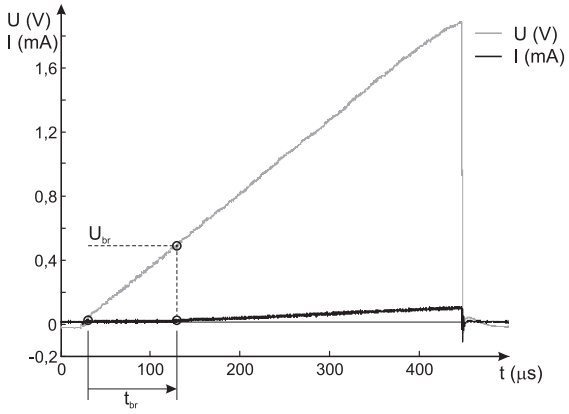

Slika 9. Določitev življenjske dobe ter porušitvene napetosti ravninskega lipidnega dvosloja. Svetla krivulja predstavlja pritisnjeno napetost, temna krivulja pa tok skozi ravninski lipidni dvosloj. Čas med začetkom naraščanja pritisnjene napetosti ter začetkom naraščanja toka definiramo kot življenjsko dobo ravninskega lipidnega dvosloja t_{br}. Ob času ko začne naraščati tok iz napetostnega signala odčitamo porušitveno napetost ravninskega lipidnega dvosloja U_{br}.
Figure 9. Planar lipid bilayer breakdown and lifetime determination. The light curve on the plot represents the applied voltage and the dark curve the current trough the planar lipid bilayer. The lifetime of planar lipid bilayer t_{br} is defined as the time between the beginning of the rising applied linear rising voltage and a time the current starts to flow across the membrane. Voltage breakdown U_{br} is defined as the value of the applied voltage at t_{br}.

6 Zahvala

Avtorji se zahvaljujejo Agenciji za raziskovalno dejavnost Republike Slovenije za finančno podporo.

7 Literatura

[1] H.T.Tien and A.Ottova, *The lipid bilayer concept: Experimental realization and current applications*. In Planar lipid bilayers (BLMs) and their applications. (Ed. H.T.Tien and A.Ottova-Leitmannova) 1−74, Elsevier, New York 2003.

[2] H.T.Tien, *Bilayer Lipid Membranes (BLM)*, Marcel Dekker, inc., New York 1974.

[3] M.Smeyers, M.Leonetti, E.Goormaghtigh and F.Homble, *Structure and function of plant membrane ion channels reconstituted in planar lipid bilayers*. In Planar Lipid Bilayers (BLMs) and their Applications. (Ed. H.T.Tien and A.Ottova-Leitmannova) 449−478, Elsevier, New York 2003.

[4] B.E.Ehrlich, *Incorporation of Ion Channels in Planar Lipid Bilayers: How to Make Bilayers Work for You*. In The Heart and Cardiovascular System. (Ed. H.A.Fozzard et al.) 551−560, Raven Press, New York 1992.

[5] P. Mueller, DO. Rudin, HT. Tien, WC. Wescott, *Methods for the formation of single bimolecular lipid membranes in aqueous solutions*. J. Phys. Chem. 67, 534−535 (1963).

[6] R. Coronado and R. Latorre, *Phospholipid-bilayers made from monolayers on patch-clamp pipettes*. Biophysical Journal 43, 231−236 (1983).

[7] M. Montal and P. Mueller, *Formation of bimolecular membranes from lipid monolayers and a study of their electrical properties*. Proceedings of the National Academy of Sciences of the United States of America, 69, 3561−3566 (1972).

[8] G.C.Troiano, L.Tung, V.Sharma and K.J.Stebe, *The Reduction in Electroporation Voltages by the Addition of Surfactant to Planar Lipid Bilayer*. Biophisical Journal 75, 880−888 (1998).

[9] V.Sharma, K.Uma Maheswari, J.C.Murphy and L.Tung, *Poloxamer 188 Decreases Susceptibility of Artificial Lipid Membranes to Electroporation*. Biophisical Journal 71, 3229−3241 (1996).

[10] T.F.Eibert, M.Alaydrus, F.Wilczewski and V.W.Hansen, *Electromagnetic and Thermal Analysis for Lipid Bilayer Membranes Exposed to RF Fields*. IEEE transactions on biomedical engineering 46, 1013−1021 (1999).

[11] A.Iglič and V.Kralj-Iglič, *Effect of anisotropic properties of membrane constituents on stable shapes of membrane bilayer structure*. In Planar Lipid Bilayers (BLMs) and their Applications. (Ed. H.T.Tien and A.Ottova-Leitmannova) 143−172, E lsevier, New York 2003.

[12] R.Benz and K.Janko, *Voltage-induced capacitance relaxation of lipid bilayer membranes; effects on membrane composition*. Biochimica et Biophysica Acta 455, 721−738 (1976).

[13] S.Kalinovski and Z.Figaszevski, *A new system for bilayer lipid membrane capacitance measurements: method, apparatus and applications*. Biochimica et Biophysica Acta 1112, 57−66 (1992).

[14] E.Gallucci, S.Micelli and G.Monticelli, *Pore Formation in Lipid Bilayer Membranes Made of Phosphatidylinositol and Oxidized Cholesterol Followed by Means of Alternating Current*. Biophisical Journal 71, 824−831 (1996).

[15] M.Pavlin, T.Kotnik, D.Miklavčič, P.Kramar, A.Maček Lebar, *Electroporation of Planar Lipid Bilayers*. In Membranes Advances in Planar Lipid Bilayers and Liposomes Volume 6. (Ed. A. Leitmannova Liu) 165−226, Academic Press 2008.

[16] D.P.Tieleman, H.Leontiadou, A.E.Mark, S.J.Marrink, *Simulation of pore formation in lipid bilayers by mechanical stress and electric fields*. Journal of the American Chemical Society 125, 6382−6383 (2003).

[17] M.Tarek, *Membrane electroporation: A molecular dynamics simulation*. Biophysical Journal, 88, 4045−4053 (2005).

[18] I.G.Abidor, V.B.Arakelyan, L.V.Chernomordik, Y.A.Chizmadzhev, V.F.Pastushenko and M.R.Tarasevich, *246 - Electric Breakdown of Bilayer Lipid Membranes I. The Main Experimental Facts and Their Qualitative Discussion*. Bioelectrochemistry and Bioenergetics 6, 37−52 (1979).

[19] A.Maček Lebar, G.C.Troiano, L.Tung, D.Miklavčič, *Inter-pulse interval between rectangular voltage pulses affects electroporation threshold of artificial lipid bilayers*. IEEE Transactions on Nanobioscience 1, 116−120 (2002).

[20] P.Kramar, D.Miklavcic, A.Macek Lebar, *Determination of lipid bilayer breakdown voltage by means of linear rising signal*. Bioelectrochemistry, 70, 23−27 (2007).

[21] P.Kramar, D.Miklavcic, A. Macek Lebar, *A system for the determination of planar lipid bilayer breakdown voltage and its applications*. IEEE Transactions on Nanobioscience 8, 132−138 (2009).

Peter Kramar je diplomiral leta 2003 in magistriral leta 2005 na Fakulteti za elektrotehniko Univerze v Ljubljani. Na isti fakulteti je od leta 2003 zaposlen, najprej kot raziskovalec, zdaj pa kot asistent. Raziskovalno se ukvarja z elektroporacijo ravninskih lipidnih dvoslojev.

Alenka Maček Lebar je diplomirala leta 1991, magistrirala leta 1995 ter doktorirala leta 1999 na Fakulteti za elektrotehniko Univerze v Ljubljani. Je docentka na Fakulteti za elektrotehniko Univerze v Ljubljani. Raziskovalno in pedagoško se ukvarja z vplivom električnega polja na biološke sisteme.

Damijan Miklavčič je diplomiral leta 1987, magistriral leta 1991 ter doktoriral leta 1993 na Fakulteti za elektrotehniko, Univerze v ljubljani. Je redni profesor na Fakulteti za elektrotehniko Univerze v Ljubljani. Raziskovalno in pedagoško se ukvarja z vplivom električnega polja na biološke sisteme.

Poglavje v knjigi

Voltage and current clamp methods for determination of planar lipid bilayer properties

Peter Kramar, Damijan Miklavčič, Malgorzata Kotulska, Alenka Maček Lebar

Objavljen v: Advances in Planar Lipid Bilayers and Liposomes, Volume 11, Elsevier 2010

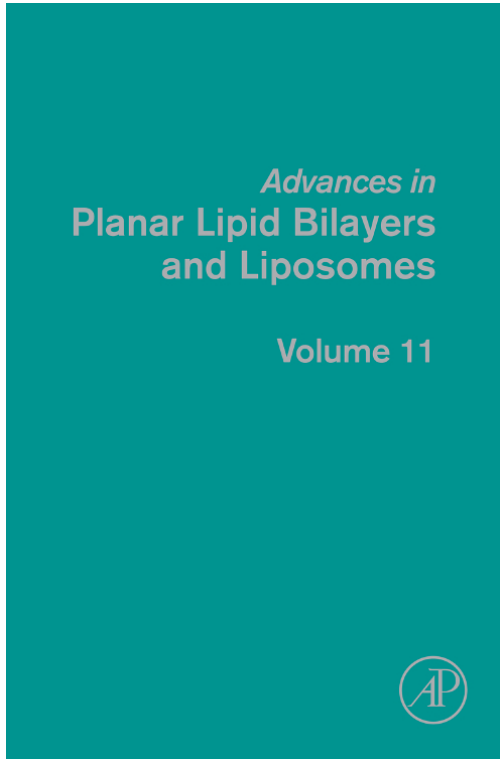

From: Peter Kramar, Damijan Miklavčič, Malgorzata Kotulska, and Alenka Maček Lebar, Voltage- and Current-Clamp Methods for Determination of Planar Lipid Bilayer Properties. In Ales Iglic, editor: *Advances in Planar Lipid Bilayers and Liposomes*, Vol. 11, Burlington: Academic Press, 2010, pp. 29-69.
ISBN: 978-0-12-381013-7

CHAPTER TWO

Voltage- and Current-Clamp Methods for Determination of Planar Lipid Bilayer Properties

Peter Kramar,[1] Damijan Miklavčič,[1] Malgorzata Kotulska,[2] *and* Alenka Maček Lebar[1,*]

Contents

1. Introduction 30
2. Measurement Systems 32
   2.1. Voltage Clamp 33
   2.2. Current Clamp 46
3. Methods for Determination of Planar Lipid Bilayer Properties 49
   3.1. Capacitance (C) 49
   3.2. Resistance (R) 53
   3.3. Breakdown Voltage (U_{br}) 54
   3.4. Fluctuations (ψ) 57
   3.5. Other Physical Properties 58
4. Conclusions 60
References 66

Abstract

Biological membranes, the barriers that envelope the cell and its inner organelles, play a crucial role in the normal functioning of cells. The simplest model of these biological membranes is the planar lipid bilayer. Because its geometry allows chemical and electrical access to both sides of the bilayer, the physical properties of this model membrane can be easily measured. Usually, a thin bimolecular film composed of specified phospholipids and organic solvent is formed on a small aperture in a hydrophobic partition separating two compartments containing aqueous solutions. From the electrical point of view, a planar lipid bilayer can be considered as an imperfect capacitor; therefore, two electrical properties,

* Corresponding author: Tel.: +386 1 4768 770; Fax: +386 1 4264 658
E-mail address: alenka.macek.lebar@fe.uni-lj.si

[1] Faculty of Electrical Engineering, University of Ljubljana, Ljubljana, Slovenia
[2] Institute of Biomedical Engineering and Instrumentation, Wroclaw University of Technology, Wroclaw, Poland

Advances in Planar Lipid Bilayers and Liposomes, Volume 11
ISSN 1554-4516, DOI: 10.1016/S1554-4516(10)11002-3

capacitance (*C*) and resistance (*R*), determine most of its behavior. Electrodes placed in the aqueous compartments on each side of the planar lipid bilayer permit the measurement of current and voltage across the model membrane. The two measuring techniques most commonly used to measure the properties of planar lipid bilayers are voltage-clamp methods and current-clamp methods.

The focus of this chapter is to review measurement systems and methods for the determination of the physical properties of planar lipid bilayers.

1. Introduction

Biological membranes, the barriers that envelope the cell and its inner organelles, play an important role in normal functioning of the cells. The membranes maintain crucial concentration gradients by acting as a selective filter for water-soluble ions and molecules [1]. Although biological membranes are composed of lipids, proteins, and small amounts of carbohydrates, the barrier function is assured by the thin layer of amphipathic phospholipids, which in polar liquid environments spontaneously arranges in various forms of lipid bilayers. A basic understanding of the properties and functioning of biological membranes can be obtained by investigating model systems, such as artificial liposomes or vesicles, which mimic the geometry and size of cell membranes, but are void of ion channels and the multitude of other embedded components commonly present in cells. The artificial planar bilayer lipid membrane (BLM) is the simplest model of a lipid system. It is usually formed across a small hole in a hydrophobic partition that separates two compartments filled with aqueous solutions. The advantage of the BLM is that both sides of the membrane can be easily altered and probed by electrodes.

Two methods of BLM formation are in common use. In one technique, the BLM is created by spreading a solution of lipids dissolved in an organic solvent. This method was introduced by Mueller and colleagues [2] and is named the painting technique. Both compartments of the chamber are filled with salt solutions and a dispersion of lipids is drawn across the hole in the partition separating them using a small paintbrush or a plastic rod. The cluster of lipids thins out in the center of the hole spontaneously forming a bilayer (Fig. 1). In the other procedure, the bilayer is formed from the apposition of two lipid monolayers [3]. A lipid solution in a volatile solvent is spread on the water–air interface of each compartment. Evaporation of the solvent creates a monolayer on the surface of the aqueous solution. When the monolayer formation is completed the water level in both compartments is raised above the hole and the bilayer is formed (Fig. 2).

A number of techniques have been developed to allow investigations of the functions and physical properties of these thin and fragile structures. Electrical measurements are a straightforward way to characterize the barrier

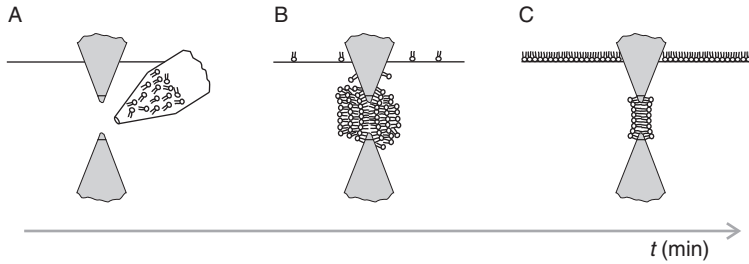

Figure 1 Planar lipid bilayer formation by the painted technique [2]. (A) Lipid molecules are painted on the aperture by pipette or brush. (B) The cluster of lipid molecules on the aperture. Lipid molecules are slowly spreading across the aperture. Nonused lipid molecules flow to the water solution surface. (C) Planar lipid bilayer is formed on the hole by thinning process.

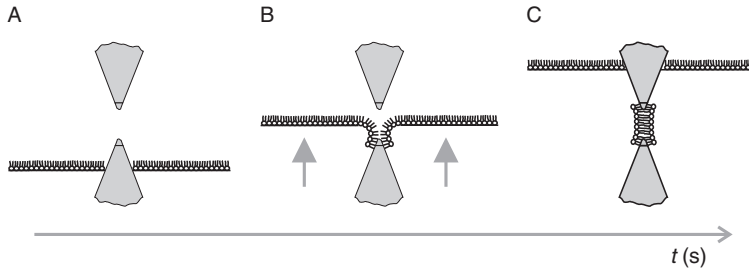

Figure 2 The folding method [3]. (A) Layer of lipid molecules on the salt solution. (B) The levels of the salt solution are slowly raised above the hole. (C) Planar lipid bilayer is formed on the hole.

function of a bilayer—its ability to prevent the flow of ions. From an electrical point of view, a planar lipid bilayer can be easily imagined as an imperfect capacitor, which means that the capacitance (C) has a finite parallel resistance (R). The typical resistance is very high since the hydrophobic core is impermeable to any charged species, and it is called a gigaseal. But the resistance drops dramatically even if a few nanometer-sized holes are present in a lipid bilayer. Formation of pores can be induced by a strong electric field externally applied to the BLM, and electrical measurements permit determination of BLM breakdown voltage (U_{br}). The electrical properties of the BLM are dependent on the physical properties of the lipids that compose the bilayer. Elasticity modulus and surface tension, for example, can be calculated from the electrical characteristics of the BLM.

Two electrical measurement methods are common (Fig. 3): the voltage-clamp method and the current-clamp method. When the voltage-clamp method is used, a voltage signal is applied to the planar lipid bilayer: a step change [4], pulse [5–7], linear rising [8], or some other shape of the

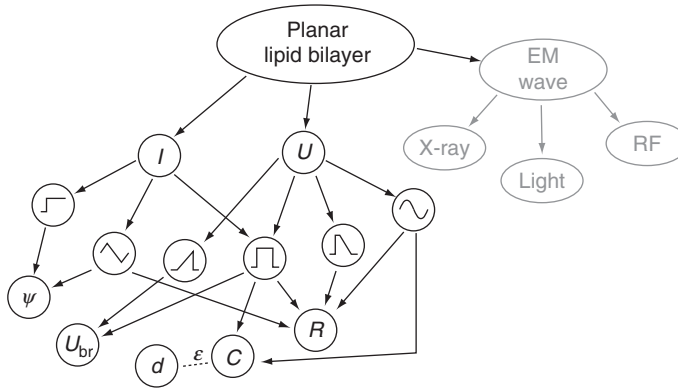

Figure 3 Measuring concepts and electrical properties of planar lipid bilayers. Resistance (R), capacitance (C), thickness (d), voltage breakdown (U_c), and mass fluctuation (Ψ) are measured with application of current (I) or voltage (U) signals of various shapes.

voltage signal. When the current-clamp method is used, a current is applied to the lipid bilayer [9]. Although these two methods are interchangeable when applied to objects of constant impedance, the situation changes when the electrical properties of a measurement subject are transient and related to the electrical signal. Separation of these two methods is useful, for example, in BLMs when electrically induced pores are studied. The shape of these pores is very unstable and their conductance is constantly changing throughout experiments.

A combination of electrical recording techniques with different kinds of high-frequency electromagnetic fields offers additional possibilities of investigating the structure–function relationships of planar lipid bilayer and of membrane interacting peptides [10–13].

In the following, we review electrical measuring principles and methods that have been applied for determination of planar lipid bilayer properties. According to the fact that each planar lipid bilayer property can be measured in many ways (Fig. 3) and therefore by different measuring systems, the main goal of the chapter is only to describe the existing measuring principles and to point out their experimental abilities. The choice of the most appropriate measuring system should be determined by combination of planar lipid bilayer properties that has to be followed.

2. Measurement Systems

The first stable planar lipid bilayer membranes were reported by Mueller and coworkers in 1962 [14]. Since then, a variety of measuring systems have been designed for studying planar lipid bilayer properties.

Measuring principles have been improved during the years, as well as the lipid chambers and measurement instrument accuracies. This review of measuring systems is divided into two parts according to the nature of the stimulus—voltage or current. Some basic characteristics of the systems, such as type of stimulating signal, number and material of electrodes volume of the chamber, etc., are given in Appendix A.

2.1. Voltage Clamp

2.1.1. System Hanai–Haydon–Taylor

The system was published in 1964 [15]. Within this system, DC and AC signals were applied to a planar lipid bilayer (Fig. 4). The DC signal was supplied by an accumulator. The voltage was controlled by a potentiometer. The current and resistance measurements were taken by electrometer. In the AC measurements, the capacitance and conductance were measured by two bridges, the Universal Bridge and Radio Frequency Bridge, which were designed on the basis of the transformer ratio-arm principle. The accuracy of the measurements was generally better than 1%. Two signal generators covering the ranges 50 Hz–100 kHz and 100 kHz–5 MHz were used, calibrated against standard frequencies. The bridge balance was detected with an oscilloscope with a preamplifier and a communications receiver. Two Ag–AgCl electrodes for DC measurements and two black platinum electrodes for AC measurements were immersed in salt solution.

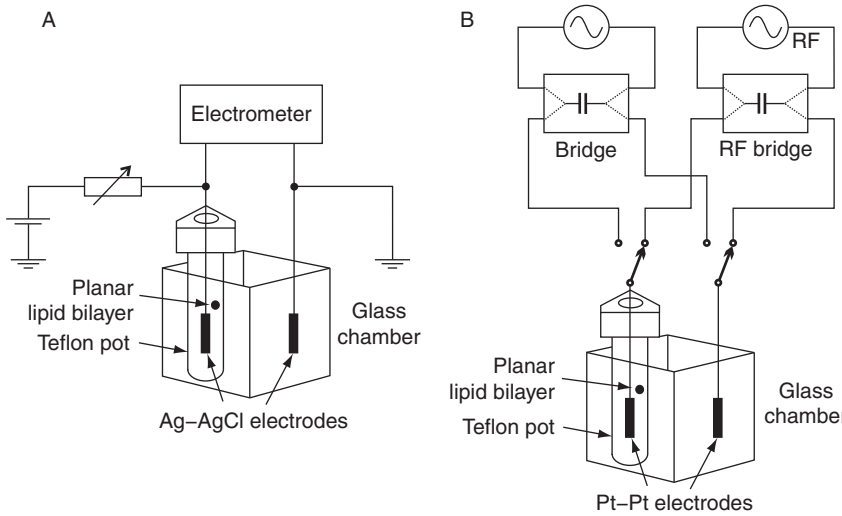

Figure 4 System Hanai–Haydon–Taylor. The figure was drawn according to description in Ref. [15].

The chamber had outer and inner parts. The outer part was made of glass cell from tubing of 4 cm × 4 cm bore. The inner part was made out of Teflon rod. The aperture for planar lipid bilayer was about 0.141 cm in diameter made by punching. The thickness of Teflon around the aperture was about 0.05 cm. The whole chamber was enclosed in a double-walled box for temperature stabilization by a water shell. The temperature during experiments was controlled with an accuracy of ±0.5 °C. Planar lipid bilayer was formed by the painted technique with a small brush.

The system was applied to quantitative assessment of the BLM molecular composition. Membrane thickness was obtained from the capacitance measurements that were obtained by a capacitance to voltage conversion method.

2.1.2. System Rosen–Sutton

The system was first published in 1968 [16]. Its main part was an AC signal generator with amplitude of 5 mV and frequency range from 100 Hz to 2 MHz (Fig. 5). Electrodes were connected to the transformer ratio-arm bridge. The bridge was initially balanced at a given planar lipid bilayer capacitance, which allowed DC potential to be applied between the electrodes during the AC measurements. The amplitudes of the DC potentials were up to 200 mV. An oscilloscope monitored Lassajous figures to permit observation of the conductance and capacitance contribution. The AC signal was applied through the bridge to planar lipid bilayer and to X channel of the oscilloscope. The planar lipid bilayer response was traced on Y channel. Four electrodes were immersed in salt solution. Two Calomel electrodes were used for measurement of transmembrane voltage by electrometer while voltage signal was delivered by two platinum electrodes. The planar lipid bilayer was painted across a round hole of about 1 mm in diameter.

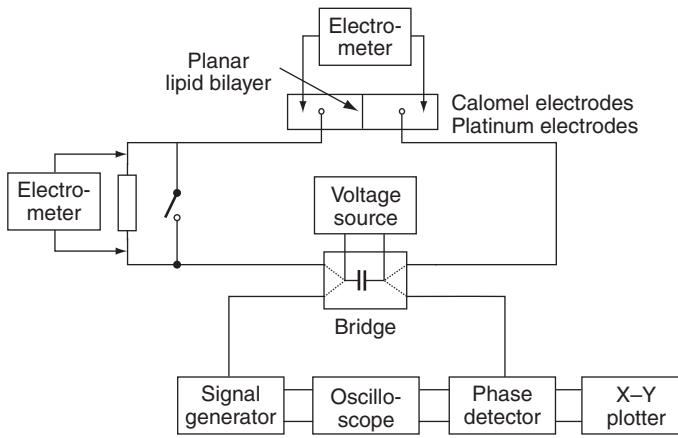

Figure 5 System Rosen–Sutton [16].

The system was applied to study an influence of the temperature and concentration of the salt solution on the electrical parameters of planar lipid bilayer [16].

2.1.3. System White

The system was first published in 1970 [17]. The basic idea follows the construction of the Rosen–Sutton system. The planar lipid bilayer capacitance was obtained from impedance measurements with an AC Winston bridge (Fig. 6). The chamber was made of Plexiglas with Teflon partition. Four platinized Ag–AgCl electrodes were used. A planar lipid bilayer was painted across round aperture of about 1 mm in diameter [17,18].

The authors studied the influence of the BLM thickness changes on BLM capacitance. They also investigated the planar lipid bilayer capacitance in dependence of the transmembrane voltage. The capacitance measurements were done by a capacitance to voltage conversion method.

2.1.4. System Wobschall

The system was published in 1971 [19,20]. The basic idea follows the construction of the Rosen–Sutton system but it was upgraded for planar lipid bilayer elasticity measurements (Fig. 7). The volume of one compartment of the chamber could be regulated by a flexible diaphragm with an acoustic oscillator. Pressure changes were measured with a pressure-sensitive transistor. The AC voltage signal was supplied by a function generator and a DC source. Both were regulated by a feedback circuit. The bridge excitation voltage with a frequency of 4 kHz varied from 5 to 15 mV. Four Ag–AgCl electrodes were immersed in a salt solution. The planar lipid bilayer was formed by the painted technique.

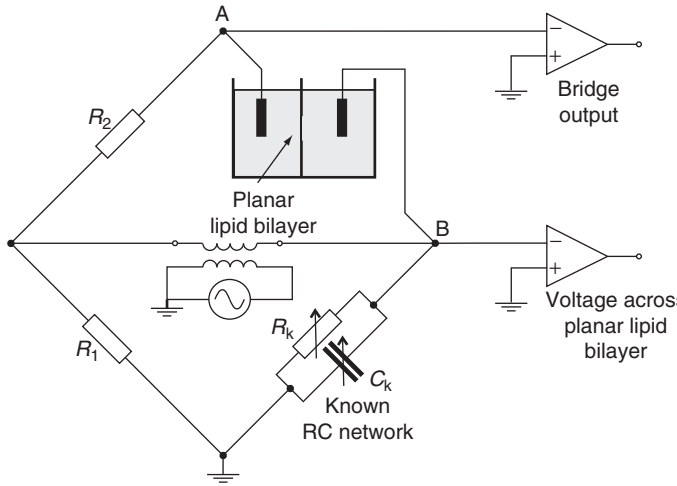

Figure 6 System White [17].

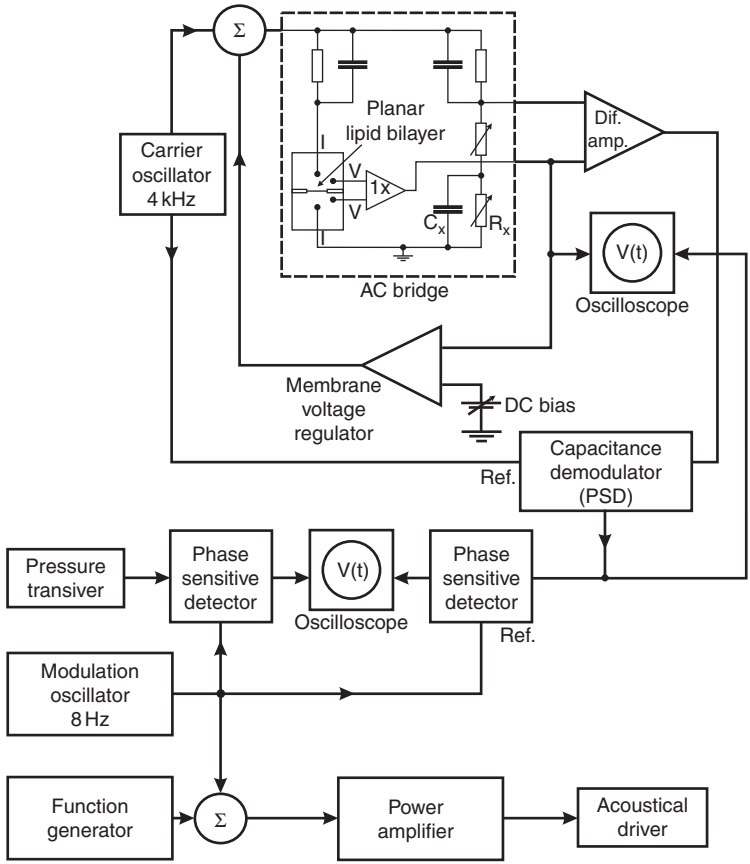

Figure 7 System Wobshall [19,20].

The capacitance of planar lipid bilayer in dependence of voltage and frequency was measured by a capacitance to voltage conversion method.

The construction of the chamber had a possibility of concaving the planar lipid bilayer in the shape of lens, which extended the area of BLM. This idea was employed to study the BLM capacitance in relation to its surface [20]. The elasticity of planar lipid bilayer at its breakdown was determined [19].

In the latter versions of this experimental system, the bridge was replaced by an impedance meter [21].

2.1.5. System Montal–Mueller

Montal and Mueller published the design of their measuring system in 1972 [3]. It was one of the first measuring systems that combined concepts of both measuring principles: voltage clamp and current clamp. The measuring

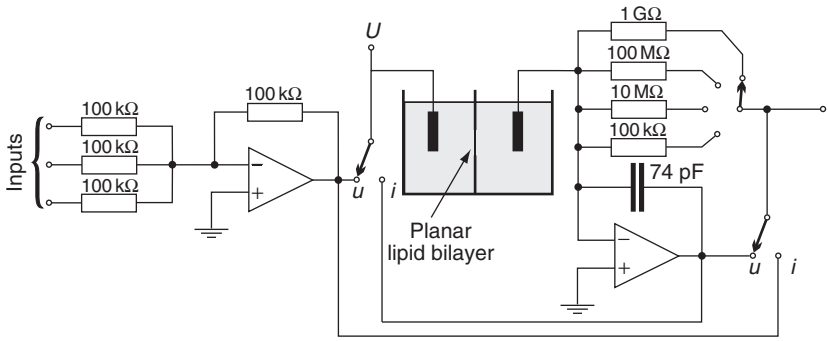

Figure 8 System Montal–Mueller [3].

principle was selected by two switches (Fig. 8). In the scheme, two amplifier circuits are present; the circuit on the left is voltage amplifier while the circuit on the right is current to voltage converter in the voltage-clamp mode (the switches are in position u) and voltage to current converter in the current-clamp mode (the switches are in position i). In voltage-clamp mode, the applied voltage is measured at connecting point U and the voltage that corresponds to current flowing through the planar lipid bilayer is measured at connecting point I. In the current-clamp mode, the applied current is recorded at connecting point I and the transmembrane voltage is measured at connecting point U. For planar lipid bilayer stimulation and corresponding measurements, two Calomel electrodes immersed in salt solution were used. The salt solution filled the Teflon chamber, which was divided into two compartments by 25 μm thick Teflon foil with an aperture of about 0.25 mm in diameter. The dimension of each compartment was (18 × 12) mm^2. The planar lipid bilayer was formed by the folding method [3].

The system was used for measurement of BLM capacitance and resistance. The capacitance was measured by charging method.

2.1.6. System Benz

The system was published in 1976 [6,7]. It is one of the simplest systems for observing planar lipid bilayers (Fig. 9). It consists of DC signal generator with the amplitude range from 10 mV to 5.4 V, switch, and battery supplied charge generator. The function of the switch was accomplished with FET transistor 2N5653. The output signal was a square pulse with duration from 500 μs to 500 ms. Oscilloscope Tektronix 7633 was used to measure the voltage response on planar lipid bilayer. The signal was filtered to the band of 80 Hz to 40 MHz. Two Ag–AgCl electrodes were immersed in a salt solution. The volume of each compartment of the Teflon chamber was of about 3 cm^3. In most cases, the area of the aperture was of about 2 mm^2. The planar lipid bilayer was formed by painted technique.

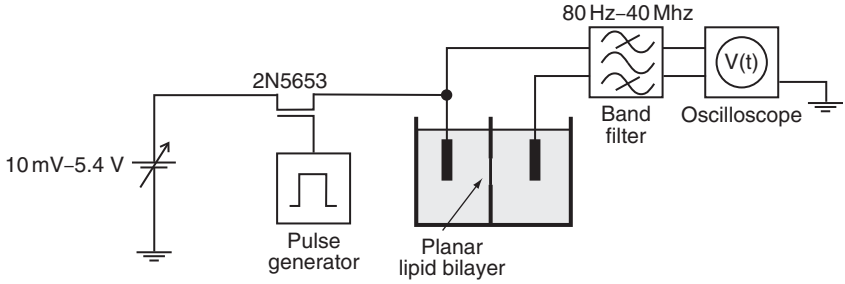

Figure 9 System Benz. The figure was drawn according to description in Ref. [6].

Benz *et al.* studied the capacitance of planar lipid bilayers using a discharge method. Most of the phospholipids used in their studies were synthesized in their own laboratory. In most cases, they used 0.1 M NaCl as the salt solution. They estimated thickness of the planar lipid bilayers and observed the thinning process of the planar lipid bilayers by capacitance measurement. The same system was used to investigate voltage breakdown as a function of salt concentration and pH [7].

The system was applied by the group of Chernomordik, whose experimental and theoretical studies made a great impact on understanding of the planar lipid bilayer breakdown process and related phenomena [4,22,23]. They observed fluctuations of the current with amplitude of about 10^{-11} A as a consequence of applying the voltage (100 mV–1 V) to the BLM. The membrane lifetime at a given voltage was also tested, defined as the time corresponding to the onset of an irreversible growth of current.

2.1.7. System Alvarez–Latorre

The system was published in 1978 [24]. The construction of the system was similar to the measuring systems based on the Winston Bridge [16,17,19]. Since the authors were interested in measuring changes in membrane capacitance rather than the absolute capacitance, they used differential amplifier to subtract the charging current of the membrane from the charging current of the equivalent *RC* network (Fig. 10). The resistance and capacitance of the equivalent *RC* network was set by the planar lipid bilayer capacitance measurement. The method based on 5 kHz, 10 mV peak-to-peak voltage waveform, which was only applied on a planar lipid bilayer. Two Ag–AgCl electrodes, one on each side of planar lipid bilayer, were immersed in the salt solution. The Teflon chamber consisted of two parts; each part had an area of 4 cm^2. A thin Teflon sheet of 19 μm was inserted between the reservoirs. The planar lipid bilayer was formed by the folding method. The output of the differential amplifier was further amplified and recorded with a sampling frequency of 2 MHz.

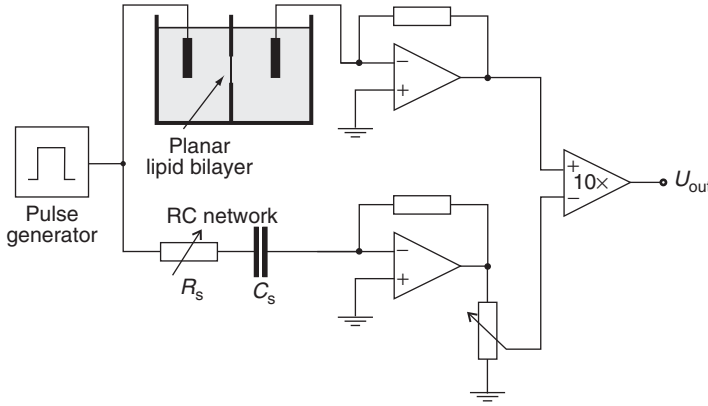

Figure 10 System Alvarez–Latorre [24].

They observed the capacitance of a planar lipid bilayer as a function of transmembrane potential and derived the thickness of planar lipid bilayers.

2.1.8. System Chanturya

The system proposed by Chanturya [25] was based on the system Benz [6]. The only difference in their designs is in a compensating capacitor, placed between the input of the operational amplifier and the inverter of the transmembrane potential (Fig. 11). The capacitor compensated almost all the reactive component of the current. Therefore, the author was able to use high-speed potential changes and obtain high resolution of measurements.

The system was applied for a study on the capacitance and resistance changes due to insertion of channel-forming proteins into the planar lipid bilayer [25].

2.1.9. System Wilhelm–Winterhalter–Zimmermann–Benz

The system was published in 1993 [26]. It was used in many other subsequent studies because it was simple and well defined [26–30]. The planar lipid bilayer was charged by a short voltage pulse with a commercial pulse generator. Instead of the switch, a diode with a reverse resistance $\gg 10^{12}\ \Omega$ was used to discharge the planar lipid bilayer only through the oscilloscope (Fig. 12). The pulse generator produced square pulses with durations from 0.2 to 10.0 μs. Two Ag–AgCl electrodes were immersed in salt solution that filled the Teflon chamber. Authors used different sizes of the apertures in the wall between two compartments—their areas were between 0.3 and 3 mm^2. The planar lipid bilayers were formed by the painted technique. The actual voltage on planar lipid bilayer was amplified with an operational amplifier and recorded with an oscilloscope. The data was processed by a connected computer.

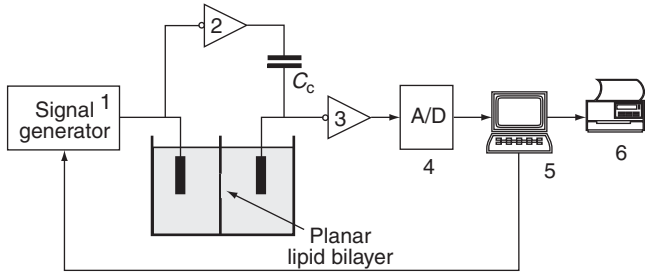

Figure 11 Sistem Chanturya [25]. 1. Signal Generator, 2. and 3. invertors, 4. analog to digital converter, 5. Personal Computer, 6. Printer.

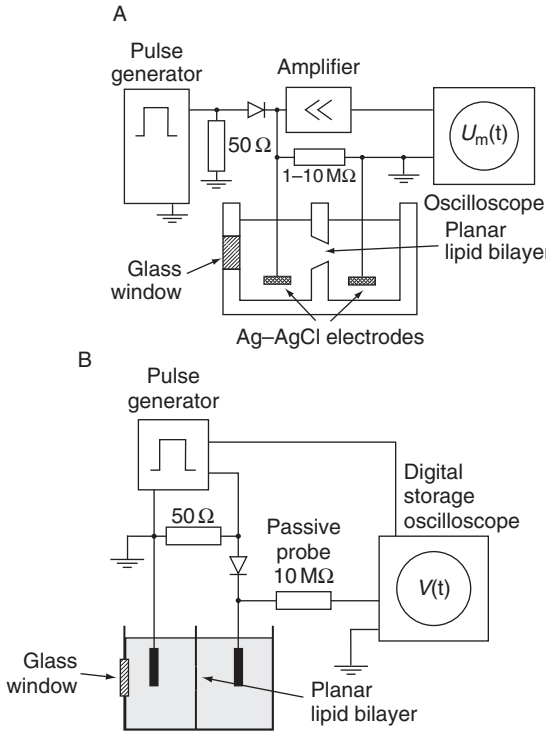

Figure 12 (A) System Wilhelm–Winterhalter–Zimmermann–Benz [26]. (B) Updated version of the system with an Digital Storage Oscilloscope described in Refs. [27–30].

Because many studies were based on this measuring system, a palette of lipids was tested [27–30]. Salt solutions differed from study to study as well as the volume of the lipids. The influence of the planar lipid bilayer composition on the breakdown voltage, capacitance, and rupture kinetics [27–29] was investigated [26,30].

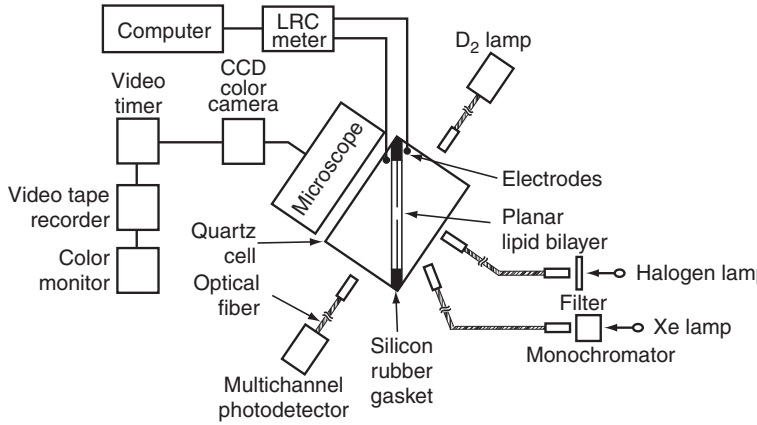

Figure 13 Sistem Yamaguchi–Nakanishi [12].

2.1.10. System Yamaguchi–Nakanishi

The system was published in 1993 [12]. It used combination of electric and optic measurements of planar lipid bilayer properties (Fig. 13). The authors simultaneously measured electrical characteristics and molecular structures of planar lipid bilayer as well as morphological changes. Planar lipid bilayer was exposed to sinus signal 7 mV_{RMS}/1 KHz. The response was measured with LCR meter. The measured data was acquired to the computer. During the electric measurement, the halogen or xenon light was used. Light reflection of planar lipid bilayer was observed and recorded by a color video camera. Two platinum/platinum electrodes were immersed in a salt solution. Chamber consisted of two quartz cells separated by Teflon 0.05 mm thick film, where an aperture of 0.7 mm in diameter was formed. The planar lipid bilayer was formed by the painted technique [12].

The authors measured changes in capacitance and resistance of planar lipid bilayer upon the irradiation by light.

2.1.11. System Sharma–Stebe–Tung

The system was an upgrade of the Benz system and it was described in 1996 [5,31]. FET switch was replaced by fast two pole analog switch. One of the switch poles was connected to the signal generator output and the other pole was connected on resistor of 1 MΩ. Voltage source consisted of an arbitrary waveform synthesizer board interfaced to a computer (Fig. 14). A square voltage pulse, which decayed linearly to zero to constitute a negative sloped ramp, and square voltage pulses from 10 μs to 10 s were generated. Four Ag–AgCl electrodes were inserted in the Teflon chamber via agar bridges. Two electrodes served to measure voltage across the bilayer by differential amplifier and the other two to apply voltage across the planar

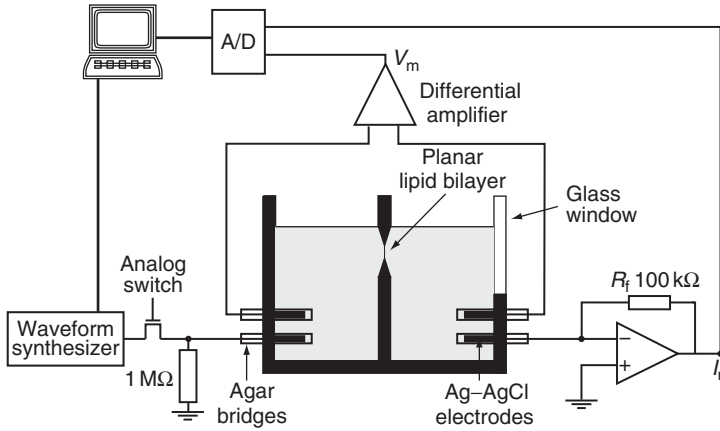

Figure 14 Sistem Sharma–Stebe–Tung [5,31].

lipid bilayer and measure the transmembrane current. The volume of each compartment of the Teflon chamber was about 3 cm^3. The diameter of the aperture in the Teflon foil was 105 μm. The planar lipid bilayers were formed by the folding technique. Current and voltage signals were recorded by a digital oscilloscope.

The system was used for studying the effects of nonionic surfactants (poloxamer 188, $C_{12}E_8$) on capacitance, conductance, and voltage breakdown of planar lipid bilayers [5,31]. Breakdown voltages of planar lipid bilayers were determined by applying a rectangular voltage pulse.

2.1.12. System Gallucci–Micelli

The system was published in 1996 [32]. The dynamic capacitance and resistance of a planar lipid bilayer could be measured simultaneously as is described in Section 3.2. Voltage signal of 1 kHz and adjustable amplitude, which was applied on planar lipid bilayer, was modulated by the signal of amplitude 2 mV and frequency of 1 kHz (Fig. 15). The electrodes were made of platinum. Experiments were performed in a Teflon chamber. The volume of each compartment was 4 ml. The aperture between the two compartments had a diameter of 1.3 mm. Current through the planar lipid bilayer was measured and amplified. The output signal from the amplifier was divided into two parts. In the first part, active two-stage 1 kHz band filter was used. The signal was then amplified, level adjusted, and rectified. Rectified voltage corresponds to the capacitance of planar lipid bilayer. In the second part, two-stage 1 kHz low pass filter was used. The signal was then amplified, level adjusted, and filtered to measure the resistance of the planar lipid bilayer [32–34].

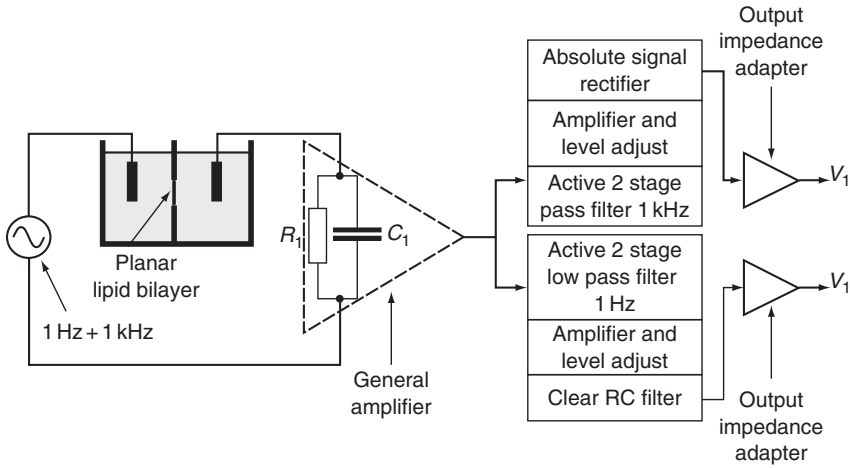

Figure 15 Sistem Gallucci–Micelli [32–34].

The general aim of the authors was investigation of channel insertion into planar lipid bilayer and corresponding electrical properties. The dynamic capacitance and resistance of planar lipid bilayers were measured simultaneously.

2.1.13. System Hanyu–Yamada–Matsumoto

Hanyu and coworkers [11] developed an experimental system that could measure ionic current and fluorescence emission of an artificial planar lipid bilayer, while controlling the membrane potential. Their experimental work was mostly dedicated to structural changes and functioning of ion channels.

The main part of the measuring system was an Axopatch200A (Axon Instruments, Inc. Foster City, USA). The program pClamp was used for voltage generation as well as for measuring the current through the planar lipid bilayer and analyses. Four Ag–AgCl electrodes were inserted in the specially designed chamber via agar bridges. Two electrodes served to measure current across the bilayer while the other two applied the voltage across the planar lipid bilayer. As in the previous system designed by Sharma *et al.* [31], the thin Teflon foil (25 μm thick) was inserted between two symmetrical parts of Teflon chamber. The diameter of the hole in the foil was 120 μm. The planar lipid bilayer was formed by the folding technique.

Schematic diagram of the experimental system developed for measuring the fluorescent emissions from the planar lipid bilayer is shown in Fig. 16. The excitation light was focused on the planar lipid bilayer (80 μm in diameter) with an objective lens so that only an area of the planar lipid bilayer was irradiated. The fluorescent emissions were collected through the

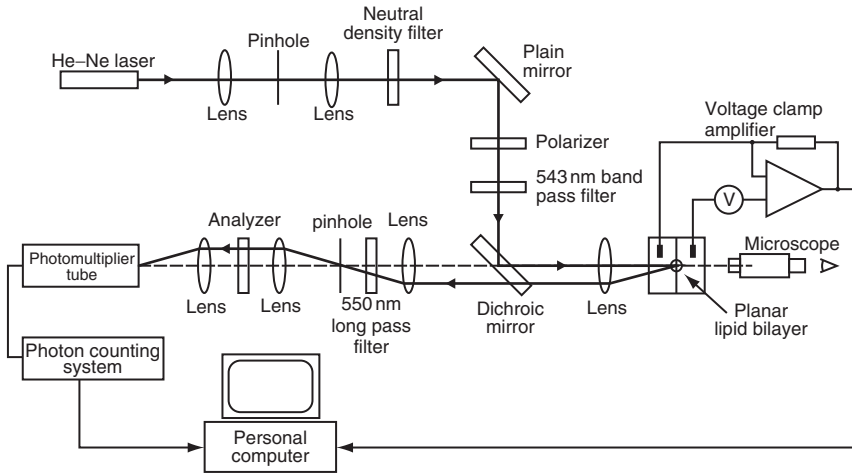

Figure 16 Hanyu–Yamada–Matsumoto [11].

objective lens and sent to the photomultiplier. Any fluorescence from other areas was blocked and scattered light was eliminated. The intensity of fluorescence was measured by photon-counting methods, while a multichannel analyzer was used for the emission spectrum measurements.

2.1.14. System Naumowicz–Petelska–Figaszewski

The system was published in 2003 [35]. It was similar to the system of Wobschall and the Rosen–Sutton system. It allowed applying pressure to planar lipid bilayer. Electrical properties of BLM were examined by impedance spectroscopy (Fig. 17). Four electrodes were immersed in a salt solution: two platinum current electrodes (CE) and two Ag–AgCl measuring electrodes (RE). The volume of one side of the organic glass chamber was modulated by external thread screw. The planar lipid bilayer was formed by the painted technique. Impedance measurement was carried out using an AC impedance system with a personal computer, two-phase lock-in amplifier, and potentiostat/galvanostat. Measuring electrodes were connected with a potentiostat via a high impedance input differential amplifier.

Impedance spectroscopy was used to measure planar lipid bilayer capacitance and resistance [35–37]. The interfacial tension of planar lipid bilayer was measured [38].

2.1.15. System Kramar–Miklavcic–Macek Lebar

The system was published in 2007 [8,39]. It was based on the Sharma–Stebe–Tung system. It included a signal generator, Teflon chamber, voltage and current measurement circuit, and digital storage oscilloscope (Fig. 18). Signal generator was a generator of an arbitrary type. It provided voltage amplitudes

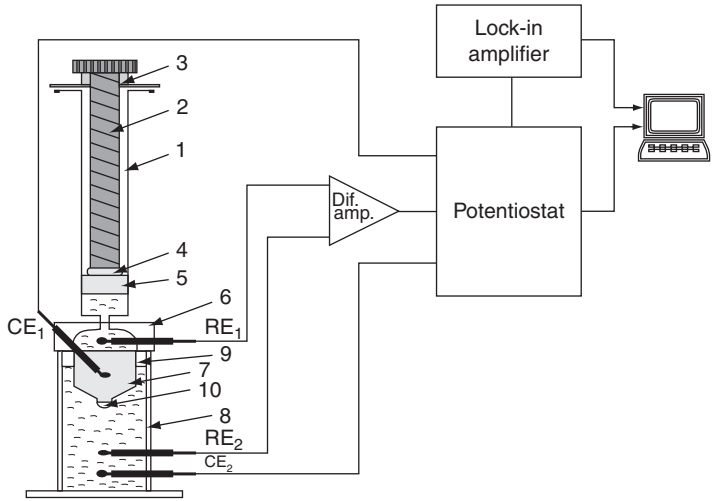

Figure 17 System Naumowicz–Petelska–Figaszewski [37]. 1. Syringe, 2. External thread screw, 3. Handwheel, 4. Steel tube, 5. Tight Teflon Piston, 6. Connector made of organic glass, 7. Platinum current electrode, 8. The chamber made of organic glass, 9. A tight Teflon attachement, 10. A forming sphere for planar lipid bilayer.

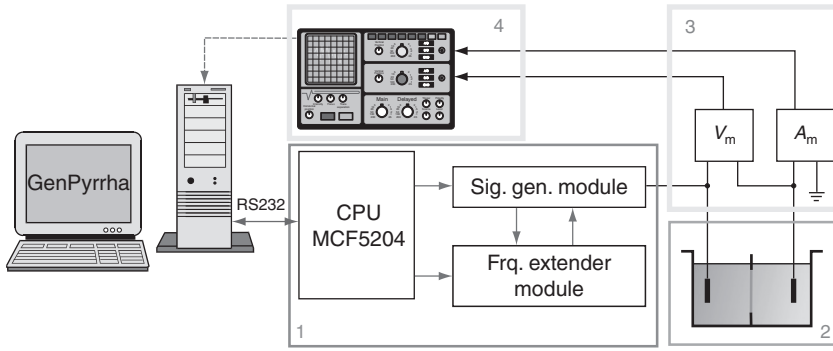

Figure 18 Experimental system. 1. The microprocessor board with MCF5024 processor and two modules. Signal generator module generates arbitrary signals. Frequency extender module is realized in programmable integrated circuit (FPGA) and is used for frequency extension. 2. Chamber for forming planar lipid bilayer and two Ag–AgCl electrodes. 3. Modules for current and voltage amplification. 4. Oscilloscope for data collection and storage.

from −5 to +5 V. It was controlled by custom designed software (Genpyrrha), which allowed drawing of arbitrary voltage signals. On the output of the signal generator was a switch that disconnected the output of the signal generator and connected the electrodes to the 1 MΩ resistor. The switch was able to turn off

the signal generator in 2 ns. This way planar lipid bilayer capacitance was measured. Two Ag–AgCl electrodes, one on each side of the planar lipid bilayer, were inserted into the salt solution. The Teflon chamber consisted of two parts—each part was a cubed reservoir of 5.3 cm^3 in volume. Between the reservoirs a 25 μm thin Teflon sheet was inserted. A diameter of the aperture was 105 μm. The planar lipid bilayer was formed by the folding method. Transmembrane voltage was measured by LeCroy differential amplifier 1822. The same electrodes were also used to measure the transmembrane current. Both signals were stored by the oscilloscope LeCroy Waverunner-2 354M in Matlab format. All sampled signals could be analyzed in Matlab^{TM} software after the experiments.

The authors measured U_{br} by means of a linearly rising signal and the capacitance of the planar lipid bilayers of various compositions [8].

2.2. Current Clamp

2.2.1. System Carius

The system was published in 1976 [40]. Symmetric AC Bridge was the main part of the measuring system (Fig. 19). The variable resistor R_K and the capacitor decade C_K, used for compensation, were in series. Without a planar lipid bilayer in the chamber, the electrode and electrolyte resistance were compensated with $R_K = R_0$ and $C_K = C_0$, when the capacitor C_0 was in series with the cell by means of switch S. With the planar lipid bilayer in the chamber, the increase in the compensation resistance needed ($R_K - R_0$) corresponded to the loss of the planar lipid bilayer capacitor, represented by the equivalent series planar lipid bilayer resistance. A DC bias voltage up to ± 200 mV was provided at the planar lipid bilayer by a voltage controlled current source. The bridge balance was controlled by a phase-sensitive detector (lock-in amplifier) tuned to the frequency of the oscillator. When the out-of-phase signal vanished at proper settings R_K, the in-phase signal output of the lock-in amplifier was proportional to ($C_{BLM} - C_K$), provided that the difference was small compared to C_K. The AC voltage on the planar lipid bilayer was 3 or 6 mV_{RMS}, when only the capacitance was recorded. Another lock-in amplifier was used for the detection of the second harmonic. For these measurements, the AC voltage on the planar lipid bilayer was 20–60 mV_{RMS} and the DC voltage varied between 0 and ± 160 mV. When the second and third harmonics were measured simultaneously by the two lock-in amplifiers, bridge balance was controlled by an AC voltmeter with a band pass filter at the input. The electrodes were Ag–AgCl–platinum black electrodes. The chamber was made of Teflon. In most cases, the diameter of the aperture was about 0.9 mm. The planar lipid bilayer was formed by the painted technique. The output signals were recorded.

The system was applied to measurements of the transmembrane voltage dependence on the BLM capacitance.

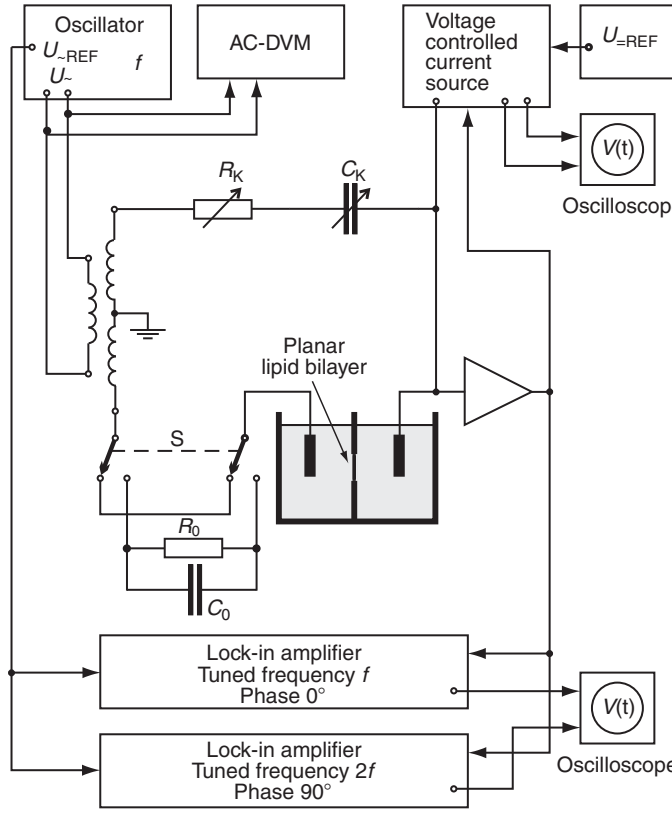

Figure 19 System Carius [40].

2.2.2. System Robello–Gliozzi

The system was published in 1989 [41]. The group performed experiments on current–voltages relationship of planar lipid bilayer under voltage-clamp condition in previous years [42]. Later on, they changed their measuring system to a current-clamp mode. The planar lipid bilayer was in a feedback network of the operational amplifier which acted as a current–voltage converter (Fig. 20). The current value was selected with resistor on the amplifier input. The current–voltage characteristics were obtained by exposing the planar lipid bilayer to a triangular signal with 8–10 min period [41]. By constant current of 10–20 pA, the fluctuations in planar lipid bilayers were studied [43–45]. Two Ag–AgCl electrodes were immersed in salt solution. The volume of each compartment of the Teflon chamber was about 2 ml. The Teflon foil between two compartments was 12 μm thick. The diameter of the apertures was from 100 to 200 μm. The planar lipid bilayer was formed by the folding method. The output signal was low-pass filtered at 250 Hz (24 db/octave) and recorded to the computer with a sampling frequency of 1 kHz.

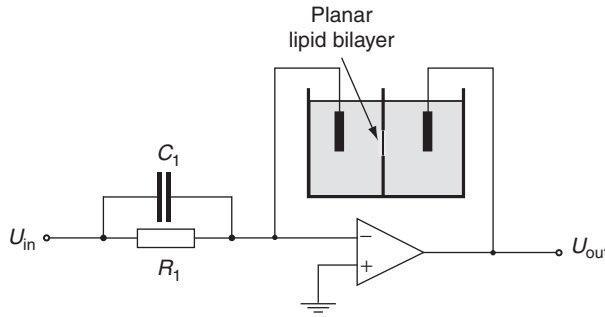

Figure 20 System Robello–Gliozzi [41–47].

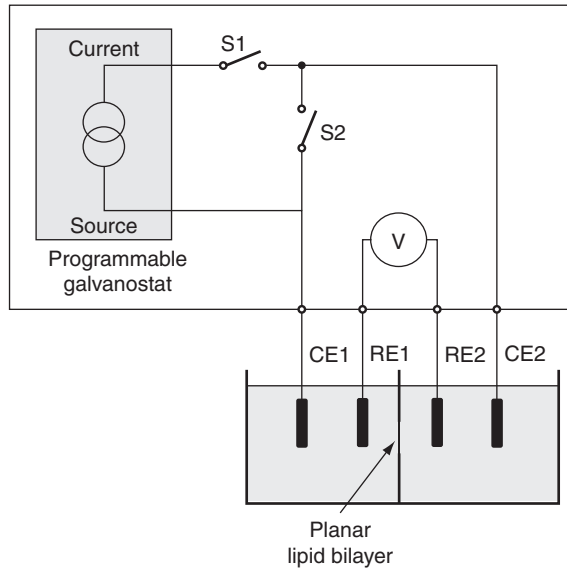

Figure 21 System Kalinowski–Figaszewski [48–51].

The authors observed voltage breakdown, current–voltage characteristic, and fluctuations of planar lipid bilayer. The system was later on upgraded to extremely low current value source (10 pA) [47].

2.2.3. System Kalinowski–Figaszewski

The system was published in 1992 [48]. The system included two modules (Fig. 21). The first module was capacity to period converter, used for measuring the BLM capacitance [48,49] (see Section 3.1). The second module was a potentiostat–galvanostat for planar lipid bilayer studies under current clamp [50]. Both modules were controlled with a personal computer.

The output signal was programmable [51]. The potentiostat had a negative feedback for equalization of operational amplifier input voltage. The chamber was made of one piece Teflon with two compartments, each 10 cm^3 of volume. Between the compartments was the aperture of 1 mm in diameter. Four Ag–AgCl electrodes were immersed in a salt solution; two of them were CE and two other reference electrodes (RE). The switch S1 disconnected the current flowing through the electrodes. The switch S2 caused short circuit of the CE and forced planar lipid bilayer potential to zero.

The system was applied for recording the transmembrane voltage, especially for the electroporation studies the trace of building voltage on planar lipid bilayer was observed due to constant current clamp [9,52].

3. Methods for Determination of Planar Lipid Bilayer Properties

3.1. Capacitance (*C*)

The capacitance (*C*) is the parameter considered the best tool for probing the stability and integrity of planar lipid bilayers and for this reason it is measured for every bilayer, even when other properties are the main focus of the measurements. There are three main methods for determination of planar lipid bilayer capacitance: a discharge method, a capacitance to period conversion method, and a capacitance to voltage conversion method. For comparison between different studies, the measured value of the capacitance must be normalized to the size of the planar lipid bilayer surface and the specific capacitance of the planar lipid bilayer, that is, the capacitance per unit area, is usually given.

3.1.1. Discharge method

The most common and simplest method for measuring planar lipid bilayer capacitance is measurement of the voltage discharge time constant [5,6,8,26,27,30,31,39,53]. Only a voltage generator, a fast switch, and an oscilloscope are needed for its implementation. To make the measurement, a planar lipid bilayer is first charged by a voltage pulse. At the end of the pulse, the charged lipid bilayer is discharged through a resistor of known resistance and the discharging process monitored with an oscilloscope (Fig. 22).

The voltage $u(t)$ on the planar lipid bilayer decreases exponentially:

$$u(t) = U_0 e^{-t/\tau}. \tag{1}$$

Here, U_0 is the amplitude of the voltage pulse and τ is a time constant. The time constant depends on the capacitance (C) and resistance (R) which come from the planar lipid bilayer and the electronic system,

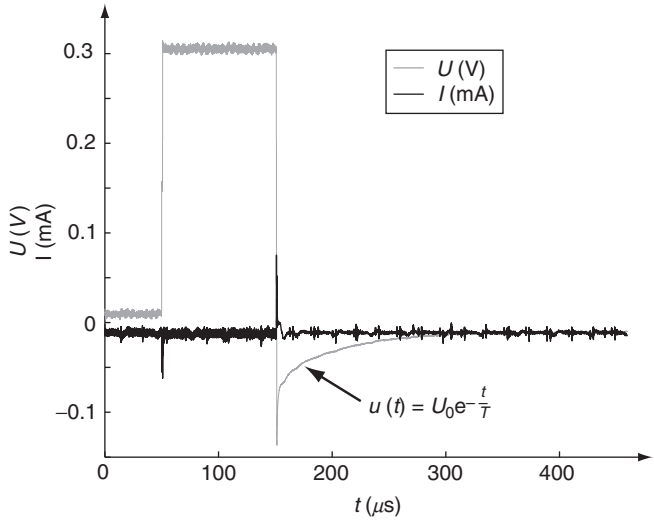

Figure 22 Planar lipid bilayer capacitance measurement by discharge method.

$$\tau = RC. \tag{2}$$

The resistance of the electronic system is usually known and is much lower than the resistance of planar lipid bilayer ($\sim 10^8$ **Ω**); therefore, the capacitance of planar lipid bilayer can be determined in two steps. First, the capacitance of the electronic system is measured without the planar lipid bilayer, C_{SYS}. Then, the capacitance of the electronic system with the planar lipid bilayer and salt solution C_{SBLM} is determined. The capacitance of planar lipid bilayer C_{BLM} is then obtained as a difference between C_{SYS} and C_{SBLM}:

$$C_{BLM} = C_{SYS} - C_{SBLM}. \tag{3}$$

In early experiments, the planar lipid bilayer charging process was also used for planar lipid bilayer capacitance determination. Montal and Mueller [3] calculated the capacitance of planar lipid bilayers from the current records in response to a voltage step signal:

$$C = \frac{I}{\Delta U} \int_0^\infty I \, \mathrm{dt}, \tag{4}$$

where I is the current and ΔU the amplitude of the voltage. In the constant voltage mode, the time constant and gain of the current record depends on the value of the feedback resistor in the current measuring amplifier. Because the capacity currents are small, the feedback resistance was kept about 100 k**Ω**.

3.1.2. A capacitance to period conversion method

The electrical parameters of the planar lipid bilayer can also be measured by means of an alternating voltage signal, which offers the advantage of eliminating the effect of possible electrode polarization.

Kalinowski and Figaszewski [48] constructed an instrument (Fig. 23), which converts planar lipid bilayer capacitance to a train of rectangular pulses. During the measurement, the planar lipid bilayer is charged and discharged with a constant current. The charge–discharge cycle duration is proportional to the membrane capacitance.

In the circuit in Fig. 23, the capacitance of planar lipid bilayer is represented by the capacitor C_{BLM}. The voltage at the point D is amplified by a noninverting amplifier with the gain k:

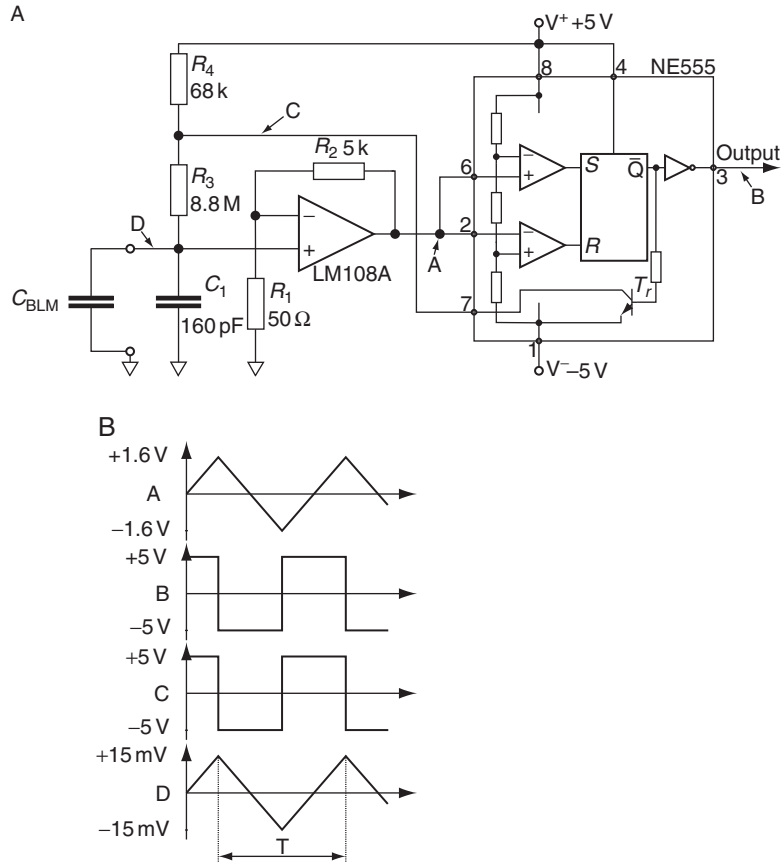

Figure 23 Measurement of planar lipid bilayer capacitance by capacitance to period conversion method. (A) Schematic diagram of the capacity-to-period converter [48]. (B) Voltage wave of the capacity-to-period converter [48].

$$k = \frac{R_1 + R_2}{R_2}. \tag{5}$$

The amplified signal is an input of the integrated circuit NE555. Two voltage comparators are contained in the integrated circuit, both with one of their inputs connected to the voltage from the amplifier output (A) while the other input is one of the voltages from the voltage divider, which is realized by three resistors. Depending on the voltage levels at the inputs R and S, the output of the cell (B) is switched to a low or high state. The result is a square wave signal, which has a well-defined period. The voltage across the planar lipid bilayer can be calculated as

$$U_{\mathrm{BLM}} = \frac{2}{3} V \frac{1}{k} = \frac{2VR_1}{3(R_1 + R_2)}. \tag{6}$$

The measurement is divided into two steps. First, the capacitor is charged with the current passing across resistors R_4 in R_3 and transistor T_{r} is off. Then, the capacitor is discharged due to the current across the transistor, which is a consequence of a changed state of the cell. The current flows across resistor R_3 and transistor T_{r}. The product of the voltage and time in one period is:

$$TV = U_{\mathrm{BLM}}(R_3 + R_4)C_{\mathrm{BLM}} + U_{\mathrm{BLM}}R_3C_{\mathrm{BLM}}. \tag{7}$$

If $R_4 \ll R_3$ and $V = V^+ = |V^-|$, then the period is:

$$T = \frac{2U_{\mathrm{BLM}}R_3C_{\mathrm{BLM}}}{V}. \tag{8}$$

3.1.3. A capacitance to voltage conversion method

When a sinusoidally varying signal is applied to the planar lipid bilayer, its impedance is important. Since capacitors "conduct" current in proportion to the rate of voltage change, they pass more current for faster changing voltages, and less current for slower changing voltages. Therefore, the capacitive part of the impedance–capacitive reactance in ohms for any capacitor is inversely proportional to the frequency of the alternating current. According to this theory, the capacitances of planar lipid bilayers were often measured using AC Wheatstone bridge [15–17], which contain a variable resistor in parallel with a variable capacitor in the known arm. When the bridge is balanced at a given frequency, the settings of the known arm give the parallel equivalent capacitance and resistance of the circuit connected to its unknown terminals. Since the planar lipid bilayer is immersed in electrolyte, the bridge measures the parallel equivalent impedance of the membrane–electrolyte system.

The parallel equivalent capacitance can be represented by the membrane capacitance and the stray capacitance associated with electrodes in series with electrolyte resistance; therefore, appropriate equivalent circuit and transform equations should be used to relate membrane capacitance to the elements of the bridge. A convenient technique for displaying AC impedance data is the Cole–Cole diagram.

Micelli *et al.* [33] measured the capacitance of planar lipid bilayers by applying sinusoidally varying voltage with amplitude of 2 mV and the frequency of 1 kHz. At this high frequency, almost all of the current crosses the reactive part of the planar lipid bilayer and its resistance is negligible. The rectified voltage is proportional to the planar lipid bilayer capacitance. By using a set of test values for the capacitance, which were one by one included in measuring system, they parameterized the relation between measured voltage and capacitance. The hyperbolic relation with two known parameters a and b was obtained:

$$C_{\mathrm{BLM}} = a\frac{V_{1h}}{b - V_{1h}}. \tag{9}$$

3.2. Resistance (*R*)

Planar lipid bilayer membranes exhibit resistance in the range of few gigaohms. The resistance is usually calculated in accordance with Ohm's law as a ratio of voltage applied to (or measured on) the planar lipid bilayer and current which flows through it. As mentioned earlier, the electrical parameters of planar lipid bilayer can also be measured by means of an alternating current. The continuous monitoring of capacitance is useful in tracking membrane thickness, while the continuous monitoring of the resistance allows studies of protein–lipid interactions and planar lipid bilayer fluctuations.

Gallucci and coworkers [32] presented an electrical circuit appropriate for continuous monitoring of planar lipid bilayer capacitance and resistance simultaneously. An input voltage was composed of two sinusoidally varying signals: one with variable amplitude (0.1–1.5 V) and frequency of 1 Hz and another with amplitude of 2 mV and frequency of 1 kHz. The planar lipid bilayer and the measuring device are shown with equivalent circuits on the left side in Fig. 24. According to the associated vector graph on the right side in Fig. 24, the following relations can be written:

$$V_1\cos(\varphi - \varphi_1) + V_{\mathrm{BLM}}\cos(\varphi_{\mathrm{BLM}} - \varphi) = V_{\mathrm{s}} \tag{10}$$

$$V_1\sin(\varphi - \varphi_1) = V_{\mathrm{BLM}}\sin(\varphi_{\mathrm{BLM}} - \varphi) \tag{11}$$

$$\omega C_{\mathrm{BLM}} V_{\mathrm{BLM}} = I\sin\varphi_{\mathrm{BLM}}. \tag{12}$$

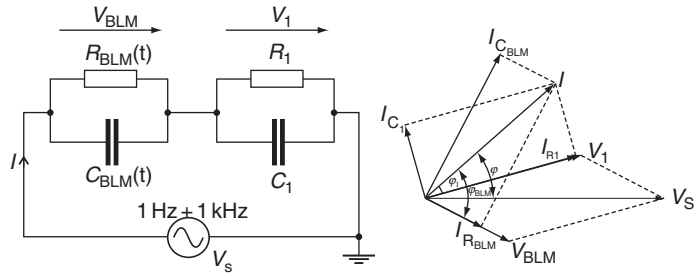

Figure 24 Left: Equivalent circuit of the planar lipid bilayer (BLM) and of the measurement device. V_s is an input voltage. V_{BLM} and V_1 are the planar lipid bilayer and output voltages, respectively. R_1 is electrical resistance and C_1 the capacitance of the measuring circuit; R_{BLM} and C_{BLM} are the resistance of planar lipid bilayer and capacitance, respectively. Right: Vector scheme of the voltages and currents in the circuit no the left [32–34].

The current I is the vector sum of the currents crossing the resistance R_1 and capacitance C_1 of the measuring device:

$$I = V_1\sqrt{(\omega C_1)^2 + \left(\frac{1}{R_1}\right)}. \tag{13}$$

If the capacitance of the planar lipid bilayer has already been measured (see Section 3.1), the phase angles φ_{BLM} and φ as well as the voltage V_{BLM} can be determined. The resistance of the planar lipid bilayer is then obtained from the relation:

$$R_{BLM} = \frac{V_{BLM}}{I\cos\varphi}. \tag{14}$$

3.3. Breakdown Voltage (U_{br})

The electrical modulation of biological membrane physical properties caused by electrical oscillations and excitations are natural processes in living organisms. Applications of external electric fields, especially those based on the phenomenon of electroporation, have gained increasing importance for manipulations in biological cells and tissues [54]. The structural changes in biological membranes induced by an external electric field involve rearrangement of the phospholipid bilayer and lead to the formation of aqueous pores. If the electric field does not exceed some critical adequate strength and duration, the membrane returns to its normal state after the end of the exposure to the electric field; the electroporation is reversible. However, if the exposure to the electric field is too long or the strength of the electric field is too high, the membrane does not reseal after the end of the exposure,

and the electroporation is irreversible. The underlying mechanisms for these properties are dependent on the lipid component of biological membrane, and can be studied on planar lipid bilayers.

Application of a steady voltage in the order of few hundred millivolts across a planar lipid bilayer causes the membrane to break. Most often the breakdown voltage (U_{br}) of the planar lipid bilayer is determined by applying a rectangular voltage pulse (10 μs–10 s) (Fig. 25). The amplitude of the voltage pulse is increased in small steps until the breakdown of the bilayer is obtained [5]. First, the voltage pulse charges up the planar lipid bilayer. Above a critical voltage (U_{br}) defects are created in the planar lipid bilayer allowing an increase of the current through the bilayer [4]. Usually, planar lipid bilayer collapses when the breakdown voltage is exceeded.

Using the rectangular voltage pulse measuring protocol, the number of applied voltage pulses is not known in advance and each planar lipid bilayer is exposed to a voltage stress many times. Such a pretreatment of the planar lipid bilayer affects its stability and consequently the determined breakdown voltage of the planar lipid bilayer [4]. Another approach for the breakdown voltage determination was suggested by Kramar *et al.* [8]. Using a linear rising signal, the breakdown voltage of a planar lipid bilayer is determined by only a single voltage exposure (Fig. 26).

The slope of the linear rising signal and the peak voltage of the signal must be selected in advance. The breakdown voltage (U_{br}) is defined as the voltage at the moment t_{br} when a sudden increase of the current through the planar lipid bilayer is observed. Time (t_{br}) is defined as the lifetime of the planar lipid bilayer at a chosen slope of the linear rising signal (Fig. 26). Because the planar lipid bilayer lifetime depends on the applied voltage [5,55] and the planar lipid bilayer pretreatment [4], U_{br} and t_{br} are measured at a variety of slopes. Using nonlinear regression (Fig. 27), a two parameter curve can be fitted to the data

$$U = \frac{a}{1 - e^{-t/b}}, \tag{15}$$

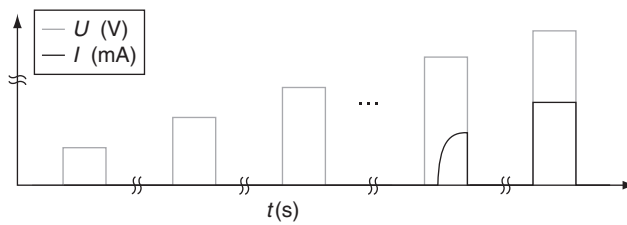

Figure 25 Measurement of planar lipid bilayer breakdown voltage (U_{br}) by successional rectangular pulses. The amplitude of the voltage pulse (gray) is incremented in small steps until the breakdown of the bilayer is observed as sudden increase of current (black) [5].

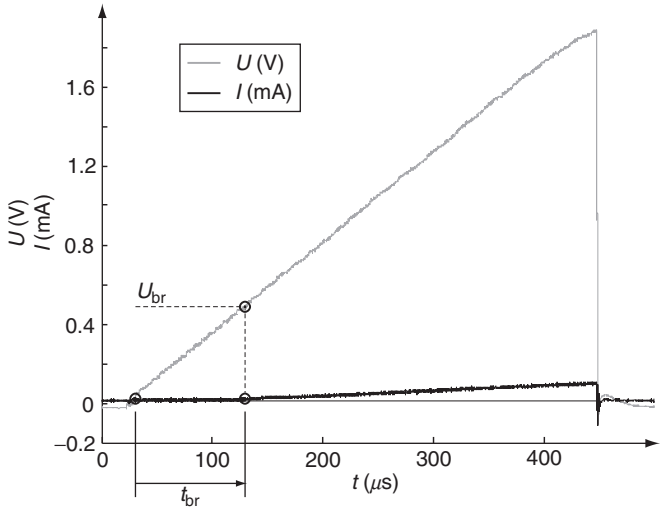

Figure 26 Measurement of planar lipid bilayer breakdown voltage (U_{br}) by linear rising signal. Breakdown voltage is defined as the voltage (gray) at the moment t_{br} when sudden increase of the current (black) through the planar lipid bilayer is observed [8].

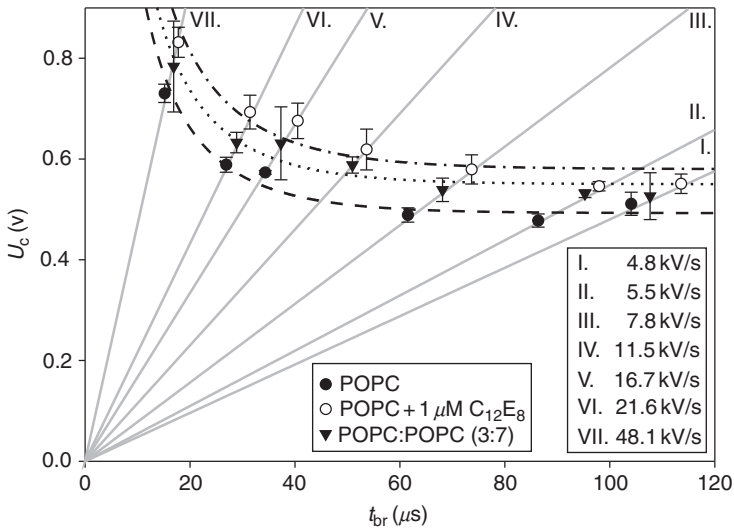

Figure 27 The breakdown voltage (U_{br}) (dots and triangles) of planar lipid bilayers with different chemical composition as a function of lifetime t_{br}. The gray lines show seven different slopes of applied liner rising voltage signal. Dash, dotted, and dash-dotted curves represent two parameters curve [15] fitted to data.

where U is U_{br} measured at different slopes; t is corresponding t_{br}; and a and b are parameters. Parameter a is an asymptote of the curve which corresponds to minimal breakdown voltage U_{brMIN} for a specific planar lipid bilayer chemical composition. Parameter b governs the inclination of the curve.

3.4. Fluctuations (ψ)

Fluidity of the lipid membrane must produce local fluctuations of the membrane microscopic parameters. Appearance of transient defects and pores in the membrane structure affects its conductance, producing fluctuations. Transient changes of the membrane electrical properties also accompany protein insertion into the membrane. Voltage-clamp studies with low-value fields are typically applied for recording capacitance and conductance changes, following insertion of channel-forming proteins into the planar lipid bilayer (e.g., Ref. [25]).

The fluctuations are even more pronounced under a strong electric field that is sufficient to electroporate the membrane. The pore appearance is preceded by lipid reorganization resulting in the events of transient membrane permeability to ions. Related to these phenomena, fluctuations of the current were observed prior to an irreversible breakdown of a planar lipid bilayer [4]; the fluctuation amplitude was about 10^{-11} A. After electroporation, it is very unlikely for an electropore to maintain its rim fixed, hence pore fluctuations are theoretically expected. Since the electroporation under voltage-clamp conditions results in very fast pore expansion leading to rapid membrane breakdown, an experimental study on the pore dynamics, in the voltage-clamp mode, required application of very short pulses that could protect the membrane from destruction [56,57]. The experiment reported in Ref. [57] approximated a typical lifetime of an electropore created under voltage-clamp conditions (250 mV) as 3 ms. Conductance fluctuations recorded in these experiments were attributed to a pore dynamics. In such a study, however, the voltage was clamped above the breaking potential and, because of the high value of the potential, the appearance of multiple pores is almost certain. The combined dynamics of several pores may have accounted for the observed fluctuations and single pore dynamics was blurred. At higher voltages, an irreversible membrane breakdown was studied by voltage-clamp techniques [27,31].

Exposure of the planar lipid bilayer to a constant current (0.1–2.0 nA) does not rupture the bilayer rapidly. The membrane slowly accumulates the charge and when the first pore appears, the transmembrane potential decreases, preventing subsequent electropore appearance, which permits the hypothesis of a single pore formation. Fluctuations observed in these current-clamp experiments are caused by opening and closing of a single pore [9,49–52,58]. The natural electropore fluctuations are enhanced by a negative feedback inherent to the current-clamp electroporation method.

The feedback results from interplay between the pore surface and the transmembrane voltage. As a consequence of the electropore expansion, the membrane resistance decreases and the voltage across planar lipid bilayer is reduced. This prevents further increase of the electropore, which usually starts shrinking instead—increasing the transmembrane voltage. This chain of events accounts for the pore stabilization and its fluctuations. The pore can live for several hours. The fluctuations show regular stochastic properties, which are partly due to the feedback and partly due to the pore dynamics and membrane elastic properties [58,59]. Elimination of the feedback in the voltage-clamp experiment, before which the pore that is formed and stabilized under current-clamp conditions, shows very interesting non-Gaussian properties of the electropore dynamics. The parameters of the long-tailed Levy-stable probability density function, which characterizes electropore dynamics, are related to the lipid composition of the membrane, salt properties, and the pore diameter (Fig. 28) [52].

3.5. Other Physical Properties

3.5.1. Thickness (*d*)

The thickness of planar lipid bilayer is usually determined from its capacitance according to the relation valid for parallel plate capacitor:

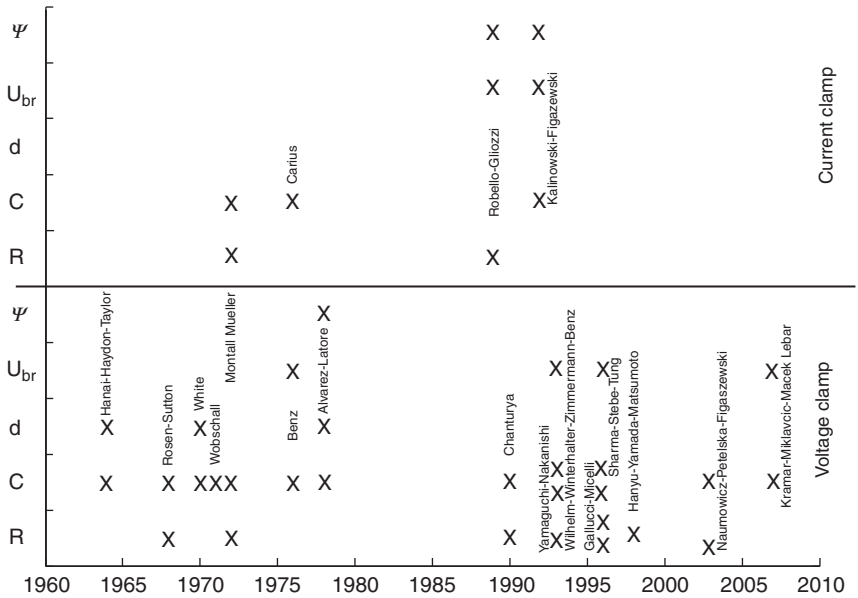

Figure 28 Time perspective of systems for planar lipid bilayer properties determination.

$$d = \varepsilon\varepsilon_0 \frac{A}{C_{\mathrm{BLM}}}. \tag{16}$$

In this equation, A stands for the area of planar lipid bilayer and C_{BLM}, ε_0, and ε for its capacitance, the permittivity of the free space, and the relative static permittivity, respectively. It is usually assumed that the relative static permittivity inside lipid bilayer equals to 2.1 [24].

3.5.2. Elasticity (E) and surface tension (σ)

A macroscopic approach using the theory of elasticity of solid bodies and liquid crystals can be applied to describe mechanical properties of lipid bilayers. In 1973, Helfrich proposed a theory and possible experiments of elastic properties measurements on planar lipid bilayers [60]. As the anisotropy of lipid bilayers is clearly expressed, several elasticity modules are required to describe its viscoelastic properties. Depending on the directions of the membrane deformation, we distinguish volume compressibility, area compressibility, unilateral extension along membrane plane, and transversal compression.

Experimentally, lipid bilayer mechanical properties were commonly measured on giant unilamellar vesicles [61–64]. Pressure was applied on a membrane with micropipette aspiration method; the properties were measured by means of video microscopy [65]. From experiments on planar lipid bilayer, Winterhalter and coworkers [66] reported that dynamics light scattering allowed quantifying viscoelastic properties in nonperturbative way, while Wobschall calculated membrane elasticity and breaking strength from measurement of capacitance of the planar lipid bilayer as it was bowed under a known pressure. Transversal elasticity modulus cannot be measured directly due to small thickness of the membrane and extremely small changes of the thickness upon deformation. It can be estimated through capacitance measurement with a special electrostriction method which is based on measurements of the amplitude of higher current harmonics [67].

Sabotin with coworkers [68] presented an estimation of the planar lipid bilayer transversal elasticity (E) and surface tension (σ) by means of viscoelastic predictive model of Dimitrov [69] and measured planar lipid bilayer capacitance and break down voltage. The model considers the lipid bilayer as a viscoelastic, isotropic material that can be represented as a standard solid model, composed of a Kelvin body in series with a linear spring. Originally, this model predicts the critical voltage and critical time needed to collapse a membrane at applied voltage. Critical voltage corresponds to breakdown voltage (U_{brMIN}) and critical time to life time (t_{br}) of planar lipid bilayer. The parameters of model are Young's transversal elasticity modulus (E), surface tension (σ), viscosity (μ), thickness of the membrane (h), and

permittivity of membrane (ε_m). If U_{br} is measured by linear rising signal (Fig. 26), the corresponding planar lipid bilayer lifetime (t_{br}) is always finite [8]. Generic model equation that still contains t_{br} [69] gives the relation:

$$U_{br} = \sqrt[4]{n + \frac{k}{t_{br}}}\,. \tag{17}$$

The relation can be fitted to the data obtained experimentally by the breakdown voltage determination using linear rising signal [8]. Parameters n and k, which are obtained through fitting, served to calculate Young's elasticity modulus (E) and surface tension (σ) of planar lipid bilayer. Specific capacitance (c_{BLM}) has to be measured, while other parameters such as thickness ($h = 3.5$ nm) and viscosity ($\mu = 6$ Ns/m^2) can be taken from Ref. [69].

4. Conclusions

In this chapter, we have reviewed setups and experimental methods applied to study of the properties of planar lipid bilayers. The planar lipid bilayer presents a good model of the plasma membrane where the behavior of the lipid part is not obscured by other components of the real cell membrane. In particular, the influence of the conductive protein ion channels could be eliminated. The development of measuring systems was enabled by discovery of the first technique for forming stable planar lipid bilayers in 1962. This discovery permitted design of a range of instruments useful for measuring planar lipid bilayer characteristics by different methods, allowing a more complete picture of planar lipid bilayer physical properties and membrane-related phenomena like electroporation. The measurement methods vary from simple electrical setups, which allowed for the first experiments and demonstrated basic lipid bilayer characteristics, to more recent advanced systems, frequently combining electrical and nonelectrical methods, such as optical or mechanical.

In the field of electrical measurements on biological objects with non-constant resistance, there are two major approaches to the topic. One method is based on the voltage-controlled measurements, in which different shapes of an alternating voltage are applied on the planar lipid bilayer. In the other method, the current shape and value are controlled. The planar lipid bilayer characteristics that are observed during the experiment dictate the choice of the measuring principle. The experiments carried out by the presented systems showed viscoelastic properties of planar lipid bilayers, temporal changes in the electroporated membrane, and fluctuation characteristics of an electropore.

Appendix A. Review of Measuring Systems

Table 1 Description of measuring systems

System	Stimulating signal	Lipid	Salt solution	Lipid preparation	Volume of the chamber	Electrodes	Aperture diameter	Temperature (°C)
Rosen–Sutton [16]	AC: 5 mV/500 Hz, DC: ±200 mV	Lecitin	1 mM, 10 mM, 100 mM, 1 M KCl or NaCl	1% (w/v)	–	2 Calomel + 2 Pt	1 mm	22
White [17,18]	AC: 20 mV/100 Hz	Oxidized cholesterol, lecithin	KCl, pH 7.1	35 mg/ml	–	4 platinized Ag–AgCl	1.6 mm	20
Wobshall [19,20]	AC: 5–15 mV_{RMS}/4kHz	Cholesterol, HDTAC	40 mM KCl, pH 6.7	12 mg/ml	–	4 Ag–AgCl	1.68 mm	30
Montal–Mueller [3]	Voltage pulse 10 ms, 37.5 mV; Constant current 20 pA	Egg lecithin, cholesterol, glyceroldioleate, bovin cardiolipin, gramicidin	0.01 M NaCl, pH 5.5	–	(18 × 12) mm^2/compartment	2 Calomel	0.25 mm	Room temperature
Benz [6,7]	10 mV–2 V/500 μs–500 ms	PC, DPhPC, DOPC, POPC, PE, Ox Ch	1 M KCl, 0.1 M NaCl, pH 6	2% (w/v)	3 cm^3/compartment	2 Ag–AgCl	2 mm^2 (area); 0.2–0.3 mm	25
Abidor-Chernomordik-Chizmadzhev-Pastushenko [4]	100 mV/1 μs, 400 mV/1 μs	Egg lecithin; Ch: lecitin 2:1	0.1 M NaCl + 10 M Tris–HCl, pH 7.4	40 mg/cm^3	–	–	1 mm	27

(*continued*)

Table 1 (*continued*)

System	Stimulating signal	Lipid	Salt solution	Lipid preparation	Volume of the chamber	Electrodes	Aperture diameter	Temperature (°C)
Alvares-Latore [24]	10 mV/5 kHz	–	–	–	4 cm^2/ compartment	2 Ag–AgCl	–	–
Robello–Gliozzi [41,43–45]	Square waves 40 mV, current ramp (0.17 pA/s), triangular signal 2.5×10^{-3} Hz	Egg lecithin:Ch 1:1, PC:Ch (4:1), PC, Ch, DPhPC, PS	10 mM Tris–Cl, pH=7.5, 0.1 M, 1 M KCl	10 mg/ml	2 ml / compartment	2 Ag–AgCl	100–150, 160, 200 μm	25
Chanturya [25,70]	10 mV–1 V/10–100 μs	PC:Ch 2:1	10 mM Tris, pH=7.4	20 mg/ml	9 ml	Ag–AgCl	0.6 mm	26–29
Kalinovski-Figazewski [48–50]	Constant current: 0.005, 0.2, 0.3, 2 nA; step 0.2 nA/10 s; rectangular signal: 8 × 0.2 nA/10 s	PC:Ch, lecithin, PS	0.1 M KCl, pH 7.0	20 mg/ml	10 cm^3/ compartment	4 Ag–AgCl (0.5 × 80) mm	1 mm	23–25
Wilhelm–Winterhalter–Zimmermann–Benz [26–30]	10 mV–2 V/500 μs–500 ms	Ox Ch (+ DOPC or + PE), azolectin, DPHPC, PS, DOPC, DOPE	10 mM, 100 mM, 1 M, 2 M, 3 M KCl. pH=6,7	1 μl, 5 mg/ml, 10 mg/ml, 40 mg/ml	5 ml/ compartment, 15 ml/ compartment	2 Ag–AgCl	100–200 μm, 0.3–3 mm, 1 mm, 2 mm^2 (area)	20, 22, 25, 30
Yamaguchi–Nakanishi [12]	7 mV_{RMS}/1 kHz	GMO	0.1 M KCl	62 mg/ml	–	2 Pt	0.7 mm	25
Sharma–Stebe–Tung [5,31]	100 mV/10 μs, 510 μs 	POPC, azolectin	100 mM KCl, pH=7.4	10 mg/ml 20 mg/ml	3 ml/compartment	4 Ag–AgCl	75–100 μm, 105 μm	22–24

Gallucci–Micelli [32–34]	Variable amplitude V_{pp}/1 Hz + 2 mV/1 kHz	PI, Ox Ch	0.1 M, 0.5 M, 1 M KCl, pH 7.0	1% (w/v)	4 ml/compartment	2 Pt	1.3 mm	22–24
Hanyu–Yamada–Matsumoto [11]	0.1–1 V	Azolectin	–	5 mg/ml	–	4 Ag–AgCl	120 μm	–
Naumowicz–Petelska–Figaszewski [35–37]	4 mV/0.01–10 kHz	Lecithin, Ch, lecithin:Ch 1:1	0.1 M KCl, pH 7.4	20 mg/cm^3	–	2 Ag–AgCl, 1 Pt	–	–
Kramar [8,68]	Linar rising voltage (4.8–48.1 kV/s)	POPC, POPS	0.1 M KCl	10 mg/ml	5.3 cm^3/ compartment	2 Ag–AgCl	105 μm	Room temperature

For each system the stimulating signal, number and material of electrodes, volume of the chamber, and a diameter of the aperture are given. Lipids, which were used in described experiments, corresponding salt solutions and the temperature, at which the experiments were conducted, are also listed. Ch, cholesterol.

Appendix B. Review of Measured Properties on Planar Lipid Bilayer

Table 2 Properties of planar lipid bilayers of various lipid compositions and parameters at which they were measured

Lipid	Salt solution	T (μs)	Shape of the signal	U_{br} (mV)	C (μF/cm^2)	R (MΩcm^2)	d (nm)	References
Azolecitin	0.1 M KCl	10	⎍	423.4±29.4	0.59±0.21	–	–	[31]
		510	⎍	441.6±23.2				
DOPC	0.1 M NaCl	–	⎍	–	0.37±0.01	0.40	4.97±0.17	[6]
DOPE	0.1 M NaCl	–	⎍	–	0.37±0.01	0.40	5.00±0.16	[6]
DPhPC	0.1 M KCl	–	⎍	390±20	0.6–0.75	7.85–17.76	–	[41,43,45,46]
	1 M KCl	–	⎍	–	0.74–1.13	24.3–54.9	–	[43,44]
	0.1 M KCl	10	⎍	546±15	–	–	–	[27,30,44]
	0.1 M NaCl	–	⎍	–	0.36±0.02	0.40	5.08±0.21	[6]
	0.1 M KCl	–	⎍	–	0.9–1	–	–	[57]
DPhPS	0.1 M KCl	10	⎍	530±15	–	–	–	[27,30]
Lecithin	1e-3–1 M NaCl or KCl	–	∿	–	0.32–0.64	1–10	–	[16]
Ox Ch	1 M KCl	–	∿	–	0.40	0.25	–	[34]
	0.1 M KCl	–	∿	–	0.45±0.01	0.21±0.01	–	[32]
	0.5 M KCl				0.47±0.04	0.23±0.01		
	1 M KCl				0.40±0.01	0.20±0.03		
	1 M KCl	10	⎍	–	0.56	–	3.3	[7]
PC	0.1 M KCl	–	⎍	280±30	0.75	–	–	[41,46]
	0.1 M NaCl	–	⎍	–	0.34±0.01	0.40	5.48±0.17	[6]
PE	0.1 M NaCl	–	⎍	–	0.33±0.01	0.40	5.67±0.22	[6]

PI	1 M KCl	–	∿	–	0.25	0.4	–	[34]
	0.1 M KCl	–	∿	–	0.30±0.01	0.37±0.01	–	[32]
	0.5 M KCl				0.27±0.01	0.34±0.01		
	1 M KCl				0.25±0.01	0.38±0.06		
POPC	0.1 M KCl	10	⊓	400±6	–	–	–	[27,30]
	0.1 M KCl	10	⊓	450±24	0.59±0.15	–	–	[5]
		100		398±19				
		10^3		331±20				
		10^4		282±26				
		10^5		258±9				
		10^6		213±18				
		10^7		167±6				
POPS	0.1 M KCl	10	⊓	410±20	–	–	–	[27,30]
PS	0.1 M KCl	–	⊓	500 ± 50	–	–	–	[46]
PC + Ch	0.1 M KCl	–	⊓	270 ± 20	–	–	–	[46]
PC + PE	0.1 NaCl	–	∿	–	0.1	–	–	[25]
Lecithin	0.1 M KCl	–	∿	–	0.38–0.61	0.014–2.12	–	[20]
+ Ch 1:1	10 mM Tris–Cl	–	⊓	–	–	–	–	[21]

For each lipid composition break down voltage ($U_{\mathbf{br}}$), capacitance (C), resistance (R), and thickens (d) are given. Salt solution that was used in experiments, as well as shape and duration of the stimulating signal are also presented.

REFERENCES

[1] R.B. Gennis, Biomembranes, Molecular Structure and Function, Springer, New York, 1989.
[2] P. Mueller, D.O. Rudin, H.T. Tien, W.C. Wescott, Methods for the formation of single bimolecular lipid membranes in aqueous solution, J. Phys. Chem. 67 (1963) 534–535.
[3] M. Montal, P. Mueller, Formation of bimolecular membranes from lipid monolayers and a study of their electrical properties, PNAS 69 (1972) 3561–3566.
[4] I.G. Abidor, V.B. Arakelyan, L.V. Chernomordik, Y.A. Chizmadzhev, V.F. Pastushenko, M.R. Tarasevich, Electric breakdown of bilayer lipid membranes I. The main experimental facts and their qualitative discussion, Bioelectrochem. Bioenerg. 6 (1979) 37–52.
[5] G.C. Troiano, L. Tung, V. Sharma, K.J. Stebe, The reduction in electroporation voltages by the addition of surfactant to planar lipid bilayer, Biophys. J. 75 (1998) 880–888.
[6] R. Benz, K. Janko, Voltage-induced capacitance relaxation of lipid bilayer membranes; effects on membrane composition, Biochim. Biophys. Acta 455 (1976) 721–738.
[7] R. Benz, F. Beckers, U. Zimmermann, Reversible electrical breakdown of lipid bilayer membranes: A charge-pulse relaxation study, J. Membr. Biol. 48 (1979) 181–204.
[8] P. Kramar, D. Miklavčič, A. Maček Lebar, Determination of the lipid bilayer breakdown voltage by means of a linear rising signal, Bioelectrochemistry 70 (2007) 23–27.
[9] S. Kalinowski, G. Ibron, K. Bryl, Z. Figaszewski, Chronopotentiometric studies of electroporation of bilayer lipid membranes, Biochim. Biophys. Acta 1396 (1998) 204–212.
[10] A. Blume, Lipids, in: D. Waltz, J. Teissie, G. Milazzo (Eds.), Bioelectrochemistry of Membranes Birkhauser, Basel-Boston-Berlin, 2004, pp. 24–61.
[11] Y. Hanyu, T. Yamada, G. Matsumoto, Simultaneous measurement of spectroscopic and physiological signals from a planar bilayer system: Detecting voltage-dependent movement of a membrane-incorporated peptide, Biochemistry 1998 (1998) 15376–15382.
[12] H. Yamaguchi, H. Nakanishi, Characterization of the preparation process and the photochemical control of electrical properties of bilayer lipid membranes containing azobenzene chromopores, Biochim. Biophys. Acta 1148 (1993) 179–184.
[13] T.F. Eibert, M. Alaydrus, F. Wilczewski, V.W. Hansen, Electromagnetic and thermal analysis for lipid bilayer membranes exposed to RF fields, IEEE Trans. Biomed. Eng. 46 (1999) 1013–1021.
[14] P. Mueller, D.O. Rudin, H.T. Tien, W.C. Wescott, Reconstitution of a cell membrane structure in vitro and its transformation into an excitable system, Nature 194 (1962) 979–980.
[15] T. Hanai, D.A. Haydon, J. Taylor, An investigation by electrical methods of lecitin-in-hydrocarbon films in aqueous solutions, Proc. R. Soc. Lond. Ser. A Math. Phys. Sci. 281 (1964) 377–391.
[16] D. Rosen, A.M. Sutton, The effects of a direct current potential bias on the electrical properties of bimolecular lipid membranes, Biochim. Biophys. Acta 163 (1968) 226–233.
[17] S.H. White, A study of lipid bilayer membrane stability using precise measurements of specific capacitance, Biophys. J. 10 (1970) 1127–1147.
[18] S.H. White, T.E. Thompson, Capacitance, area, and thickness variations in thin lipid films, Biochim. Biophys. Acta 323 (1973) 7–22.
[19] D. Wobschall, Bilayer membrane elasticity and dynamic response, J. Colloid Interface Sci. 36 (1971) 385–423.

[20] D. Wobschall, Voltage dependance of bilayer membrane capacitance, J. Colloid Interface Sci. 40 (1972) 417–423.
[21] K.U. Maheswari, T. Ramachandran, D. Rajaji, Interaction of cisplatin with planar model membranes—dose dependent change in electrical characteristics, Biochim. Biophys. Acta 1463 (2000) 230–240.
[22] L.V. Chernomordik, S.I. Sukharev, I.G. Abidor, Y.A. Chizmadzhev, Breakdown of lipid bilayer membranes in an electric field, Biochim. Biophys. Acta 736 (1983) 203–213.
[23] L.V. Chernomordik, S.I. Sukharev, S.V. Popov, V.F. Pastushenko, A.V. Sokirko, I.G. Abidor, et al. The electrical breakdown of cell and lipid membranes: the similarity of phenomenologies, Biochim. Biophys. Acta 902 (1987) 360–373.
[24] O. Alvarez, R. Latorre, Voltage-dependent capacitance in lipid bilayers made from monolayers, Biophys. J. 21 (1978) 1–17.
[25] A.N. Chanturiya, Detection of transient capacitance increase associated with channel formation in lipid bilayers, Biochim. Biophys. Acta 1026 (1990) 248–250.
[26] C. Wilhelm, M. Winterhalter, U. Zimmermann, R. Benz, Kinetics o pore size during irreversible electrical breakdown of lipid bilayer membranes, Biophys. J. 64 (1993) 121–128.
[27] A. Diederich, G. Bahr, M. Winterhalter, Influence of surface charges on the rupture of black lipid membranes, Phys. Rev. E 58 (1998) 4883–4889.
[28] A. Diederich, G. Bahr, M. Winterhalter, Influence of polylysine on the rupture of negatively charged membranes, Langmuir 14 (1998) 4597–4605.
[29] A. Diederich, M. Strobel, W. Meier, M. Winterhalter, Viscosity- and inertia-limited rupture of dextran-supported black lipid membranes, J. phys. Chem. B 103 (1999) 1402–1407.
[30] W. Meier, A. Graff, A. Diederich, M. Winterhalter, Stabilization of planar lipid membranes: a stratified layer approach, Biochim. Biophys. Acta 2000 (2000) 4559–4562.
[31] V. Sharma, K. Uma Maheswari, J.C. Murphy, L. Tung, Poloxamer 188 decreases susceptibility of artificial lipid membranes to electroporation, Biophys. J. 71 (1996) 3229–3241.
[32] E. Gallucci, S. Micelli, G. Monticelli, Pore formation in lipid bilayer membranes made of phosphatidylinositol and oxidized cholesterol followed by means of alternating current, Biophys. J. 71 (1996) 824–831.
[33] S. Micelli, E. Gallucci, V. Picciarelli, Studies of mitochondrial porin incorporation parameters and voltage-gated mechanism with different black lipid membranes, Bioelectrochemistry 52 (2000) 63–75.
[34] S. Micelli, E. Gallucci, D. Meleleo, V. Stipani, V. Picciarelli, Mitochondrial porin incorporation into black lipid membranes: ionic and gating contribution to the total current, Bioelectrochemistry 75 (2002) 97–106.
[35] M. Naumowicz, A.D. Petelska, Z.A. Figaszewski, Capacitance and resistance of the bilayer lipid membrane formed of phosphatidylcholine and cholesterol, Cell. Mol. Biol. Lett. 8 (2003) 5–18.
[36] M. Naumowicz, Z.A. Figaszewski, Impedance spectroscopic investigation of the bilayer lipid membranes formed from the phosphatidylserine–ceramide mixture, J. Membr. Biol. 227 (2009) 67–75.
[37] M. Naumowicz, A.D. Petelska, Z.A. Figaszewski, Impedance analysis of phosphatidylcholine–cholesterol system in bilayer lipid membranes, Electrochim. Acta 50 (2005) 2155–2161.
[38] A.D. Petelska, M. Naumowicz, Z.A. Figaszewski, Complex formation equilibria in two-component bilayer lipid membrane: interfacial tension method, J. Membr. Biol. 228 (2009) 71–77.

[39] P. Kramar, D. Miklavčič, A. Maček-Lebar, A system for the determination of planar lipid membrane voltage and its applications, IEEE Trans. Nanobiosci. 8 (2009) 132–138.
[40] W. Carius, Voltage dependence of bilayer membrane capacitance. Harmonic response to ac excitation with dc bias, J. Colloid Interface Sci. 57 (1976) 301–307.
[41] M. Robello, A. Gliozzi, Conductance transition induced by an electric field in lipid bilayers, Biochim. Biophys. Acta 982 (1989) 173–176.
[42] M. Robello, M. Fresia, L. Maga, A. Grasso, S. Ciani, Permeation of divalent cations through α-latrotoxin channels in lipid bilayers: steady-state current-voltage relationships, J. Membr. Biol. 95 (1987) 55–62.
[43] A. Ridi, E. Scalas, M. Robello, A. Gliozzi, Linear response of a fluctuating lipid bilayer, Thin Solid Films 327–329 (1998) 796–799.
[44] E. Scalas, A. Ridi, M. Robello, A. Gliozzi, Flicker noise in bilayer lipid membranes, Europhys. Lett. 43 (1998) 101–105.
[45] A. Ridi, E. Scalas, A. Gliozzi, Noise measurements in bilayer lipid membranes during electroporation, The Eur. Phys. J. E 2 (2000) 161–168.
[46] I. Genco, A. Gliozzi, A. Relini, M. Robello, E. Scalas, Electroporation in symmetric and asymmetric membranes, Biochim. Biophys. Acta 1149 (1993) 10–18.
[47] E. Pescio, A. Ridi, A. Gliozzi, A picoampere current generator for membrane electroporation, Rev. Sci. Instrum. 71 (2000) 1740–1744.
[48] S. Kalinowski, Z. Figaszewski, A new system for bilayer lipid membrane capacitance measurements: method, apparatus and applications, Biochim. Biophys. Acta 1112 (1992) 57–66.
[49] S. Kalinowski, Z. Figaszewski, A four-electrode system for measurement of bilayer lipid membrane capacitance, Meas. Sci. Technol. 6 (1995) 1034–1049.
[50] S. Kalinowski, Z. Figaszewski, A four-electrode potentiostat–galvanostat for studies of bilayer lipid membranes, Meas. Sci. Technol. 6 (1995) 1050–1055.
[51] S. Koronkiewicz, S. Kalinowski, K. Bryl, Programmable chronopotentiometry as a tool for the study of electroporation and resealing of pores in bilayer lipid membranes, Biochim. Biophys. Acta 1561 (2002) 222–229.
[52] M. Kotulska, Natural fluctuations of an electropore show fractional Levy stable motion, Biophys. J. 92 (2007) 2412–2421.
[53] J. Vargas, J.M. Alarcon, E. Rojas, Displacement currents associated with the insertion of Alzheimer Disease amyloid (beta)-peptide into planar bilayer membranes, Biophys. J. 79 (2000) 934–944.
[54] D. Miklavčič, M. Puc, Electroporation, Wiley Encyclopedia of Biomedical Engineering, Wiley, New York, 2006.
[55] A. Maček-Lebar, G.C. Troiano, L. Tung, D. Miklavčič, Inter-pulse interval between rectangular voltage pulses affects electroporation threshold of artificial lipid bilayers, IEEE Trans. Nanobiosci. 1 (2002) 116–120.
[56] V.F. Antonov, V.V. Petrov, A.A. Molnar, D.A. Predvoditelev, A.S. Ivanov, The appearance of single ion channels in unmodified lipid bilayer membrane at the phase transition temperature, Nature 283 (1980) 585–588.
[57] K.C. Melikov, V.A. Frolov, A. Shcherbakov, A.V. Samsonov, Y.A. Chizmadzhev, L.V. Chernomordik, Voltage-induced nonconductive pre-pores and metastable single pores in unmodified planar lipid bilayer, Biophys. J. 80 (2001) 1829–1836.
[58] M. Kotulska, S. Koronkiewicz, S. Kalinowski, Self-similar processes and flicker noise from a fluctuating nanopore in a lipid membrane, Phys. Rev. E 69 (2004) 031920–031930.
[59] S. Koronkiewicz, K. Bryl, Cholesterol-induced variations in fluctuations of the pores in bilayer lipid membrane, Cell. Mol. Biol. Lett. 4 (1999) 567–582.

[60] W. Helfrich, Elastic properties of lipid bilayers—theory and possible experiments, Z. Naturforsch. C J. Biosci. C 28 (1973) 693–703.
[61] R. Kwok, E.A. Evans, Thermoelasticity of large lecithin bilayer vesicles, Biophys. J. 35 (1981) 637–652.
[62] E. Evans, D. Needham, Physical properties of surfactant bilayer membranes: thermal transitions, elasticity, rigidity, cohesion, and colloidal interactions, J. Phys. Chem. 91 (1987) 4219–4228.
[63] B.L.-S. Mui, P.R. Cullis, E.A. Evans, T.D. Madden, Osmotic properties of large unilamellar vesicles prepared by extrusion, Biophys. J. 64 (1993) 443–453.
[64] E. Evans, W. Rawicz, Elasticity of ''fuzzy'' biomembranes, Phys. Rev. Lett. 79 (1997) 2379–2382.
[65] J. Genova, A. Zheliaskova, M.D. Mitov, The influence of sucrose on the elasticity of SOPC lipid membrane studied by the analysis of thermally induced shape fluctuations, Colloids Surf. A—Physicochem. Eng. Asp. 282 (2006) 420–422.
[66] M. Winterhalter, Black lipid membranes, Curr. Opin. Colloid Interface Sci. 5 (2000) 250–255.
[67] T. Hianik, Structure and physical properties of biomembranes and model membranes, Acta Phys. Slovaca 56 (2006) 687–806.
[68] I. Sabotin, A. Maček Lebar, D. Miklavčič, P. Kramar, Measurement protocol for planar lipid bilayer viscoelastic properties, IEEE Trans. Dielectr. Electr. Insul. 16 (2009) 1236–1242.
[69] D.S. Dimitrov, Electric field-induced breakdown of lipid bilayers and cell-membranes—a thin viscoelastic film model, J. Membr. Biol. 78 (1984) 53–60.
[70] A.N. Chanturiya, G. Basanez, U. Schubert, P. Henklein, J.W. Yewdell, J. Zimmerberg, PB1-F2, an influenza A virus-encoded proapoptotic mitochondrial protein, creates variably sized pores in planar lipid membranes, J. Virol. 78 (2004) 6304–6312.